

**Uncovering the molecular mechanisms of human  
cytomegalovirus immunoevasins US2 and US11  
using genetic screens**

**Michael Laurentius van de Weijer**

Title: Uncovering the molecular mechanisms of human cytomegalovirus immunoevasins  
US2 and US11 using genetic screens  
PhD Thesis, Utrecht University, The Netherlands

Author: Michael L van de Weijer

Cover Artwork: iStock by Getty Images - 494735914

Printed and published by: ProefschriftMaken || [www.proefschriftmaken.nl](http://www.proefschriftmaken.nl)

ISBN: 978-94-6295-660-5

© Michael L van de Weijer, Utrecht, The Netherlands. All rights reserved. No parts of this thesis may be reproduced, stored in a retrieval system or transmitted in any form or by any means without permission of the author. The copyright of articles that have been published or accepted for publication has been transferred to the respective journals.

# **Uncovering the molecular mechanisms of human cytomegalovirus immunoevasins US2 and US11 using genetic screens**

Het ophelderen van de moleculaire mechanismen van de immuonevasie eiwitten US2 en US11 van het humane cytomegalovirus met behulp van genetische screeningsmethoden  
(met een samenvatting in het Nederlands)

## **Proefschrift**

ter verkrijging van de graad van doctor aan de Universiteit Utrecht op gezag van de rector magnificus, prof.dr. G.J. van der Zwaan, ingevolge het besluit van het college voor promoties in het openbaar te verdedigen op

donderdag 8 juni 2017 des ochtends te 10.30 uur

door

**Michael Laurentius van de Weijer**

geboren op 29 september 1988  
te Baarn

**Promotor:** Prof. Dr. E.J.H.J. Wiertz

**Copromotor:** Dr. Ir. R.J. Lebbink

*"Far out in the uncharted backwaters of the unfashionable end of the Western spiral arm of the galaxy lies a small unregarded yellow sun. Orbiting this, at a distance of roughly ninety million miles is an utterly insignificant little blue-green planet, whose ape descended life forms are so amazingly primitive that they still think digital watches are a pretty neat idea. This planet has, or had, a problem, which was this. Most of the people living on it were unhappy for pretty much of the time. Many solutions were suggested for this problem, but most of these were largely concerned with the movements of small, green pieces of paper, which is odd, because on the whole, it wasn't the small, green pieces of paper which were unhappy. And so the problem remained, and lots of the people were mean, and most of them were miserable, even the ones with digital watches. Many were increasingly of the opinion that they'd all made a big mistake coming down from the trees in the first place, and some said that even the trees had been a bad move, and that no-one should ever have left the oceans."*

**- Douglas Adams (The Hitchhiker's Guide to the Galaxy)**

**Reading committee:**

Prof. Dr. J.A.G. van Strijp  
Prof. Dr. F.G. Förster  
Dr. E.J.A.M. Sijts  
Prof. Dr. H. Ovaa  
Prof. Dr. I. Braakman

**Defense committee:**

Prof. Dr. F.G. Förster  
Dr. E.J.A.M. Sijts  
Prof. Dr. H. Ovaa  
Prof. Dr. A.S. Akhmanova  
Prof. Dr. R.J.L. Willems

**Paranymphs:**

F.R. van Diemen, MSc  
A.B.C. Schuren, MSc

# Contents

<b>Chapter 1</b>	<b>General introduction</b>	9
<b>Chapter 2</b>	<b>Viral immune evasion: lessons in MHC class I antigen presentation</b> Michael L. van de Weijer*, Rutger D. Luteijn*, Emmanuel J.H.J. Wiertz <i>Seminars in Immunology 27 (2015). doi:10.1016/j.smim.2015.03.010</i>	21
<b>Chapter 3</b>	<b>A high-coverage shRNA screen identifies TMEM129 as an E3 ligase involved in ER-associated protein degradation</b> Michael L. van de Weijer, Michael C. Bassik, Rutger D. Luteijn, Cornelia M. Voorburg, Mirjam A.M. Lohuis, Elisabeth Kremmer, Rob C. Hoeben, Emily M. LeProust, Siyuan Chen, Hanneke Hoelen, Maaïke E. Rensing, Weronika Patena, Jonathan S. Weissman, Michael T. McManus, Emmanuel J.H.J. Wiertz*, Robert Jan Lebbink* <i>Nature Communications 5 (2014) 3832. doi:10.1038/ncomms4832</i>	55
<b>Chapter 4</b>	<b>The E3 ubiquitin ligase TMEM129 is a tri-spanning transmembrane protein</b> Michael L. van de Weijer, Guus H. van Muijlwijk, Linda J. Visser, Ana I. Costa, Emmanuel J.H.J. Wiertz* and Robert Jan Lebbink* <i>Viruses 8 (2016). doi:10.3390/v8110309</i>	103
<b>Chapter 5</b>	<b>The p97-cofactor UBXD8 is essential for HCMV US11-mediated HLA class I degradation</b> Michael L. van de Weijer, Robert Jan Lebbink*, Emmanuel J.H.J. Wiertz* <i>Manuscript in preparation</i>	125
<b>Chapter 6</b>	<b>Multiple E2 ubiquitin-conjugating enzymes regulate immunoreceptor degradation by cytomegalovirus US2</b> Michael L. van de Weijer*, Anouk B.C. Schuren*, Dick J. van den Boomen, Arend Mulder, Frans H.J. Claas, Paul J. Lehner, Robert Jan Lebbink#, Emmanuel J.H.J. Wiertz# <i>Manuscript submitted</i>	143
<b>Chapter 7</b>	<b>Summarizing discussion</b>	171
<b>Addendum</b>	<b>Nederlandse samenvatting</b> <b>Dankwoord</b> <b>Curriculum Vitae</b>	183

\*, # These authors contributed equally to this work





# **CHAPTER 1**

## **General introduction**

Michael L. van de Weijer

## **An evolutionary arms race**

During millions of years, the evolutionary arms race between viruses and their hosts has resulted in mutual adaptation. The host has equipped itself with an extensive arsenal of antiviral mechanisms to defend itself against these intruders, while viruses have developed strategies to counter, evade and even exploit host immune responses. RNA viruses, such as myxoviruses, picornaviruses, and retroviruses, evade immune responses mostly through antigenic variation. This may be related due to their limited coding capacity. DNA viruses, such as poxviruses and herpesviruses, have a larger coding capacity and can afford to encode proteins dedicated to manipulating the hosts immune system.

Herpesviruses are large, enveloped double-stranded DNA (dsDNA) viruses belonging to the family of Herpesviridae, which can be further subdivided into  $\alpha$ -,  $\beta$ -, and  $\gamma$ -subfamilies based on their biological properties and nucleotide sequences. Nine herpesvirus types are known to infect humans: herpes simplex virus type 1 and 2 (HSV-1 and HSV-2, also known as human herpesvirus 1 and 2 (HHV-1 and HHV-2)); varicella-zoster virus (VZV; HHV-3); Epstein-Barr virus (EBV; HHV-4); human cytomegalovirus (HCMV; HHV-5); human herpesvirus 6A, 6B and 7 (HHV-6A, HHV-6B, and HHV-7); and Kaposi's sarcoma-associated herpesvirus (KSHV; HHV8) [1]. Herpesvirus infections are generally asymptomatic or cause only mild symptoms, but under certain conditions, complications may arise. For instance, HCMV infections in pregnant women can cause serious congenital disease to the developing child, and severe complications in immunocompromised individuals. EBV and KSHV infections are associated with the emergence of certain malignancies [2].

Herpesviruses are true masters of immune evasion, which is illustrated by the fact that a majority of the human population is infected for life with one or more herpesviruses. Virtually every single stage of innate and adaptive immune responses is targeted. Herpesviruses interfere with the host's cytokine and chemokine signaling [3], impair complement activation [4], and inhibit pathogen recognition receptor (PRRs) signaling [5]. To evade adaptive immune responses, herpesviruses manipulate MHC class I- and II-mediated antigen presentation [6] and prevent recognition and elimination of infected cells by natural killer (NK) cells [7]. In addition, herpesviruses are able to achieve a quiescent state called latency, during which viral gene expression is limited and, hence, the availability of viral antigens is greatly reduced. Ultimately, this prevents the detection by surveying CD8-positive cytotoxic T-lymphocytes (CD8<sup>+</sup> CTLs) and, consequently, hampers the eradication of the virus-infected cells [8].

## **Human cytomegalovirus – a master of immune evasion**

Human cytomegalovirus (HCMV) is a member of the  $\beta$ -herpesviridae and carries the largest dsDNA genome of the human herpesviruses [9]. HCMV is a common virus with a

seroprevalence of 40–100%, depending on the socioeconomic status of the host population. HCMV encodes multiple immunomodulatory proteins that facilitate interference with the host's immune system, thereby enabling HCMV to establish a lifelong infection [10–12]. The MHC-I antigen presentation pathway is a major target for immune-evasive strategies of HCMV, resulting in effective elusion of CD8<sup>+</sup> CTLs.

Most nucleated cells express MHC-I on their cell surface. MHC-I is a heterotrimeric complex consisting of  $\beta_2$ -microglobulin ( $\beta_2m$ ), MHC-I heavy chain (HC) and a variable peptide. MHC-I complex assembly is a highly specialized process that demands tight regulation by additional proteins. The MHC-I HC is a type I membrane protein that is co-translationally inserted into the ER-membrane. Once inserted, it associates with the ER-resident chaperones calnexin and BiP, which aid in correct folding of the HC. Upon engagement with  $\beta_2m$ , the  $\beta_2m$ -HC complex dissociates from calnexin and BiP, and interacts with calreticulin, ERp57, tapasin, and the transporter associated with antigen processing (TAP), which together form the MHC-I peptide-loading complex (PLC). The PLC promotes folding of MHC-I, stabilizes the complex, and facilitates efficient loading of peptides into the peptide binding groove of the  $\beta_2m$ -HC complex [13]. TAP transports cytosolic peptides into the ER, and thereby serves as the major provider of peptides loaded onto MHC-I molecules. After the formation of the trimeric complex of  $\beta_2m$ -HC and a high-affinity peptide, the complex dissociates from the PLC and travels through the Golgi-network to the cell surface. At the cell surface, MHC-I molecules are continuously surveyed by CD8<sup>+</sup> CTLs, which mount an immune response when the presented peptide is recognized by their T-cell receptor [14].

At least five unique short (US) regions in the HCMV genome are known to encode proteins that specifically interfere with the expression of MHC-I molecules [6]. US2 directs newly synthesized MHC-I HCs and various other immunoreceptors for proteasomal degradation in order to modulate cellular migration and immune signaling [15,16]. US3 retains newly synthesized MHC-I proteins in the ER and blocks tapasin-dependent peptide loading [17,18]. US6 interacts with the TAP complex and induces conformational changes of TAP that prevent ATP binding, thereby inhibiting TAP-mediated peptide translocation into the ER [19–22]. US10 specifically targets HLA-G molecules for degradation [23]. US11 causes proteasomal degradation of newly synthesized MHC-I HCs [16].

The aforementioned viral MHC-I inhibitors not only demonstrate how HCMV evades the immune system, but they also represent valuable tools to further dissect the MHC-I antigen presentation pathway. In addition, these viral MHC-I inhibitors have helped to unravel general cellular processes, including ER-associated protein degradation (ERAD). A more detailed discussion of the aforementioned and other viral immune evasion strategies and how they helped shape our current understanding of the MHC-I antigen presentation pathway is provided in **Chapter 2**.

## ER-associated protein degradation

Approximately one-third of the mammalian proteome consists of secreted and integral membrane proteins that insert into the ER co- or post-translationally. Folding failures may result in protein accumulation and aggregation, thereby compromising protein and cellular homeostasis. To maintain homeostasis, quality control systems in the ER ensure that newly-synthesized proteins fold properly. ER proteins that are terminally misfolded are targeted for degradation through ER-associated protein degradation (ERAD). In ERAD, ER-luminal or integral proteins are transported from the ER into the cytosol in a retrograde fashion (also known as retrotranslocation or dislocation) for degradation by the proteasome. At the center of the ERAD pathway lie multiprotein complexes that combine the functions essential to this process, namely substrate recognition, dislocation, ubiquitination, and degradation [24,25].

The ERAD pathway is not only responsible for degradation of terminally misfolded proteins, but it also regulates the expression level and processing of certain proteins. The list of sporadic and genetic human diseases associated with ERAD is constantly expanding, illustrating the importance of ERAD in protein and cellular homeostasis [26].

## Exploiting the exploiters

Under physiological conditions, only a minor fraction of newly-synthesized MHC-I molecules undergo ERAD due to a failure to either associate with  $\beta_2m$  or to be loaded with a peptide [27]. HCMV US2 and US11 hijack the ERAD pathway to force dislocation of newly synthesized MHC-I HCs for degradation by the proteasome [15,28] (**figure 1**). As such, US2 and US11 reduce the half-life of MHC-I to less than a minute. US2 and US11 have proven to be valuable models for studying MHC-I degradation in particular and mammalian ERAD in general. Especially US11 has been instrumental in the identification of key players in mammalian ERAD.

US2 and US11 are ER-localized type I membrane glycoproteins of respectively 199 and 215 amino acid residues in length [29,30]. While US2 and US11 both target MHC-I for degradation, they utilize distinct ERAD complexes (**see figure 2A vs 2B**). US11 uses Derlin-1 and the E3 ubiquitin ligase TMEM129 in cooperation with the E2 ubiquitin-conjugating enzymes UBE2J2 and UBE2K to dislocate MHC-I [31–34]. Interestingly, US2 does not depend on these proteins, but instead usurps the E3 ubiquitin ligase TRC8 and the E2 UBE2G2 to mediate MHC-I downregulation [35] (**see also Chapter 6**). On the cytosolic side, both US2 and US11 rely on the ATPase p97/VCP for extraction of MHC-I from the membrane [36,37]. While the E3 ubiquitin ligases TRC8 and TMEM129 are essential for MHC-I dislocation by US2 and US11 respectively, ERAD of endogenously misfolded HCs does not rely on either E3, but instead requires yet another E3 ubiquitin ligase, HRD1, that together with the E2-

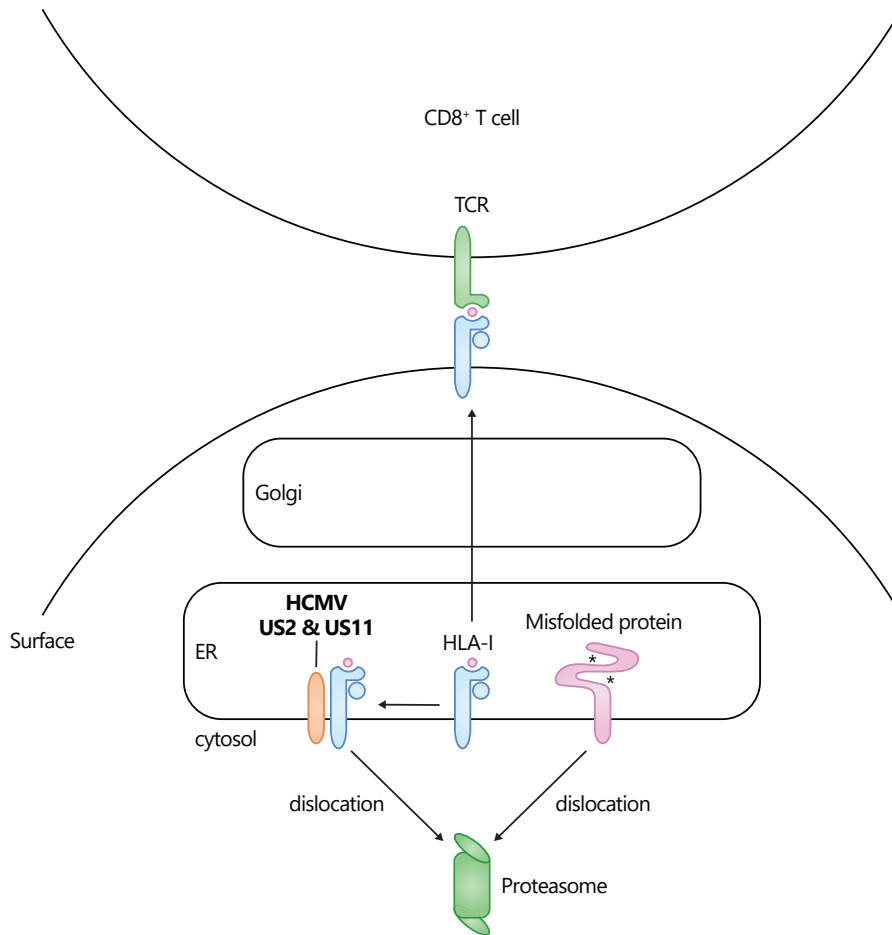


**Figure 1. MHC-I downregulation by HCMV US2 and US11.** Virtually all nucleated cells express MHC-I on their cell surface. MHC-I is a heterotrimeric complex consisting of  $\beta$ 2-microglobulin ( $\beta$ 2m), MHC-I heavy chain (HC) and a variable high-affinity peptide. After its formation, the complex dissociates and travels from the ER through the Golgi-network to the cell surface. At the cell surface, MHC-I molecules are continuously surveyed by CD8<sup>+</sup> CTLs, which mount an immune response when the presented peptide is recognized by their T-cell receptor. HCMV US2 and US11 hijack the ER-associated protein degradation (ERAD) pathway to force dislocation of newly synthesized MHC-I for degradation by the proteasome. Ultimately, this prevents the detection by surveying CD8<sup>+</sup> cytotoxic T-lymphocytes (CD8<sup>+</sup> CTLs) and, consequently, hampers the eradication of the virus-infected cells. Under physiological conditions, the ERAD pathway is responsible for degradation of terminally misfolded secretory proteins.

conjugating enzyme UBE2J1 catalyzes the ubiquitination of MHC-I HCs [38]. To facilitate the dislocation of the misfolded HCs, HRD1 forms a complex with Derlin-1 and p97, previously discovered in the context of US11 [38].

Thus, depending on its context, the dislocation of MHC-I HCs may be catalyzed by at least three different ERAD complexes containing different E3 ubiquitin ligases. This observation testifies to the versatility of ERAD and underscores the essential role E3 ubiquitin ligases play in regulating the dislocation of substrates into the cytosol for degradation by the ubiquitin-proteasome system.

## Scope of this thesis

Most of our current knowledge on ERAD stems from early studies performed in *Saccharomyces cerevisiae* [39]. This is related to the difficulty of gene manipulation in mammalian cells compared to yeast. In addition, the ERAD pathway in mammals is considerably more intricate than in yeast, probably because the ERAD pathway has seen a high diversification and specialization due to the emergence of complex life and the expansion of the proteome. While many of the findings in yeast can be translated to mammals due to the high conservation among eukaryotes, our current understanding of ERAD in mammalian cells is still far from complete.

Recent advances in mammalian gene manipulation have created new ways for extensive interrogation, such as the generation of lentivirus-based high-throughput whole-genome shRNA libraries for conducting RNAi screens [40]. Additionally, in early 2013, a groundbreaking new gene manipulation technique for use in mammalian cells emerged: CRISPR/Cas9-mediated genome engineering [41,42]. This technique utilizes the bacterial nuclease protein Cas9 in combination with a guide RNA (gRNA) to promote programmed editing of DNA within mammalian cells. By matching the gRNA sequence to a desired sequence present in the human genome, the Cas9 molecule can be programmed to cleave any given site in the human genome, thereby producing a double-stranded break (DSB). The DSB is recognized and repaired by the non-homologous end joining (NHEJ) system, but due to the error-prone nature of NHEJ, the introduction of mutations is inevitable. These mutations may result in gene disruption, ultimately producing a target gene knockout. The CRISPR/Cas9 genome-engineering technique was quickly adopted to efficiently produce gene knockouts and knockins, in both small and large scale setups. After a publication in early 2013, in which the CRISPR/Cas9-tool was first used to modify the mammalian genetic code, the amount of publications using this technique for gene editing has skyrocketed.

Herpesvirus immunoevasins not only demonstrate how viruses evade the immune system, but also represent valuable tools to further unravel the MHC-I antigen presentation pathway and general cellular processes, including ER-associated protein degradation. We decided to study mammalian ERAD using the HMCV immunoevasins US2 and US11 as a

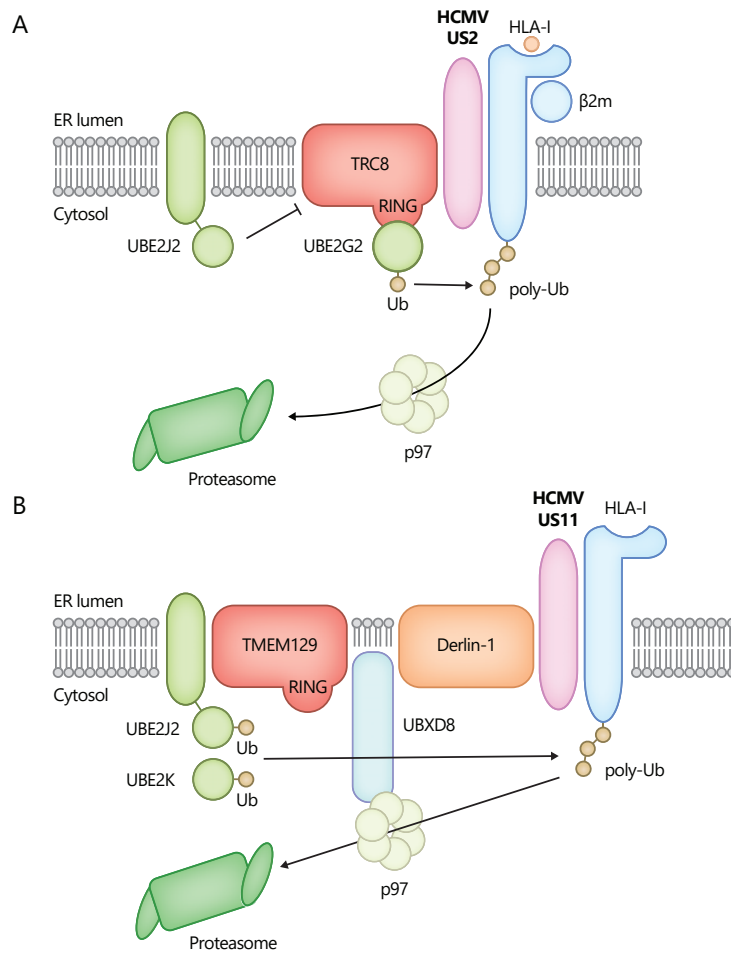


**Figure 2. Molecular model of the HCMV-induced degradation of MHC-I.** (A) The HCMV US2 protein engages newly-synthesized  $\beta$ 2m-associated MHC-I and directs it towards the E3 ubiquitin ligase TRC8. In conjunction with the E2 conjugating-enzyme UBE2G2, TRC8 catalyzes the ubiquitination of the HC. The resulting poly-ubiquitin chain signals for the extraction from the ER membrane by p97, after which the HC is degraded by the proteasome. In this context, UBE2J2 depletion increases TRC8 expression levels in the presence of US2, and in this way enhances US2-mediated HLA-I downregulation. (B) The HCMV US11 protein requires the TMEM129-Derlin-1 complex to dispose of the HCs. The MHC-I HC is ubiquitinated by the E3 TMEM129 in conjunction with the E2 enzymes UBE2J2 and UBE2K. UBE2J2 is proposed to nucleate the ubiquitin chain, while UBE2K probably is responsible for chain elongation. Eventually, the MHC I molecules are dislocated into the cytosol via p97 and degraded by the proteasome.

model; the latest RNAi library screening and CRISPR/Cas9 genome-engineering techniques were employed to identify novel players in MHC I degradation. In **Chapter 2**, we review the interactions of herpesviruses with the MHC-I antigen presentation pathway. In **Chapter 3**, we employ a pooled lentiviral genome-wide shRNA library to screen for host factors essential for US11-mediated MHC-I downregulation. We identify the previously uncharacterized protein TMEM129 as the elusive E3 ubiquitin ligase and UBE2J2 and UBE2K as the E2 ubiquitin-conjugating enzymes exploited by US11 (**figure 2B**). We also find evidence that TMEM129 might play a more general role in mammalian ERAD. In **Chapter 4**, we explore the topology of TMEM129. Many of the E3 proteins involved in ERAD are multi-spanning transmembrane proteins. We show that TMEM129 is an ER-localized tri-spanning transmembrane protein with a C-terminal cytosolic RING domain. In **Chapter 5**, we generate a CRISPR/Cas9 library focused on known human p97 co-factors to find the ones that are essential for US11-mediated MHC-I degradation. We identify UBXD8 as a p97 co-factor that is essential for MHC-I degradation by US11 (**figure 2B**). In **Chapter 6**, we establish a CRISPR/Cas9 library targeting all known E2 ubiquitin-conjugating enzymes. Using this library, we screen for E2 enzymes essential for US2-induced degradation of MHC-I. We identify UBE2G2 as an E2 ubiquitin-conjugating enzyme that is critically involved in US2-mediated MHC-I degradation. Surprisingly, we find UBE2J2 to counteract degradation of MHC-I by US2 (**figure 2A**). **Chapter 7** summarizes the findings of this thesis and discusses the potential of combining various cutting-edge techniques to study mammalian ERAD.

## References

- [1] A. Arvin, G. Campadelli-Fiume, E. Mocarski, P.S. Moore, B. Roizman, R. Whitley, K. Yamanishi, *Human Herpesviruses*, Cambridge University Press, 2007. <http://www.ncbi.nlm.nih.gov/pubmed/21348071> (accessed January 10, 2017).
- [2] P. Griffiths, I. Baraniak, M. Reeves, The pathogenesis of human cytomegalovirus., *J. Pathol.* 235 (2015) 288–97. doi:10.1002/path.4437.
- [3] A. Alcamí, Viral mimicry of cytokines, chemokines and their receptors, *Nat. Rev. Immunol.* 3 (2003) 36–50. doi:10.1038/nri980.
- [4] J.D. Lambris, D. Ricklin, B. V. Geisbrecht, Complement evasion by human pathogens, *Nat. Rev. Microbiol.* 6 (2008) 132–142. doi:10.1038/nrmicro1824.
- [5] A.G. Bowie, L. Unterholzner, Viral evasion and subversion of pattern-recognition receptor signalling., *Nat. Rev. Immunol.* 8 (2008) 911–22. doi:10.1038/nri2436.
- [6] M.L.M.L. van de Weijer, R.D.R.D. Luteijn, E.J.H.J.E.J.H.J. Wiertz, Viral immune evasion: Lessons in MHC class I antigen presentation., *Semin. Immunol.* 27 (2015) 125–37. doi:10.1016/j.smim.2015.03.010.
- [7] L.L. Lanier, Evolutionary struggles between NK cells and viruses, *Nat. Rev. Immunol.* 8 (2008) 259–268. doi:10.1038/nri2276.
- [8] B.D. Griffin, M.C. Verweij, E.J.H.J. Wiertz, Herpesviruses and immunity: the art of evasion., *Vet. Microbiol.* 143 (2010) 89–100. doi:10.1016/j.vetmic.2010.02.017.
- [9] D.J. McGeoch, F.J. Rixon, A.J. Davison, Topics in herpesvirus genomics and evolution, *Virus Res.* 117 (2006) 90–104. doi:10.1016/j.virusres.2006.01.002.



- [10] W. Dunn, C. Chou, H. Li, R. Hai, D. Patterson, V. Stolc, H. Zhu, F. Liu, Functional profiling of a human cytomegalovirus genome., *Proc. Natl. Acad. Sci. U. S. A.* 100 (2003) 14223–8. doi:10.1073/pnas.2334032100.
- [11] E.S. Mocarski, Immunomodulation by cytomegaloviruses: manipulative strategies beyond evasion., *Trends Microbiol.* 10 (2002) 332–9. <http://www.ncbi.nlm.nih.gov/pubmed/12110212> (accessed January 17, 2016).
- [12] S.G. Hansen, C.J. Powers, R. Richards, A.B. Ventura, J.C. Ford, D. Siess, M.K. Axthelm, J.A. Nelson, M.A. Jarvis, L.J. Picker, K. Früh, Evasion of CD8+ T cells is critical for superinfection by cytomegalovirus., *Science.* 328 (2010) 102-6. doi:10.1126/science.1185350.
- [13] B. Sadasivan, P.J. Lehner, B. Ortmann, T. Spies, P. Cresswell, Roles for calreticulin and a novel glycoprotein, tapasin, in the interaction of MHC class I molecules with TAP., *Immunity.* 5 (1996) 103–14. <http://www.ncbi.nlm.nih.gov/pubmed/8769474> (accessed October 28, 2014).
- [14] A. Van Hateren, E. James, A. Bailey, A. Phillips, N. Dalchau, T. Elliott, The cell biology of major histocompatibility complex class I assembly: towards a molecular understanding., *Tissue Antigens.* 76 (2010) 259–75. doi:10.1111/j.1399-0039.2010.01550.x.
- [15] E.J. Wiertz, D. Tortorella, M. Bogyo, J. Yu, W. Mothes, T.R. Jones, T.A. Rapoport, H.L. Ploegh, Sec61-mediated transfer of a membrane protein from the endoplasmic reticulum to the proteasome for destruction., *Nature.* 384 (1996) 432–8. doi:10.1038/384432a0.
- [16] J.-L. Hsu, D.J.H. van den Boomen, P. Tomasec, M.P. Weekes, R. Antrobus, R.J. Stanton, E. Ruckova, D. Sugrue, G.S. Wilkie, A.J. Davison, G.W.G. Wilkinson, P.J. Lehner, Plasma membrane profiling defines an expanded class of cell surface proteins selectively targeted for degradation by HCMV US2 in cooperation with UL141., *PLoS Pathog.* 11 (2015) e1004811. doi:10.1371/journal.ppat.1004811.
- [17] T.R. Jones, E.J. Wiertz, L. Sun, K.N. Fish, J.A. Nelson, H.L. Ploegh, Human cytomegalovirus US3 impairs transport and maturation of major histocompatibility complex class I heavy chains., *Proc. Natl. Acad. Sci. U. S. A.* 93 (1996) 11327–33. <http://www.pubmedcentral.nih.gov/articlerender.fcgi?artid=38057&tool=pmcentrez&rendertype=abstract> (accessed October 30, 2014).
- [18] B. Park, Y. Kim, J. Shin, S. Lee, K. Cho, K. Früh, S. Lee, K. Ahn, Human cytomegalovirus inhibits tapasin-dependent peptide loading and optimization of the MHC class I peptide cargo for immune evasion., *Immunity.* 20 (2004) 71-85. <http://www.ncbi.nlm.nih.gov/pubmed/14738766> (accessed October 30, 2014).
- [19] K. Ahn, A. Gruhler, B. Galocha, T.R. Jones, E.J. Wiertz, H.L. Ploegh, P.A. Peterson, Y. Yang, K. Früh, The ER-luminal domain of the HCMV glycoprotein US6 inhibits peptide translocation by TAP., *Immunity.* 6 (1997) 613-21. <http://www.ncbi.nlm.nih.gov/pubmed/9175839> (accessed February 10, 2015).
- [20] H. Hengel, J.O. Koopmann, T. Flohr, W. Muranyi, E. Goulmy, G.J. Hämmerling, U.H. Koszinowski, F. Momburg, A viral ER-resident glycoprotein inactivates the MHC-encoded peptide transporter., *Immunity.* 6 (1997) 623-32. <http://www.ncbi.nlm.nih.gov/pubmed/9175840> (accessed February 10, 2015).
- [21] P.J. Lehner, J.T. Karttunen, G.W. Wilkinson, P. Cresswell, The human cytomegalovirus US6 glycoprotein inhibits transporter associated with antigen processing-dependent peptide translocation., *Proc. Natl. Acad. Sci. U.S.A.* 94 (1997) 6904–9. <http://www.pubmedcentral.nih.gov/articlerender.fcgi?artid=21257&tool=pmcentrez&rendertype=abstract> (accessed February 10, 2015).
- [22] E.W. Hewitt, S.S. Gupta, P.J. Lehner, The human cytomegalovirus gene product US6 inhibits ATP binding by TAP., *EMBO J.* 20 (2001) 387–96. doi:10.1093/emboj/20.3.387.
- [23] B. Park, E. Spooner, B.L. Houser, J.L. Strominger, H.L. Ploegh, The HCMV membrane glycoprotein US10 selectively targets HLA-G for degradation., *J. Exp. Med.* 207 (2010) 2033–41. doi:10.1084/jem.20091793.
- [24] J.A. Olzmann, R.R. Kopito, J.C. Christianson, The mammalian endoplasmic reticulum-associated degradation system., *Cold Spring Harb. Perspect. Biol.* 5 (2013). doi:10.1101/cshperspect.a013185.
- [25] J.C. Christianson, J. a Olzmann, T. a Shaler, M.E. Sowa, E.J. Bennett, C.M. Richter, R.E. Tyler, E.J. Greenblatt, J.W. Harper, R.R. Kopito, Defining human ERAD networks through an integrative mapping strategy., *Nat. Cell Biol.* 14 (2011) 93–105. doi:10.1038/ncb2383.

- [26] M. Aridor, Visiting the ER: The endoplasmic reticulum as a target for therapeutics in traffic related diseases, *Adv. Drug Deliv. Rev.* 59 (2007) 759–781. doi:10.1016/j.addr.2007.06.002.
- [27] E.A. Hughes, C. Hammond, P. Cresswell, Misfolded major histocompatibility complex class I heavy chains are translocated into the cytoplasm and degraded by the proteasome., *Proc. Natl. Acad. Sci. U.S.A.* 94(1997)1896–901. <http://www.pubmedcentral.nih.gov/articlerender.fcgi?artid=20014&tool=pmcentrez&rendertype=abstract> (accessed October 30, 2014).
- [28] E.J. Wiertz, T.R. Jones, L. Sun, M. Bogoy, H.J. Geuze, H.L. Ploegh, The human cytomegalovirus US11 gene product dislocates MHC class I heavy chains from the endoplasmic reticulum to the cytosol., *Cell.* 84 (1996) 769–79. <http://www.ncbi.nlm.nih.gov/pubmed/8625414> (accessed October 30, 2014).
- [29] a Rehm, P. Stern, H.L. Ploegh, D. Tortorella, Signal peptide cleavage of a type I membrane protein, HCMV US11, is dependent on its membrane anchor., *EMBO J.* 20 (2001) 1573–82. doi:10.1093/emboj/20.7.1573.
- [30] B.E. Gewurz, H.L. Ploegh, D. Tortorella, US2, a human cytomegalovirus-encoded type I membrane protein, contains a non-cleavable amino-terminal signal peptide., *J. Biol. Chem.* 277 (2002) 11306–13. doi:10.1074/jbc.M107904200.
- [31] B.N. Lilley, H.L. Ploegh, A membrane protein required for dislocation of misfolded proteins from the ER., *Nature.* 429 (2004) 834–40. doi:10.1038/nature02592.
- [32] M.L.M.L. Van De Weijer, M.C. Bassik, R.D.R.D. Luteijn, C.M.C.M. Voorburg, M.A.M.A.M. Lohuis, E. Kremmer, R.C.R.C. Hoeben, E.M.E.M. Leproust, S. Chen, H. Hoelen, M.E.M.E. Rensing, W. Patena, J.S.J.S. Weissman, M.T.M.T. McManus, E.J.H.J.E.J.H.J. Wiertz, R.J.R.J. Lebbink, A high-coverage shRNA screen identifies TMEM129 as an E3 ligase involved in ER-associated protein degradation., *Nat. Commun.* 5 (2014) 3832. doi:10.1038/ncomms4832.
- [33] D.J.H. van den Boomen, R.T. Timms, G.L. Grice, H.R. Stagg, K. Skødt, G. Dougan, J.A. Nathan, P.J. Lehner, TMEM129 is a Derlin-1 associated ERAD E3 ligase essential for virus-induced degradation of MHC-I., *Proc. Natl. Acad. Sci. U. S. A.* 111 (2014) 11425-30. doi:10.1073/pnas.1409099111.
- [34] D. Flierman, C.S. Coleman, C.M. Pickart, T.A. Rapoport, V. Chau, E2-25K mediates US11-triggered retrotranslocation of MHC class I heavy chains in a permeabilized cell system., *Proc. Natl. Acad. Sci. U. S. A.* 103 (2006) 11589–94. doi:10.1073/pnas.0605215103.
- [35] H.R. Stagg, M. Thomas, D. van den Boomen, E.J.H.J. Wiertz, H. a Drabkin, R.M. Gemmill, P.J. Lehner, The TRC8 E3 ligase ubiquitinates MHC class I molecules before dislocation from the ER., *J. Cell Biol.* 186 (2009) 685–92. doi:10.1083/jcb.200906110.
- [36] Y. Ye, Y. Shibata, M. Kikkert, S. van Voorden, E. Wiertz, T.A. Rapoport, Recruitment of the p97 ATPase and ubiquitin ligases to the site of retrotranslocation at the endoplasmic reticulum membrane., *Proc. Natl. Acad. Sci. U. S. A.* 102 (2005) 14132–8. doi:10.1073/pnas.0505006102.
- [37] N. Soetandyo, Y. Ye, The p97 ATPase dislocates MHC class I heavy chain in US2-expressing cells via a Ufd1-Npl4-independent mechanism., *J. Biol. Chem.* 285 (2010) 32352–9. doi:10.1074/jbc.M110.131649.
- [38] M.L. Burr, F. Cano, S. Svobodova, L.H. Boyle, J.M. Boname, P.J. Lehner, HRD1 and UBE2J1 target misfolded MHC class I heavy chains for endoplasmic reticulum-associated degradation., *Proc. Natl. Acad. Sci. U. S. A.* 108 (2011) 2034–9. doi:10.1073/pnas.1016229108.
- [39] P.G. Needham, J.L. Brodsky, How early studies on secreted and membrane protein quality control gave rise to the ER associated degradation (ERAD) pathway: the early history of ERAD., *Biochim. Biophys. Acta.* 1833 (2013) 2447–57. doi:10.1016/j.bbamcr.2013.03.018.
- [40] M.C. Bassik, R.J. Lebbink, L.S. Churchman, N.T. Ingolia, W. Patena, E.M. LeProust, M. Schuldiner, J.S. Weissman, M.T. McManus, Rapid creation and quantitative monitoring of high coverage shRNA libraries., *Nat. Methods.* 6 (2009) 443–5. doi:10.1038/nmeth.1330.
- [41] L. Cong, F.A. Ran, D. Cox, S. Lin, R. Barretto, N. Habib, P.D. Hsu, X. Wu, W. Jiang, L.A. Marraffini, F. Zhang, Multiplex genome engineering using CRISPR/Cas systems., *Science* (80-. ). 339 (2013) 819–23. doi:10.1126/

science.1231143.

- [42] M. Jinek, A. East, A. Cheng, S. Lin, E. Ma, J. Doudna, RNA-programmed genome editing in human cells., *Elife*. 2 (2013) e00471. doi:10.7554/eLife.00471.

1



## CHAPTER 2

# Viral immune evasion: lessons in MHC class I antigen presentation

Michael L. van de Weijer\*, Rutger D. Luteijn\*, Emmanuel J.H.J. Wiertz

Medical Microbiology, University Medical Center Utrecht, 3584CX Utrecht, The Netherlands

\*These authors contributed equally to this work

Published in:  
Seminars in Immunology 27 (2015). doi:10.1016/j.smim.2015.03.010

## **ABSTRACT**

The MHC class I antigen presentation pathway enables cells infected with intracellular pathogens to signal the presence of the invader to the immune system. Cytotoxic T lymphocytes are able to eliminate the infected cells through recognition of pathogen-derived peptides presented by MHC class I molecules at the cell surface. In the course of evolution, many viruses have acquired inhibitors that target essential stages of the MHC class I antigen presentation pathway. Studies on these immune evasion proteins reveal fascinating strategies used by viruses to elude the immune system. Viral immunoevasins also constitute great research tools that facilitate functional studies on the MHC class I antigen presentation pathway, allowing the investigation of less well understood routes, such as TAP-independent antigen presentation and cross-presentation of exogenous proteins. Viral immunoevasins have also helped to unravel more general cellular processes. For instance, basic principles of ER-associated protein degradation via the ubiquitin-proteasome pathway have been resolved using virus-induced degradation of MHC class I as a model. This review highlights how viral immunoevasins have increased our understanding of MHC class I-restricted antigen presentation.

## 1. MHC class I antigen presentation

Virtually all nucleated cells express major histocompatibility complex class I molecules (MHC I) on their cell surface. The heterotrimeric MHC I complex consists of  $\beta_2$ -microglobulin ( $\beta_2m$ ), the MHC I heavy chain (HC) and a variable peptide. This peptide is usually generated within the cell by degradation of endogenously expressed proteins. The resulting peptides are loaded into the peptide binding groove of the MHC I HC -  $\beta_2m$  heterodimer. At the cell surface, MHC I molecules are continuously surveyed by CD8<sup>+</sup> cytotoxic T cells (CTLs), which mount an immune response when the presented peptide is recognized by the T-cell receptor.

MHC I assembly is a highly specialized process that demands tight regulation by additional proteins. The MHC I HC is a type I membrane protein that is co-translationally inserted into the ER-membrane. Once inserted, it associates with the ER-resident chaperones calnexin and BiP, which aid in correct folding of the HC. Upon engagement with  $\beta_2m$ , the  $\beta_2m$ /HC complex dissociates from calnexin and BiP and interacts with calreticulin, ERp57, tapasin, and the transporter associated with antigen processing (TAP), which together form the MHC I class I peptide-loading complex (PLC) (**figure 1A**). The PLC promotes folding of MHC I, stabilizes the complex, and facilitates efficient loading of peptides into the binding groove of the  $\beta_2m$ /HC complex [1]. TAP transports cytosolic peptides into the ER, thus serving as the major source of peptides loaded onto MHC I molecules. After the formation of the trimeric complex of  $\beta_2m$ /HC and a high-affinity peptide, the complex dissociates from the PLC and travels through the Golgi-network to the cell surface, where it presents its cargo to CD8<sup>+</sup> CTLs.

Viral inhibitors of the MHC I antigen presentation pathway have greatly advanced our understanding of this important arm of the adaptive immune system. This is illustrated by the discovery of the adenovirus 5 protein E3-19K, the first specific viral inhibitor of MHC I antigen presentation [2]. At the time, the location of MHC I peptide loading was still elusive. Using E3-19K, it was shown that retention of MHC I in the ER prevents antigen presentation of newly synthesized peptides, thereby stressing the central role of this compartment in MHC I processing [3]. Since the discovery of E3-19K, many different viral MHC I inhibitors have been identified that together target virtually every single step within the MHC I antigen presentation pathway (**table 1**). These inhibitors not only demonstrate how viruses evade the immune system, but also represent great tools to further dissect MHC I antigen presentation, including less common PLC-independent antigen presentation pathways and cross-presentation of exogenous proteins. In addition, viral MHC I inhibitors have helped unraveling more general cellular processes, including ER-associated degradation of proteins via the ubiquitin-proteasome pathway.

**Table 1. Overview of known viral immunoevasins that target the MHC class I antigen presentation pathway.**

Virus name or family	Viral protein	Effects	Refs
$\alpha$ -herpesvirus (HSV, BHV-1, PRV)	UL41/vhs	Inhibits MHC I and pro-inflammatory cytokine synthesis through host shutoff	[166]
Varicellovirus (BHV-1; EHV-1/4; PRV)	UL49.5	Induces conformational arrest of TAP. BHV: also induces conformational arrest and degradation of TAP. EHV: also blocks ATP binding to TAP	[48–50]
HSV-1/2	ICP47	Binds and blocks peptide binding site of TAP	[38,39]
VZV	ORF66	Retains mature MHC I complexes in the ERGIC	[167,168]
EBV	EBNA1	Resists proteasomal degradation	[10–16]
	BNLF2a	Blocks both peptide and ATP binding to TAP	[51]
	BGLF5	Inhibits MHC I synthesis through host shutoff	[169,170]
	BILF1	Causes MHC I internalization and lysosomal degradation	[171]
hCMV	US2/gp24	Targets MHC I for ERAD	[87]
	US3/gp23	Binds tapasin and inhibits tapasin-dep. peptide loading	[66,67]
	US6/gp21	Prevents ATP binding by inducing conformational changes in TAP	[43–46]
	US10	Causes non-classical MHC I (MHC I-G) degradation	[172]
	US11/gp33	Targets MHC I for ERAD	[88]
mCMV	m4/gp34	Binds MHC I at the cell surface, thereby decreasing NK cell-mediated lysis and recognition of peptide-loaded MHC I complexes by CTLs	[173,174]
	m6/gp48	Targets MHC I to lysosomes, thereby decreasing cell-surface expression of MHC I molecules	[175]
	m27	Inhibitor of IFN- $\gamma$ signaling, thereby blocking immunoproteasome formation	[176]
	m152/gp40	Causes MHC I retention in the ERGIC, thereby downregulating cell-surface MHC I molecules	[177]
RhCMV	rh178/VIHCE	Inhibits MHC I HC translation in a signal peptide-dependent manner	[5,6]
HHV-6/7	U21	Reroutes MHC I to lysosomes for degradation	[178–182]
KSHV	LANA1	Resists proteasomal degradation	[18,19]
	ORF37/SOX	Inhibits MHC I and pro-inflammatory cytokine production through host shutoff	[183,184]
	kk3/MIR1	Ubiquitinates MHC I for internalization & lysosomal degradation	[120,121]
	kk5/MIR2		
MHV-68	mK3	Ubiquitinates MHC I HCs for ERAD	[102,103,108]
Cowpoxvirus	CPXV012	Prevents peptide transport by inhibiting ATP binding to TAP	[34–37]
	CPXV203	Retains MHC I in the ER	[35,114]
Adenovirus	E3-19K	Retains MHC I in the ER	[2,3]



## 2. MHC I insertion into the ER

Like other type I transmembrane (TM) proteins, the MHC I HC is inserted into the ER co-translationally. This process is guided by an N-terminal signal sequence. Upon translation, the signal peptide binds to the cytosolic signal-recognition particle (SRP). This event temporarily stalls the translation process of the HC and allows binding to the SRP receptor. This interaction mediates the delivery of the ribosome and the nascent HC to the Sec61 translocation complex, which co-translationally integrates the HC into the ER membrane (for a recent review of this process see [4]).

The signal peptide of the polymorphic MHC I HC is highly homologous between haplotypes and conserved among species. Therefore, this sequence is an ideal target for viral immunoevasins. The rhesus CMV protein Rh178 specifically blocks the translation of the HC in a signal peptide-dependent manner. Although the HC mRNA engages with the ribosome and translation is initiated, full-length HC molecules are absent in cells expressing Rh178. The mechanism of inhibition is unclear, but Rh178 is suggested to interfere with chain elongation prior to engagement of the HC with the Sec61 translocon. Likely, Rh178 inhibits proper functioning of the SRP or the SRP receptor [5,6]. Future studies on Rh178 may help to further establish the mechanism by which TM proteins are inserted into the ER membrane, a process that is still incompletely understood [4].

## 3. Proteasomal generation of antigenic peptides

The majority of the peptides presented via MHC I is derived from ubiquitinated proteins degraded by the 26S proteasome. This large cylindrical complex of 2 MDa is composed of a 20S core unit and two 19S caps. The 19S caps recognize ubiquitinated substrates and partially unfold proteins to allow them to access the 20S core. The 20S complex contains six proteolytic sites with distinct protease activities that cleave the substrate after large hydrophobic, basic, or acidic amino acid residues. Peptides released by the proteasome can be processed further for presentation via MHC I molecules [7]. In addition to the central role of the proteasome in the MHC I antigen presentation pathway, its activity is crucial for cellular homeostasis. Inhibition of the proteasome by *e.g.* chemical compounds will ultimately lead to apoptosis. While general, *in trans* inhibition of the proteasome will therefore be detrimental for the cell, viral evasion mechanisms have been found that act *in cis*, preventing the specific generation of viral epitopes by the proteasome.

The Epstein-Barr virus (EBV) nuclear antigen-1 (EBNA-1) is essential for the persistence of the viral episome and for distribution of viral genomes to daughter cells upon cell division [8]. EBNA-1 is expressed during latent EBV infections and is found in all EBV-associated tumors, thereby making it an ideal target for CD8<sup>+</sup> T cell immunity. Initial studies showed that CD8<sup>+</sup> T cell responses against EBNA-1 cannot be detected *in vitro*, despite the presence

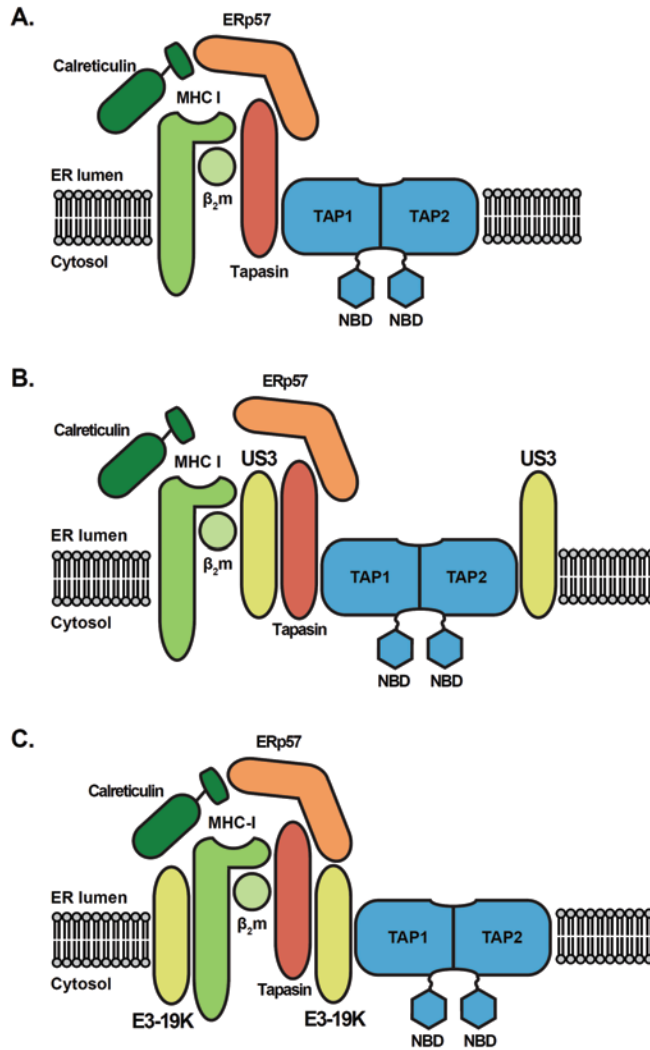


**Figure 1. The immune evasion proteins HCMV US3 and adenovirus E3-19K interfere with MHC I peptide loading and egress of MHC I from the ER.** (A) Components of the PLC. The peptide transporter TAP consists of the subunits TAP1 and TAP2; the conformational transitions of TAP that facilitate the translocation of peptides over the ER membrane are energized by the hydrolysis of ATP at the nucleotide binding domains (NBDs) of the TAP complex. The outer helices serve as a docking platform for tapasin, which also binds ERp57 and MHC I HC. The tapasin-ERp57 complex stabilizes peptide-receptive  $\beta_2m$ -HC dimers and promotes the binding of high-affinity peptides to the HC peptide-binding groove, a process that is also known as peptide-editing. Calreticulin further stabilizes the  $\beta_2m$ -HC complex until high-affinity peptide is loaded. (B and C) The immune evasion proteins HCMV US3 (B) and adenovirus E3-19K (C) interact with different components of the PLC. (B) US3 can bind to tapasin, TAP, and MHC I independently and disturbs the peptide-editing function of tapasin and ERp57. (C) E3-19K binds to MHC I independently of its interaction with TAP and tapasin. E3-19K retains MHC I in the ER. In addition, E3-19K can bind to TAP and tapasin, thereby interfering with the interaction between tapasin and MHC I.

of EBNA-1-specific CD8<sup>+</sup> T cells in EBV seropositive healthy individuals [9]. This paradox may be explained by the resistance of EBNA-1 to proteasomal degradation. This resistance was pinpointed to a Gly-Ala repeat of variable length within the central region of EBNA-1. When this repeat was coupled to other proteins, it served as a *cis*-acting inhibitory signal for proteasomal degradation [7,10,11]. The Gly-Ala repeats did not prevent ubiquitination of proteins, nor their targeting to the proteasome, but disturbed the subsequent interaction with the proteasome [12]. The mechanism of this disturbance is unclear. The Gly-Ala repeat may interfere with recognition of the ubiquitinated protein by the 19S caps [12], or it may impair the unfolding of the substrate by the 19S caps, thereby preventing access of the substrate to the 20S catalytic core of the proteasome [13].

Although initial studies failed to identify CD8<sup>+</sup> T cell responses against endogenously processed EBNA-1, later studies revealed that such responses do exist, suggesting that EBNA-1 epitopes can indeed be presented via MHC I [14–16]. These epitopes may be derived from defective ribosomal products. Prematurely abrogated EBNA-1 translation products may not contain the Gly-Ala repeat and may therefore be processed by the proteasome, resulting in presentation of EBNA-1-derived epitopes at the cell surface. Alternatively, debris of EBV-infected cells may be endocytosed by dendritic cells (DCs) and may serve as a source of peptides presented to CD8<sup>+</sup> CTLs in the context of MHC I. This cross-presentation of antigen may facilitate the induction of a primary CTL response against viral antigens, including EBNA-1 (discussed in more detail below).

Kaposi's sarcoma-associated herpesvirus (KSHV) expresses the latency-associated nuclear antigen-1 (LANA-1) during latency. Like EBNA-1, LANA-1 is essential for preserving the viral genome in daughter cells upon cell division [17]. LANA-1 has a central repeat region composed of glutamine, glutamate and aspartate residues. Comparable to the Gly-Ala repeat of EBNA-1, the repeat region of LANA-1 prevents degradation of the viral protein by the proteasome *in cis*. Coupling of this region to other proteins interfered with their proteasomal degradation and diminished their antigenic potential [18,19]. The ability to couple the repeat regions to other proteins to prevent their degradation may be utilized for clinical applications. Accelerated proteasomal breakdown of the tumor suppressor protein p53 has been associated with tumor development. To prevent breakdown and increase stability of p53, a chimera has been constructed containing the EBNA-1 Gly-Ala repeat. This chimera has an increased stability in tumor cells and reduces tumor cell growth [20].

Viral gene therapy vectors have been developed that lack all viral protein-coding regions, to avoid undesired immune responses against the viral vector [21]. However, the transgenic content of these vectors may still elicit an immune response. Gly-Ala repeats may be exploited to limit the immunogenicity of the proteins expressed by lentiviral and adenoviral gene therapy vectors, and thereby prolong the expression of the transgenic products. Insertion of the Gly-Ala repeat into proteins expressed by these viral vectors indeed lowers recognition by CD8<sup>+</sup> T cells *in vitro* [22–26]. In mouse models, survival of cells

expressing Gly-Ala-containing chimeric proteins was improved compared to cells expressing the wild-type proteins alone, suggesting that these cells were protected from CD8<sup>+</sup> T cell-mediated destruction [23–25]. These findings highlight the potential applications of *in cis*-acting immunoevasins for the protection of transgenes from the immune system.

#### 4. TAP-dependent MHC I peptide loading

The vast majority of peptides presented by MHC I are derived from proteins degraded in the cytosol [7]. These peptides have to cross the ER membrane to gain access to the peptide binding groove of newly synthesized MHC I molecules. The peptides are translocated over the ER membrane by a dedicated peptide pump, the transporter associated with antigen processing, TAP. This heterodimeric ATP-binding cassette (ABC) transporter consists of the subunits TAP1 and TAP2. Both subunits encode a C-terminal nucleotide-binding domain (NBD) and an N-terminal transmembrane domain that includes 10 (for TAP1) or 9 (for TAP2) transmembrane helices [27,28]. These transmembrane helices intertwine and form a channel in the ER membrane. At the cytosolic side of the channel, a peptide-binding pocket is formed that can accommodate peptides of 8-16 amino acid residues in length [29]. The transport of peptides into the ER is energized by ATP binding and hydrolysis at the NBDs of TAP. TAP-mediated peptide transport is a multistep process that starts with the association of peptides to the peptide-binding domain and ATP binding at the NBDs. The binding of both peptide and ATP causes conformational changes that result in translocation of the peptide over the ER membrane. Finally, ATP hydrolysis at the NBDs rearranges TAP to allow a new cycle of peptide transport [29].

The dominant role of TAP-mediated peptide transport in MHC I antigen presentation is demonstrated in cell lines that lack a functional TAP complex. MHC I surface expression is strongly reduced on these cells [30,31], allowing these cells to escape from T cell recognition [32,33]. The essential contribution of TAP to MHC I antigen presentation makes TAP an ideal target for viral immune evasion strategies. Indeed, several viruses encode gene products that specifically interfere with peptide transport by TAP. TAP inhibitors have been found in all three herpesvirus subfamilies. Recently, certain cowpoxvirus strains have also been shown to inhibit TAP-mediated peptide transport [34–37]. The identification of these TAP inhibitors has not only revealed how viruses elude the immune system, but has also helped to unravel the mechanism of TAP-mediated peptide transport, as all viral immunoevasins target TAP at distinct steps during the peptide translocation cycle (**figure 2A**).

The cytosolic Infected Cell Protein 47 (ICP47) encoded by herpes simplex virus (HSV)-1 and HSV-2 inhibits peptide transport by blocking peptide binding to TAP [38–41]. As ATP-binding to TAP remains unaffected, this finding illustrates that the binding of peptide and ATP to TAP are two independent processes. However, ATP hydrolysis is prevented in the presence of ICP47, showing that peptide binding to TAP is crucial for ATP hydrolysis [42] (**figure 2B**).

The human cytomegalovirus (HCMV) encodes the TAP inhibitor US6 [43–45]. This ER-resident type I TM protein does not affect peptide binding, but rather blocks ATP binding to the cytosolic NBDs of TAP1 [46]. As the active domain of US6 binds to the ER luminal loops of TAP, inhibition of cytosolic ATP binding by US6 must be mediated by allosteric regulation across the ER membrane. This suggests that US6 locks TAP in a translocation-incompetent conformation [46]. In line with this, US6 influences the lateral mobility of TAP in the ER membrane, which is indicative of conformational alterations of the transporter complex [47] (**figure 2C**).

In many varicelloviruses, TAP-mediated peptide transport is blocked by UL49.5 [48–50]. This type I TM protein inhibits peptide transport by arresting TAP in a translocation-incompetent conformation. Peptide and ATP binding still take place, suggesting that conformational changes of TAP following the initial steps in the transport process are blocked by UL49.5 [48]. In addition to this effect, UL49.5 of bovine herpes virus (BHV)-1, BHV-5, bubaline herpesvirus 1, and cervid herpesvirus 1 induce proteasomal degradation of both TAP subunits [50]. The UL49.5 proteins of equine herpes virus (EHV)-1 and EHV-5 do not cause degradation of TAP, but instead block ATP binding to TAP [49] (**figure 2D-E**).

EBV encodes a TAP inhibitor, BNLF2a, during the replicative phase of its life cycle [51]. This membrane protein lacks a conventional signal sequence, but is inserted into the ER membrane post-translationally through a hydrophobic C-terminal tail-anchor. BNLF2a interacts with cytosolic domains of TAP and blocks both peptide and ATP binding, thereby preventing conformational rearrangements that normally follow peptide binding [52,53] (**figure 2F**).

Several cowpox virus strains encode a TAP inhibitor as well, namely CPXV012. So far, CPXV012 is the only TAP inhibitor identified outside the herpesvirus family [34,35]. CPXV012 is a type II TM protein that binds to TAP via its ER-luminal domains. CPXV012 blocks ATP binding to the NBDs of TAP without affecting peptide binding [36,37]. As for US6, the localization of the functional domain of CPXV012 within the ER excludes a direct interaction between this domain and the NBDs of TAP. Therefore, distal allosteric effects induced by CPXV012 likely result in NBD rearrangements that are incompatible with ATP binding [36] (**figure 2G**).

The common denominator between these TAP inhibitors is their ability to impede the structural rearrangements of TAP that are essential for its function as a peptide transporter. At the same time, the expression of TAP inhibitors by so many viruses testifies to the importance of MHC I antigen presentation in antiviral defense.

## 5. Tapasin

The N-terminal transmembrane helices of TAP function as a platform for tapasin, another component of the PLC [54]. Tapasin is a type I glycoprotein with a dual role in the PLC. The

transmembrane domain of tapasin binds and stabilizes TAP [55,56], whereas the N-terminal ER-luminal domain of tapasin recruits MHC I into the PLC, thus linking MHC I to TAP [56,57]. The close proximity of MHC I to TAP ensures a local high concentration of peptides. From this pool of peptides, MHC I has to select high-affinity peptides to form a stable complex. This is important for proper expression of the MHC I/peptide complexes at the cell surface [58]. Furthermore, loading of low-affinity peptides can result in exchange for peptides with a higher affinity from the extracellular milieu [59], which may result in inappropriate immune responses.

Until high-affinity peptide loading occurs, MHC I is stabilized by both tapasin and the generic ER chaperones calreticulin and ERp57. The association of tapasin and ERp57 promotes the recruitment of high-affinity peptides to MHC I, a process that is also known as peptide editing [60]. Once stable high-affinity peptide/MHC I complexes have been formed, the fully assembled MHC I dissociates from the PLC. Not all MHC I alleles are equally dependent on tapasin [61]. Tapasin-dependency correlates with the properties of certain residues within the peptide binding groove of MHC I [61–64]. Tapasin deletion severely affects MHC I surface expression and CD8<sup>+</sup> T cell responses, although the effect is not as pronounced as for TAP deletion [65]. Nonetheless, several viruses have evolved immune escape mechanisms that target tapasin. For example, HCMV US3, a type I TM protein that binds to tapasin and TAP, inhibits the peptide editing function of tapasin [66]. In addition, US3 can also bind and retain MHC I in the ER [67]. In line with this, US3 primarily affects the maturation of tapasin-dependent MHC I alleles [66] (**figure 1B**).

Like HCMV US3, the adenovirus-encoded type I TM protein E3-19K also directly binds and retains MHC I molecules in the ER [2]. In part, ER retention is mediated by a di-lysine ER retention motif within the cytoplasmic tail of E3-19K [68]. However, removal of this retention signal does not fully restore MHC I surface levels, suggesting that E3-19K might use an additional mechanism to retain MHC I in the ER. In line with this, MHC I molecules that bind to E3-19K weakly were also retained in the ER. In a later study, E3-19K was found to also bind TAP independently of its interaction with MHC I. This leads to a decreased interaction between TAP and MHC I, while the interaction between TAP and tapasin is preserved [69]. Thus, E3-19K interferes with the bridging function of tapasin and excludes MHC I from the PLC (**figure 1C**).

Structural analysis of the tapasin-ERp57 heterodimer suggested that a conserved surface on tapasin interacts with MHC I and keeps the MHC I peptide-binding groove in an open, peptide-receptive conformation [70]. Proteins like US3 and E3-19K may help to further delineate the contribution of various components of the PLC to efficient loading of MHC I with high-affinity peptides.

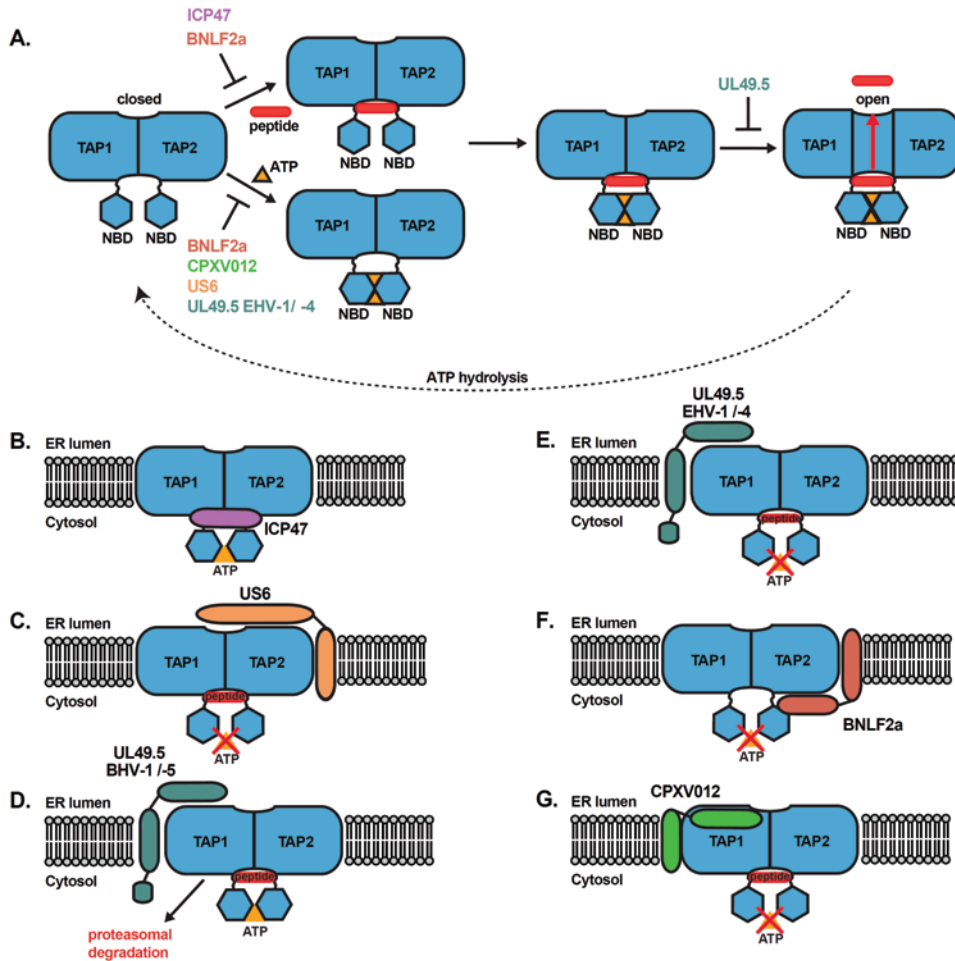


**Figure 2. Viral TAP inhibitors interfere with the peptide translocation cycle at different stages.** (A) Model of the peptide transport cycle and the effects of viral TAP inhibitors. In a closed conformation of TAP, ATP can bind to the nucleotide binding domains (NBDs) of TAP, and peptide can bind to the peptide binding domain. ATP and peptide binding occur independently of each other. When both peptide and ATP bind, TAP changes to an open conformation that allows peptide transport into the ER lumen. After ATP hydrolysis, TAP returns to a closed conformation and is again receptive for ATP and peptide. Viral TAP inhibitors arrest TAP at different stages during the peptide transport cycle. EHV-1 and EHV-4-encoded UL49.5, HCMV-encoded US6, EBV-encoded BNLF2a, and cowpox virus-encoded CPXV012 block ATP binding to TAP. HSV-1 and HSV-2-encoded ICP47 and EBV BNLF2a inhibit peptide binding to TAP. The UL49.5 proteins of BHV-1 and other ruminant herpesviruses, and pseudorabies virus (PRV) block the conformational alterations needed for peptide transport without affecting ATP and peptide binding to TAP. (B-G) TAP inhibitors bind differentially to TAP. (B) The cytosolic ICP47 proteins of HSV-1 and HSV-2 interact with the peptide binding domain of TAP, thereby competitively inhibiting peptide binding to TAP. (C) The HCMV-encoded type I TM protein US6 interacts with the ER luminal domain of TAP and blocks ATP-binding to the NBDs of TAP. (D and E) The UL49.5 gene products of varicelloviruses are type I TM proteins that bind to TAP through their TM and ER luminal domains. The interaction of UL49.5 proteins with TAP inhibits conformational transitions required

**Figure 2 (continued).** for translocation of peptides over the ER membrane. (D) In addition, UL49.5 proteins of BHV-1 and several other ruminant varicelloviruses induce degradation of TAP through their cytosolic domain. (E) The UL49.5 proteins of EHV-1 and EHV-4 inhibit ATP-binding to TAP. (F) The EBV-encoded tail-anchored protein BNLF2a binds TAP through its cytosolic domain. BNLF2a inhibits both peptide and ATP binding to TAP. (G) The interaction of the type II TM protein CPXV012 of cowpox viruses with TAP results in inhibition of ATP binding to the NBDs of TAP.

## 6. TAP-independent peptide presentation

The selective targeting of TAP by numerous viruses underscores the importance of this transporter in the MHC I antigen presentation pathway. In addition, many tumors escape CD8<sup>+</sup> T cell recognition through mutations in the *TAP1* or *TAP2* genes [71–75]. Nevertheless, cells with TAP impairments due to mutations in one or both of the transporter subunits still carry MHC I/peptide complexes at their cell surface [76,77]. However, the repertoire of peptides presented by these cells is completely different from that of cells with a functional antigen processing machinery. Many of these so-called T-cell epitopes associated with impaired antigen processing (TEIPP) are only presented in the absence of functional TAP. The lack of an ER peptide pool generated by TAP promotes the presentation of peptides from alternative sources. A proportion of these TEIPPs are formed by cleavage of signal peptides by signal peptidases (SP) or signal peptide peptidases (SPP) in the ER lumen. TAP-independent peptides can also be generated outside the ER, for example in the *trans*-Golgi network and/or endosomal compartments.

TEIPPs are capable of eliciting CD8<sup>+</sup> T cell responses and play a role in the recognition of TAP-deficient tumor cells [78,79]. Viral TAP inhibitors can promote TEIPP peptide presentation and recognition by TEIPP-specific CD8<sup>+</sup> T cells. Initially, this was shown in HeLa cells expressing a mouse TEIPP derived from the *Lass5* gene. This TEIPP is presented in the context of the classical mouse MHC I molecule H-2D<sup>b</sup>. Co-expression of the TAP inhibitor ICP47 enhanced the response of *Lass5* epitope-specific T cells, thereby indicating that the display of TEIPPs is increased upon TAP inhibition [78]. Similar results were shown for the BHV-1-encoded TAP inhibitor UL49.5 in the context of the non-classical mouse MHC I molecule Qa-1<sup>b</sup>. Qa-1<sup>b</sup>, the functional homolog of human HLA-E, mainly presents leader peptides derived from classical MHC I molecules carried by TAP-proficient cells. Upon TAP inhibition by UL49.5, recognition of the cells by leader peptide-specific CD8<sup>+</sup> T cells was abrogated, whereas activation of TEIPP-specific CD8<sup>+</sup> T cells was greatly enhanced [80,81].

Viral TAP inhibitors have also been used to identify TEIPP-specific CD8<sup>+</sup> T cells in humans. Certain CD8<sup>+</sup> T cells isolated from healthy donors recognized and killed human B-lymphoblastoid cell lines (LCLs) expressing the viral TAP inhibitors UL49.5, US6, BNLF2a, or ICP47 [82]. The CD8<sup>+</sup> T cell clones identified recognized TEIPPs in the context of various classical MHC I molecules, including HLA-A2, HLA-B8, and HLA-B4402. In TAP-proficient cells, these HLA molecules differ in their dependence on TAP; HLA-A2 and HLA-B8 are relatively TAP-independent [65,76,77,83], whereas HLA-B4402 strongly depends on TAP for



antigen presentation [84,85]. These findings show that upon viral TAP-inhibition, both TAP-dependent and TAP-independent MHC I alleles can present TEIPPs and activate the immune system.

These studies with virus-encoded TAP inhibitors indicate that, in addition to the peptides supplied by TAP, alternative peptide processing pathways can yield peptides presented by MHC I. These pathways are especially dominant in the absence of functional TAP, *e.g.* in certain tumor cells. This results in the generation of TEIPPs and recognition by a specific subset of T cells. The presence of TEIPPs on tumor cells or cells expressing viral TAP inhibitors makes them ideal targets for immunotherapy. Especially viral TAP inhibitors are interesting tools to induce such a response. For example, UL49.5 of BHV-1 promotes the presentation of TAP-independent epitopes on tumor cell lines. Furthermore, dendritic cells expressing BHV-1 UL49.5 can induce TEIPP specific T-cell responses, and may therefore be used to direct the immune system toward tumor cells that express TEIPPs [80,81]. So far, the identity of the human TEIPP peptides that stimulate these T cell responses has remained elusive.

2

## 7. Degradation of MHC I

A failure to either associate with  $\beta_2m$  or to be loaded with peptide will produce unstable MHC I HCs, which are then degraded via a cellular process that is called ER-associated protein degradation (ERAD) [86]. Under normal conditions, only a minor fraction of the MHC I molecules synthesized undergo ERAD eventually, which hampers the elucidation of the molecular mechanisms underlying ERAD of MHC I. Therefore, viral immunoevasins that specifically target MHC I for ERAD, have been used to accelerate MHC I degradation; this has facilitated the discovery of factors essentially involved in this process (figure 3). In particular, HCMV US2 and US11, and mK3 of mouse herpesvirus 68 (MHV68) have greatly contributed to our current understanding of the molecular mechanisms of general ERAD, and in particular the ERAD of MHC I. Interestingly, although all three of these viral proteins target HCs for degradation by the proteasome, the mechanisms by which the HCs are retrotranslocated or dislocated from the ER into the cytosol are distinct.

HCMV US2 and US11 are ER-resident type I membrane glycoproteins of 199 and 215 amino acid residues in length, respectively. Both proteins contain a signal peptide, a luminal domain, a transmembrane domain and a relatively short cytosolic domain. US2 and US11 cause dislocation of newly synthesized MHC I HCs from the ER into the cytosol, and ultimately their degradation by the proteasome [87,88]. Although the end result of the dislocation reaction is thus similar, US2 and US11 operate differently.

The ER luminal domain of US11 interacts with the MHC I HC, while the transmembrane region of US11 recruits the multimembrane-spanning protein Derlin-1 [89–92]. Derlin-1 then associates with other members of the dislocation complex, including the E3 ubiquitin

ligase TMEM129 [93,94] and VIMP-p97 [90,95]. In cooperation with the E2 conjugating enzymes UBE2J2 [93,94] and UBE2K [93,96], the E3 TMEM129 ubiquitinates the MHC I HC, presumably at its cytosolic tail, which consequently triggers its extraction into the cytosol via the AAA-ATPase p97 [95]. The HC is deglycosylated by a N-glycanase [88,97], and finally, the dislocated HC is degraded by the proteasome [88].

In contrast to US11, US2 seems to rely on a less-well characterized pathway, since it does not require the proteins known to be essential for US11-mediated HC dislocation, but uses others instead. For example, US2 requires SPP [98] and the E3 ubiquitin ligase TRC8 [99]. Whereas TRC8 is known to be required for HC ubiquitination, the exact role of SPP, and whether its proteolytic activity is required, remains unclear and even debated, as a recent study showed that US2 could still downregulate MHC I in SPP-knockout cells [100]. However, SPP is required for cleavage and subsequent degradation of the unfolded protein response regulator XBP1u [101] and Heme oxygenase-1 (HO-1) [100]. Interestingly, the ERAD complex responsible for the degradation of XBP1u also contains Derlin-1, besides TRC8 and SPP. This is in contrast to the composition of the ERAD complex responsible for US2-mediated MHC I downregulation, in which Derlin-1 is neither present nor required [90,91], whereas TRC8 is [99].

The mouse gamma herpesvirus 68 (MHV68) protein mK3 is itself a RING-CH-containing E3 ubiquitin ligase that induces rapid degradation of MHC I HCs [102,103]. The mK3 protein binds to the PLC-proteins TAP and tapasin, and waits for the MHC I HCs to enter the PLC [104]. Upon association with the HC, mK3 engages the E2-conjugating enzyme UBE2J2 to ubiquitinate the cytosolic tail of the HC [103,105–107], after which Derlin-1 and p97 are recruited to dislocate the HCs into the cytosol for degradation [108].

Especially the US11-mediated degradation of MHC I has been instrumental in the identification of key components of mammalian ERAD, such as Derlin-1 [90,91], the AAA-ATPase p97 [95], VIMP [90] and TMEM129 [93,94], whereas US2 facilitated the discovery of the role of SPP [98] and TRC8 [99] in ERAD. These viral proteins have demonstrated that a complex with a central E3 ubiquitin ligase is responsible for ubiquitination and subsequent dislocation of MHC I. However, while the E3 ubiquitin ligases TRC8 and TMEM129 are essential for MHC I dislocation by US2 and US11, respectively, ERAD of endogenous HCs does not rely on either E3. It was found that, upon  $\beta_2m$  depletion, yet another E3 ubiquitin ligase, HRD1, catalyzes the ubiquitination of MHC I HCs, together with the E2-conjugating enzyme UBE2J1 [109]. To facilitate the dislocation of the misfolded HCs, HRD1 forms a complex with Derlin-1 and p97, previously discovered in the US11 pathway. HFE-C282Y, a protein responsible for hereditary haemochromatosis, is also degraded by HRD1. HFE is an MHC I-like protein and functions to regulate iron absorption. The C282Y mutation causes the protein to be unable to associate with  $\beta_2m$ , which results in misfolding of HFE, resulting in its retention within the ER and ultimately degradation by HRD1 [109].

Studies on MHC I dislocation by US2 and US11 have shown that the MHC I HC is

ubiquitinated during the process of dislocation. Monoubiquitination of the HC is not sufficient to induce US11-mediated dislocation; completion of this reaction requires K48-linked polyubiquitination [110,111]. It has been suggested that lysine residues present within the HC are the main target for ubiquitination. However, beside lysine, also serine, threonine, and cysteine residues can be ubiquitinated [106,112]. For instance, mK3-UBE2J2-mediated K48-linked ubiquitination of the MHC I HC actually favors ubiquitination onto lysine, serine, or threonine residues [105–107]. In the case of misfolded HC dislocation, HRD1-UBE2J1-mediated ubiquitination can be targeted to both lysine and non-lysine residues, although lysine residues within the ER luminal domain of the HC are the preferred ubiquitin acceptor sites [113].

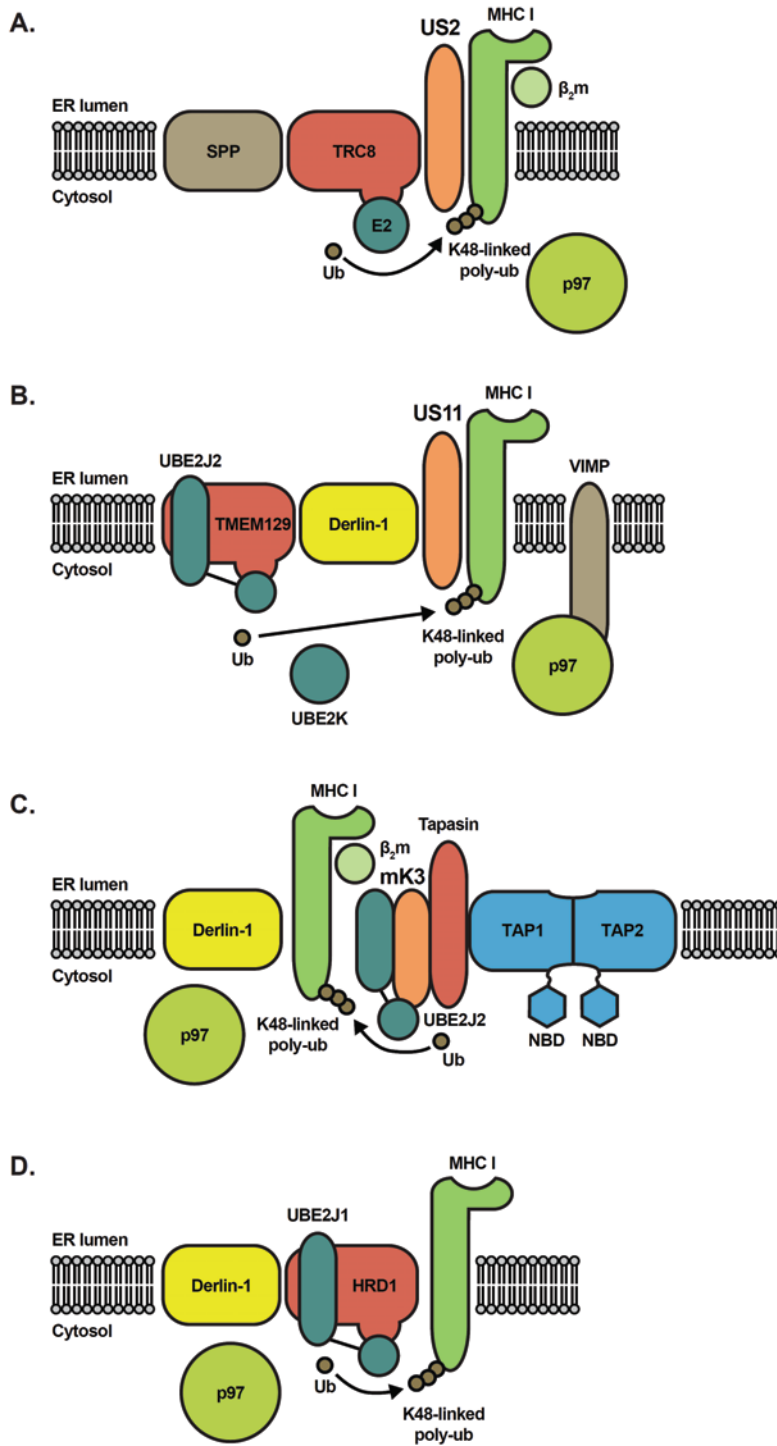
Thus, depending on its context, the dislocation of MHC I HCs may be catalyzed by at least four different ERAD complexes containing different E3 ubiquitin ligases. This observation testifies to the versatility of ERAD and underscores the essential role E3 ubiquitin ligases play in regulating the dislocation of substrates into the cytosol for degradation by the ubiquitin-proteasome system.

## 8. Sorting out MHC I

Once the MHC I HC is associated with  $\beta_2m$  and has acquired a peptide of sufficient affinity, it is released from the PLC and can be transported to the cell surface. However, these MHC I molecules have to pass the Golgi compartment, in which another quality control system is present. The poxvirus protein CPXV203 has given great insights into this quality control system.

CPXV203 is a soluble protein that retains peptide-loaded MHC I molecules in the ER through a mechanism distinct of E3-19K. Contrary to E3-19K, CPXV203 does not depend on other components of the PLC for its action [35,114]. It is capable of directly binding the luminal domains of MHC I [115]. In addition, CPXV203 contains a C-terminal KTEL sequence [35,114] that closely resembles the ER retention motif KDEL [116–118]. Thus, CPXV203 appears to hijack the KDEL-receptor to facilitate COP1-mediated retrograde transport of peptide-loaded MHC I molecules that have reached the Golgi. Later, it was found that the cellular quality control for MHC class I in the Golgi is driven by similar mechanisms. Non-PLC-bound calreticulin present in the *cis*-Golgi is able to recognize MHC I that has been loaded with sub-optimal peptides. Calreticulin contains a C-terminal KDEL sequence, which enables recruitment of the KDEL-receptor. Then, COP1-retrograde transport returns the MHC I molecule to the ER [119].

Once MHC I molecules have passed the quality control system present in the Golgi, it finally reaches the surface for presentation of peptides to CD8<sup>+</sup> T cells. Eventually, surface MHC I molecules are endocytosed, and either recycled to the cell surface after exchange of its peptide content for endosomal peptides, or transported to lysosomes for degradation.



< **Figure 3. ER-associated degradation of MHC class I.** The degradation of MHC I HCs can be catalyzed by at least three different herpesvirus-encoded immunoevasins, but can also occur in the absence of viral evasion molecules, for example if HCs fail to bind  $\beta_2m$ . (A) The HCMV US2 protein exploits the TRC8-SPP-dependent ERAD pathway, while (B) the HCMV US11 protein requires the TMEM129-Derlin-1 complex to dispose of the HCs. (C) MHV68 mK3 is an E3 ubiquitin ligase itself, binding TAP and catalyzing the ubiquitination of MHC I HCs. (D) When HCs fail to associate with  $\beta_2m$ , they are degraded by the HRD1-Derlin-1 complex. In these four instances, the MHC I HC is ubiquitinated by a specific E3 ubiquitin ligase in cooperation with one or several E2 conjugating enzymes. Eventually, the MHC I molecules are dislocated into the cytosol via p97 and degraded by the proteasome.

Two viral proteins, kK3 and kK5 of KSHV, have given new insights into the recycling of MHC I [120,121].

The KSHV proteins kK3 and kK5, also known as Modulator of Immune Recognition (MIR) 1 and 2, are highly homologous to mK3 of MHV68, earlier discussed. While kK3 and kK5 are also RING-CH-containing E3 ubiquitin ligases, they do not target MHC I for ERAD, but rather facilitate rapid endocytosis and subsequent lysosomal degradation of MHC I [120,121]. The kK3 and kK5 proteins have 40% amino acid identity and are thought to originate from a gene duplication event. The kK3 and kK5 proteins both downregulate MHC I, but their haplotype specificity is different: kK3 affects the surface expression of HLA-A, B, C, and E, whereas kK5 only affects the surface expression of human HLA-A and B [121]. In addition, they both reduce surface expression of DC-SIGN, DC-SIGNR [122], the MHC I-like molecules CD1d [123] and HFE [124], and gamma interferon receptor 1 (IFNGR1) [125]. In addition, kK5, but not kK3, reduces surface expression of the cell adhesion molecules ICAM-1 [126,127], ALCAM [128], PECAM, and VE-cadherin [129], the co-stimulatory molecule B7.2 [126,127], the NKG2D ligands MICA/B and AICL [130], bone marrow stromal antigen 2 (BST-2, CD316), and Syntaxin-4 [128]. Thus, kK3 mainly targets MHC I, while kK5 is more promiscuous. The downregulation of most of these receptors aims to prevent detection by cytotoxic T lymphocytes (CTLs) and natural killer (NK) cells.

To internalize MHC I, kK3 and kK5 both ubiquitinate the cytosolic tail of the MHC I HC, but while kK3 preferentially targets the lysine residue at position 340 of the HC [131], kK5 targets the lysine residue at position 335 [132–134]. In general, kK5 prefers to ubiquitinate lysine residues proximal to the transmembrane region, whereas kK3 preferentially targets residues that are around 15 amino acid residues away from the transmembrane region [134]. These findings explain the differences in target preference between kK3 and kK5 to some extent. If lysine residues are lacking within these regions, kK3 and kK5 are also able to mediate ubiquitination onto cysteine residues [112,134]. Remarkably, when cytosolic cysteine and lysine residues both are absent, kK3 can still ubiquitinate this mutant MHC I. These findings showed that ubiquitination can also occur onto amino acid residues other than cysteine and lysine residues, as has also been seen in the context of mK3-mediated MHC I degradation [105,106].

While Lys48-linked ubiquitination of MHC I molecules promotes their degradation via

the ERAD pathway, it was unclear which ubiquitin linkage type is required for internalization. A yeast-two-hybrid screen using the RING domain of kK3 as a bait identified UBE2-N as decisive factor in this process [135]. UBE2-N is an E2 ubiquitin-conjugating enzyme known to conjugate Lys63-linked ubiquitin chains [136]. This discovery suggested that Lys63-linked ubiquitin chains could induce for the receptor's internalization. Indeed, MHC I internalization by kK3 requires Lys63-linked ubiquitin chains [137]. Monoubiquitination of the HC was insufficient for internalization; only polyubiquitination could provide a signal that was sufficient for internalization. Depletion of UBE2N decreased the amount of polyubiquitinated MHC I, but a monoubiquitinated MHC I accumulated, indicating that another E2 enzyme had to be involved, catalyzing ubiquitin chain initiation. Additional depletion studies identified this E2 to be UBE2D2/3 [137]. Thus, two different E2 enzymes are required for this reaction. This is in agreement with other findings showing that the processivity of polyubiquitin formation is often orchestrated by at least two different E2 enzymes, one of which is responsible for ubiquitin chain initiation, while the other E2 promotes ubiquitin chain elongation of a specific type [138]. After ubiquitination of MHC I by kK3, internalization occurs via clathrin-mediated endocytosis, as clathrin, its adaptor Epsin-1, and the ESCRT I machinery were found to be required [131,137] (**figure 4**).

Similar to kK3, kK5 uses the E2 enzymes UBE2N and UBE2D2/3 to catalyze polyubiquitination of MHC I. However, the polyubiquitin chains were found to contain not only Lys63-linked, but also Lys11-linked ubiquitin [132,133]. When Lys63-linked chain formation was blocked, kK5 could still polyubiquitinate MHC I, but this did not cause endocytosis, showing that the linkage types produced in the absence of Lys63 linkage could not induce internalization. Internalization of MHC I after ubiquitination by kK5 was shown to be dependent on the GTPase dynamin [127], suggesting that kK5-mediated MHC I internalization is also dependent on clathrin-mediated endocytosis, like the kK3-induced internalization.

The discovery of the viral RING-CH proteins mK3, kK3, and kK5 prompted the search for human homologues that would regulate the internalization of surface proteins. These homologous human proteins were named Membrane-Associated RING-CH (MARCH) proteins. The first human MARCH protein to be identified was c-MIR/MARCH8. MARCH8 induces rapid endocytosis of B7-2, a co-stimulatory molecule, but not of MHC I molecules [139]. In total, eleven MARCH proteins with E3 ubiquitin ligase function have been identified so far in humans. MHC I surface expression was found to be regulated via K63 ubiquitination by MARCH4 and MARCH9 [140].

The expression of MHC class II (MHC II) is more restricted, as it is mainly expressed by antigen-presenting cells, such as DCs and B-cells. MHC II is responsible for the presentation of exogenous antigens, and the subsequent activation of CD4+ T-cells through the specific interaction between peptide-loaded MHC II and the T-cell receptor (TCR). Surface expression of MHC II is regulated by MARCH1 [141] and MARCH8 [142]. Overexpression of both MARCH

proteins reroutes the MHC II from early endocytic compartments to terminal lysosomes in B-cells and DCs [143–145]. Thus, ubiquitination of MHC II has been implicated in internalization, endocytic trafficking, and targeting to multivesicular bodies and lysosomes for degradation. The lysine residue at position 225 within the cytoplasmic tail of the MHC II  $\beta$ -chain appears to be the sole acceptor of ubiquitination, as mutation of this residue into an arginine renders the  $\beta$ -chain insensitive for MARCH1 and MARCH8-mediated ubiquitination [142,146–148].

DCs and B-cells present peptides via MHC II for recognition by CD4<sup>+</sup> T lymphocytes. A striking difference exists between DCs and B-cells with respect to their regulation of MHC II surface expression. Immature DCs express low levels of MHC II at their cell surface; most MHC II molecules are kept in late endosomal compartments, such as multivesicular bodies, or are degraded within lysosomes, through constitutive ubiquitination by MARCH1 [143,148]. Upon maturation, DCs upregulate their CD83 surface expression, which disrupts the association of MHC II with MARCH1 [149]. Moreover, these DCs downregulate their MARCH1 expression, resulting in increased expression of MHC II at the cell surface [143]. In contrast, in B-cells, MHC II expression is constitutively high, despite MHC II being ubiquitinated [141]. This is because in B-cells, MHC II is modified with only two to three ubiquitin moieties, which is insufficient for lysosomal transport and results in increased recycling to the plasma membrane. In immature DCs, MHC II is modified with four to six ubiquitin moieties, sufficient to trigger transport to late endosomal compartments for degradation [147,150]. Thus, ubiquitin chain length plays a crucial role in the regulation of MHC II trafficking in DCs and B-cells.

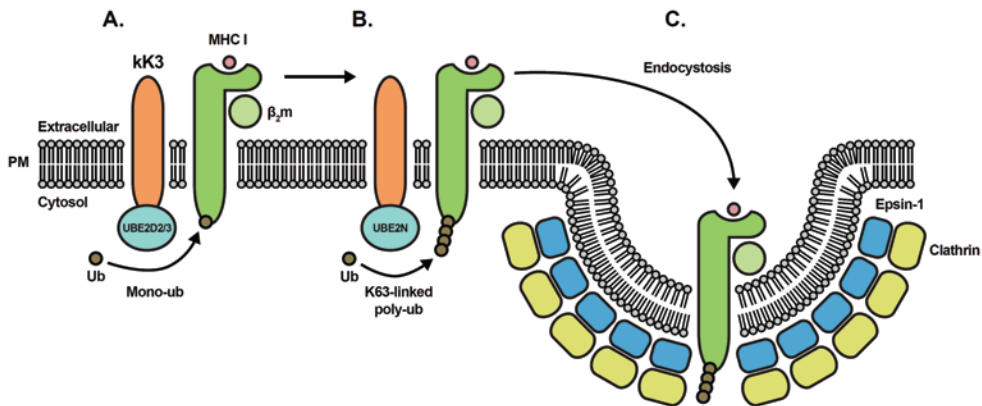


**Figure 4. kK3-mediated endocytosis of MHC I.** (A) kK3 associates with MHC I, and subsequently induces monoubiquitination of the HC in cooperation with the E2 enzyme UBE2D2/3. (B) Next, the E2 enzyme UBE2-N is recruited to facilitate Lys63-linked ubiquitin chain elongation, (C) which signals for clathrin-mediated endocytosis. The MHC I molecules are then transported to multivesicular bodies and ultimately degraded in lysosomes.

## 9. Cross-presentation

To eradicate cells infected with intracellular bacteria or viruses, naïve CD8<sup>+</sup> T cells have to be activated by DCs through a process called cross-priming. Cross-priming is the result of cross-presentation, *i.e.* the presentation of exogenous antigens by MHC I molecules. How cross-presentation is regulated, has been a subject of intense investigation. For exogenous antigens to be presented by MHC I, these antigens have been suggested to be transported into the cytosol, where they are processed into peptides. These peptides may be transported into the ER via TAP. Other studies have however indicated that peptide loading of MHC I also takes place in endocytic or phagocytic compartments. Several viral TAP inhibitors, such as HCMV US6 and HSV-1 ICP47 have greatly aided in the elucidation of the cross-presentation pathway.

Uptake of soluble exogenous antigens relies on endocytosis or macropinocytosis. Subsequent cross-presentation of these antigens has been elucidated to some detail by using the viral TAP inhibitor HCMV US6. US6 blocks TAP through its ER luminal domain, in particular the amino acid residues 20-146. When a soluble, truncated version of US6 encompassing its functional domain is added to DCs exogenously, it is internalized into TAP-containing compartments, where it interferes with TAP function [151,152]. The latter results in strong inhibition of cross-presentation of soluble exogenous antigens. This suggests that TAP-mediated peptide translocation is essential for cross-presentation. However, the location of the TAP complexes inhibited by US6 remained unresolved by these experiments. Soluble US6 could inhibit TAP within an endocytic/phagocytic compartment or the ER. To address this important question, soluble US6 was fused to transferrin to localize it exclusively to early endosomes [151]. In this way, cross-presentation of OVA peptides was severely reduced. These experiments indicate that the re-import of antigenic peptides derived from soluble antigens for cross-presentation is mainly facilitated by TAP present in early endosomes.

Since particulate antigens are internalized via phagocytosis [152,153], phagosomes may facilitate retrotranslocation of particulate exogenous antigens. Indeed, DC phagosomes have been found to contain ERAD components, in addition to PLC proteins including TAP [152–154]. Thus, phagosomes appear to contain all necessary components to facilitate cross-presentation. To supply the phagosomes with ERAD factors, phagosomes have been suggested to fuse with ER membranes [153,155], although this subject has remained controversial [156]. Exogenous antigens may also reach the cytosol via alternative pathways, *e.g.* via retrotranslocation from the ER.

Several exogenous proteins that enter the cell via endocytosis have been found to reach the ER compartment. Certain toxins, such as cholera toxin and ricin toxin, which have their mode of action inside the cytosol, are endocytosed and are retrotransported via the Golgi network back to the ER, where they enter the cytosol via retrotranslocation [157,158]. When offered to DCs, endocytosed soluble HCMV US6 and exogenous  $\beta_2m$  were



able to reach the ER after endocytosis [159]. Thus, dependent on the type of antigen, cross-presentation may occur within phagosomes, endosomes, or the ER.

More insight into the retrotranslocation of exogenous antigens was obtained using the HSV-1 encoded TAP inhibitor ICP47 and the Sec61 inhibitor Exotoxin A (ExoA) from *Pseudomonas aeruginosa* [160]. As discussed above, ICP47 blocks peptide translocation via interaction with the cytosolic part of TAP [38,39]. It was found that soluble, exogenous ICP47 is able to block both endogenous and exogenous antigen presentation in DCs [155]. Soluble ICP47 is phagocytosed and subsequently dislocated into the cytosol, where it can act upon the cytosolic side of TAP, regardless of its location. Thus, ICP47 can block peptide transport of both endogenous and exogenous antigens. Exogenous addition of ExoA was found to reverse the ICP47-mediated TAP inhibition. Also, when only ExoA was supplied exogenously, cross-presentation of the OVA peptide was inhibited. These findings suggest that Sec61 plays a crucial role in the retrotranslocation of exogenous proteins. However, the exact role of Sec61 in retrotranslocation remains to be determined. The retrotranslocation of exogenous antigens appears to be also dependent on p97, as a dominant-negative version inhibited cross-presentation [155,161]. Remarkably, the ERAD factor Derlin-1 does not seem to be crucial in this process [161].

## 10. Concluding remarks

The wide variety of viral gene products targeting MHC I antigen presentation underlines the importance of this pathway in combating viral infections. In addition, this arm of the immune system plays a role in immune recognition of other pathogens, including (intracellular) bacteria (reviewed by [162]). To counteract such responses, certain bacteria encode gene products that target MHC I antigen presentation directly, such as the Cif protein from *P. aeruginosa*. This protein is delivered to target cells by membrane vesicles, where it induces TAP degradation through the ubiquitin-proteasome pathway [163]. Other bacteria manipulate MHC I antigen presentation more indirectly; *e.g.* by reducing their antigenic content within infected cells [164], or by mutating the epitopes expressed by MHC I molecules [165].

The discovery of virus-encoded immunoevasins in recent years has greatly contributed to the characterization of the MHC class I antigen presentation pathway, including TAP-mediated peptide transport, degradation of MHC I, recycling of MHC I, and cross-presentation. The specific and potent effect of these immunoevasins on the aforementioned processes makes them ideal molecular probes. Especially herpesviruses and poxviruses have been extremely useful in this context, since these viruses encode numerous immune evasion proteins that allow them to elude the host immune system. Moreover, these immunoevasins are potentially useful in gene therapy, transplantation and tumor-specific immunotherapy, as they allow specific manipulation of the immune system.

## References

- 1 Sadasivan B, Lehner PJ, Ortmann B, Spies T, Cresswell P. Roles for calreticulin and a novel glycoprotein, tapasin, in the interaction of MHC class I molecules with TAP. *Immunity* 1996;5:103–14.
- 2 Burgert HG, Kvist S. An adenovirus type 2 glycoprotein blocks cell surface expression of human histocompatibility class I antigens. *Cell* 1985;41:987–97.
- 3 Cox JH, Yewdell JW, Eisenlohr LC, Johnson PR, Bennink JR. Antigen presentation requires transport of MHC class I molecules from the endoplasmic reticulum. *Science* 1990;247:715–8.
- 4 Akopian D, Shen K, Zhang X, Shan S. Signal recognition particle: an essential protein-targeting machine. *Annu Rev Biochem* 2013;82:693–721. doi:10.1146/annurev-biochem-072711-164732.
- 5 Powers CJ, Früh K. Signal peptide-dependent inhibition of MHC class I heavy chain translation by rhesus cytomegalovirus. *PLoS Pathog* 2008;4:e1000150. doi:10.1371/journal.ppat.1000150.
- 6 Richards R, Scholz I, Powers C, Skach WR, Früh K. The cytoplasmic domain of rhesus cytomegalovirus Rh178 interrupts translation of major histocompatibility class I leader peptide-containing proteins prior to translocation. *J Virol* 2011;85:8766–76. doi:10.1128/JVI.05021-11.
- 7 Rock KL, Goldberg AL. Degradation of cell proteins and the generation of MHC class I-presented peptides. *Annu Rev Immunol* 1999;17:739–79. doi:10.1146/annurev.immunol.17.1.739.
- 8 Leight ER, Sugden B. EBNA-1: a protein pivotal to latent infection by Epstein-Barr virus. *Rev Med Virol* 2000;10:83–100.
- 9 Blake N, Haigh T, Shaka'a G, Croom-Carter D, Rickinson A. The importance of exogenous antigen in priming the human CD8+ T cell response: lessons from the EBV nuclear antigen EBNA1. *J Immunol* 2000;165:7078–87.
- 10 Levitskaya J, Coram M, Levitsky V, Imreh S, Steigerwald-Mullen PM, Klein G, et al. Inhibition of antigen processing by the internal repeat region of the Epstein-Barr virus nuclear antigen-1. *Nature* 1995;375:685–8. doi:10.1038/375685a0.
- 11 Levitskaya J, Sharipo A, Leonchiks A, Ciechanover A, Masucci MG. Inhibition of ubiquitin/proteasome-dependent protein degradation by the Gly-Ala repeat domain of the Epstein-Barr virus nuclear antigen 1. *Proc Natl Acad Sci U S A* 1997;94:12616–21.
- 12 Sharipo A, Imreh M, Leonchiks A, Imreh S, Masucci MG. A minimal glycine-alanine repeat prevents the interaction of ubiquitinated I kappaB alpha with the proteasome: a new mechanism for selective inhibition of proteolysis. *Nat Med* 1998;4:939–44.
- 13 Daskalogianni C, Apcher S, Candeias MM, Naski N, Calvo F, Fåhræus R. Gly-Ala repeats induce position- and substrate-specific regulation of 26 S proteasome-dependent partial processing. *J Biol Chem* 2008;283:30090–100. doi:10.1074/jbc.M803290200.
- 14 Lee SP, Brooks JM, Al-Jarrah H, Thomas WA, Haigh TA, Taylor GS, et al. CD8 T cell recognition of endogenously expressed Epstein-Barr virus nuclear antigen 1. *J Exp Med* 2004;199:1409–20. doi:10.1084/jem.20040121.
- 15 Tellam J, Connolly G, Green KJ, Miles JJ, Moss DJ, Burrows SR, et al. Endogenous presentation of CD8+ T cell epitopes from Epstein-Barr virus-encoded nuclear antigen 1. *J Exp Med* 2004;199:1421–31. doi:10.1084/jem.20040191.
- 16 Voo KS, Fu T, Wang HY, Tellam J, Heslop HE, Brenner MK, et al. Evidence for the presentation of major histocompatibility complex class I-restricted Epstein-Barr virus nuclear antigen 1 peptides to CD8+ T lymphocytes. *J Exp Med* 2004;199:459–70. doi:10.1084/jem.20031219.
- 17 Ballestas ME, Chatis PA, Kaye KM. Efficient persistence of extrachromosomal KSHV DNA mediated by latency-associated nuclear antigen. *Science* 1999;284:641–4.
- 18 Zaldumbide A, Ossevoort M, Wiertz EJHJ, Hoeben RC. In cis inhibition of antigen processing by the latency-associated nuclear antigen I of Kaposi sarcoma herpes virus. *Mol Immunol* 2007;44:1352–60. doi:10.1016/j.

- molimm.2006.05.012.
- 19 Kwun HJ, da Silva SR, Shah IM, Blake N, Moore PS, Chang Y. Kaposi's sarcoma-associated herpesvirus latency-associated nuclear antigen 1 mimics Epstein-Barr virus EBNA1 immune evasion through central repeat domain effects on protein processing. *J Virol* 2007;81:8225–35. doi:10.1128/JVI.00411-07.
  - 20 Heessen S, Leonchiks A, Issaeva N, Sharipo A, Selivanova G, Masucci MG, et al. Functional p53 chimeras containing the Epstein-Barr virus Gly-Ala repeat are protected from Mdm2- and HPV-E6-induced proteolysis. *Proc Natl Acad Sci U S A* 2002;99:1532–7. doi:10.1073/pnas.022306499.
  - 21 Alba R, Bosch A, Chillon M. Gutless adenovirus: last-generation adenovirus for gene therapy. *Gene Ther* 2005;12 Suppl 1:518–27. doi:10.1038/sj.gt.3302612.
  - 22 Eggers R, Hendriks WTJ, Tannemaat MR, van Heerikhuizen JJ, Pool CW, Carlstedt TP, et al. Neuroregenerative effects of lentiviral vector-mediated GDNF expression in reimplanted ventral roots. *Mol Cell Neurosci* 2008;39:105–17. doi:10.1016/j.mcn.2008.05.018.
  - 23 Hendriks WTJ, Eggers R, Carlstedt TP, Zaldumbide A, Tannemaat MR, Fallaux FJ, et al. Lentiviral vector-mediated reporter gene expression in avulsed spinal ventral root is short-term, but is prolonged using an immune “stealth” transgene. *Restor Neurol Neurosci* 2007;25:585–99.
  - 24 Hoyng SA, Gnavi F, de Winter F, Eggers R, Ozawa T, Zaldumbide A, et al. Developing a potentially immunologically inert tetracycline-regulatable viral vector for gene therapy in the peripheral nerve. *Gene Ther* 2014;21:549–57. doi:10.1038/gt.2014.22.
  - 25 Ossevoort M, Visser BMJ, van den Wollenberg DJM, van der Voort EIH, Offringa R, Melief CJM, et al. Creation of immune “stealth” genes for gene therapy through fusion with the Gly-Ala repeat of EBNA-1. *Gene Ther* 2003;10:2020–8. doi:10.1038/sj.gt.3302098.
  - 26 Zaldumbide A, Weening S, Cramer SJ, Rabelink MJWE, Verhaagen J, Hoebe RC. A potentially immunologically inert derivative of the reverse tetracycline-controlled transactivator. *Biotechnol Lett* 2010;32:749–54. doi:10.1007/s10529-010-0218-8.
  - 27 Vos JC, Spee P, Momburg F, Neefjes J. Membrane topology and dimerization of the two subunits of the transporter associated with antigen processing reveal a three-domain structure. *J Immunol* 1999;163:6679–85.
  - 28 Vos JC, Reits EA, Wojcik-Jacobs E, Neefjes J. Head-head/tail-tail relative orientation of the pore-forming domains of the heterodimeric ABC transporter TAP. *Curr Biol* 2000;10:1–7.
  - 29 Parcej D, Tampé R. ABC proteins in antigen translocation and viral inhibition. *Nat Chem Biol* 2010;6:572–80. doi:10.1038/nchembio.410.
  - 30 Attaya M, Jameson S, Martínez CK, Hermel E, Aldrich C, Forman J, et al. Ham-2 corrects the class I antigen-processing defect in RMA-S cells. *Nature* 1992;355:647–9. doi:10.1038/355647a0.
  - 31 Spies T, DeMars R. Restored expression of major histocompatibility class I molecules by gene transfer of a putative peptide transporter. *Nature* 1991;351:323–4. doi:10.1038/351323a0.
  - 32 Franksson L, Petersson M, Kiessling R, Kärre K. Immunization against tumor and minor histocompatibility antigens by eluted cellular peptides loaded on antigen processing defective cells. *Eur J Immunol* 1993;23:2606–13. doi:10.1002/eji.1830231034.
  - 33 Ohlén C, Bastin J, Ljunggren HG, Foster L, Wolpert E, Klein G, et al. Resistance to H-2-restricted but not to allo-H2-specific graft and cytotoxic T lymphocyte responses in lymphoma mutant. *J Immunol* 1990;145:52–8.
  - 34 Alzhanova D, Edwards DM, Hammarlund E, Scholz IG, Horst D, Wagner MJ, et al. Cowpox virus inhibits the transporter associated with antigen processing to evade T cell recognition. *Cell Host Microbe* 2009;6:433–45. doi:10.1016/j.chom.2009.09.013.
  - 35 Byun M, Verweij MC, Pickup DJ, Wiertz EJHJ, Hansen TH, Yokoyama WM. Two mechanistically distinct immune evasion proteins of cowpox virus combine to avoid antiviral CD8 T cells. *Cell Host Microbe* 2009;6:422–32. doi:10.1016/j.chom.2009.09.012.

- 36 Luteijn RD, Hoelen H, Kruse E, van Leeuwen WF, Grootens J, Horst D, et al. Cowpox virus protein CPXV012 eludes CTLs by blocking ATP binding to TAP. *J Immunol* 2014;193:1578–89. doi:10.4049/jimmunol.1400964.
- 37 Lin J, Eggensperger S, Hank S, Wycisk AI, Wieneke R, Mayerhofer PU, et al. A negative feedback modulator of antigen processing evolved from a frameshift in the cowpox virus genome. *PLoS Pathog* 2014;10:e1004554. doi:10.1371/journal.ppat.1004554.
- 38 Fruh K, Ahn K, Djaballah H, Sempé P, van Endert PM, Tampe R, et al. A viral inhibitor of peptide transporters for antigen presentation. *Nature* 1995;375:415–8. doi:10.1038/375415a0.
- 39 Hill A, Jugovic P, York I, Russ G, Bennink J, Yewdell J, et al. Herpes simplex virus turns off the TAP to evade host immunity. *Nature* 1995;375:411–5. doi:10.1038/375411a0.
- 40 Tomazin R, Hill AB, Jugovic P, York I, van Endert P, Ploegh HL, et al. Stable binding of the herpes simplex virus ICP47 protein to the peptide binding site of TAP. *EMBO J* 1996;15:3256–66.
- 41 Ahn K, Meyer TH, Uebel S, Sempé P, Djaballah H, Yang Y, et al. Molecular mechanism and species specificity of TAP inhibition by herpes simplex virus ICP47. *EMBO J* 1996;15:3247–55.
- 42 Gorbulev S, Abele R, Tampé R. Allosteric crosstalk between peptide-binding, transport, and ATP hydrolysis of the ABC transporter TAP. *Proc Natl Acad Sci U S A* 2001;98:3732–7. doi:10.1073/pnas.061467898.
- 43 Ahn K, Gruhler A, Galocha B, Jones TR, Wiertz EJ, Ploegh HL, et al. The ER-luminal domain of the HCMV glycoprotein US6 inhibits peptide translocation by TAP. *Immunity* 1997;6:613–21.
- 44 Hengel H, Koopmann JO, Flohr T, Muranyi W, Goulmy E, Hämmerling GJ, et al. A viral ER-resident glycoprotein inactivates the MHC-encoded peptide transporter. *Immunity* 1997;6:623–32.
- 45 Lehner PJ, Karttunen JT, Wilkinson GW, Cresswell P. The human cytomegalovirus US6 glycoprotein inhibits transporter associated with antigen processing-dependent peptide translocation. *Proc Natl Acad Sci U S A* 1997;94:6904–9.
- 46 Hewitt EW, Gupta SS, Lehner PJ. The human cytomegalovirus gene product US6 inhibits ATP binding by TAP. *EMBO J* 2001;20:387–96. doi:10.1093/emboj/20.3.387.
- 47 Reits EA, Vos JC, Grommé M, Neeffjes J. The major substrates for TAP in vivo are derived from newly synthesized proteins. *Nature* 2000;404:774–8. doi:10.1038/35008103.
- 48 Koppers-Lalic D, Reits EAJ, Rensing ME, Lipinska AD, Abele R, Koch J, et al. Varicelloviruses avoid T cell recognition by UL49.5-mediated inactivation of the transporter associated with antigen processing. *Proc Natl Acad Sci U S A* 2005;102:5144–9. doi:10.1073/pnas.0501463102.
- 49 Koppers-Lalic D, Verweij MC, Lipińska AD, Wang Y, Quinten E, Reits EA, et al. Varicellovirus UL 49.5 proteins differentially affect the function of the transporter associated with antigen processing, TAP. *PLoS Pathog* 2008;4:e1000080. doi:10.1371/journal.ppat.1000080.
- 50 Verweij MC, Lipinska AD, Koppers-Lalic D, van Leeuwen WF, Cohen JI, Kinchington PR, et al. The capacity of UL49.5 proteins to inhibit TAP is widely distributed among members of the genus Varicellovirus. *J Virol* 2011;85:2351–63. doi:10.1128/JVI.01621-10.
- 51 Hislop AD, Rensing ME, van Leeuwen D, Pudney VA, Horst D, Koppers-Lalic D, et al. A CD8+ T cell immune evasion protein specific to Epstein-Barr virus and its close relatives in Old World primates. *J Exp Med* 2007;204:1863–73. doi:10.1084/jem.20070256.
- 52 Horst D, Favaloro V, Vilardi F, van Leeuwen HC, Garstka MA, Hislop AD, et al. EBV protein BNLF2a exploits host tail-anchored protein integration machinery to inhibit TAP. *J Immunol* 2011;186:3594–605. doi:10.4049/jimmunol.1002656.
- 53 Wycisk AI, Lin J, Loch S, Hobohm K, Funke J, Wieneke R, et al. Epstein-Barr viral BNLF2a protein hijacks the tail-anchored protein insertion machinery to block antigen processing by the transport complex TAP. *JBiolChem* 2011;286:41402–12.
- 54 Koch J, Guntrum R, Heintke S, Kyritsis C, Tampé R. Functional dissection of the transmembrane domains of the transporter associated with antigen processing (TAP). *J Biol Chem* 2004;279:10142–7. doi:10.1074/jbc.

M312816200.

- 55 Bangia N, Lehner PJ, Hughes EA, Surman M, Cresswell P. The N-terminal region of tapasin is required to stabilize the MHC class I loading complex. *Eur J Immunol* 1999;29:1858–70. doi:10.1002/(SICI)1521-4141(199906)29:06<1858::AID-IMMU1858>3.0.CO;2-C.
- 56 Lehner PJ, Surman MJ, Cresswell P. Soluble tapasin restores MHC class I expression and function in the tapasin-negative cell line .220. *Immunity* 1998;8:221–31.
- 57 Ortmann B, Copeman J, Lehner PJ, Sadasivan B, Herberg JA, Granda AG, et al. A critical role for tapasin in the assembly and function of multimeric MHC class I-TAP complexes. *Science* 1997;277:1306–9.
- 58 Van der Burg SH, Visseren MJ, Brandt RM, Kast WM, Melief CJ. Immunogenicity of peptides bound to MHC class I molecules depends on the MHC-peptide complex stability. *J Immunol* 1996;156:3308–14.
- 59 Barnden MJ, Purcell AW, Gorman JJ, McCluskey J. Tapasin-mediated retention and optimization of peptide ligands during the assembly of class I molecules. *J Immunol* 2000;165:322–30.
- 60 Wearsch PA, Cresswell P. Selective loading of high-affinity peptides onto major histocompatibility complex class I molecules by the tapasin-ERp57 heterodimer. *Nat Immunol* 2007;8:873–81. doi:10.1038/ni1485.
- 61 Park B, Lee S, Kim E, Ahn K. A single polymorphic residue within the peptide-binding cleft of MHC class I molecules determines spectrum of tapasin dependence. *J Immunol* 2003;170:961–8.
- 62 Beissbarth T, Sun J, Kavathas PB, Ortmann B. Increased efficiency of folding and peptide loading of mutant MHC class I molecules. *Eur J Immunol* 2000;30:1203–13. doi:10.1002/(SICI)1521-4141(200004)30:4<1203::AID-IMMU1203>3.0.CO;2-L.
- 63 Turnquist HR, Thomas HJ, Prilliman KR, Lutz CT, Hildebrand WH, Solheim JC. HLA-B polymorphism affects interactions with multiple endoplasmic reticulum proteins. *Eur J Immunol* 2000;30:3021–8. doi:10.1002/1521-4141(200010)30:10<3021::AID-IMMU3021>3.0.CO;2-U.
- 64 Williams AP, Peh CA, Purcell AW, McCluskey J, Elliott T. Optimization of the MHC class I peptide cargo is dependent on tapasin. *Immunity* 2002;16:509–20.
- 65 Granda AG, Golovina TN, Hamilton SE, Sriram V, Spies T, Brutkiewicz RR, et al. Impaired assembly yet normal trafficking of MHC class I molecules in Tapasin mutant mice. *Immunity* 2000;13:213–22.
- 66 Park B, Kim Y, Shin J, Lee S, Cho K, Früh K, et al. Human cytomegalovirus inhibits tapasin-dependent peptide loading and optimization of the MHC class I peptide cargo for immune evasion. *Immunity* 2004;20:71–85.
- 67 Jones TR, Wiertz EJ, Sun L, Fish KN, Nelson JA, Ploegh HL. Human cytomegalovirus US3 impairs transport and maturation of major histocompatibility complex class I heavy chains. *Proc Natl Acad Sci U S A* 1996;93:11327–33.
- 68 Cox JH, Bennink JR, Yewdell JW. Retention of adenovirus E19 glycoprotein in the endoplasmic reticulum is essential to its ability to block antigen presentation. *J Exp Med* 1991;174:1629–37.
- 69 Bennett EM, Bennink JR, Yewdell JW, Brodsky FM. Cutting edge: adenovirus E19 has two mechanisms for affecting class I MHC expression. *J Immunol* 1999;162:5049–52.
- 70 Dong G, Wearsch PA, Peaper DR, Cresswell P, Reinisch KM. Insights into MHC class I peptide loading from the structure of the tapasin-ERp57 thiol oxidoreductase heterodimer. *Immunity* 2009;30:21–32. doi:10.1016/j.immuni.2008.10.018.
- 71 Agrawal S, Reemtsma K, Bagiella E, Oluwole SF, Braunstein NS. Role of TAP-1 and/or TAP-2 antigen presentation defects in tumorigenicity of mouse melanoma. *Cell Immunol* 2004;228:130–7. doi:10.1016/j.cellimm.2004.04.006.
- 72 Cromme F V, Airey J, Heemels MT, Ploegh HL, Keating PJ, Stern PL, et al. Loss of transporter protein, encoded by the TAP-1 gene, is highly correlated with loss of HLA expression in cervical carcinomas. *J Exp Med* 1994;179:335–40.
- 73 Kasajima A, Sers C, Sasano H, Jöhrens K, Stenzinger A, Noske A, et al. Down-regulation of the antigen processing machinery is linked to a loss of inflammatory response in colorectal cancer. *Hum Pathol* 2010;41:1758–69.

- doi:10.1016/j.humpath.2010.05.014.
- 74 Restifo NP, Esquivel F, Kawakami Y, Yewdell JW, Mulé JJ, Rosenberg SA, et al. Identification of human cancers deficient in antigen processing. *J Exp Med* 1993;177:265–72.
  - 75 Seliger B, Hohne A, Knuth A, Bernhard H, Meyer T, Tampe R, et al. Analysis of the major histocompatibility complex class I antigen presentation machinery in normal and malignant renal cells: evidence for deficiencies associated with transformation and progression. *Cancer Res* 1996;56:1756–60.
  - 76 Henderson RA, Michel H, Sakaguchi K, Shabanowitz J, Appella E, Hunt DF, et al. HLA-A2.1-associated peptides from a mutant cell line: a second pathway of antigen presentation. *Science* 1992;255:1264–6.
  - 77 Wei ML, Cresswell P. HLA-A2 molecules in an antigen-processing mutant cell contain signal sequence-derived peptides. *Nature* 1992;356:443–6. doi:10.1038/356443a0.
  - 78 Van Hall T, Wolpert EZ, van Veelen P, Laban S, van der Veer M, Roseboom M, et al. Selective cytotoxic T-lymphocyte targeting of tumor immune escape variants. *Nat Med* 2006;12:417–24. doi:10.1038/nm1381.
  - 79 Wolpert EZ, Petersson M, Chambers BJ, Sandberg JK, Kiessling R, Ljunggren HG, et al. Generation of CD8+ T cells specific for transporter associated with antigen processing deficient cells. *Proc Natl Acad Sci U S A* 1997;94:11496–501.
  - 80 Chambers B, Grufman P, Fredriksson V, Andersson K, Roseboom M, Laban S, et al. Induction of protective CTL immunity against peptide transporter TAP-deficient tumors through dendritic cell vaccination. *Cancer Res* 2007;67:8450–5. doi:10.1158/0008-5472.CAN-07-1092.
  - 81 Van Hall T, Laban S, Koppers-Lalic D, Koch J, Precup C, Asmawidjaja P, et al. The varicellovirus-encoded TAP inhibitor UL49.5 regulates the presentation of CTL epitopes by Qa-1b1. *J Immunol* 2007;178:657–62.
  - 82 Lampen MH, Verweij MC, Querido B, van der Burg SH, Wiertz EJHJ, van Hall T. CD8+ T cell responses against TAP-inhibited cells are readily detected in the human population. *J Immunol* 2010;185:6508–17. doi:10.4049/jimmunol.1001774.
  - 83 Guéguen M, Biddison WE, Long EO. T cell recognition of an HLA-A2-restricted epitope derived from a cleaved signal sequence. *J Exp Med* 1994;180:1989–94.
  - 84 Thammavongsa V, Raghuraman G, Filzen TM, Collins KL, Raghavan M. HLA-B44 polymorphisms at position 116 of the heavy chain influence TAP complex binding via an effect on peptide occupancy. *J Immunol* 2006;177:3150–61.
  - 85 Zernich D, Purcell AW, Macdonald WA, Kjer-Nielsen L, Ely LK, Laham N, et al. Natural HLA class I polymorphism controls the pathway of antigen presentation and susceptibility to viral evasion. *J Exp Med* 2004;200:13–24. doi:10.1084/jem.20031680.
  - 86 Hughes EA, Hammond C, Cresswell P. Misfolded major histocompatibility complex class I heavy chains are translocated into the cytoplasm and degraded by the proteasome. *Proc Natl Acad Sci U S A* 1997;94:1896–901.
  - 87 Wiertz EJ, Tortorella D, Bogoy M, Yu J, Mothes W, Jones TR, et al. Sec61-mediated transfer of a membrane protein from the endoplasmic reticulum to the proteasome for destruction. *Nature* 1996;384:432–8. doi:10.1038/384432a0.
  - 88 Wiertz EJ, Jones TR, Sun L, Bogoy M, Geuze HJ, Ploegh HL. The human cytomegalovirus US11 gene product dislocates MHC class I heavy chains from the endoplasmic reticulum to the cytosol. *Cell* 1996;84:769–79.
  - 89 Lilley BN, Tortorella D, Ploegh HL. Dislocation of a type I membrane protein requires interactions between membrane-spanning segments within the lipid bilayer. *Mol Biol Cell* 2003;14:3690–8. doi:10.1091/mbc.E03-03-0192.
  - 90 Ye Y, Shibata Y, Yun C, Ron D, Rapoport T a. A membrane protein complex mediates retro-translocation from the ER lumen into the cytosol. *Nature* 2004;429:841–7. doi:10.1038/nature02656.
  - 91 Lilley BN, Ploegh HL. A membrane protein required for dislocation of misfolded proteins from the ER. *Nature* 2004;429:834–40. doi:10.1038/nature02592.

- 92 Cho S, Lee M, Jun Y. Forced interaction of cell surface proteins with Derlin-1 in the endoplasmic reticulum is sufficient to induce their dislocation into the cytosol for degradation. *Biochem Biophys Res Commun* 2013;430:787–92. doi:10.1016/j.bbrc.2012.11.068.
- 93 Van de Weijer ML, Bassik MC, Luteijn RD, Voorburg CM, Lohuis MAM, Kremmer E, et al. A high-coverage shRNA screen identifies TMEM129 as an E3 ligase involved in ER-associated protein degradation. *Nat Commun* 2014;5:3832. doi:10.1038/ncomms4832.
- 94 Van den Boomen DJH, Timms RT, Grice GL, Stagg HR, Skødt K, Dougan G, et al. TMEM129 is a Derlin-1 associated ERAD E3 ligase essential for virus-induced degradation of MHC-I. *Proc Natl Acad Sci U S A* 2014;111:11425–30. doi:10.1073/pnas.1409099111.
- 95 Ye Y, Meyer HH, Rapoport TA. The AAA ATPase Cdc48/p97 and its partners transport proteins from the ER into the cytosol. *Nature* 2001;414:652–6. doi:10.1038/414652a.
- 96 Flierman D, Coleman CS, Pickart CM, Rapoport TA, Chau V. E2-25K mediates US11-triggered retro-translocation of MHC class I heavy chains in a permeabilized cell system. *Proc Natl Acad Sci U S A* 2006;103:11589–94. doi:10.1073/pnas.0605215103.
- 97 Hirsch C, Blom D, Ploegh HL. A role for N-glycanase in the cytosolic turnover of glycoproteins. *EMBO J* 2003;22:1036–46. doi:10.1093/emboj/cdg107.
- 98 Loureiro J, Lilley BN, Spooner E, Noriega V, Tortorella D, Ploegh HL. Signal peptide peptidase is required for dislocation from the endoplasmic reticulum. *Nature* 2006;441:894–7. doi:10.1038/nature04830.
- 99 Stagg HR, Thomas M, van den Boomen D, Wiertz EJHJ, Drabkin H a, Gemmill RM, et al. The TRC8 E3 ligase ubiquitinates MHC class I molecules before dislocation from the ER. *J Cell Biol* 2009;186:685–92. doi:10.1083/jcb.200906110.
- 100 Boname JM, Bloor S, Wandel MP, Nathan JA, Antrobus R, Dingwell KS, et al. Cleavage by signal peptide peptidase is required for the degradation of selected tail-anchored proteins. *J Cell Biol* 2014;205:847–62. doi:10.1083/jcb.201312009.
- 101 Chen C-Y, Malchus NS, Hehn B, Stelzer W, Avci D, Langosch D, et al. Signal peptide peptidase functions in ERAD to cleave the unfolded protein response regulator XBP1u. *EMBO J* 2014. doi:10.15252/embj.201488208.
- 102 Stevenson PG, Efstathiou S, Doherty PC, Lehner PJ. Inhibition of MHC class I-restricted antigen presentation by gamma 2-herpesviruses. *Proc Natl Acad Sci U S A* 2000;97:8455–60. doi:10.1073/pnas.150240097.
- 103 Boname JM, Stevenson PG. MHC class I ubiquitination by a viral PHD/LAP finger protein. *Immunity* 2001;15:627–36.
- 104 Lybarger L, Wang X, Harris MR, Virgin HW, Hansen TH. Virus subversion of the MHC class I peptide-loading complex. *Immunity* 2003;18:121–30.
- 105 Wang X, Herr RA, Chua W-J, Lybarger L, Wiertz EJHJ, Hansen TH. Ubiquitination of serine, threonine, or lysine residues on the cytoplasmic tail can induce ERAD of MHC-I by viral E3 ligase mK3. *J Cell Biol* 2007;177:613–24. doi:10.1083/jcb.200611063.
- 106 Wang X, Herr R a, Rabelink M, Hoeben RC, Wiertz EJHJ, Hansen TH. Ube2j2 ubiquitinates hydroxylated amino acids on ER-associated degradation substrates. *J Cell Biol* 2009;187:655–68. doi:10.1083/jcb.200908036.
- 107 Herr RA, Harris J, Fang S, Wang X, Hansen TH. Role of the RING-CH domain of viral ligase mK3 in ubiquitination of non-lysine and lysine MHC I residues. *Traffic* 2009;10:1301–17. doi:10.1111/j.1600-0854.2009.00946.x.
- 108 Wang X, Ye Y, Lencer W, Hansen TH. The viral E3 ubiquitin ligase mK3 uses the Derlin/p97 endoplasmic reticulum-associated degradation pathway to mediate down-regulation of major histocompatibility complex class I proteins. *J Biol Chem* 2006;281:8636–44. doi:10.1074/jbc.M513920200.
- 109 Burr ML, Cano F, Svobodova S, Boyle LH, Boname JM, Lehner PJ. HRD1 and UBE2J1 target misfolded MHC class I heavy chains for endoplasmic reticulum-associated degradation. *Proc Natl Acad Sci U S A* 2011;108:2034–9. doi:10.1073/pnas.1016229108.
- 110 Shamu CE, Flierman D, Ploegh HL, Rapoport TA, Chau V. Polyubiquitination is required for US11-dependent

- movement of MHC class I heavy chain from endoplasmic reticulum into cytosol. *Mol Biol Cell* 2001;12:2546–55.
- 111 Flierman D, Ye Y, Dai M, Chau V, Rapoport TA. Polyubiquitin serves as a recognition signal, rather than a ratcheting molecule, during retrotranslocation of proteins across the endoplasmic reticulum membrane. *J Biol Chem* 2003;278:34774–82. doi:10.1074/jbc.M303360200.
- 112 Cadwell K, Coscoy L. Ubiquitination on nonlysine residues by a viral E3 ubiquitin ligase. *Science* 2005;309:127–30. doi:10.1126/science.1110340.
- 113 Burr ML, van den Boomen DJH, Bye H, Antrobus R, Wiertz EJ, Lehner PJ. MHC class I molecules are preferentially ubiquitinated on endoplasmic reticulum luminal residues during HRD1 ubiquitin E3 ligase-mediated dislocation. *Proc Natl Acad Sci U S A* 2013;110:14290–5. doi:10.1073/pnas.1303380110.
- 114 Byun M, Wang X, Pak M, Hansen TH, Yokoyama WM. Cowpox virus exploits the endoplasmic reticulum retention pathway to inhibit MHC class I transport to the cell surface. *Cell Host Microbe* 2007;2:306–15. doi:10.1016/j.chom.2007.09.002.
- 115 McCoy WH, Wang X, Yokoyama WM, Hansen TH, Fremont DH. Structural mechanism of ER retrieval of MHC class I by cowpox. *PLoS Biol* 2012;10:e1001432. doi:10.1371/journal.pbio.1001432.
- 116 Munro S, Pelham HR. A C-terminal signal prevents secretion of luminal ER proteins. *Cell* 1987;48:899–907.
- 117 Pelham HR. Evidence that luminal ER proteins are sorted from secreted proteins in a post-ER compartment. *EMBO J* 1988;7:913–8.
- 118 Andres DA, Dickerson IM, Dixon JE. Variants of the carboxyl-terminal KDEL sequence direct intracellular retention. *J Biol Chem* 1990;265:5952–5.
- 119 Howe C, Garstka M, Al-Balushi M, Ghanem E, Antoniou AN, Fritzsche S, et al. Calreticulin-dependent recycling in the early secretory pathway mediates optimal peptide loading of MHC class I molecules. *EMBO J* 2009;28:3730–44. doi:10.1038/emboj.2009.296.
- 120 Coscoy L, Ganem D. Kaposi's sarcoma-associated herpesvirus encodes two proteins that block cell surface display of MHC class I chains by enhancing their endocytosis. *Proc Natl Acad Sci U S A* 2000;97:8051–6. doi:10.1073/pnas.140129797.
- 121 Ishido S, Wang C, Lee BS, Cohen GB, Jung JU. Downregulation of major histocompatibility complex class I molecules by Kaposi's sarcoma-associated herpesvirus K3 and K5 proteins. *J Virol* 2000;74:5300–9.
- 122 Lang SM, Bynoe MOF, Karki R, Tartell MA, Means RE. Kaposi's sarcoma-associated herpesvirus K3 and K5 proteins down regulate both DC-SIGN and DC-SIGNR. *PLoS One* 2013;8:e58056. doi:10.1371/journal.pone.0058056.
- 123 Sanchez DJ, Gumperz JE, Ganem D. Regulation of CD1d expression and function by a herpesvirus infection. *J Clin Invest* 2005;115:1369–78. doi:10.1172/JCI24041.
- 124 Rhodes DA, Boyle LH, Boname JM, Lehner PJ, Trowsdale J. Ubiquitination of lysine-331 by Kaposi's sarcoma-associated herpesvirus protein K5 targets HFE for lysosomal degradation. *Proc Natl Acad Sci U S A* 2010;107:16240–5. doi:10.1073/pnas.1003421107.
- 125 Li Q, Means R, Lang S, Jung JU. Downregulation of gamma interferon receptor 1 by Kaposi's sarcoma-associated herpesvirus K3 and K5. *J Virol* 2007;81:2117–27. doi:10.1128/JVI.01961-06.
- 126 Ishido S, Choi JK, Lee BS, Wang C, DeMaria M, Johnson RP, et al. Inhibition of natural killer cell-mediated cytotoxicity by Kaposi's sarcoma-associated herpesvirus K5 protein. *Immunity* 2000;13:365–74.
- 127 Coscoy L, Ganem D. A viral protein that selectively downregulates ICAM-1 and B7-2 and modulates T cell costimulation. *J Clin Invest* 2001;107:1599–606. doi:10.1172/JCI12432.
- 128 Barteel E, McCormack A, Früh K. Quantitative membrane proteomics reveals new cellular targets of viral immune modulators. *PLoS Pathog* 2006;2:e107. doi:10.1371/journal.ppat.0020107.
- 129 Mansouri M, Douglas J, Rose PP, Gouveia K, Thomas G, Means RE, et al. Kaposi sarcoma herpesvirus K5 removes CD31/PECAM from endothelial cells. *Blood* 2006;108:1932–40. doi:10.1182/blood-2005-11-4404.



- 130 Thomas M, Wills M, Lehner PJ. Natural killer cell evasion by an E3 ubiquitin ligase from Kaposi's sarcoma-associated herpesvirus. *Biochem Soc Trans* 2008;36:459–63. doi:10.1042/BST0360459.
- 131 Hewitt EW, Duncan L, Mufti D, Baker J, Stevenson PG, Lehner PJ. Ubiquitylation of MHC class I by the K3 viral protein signals internalization and TSG101-dependent degradation. *EMBO J* 2002;21:2418–29. doi:10.1093/emboj/21.10.2418.
- 132 Boname JM, Thomas M, Stagg HR, Xu P, Peng J, Lehner PJ. Efficient internalization of MHC I requires lysine-11 and lysine-63 mixed linkage polyubiquitin chains. *Traffic* 2010;11:210–20. doi:10.1111/j.1600-0854.2009.01011.x.
- 133 Goto E, Yamanaka Y, Ishikawa A, Aoki-Kawasumi M, Mito-Yoshida M, Ohmura-Hoshino M, et al. Contribution of lysine 11-linked ubiquitination to MIR2-mediated major histocompatibility complex class I internalization. *J Biol Chem* 2010;285:35311–9. doi:10.1074/jbc.M110.112763.
- 134 Cadwell K, Coscoy L. The specificities of Kaposi's sarcoma-associated herpesvirus-encoded E3 ubiquitin ligases are determined by the positions of lysine or cysteine residues within the intracytoplasmic domains of their targets. *J Virol* 2008;82:4184–9. doi:10.1128/JVI.02264-07.
- 135 Dodd RB, Allen MD, Brown SE, Sanderson CM, Duncan LM, Lehner PJ, et al. Solution structure of the Kaposi's sarcoma-associated herpesvirus K3 N-terminal domain reveals a novel E2-binding C4HC3-type RING domain. *J Biol Chem* 2004;279:53840–7. doi:10.1074/jbc.M409662200.
- 136 Hofmann RM, Pickart CM. Noncanonical MMS2-encoded ubiquitin-conjugating enzyme functions in assembly of novel polyubiquitin chains for DNA repair. *Cell* 1999;96:645–53.
- 137 Duncan LM, Piper S, Dodd RB, Saville MK, Sanderson CM, Luzio JP, et al. Lysine-63-linked ubiquitination is required for endolysosomal degradation of class I molecules. *EMBO J* 2006;25:1635–45. doi:10.1038/sj.emboj.7601056.
- 138 Ye Y, Rape M. Building ubiquitin chains: E2 enzymes at work. *Nat Rev Mol Cell Biol* 2009;10:755–64. doi:10.1038/nrm2780.
- 139 Goto E, Ishido S, Sato Y, Ohgimoto S, Ohgimoto K, Nagano-Fujii M, et al. c-MIR, a human E3 ubiquitin ligase, is a functional homolog of herpesvirus proteins MIR1 and MIR2 and has similar activity. *J Biol Chem* 2003;278:14657–68. doi:10.1074/jbc.M211285200.
- 140 Bartee E, Mansouri M, Hovey Nerenberg BT, Gouveia K, Früh K. Downregulation of major histocompatibility complex class I by human ubiquitin ligases related to viral immune evasion proteins. *J Virol* 2004;78:1109–20.
- 141 Matsuki Y, Ohmura-Hoshino M, Goto E, Aoki M, Mito-Yoshida M, Uematsu M, et al. Novel regulation of MHC class II function in B cells. *EMBO J* 2007;26:846–54. doi:10.1038/sj.emboj.7601556.
- 142 Ohmura-Hoshino M, Matsuki Y, Aoki M, Goto E, Mito M, Uematsu M, et al. Inhibition of MHC class II expression and immune responses by c-MIR. *J Immunol* 2006;177:341–54.
- 143 De Gassart A, Camosseto V, Thibodeau J, Ceppi M, Catalan N, Pierre P, et al. MHC class II stabilization at the surface of human dendritic cells is the result of maturation-dependent MARCH I down-regulation. *Proc Natl Acad Sci U S A* 2008;105:3491–6. doi:10.1073/pnas.0708874105.
- 144 Furuta K, Walseng E, Roche PA. Internalizing MHC class II-peptide complexes are ubiquitinated in early endosomes and targeted for lysosomal degradation. *Proc Natl Acad Sci U S A* 2013;110:20188–93. doi:10.1073/pnas.1312994110.
- 145 Eyster CA, Cole NB, Petersen S, Viswanathan K, Früh K, Donaldson JG. MARCH ubiquitin ligases alter the itinerary of clathrin-independent cargo from recycling to degradation. *Mol Biol Cell* 2011;22:3218–30. doi:10.1091/mbc.E10-11-0874.
- 146 Walseng E, Furuta K, Bosch B, Weih KA, Matsuki Y, Bakke O, et al. Ubiquitination regulates MHC class II-peptide complex retention and degradation in dendritic cells. *Proc Natl Acad Sci U S A* 2010;107:20465–70. doi:10.1073/pnas.1010990107.
- 147 Van Niel G, Wubbolts R, Ten Broeke T, Buschow SI, Ossendorp FA, Melief CJ, et al. Dendritic cells regulate

- exposure of MHC class II at their plasma membrane by oligoubiquitination. *Immunity* 2006;25:885–94. doi:10.1016/j.immuni.2006.11.001.
- 148 Shin J-S, Ebersold M, Pypaert M, Delamarre L, Hartley A, Mellman I. Surface expression of MHC class II in dendritic cells is controlled by regulated ubiquitination. *Nature* 2006;444:115–8. doi:10.1038/nature05261.
- 149 Tze LE, Horikawa K, Domaschenz H, Howard DR, Roots CM, Rigby RJ, et al. CD83 increases MHC II and CD86 on dendritic cells by opposing IL-10-driven MARCH1-mediated ubiquitination and degradation. *J Exp Med* 2011;208:149–65. doi:10.1084/jem.20092203.
- 150 Ma JK, Platt MY, Eastham-Anderson J, Shin J-S, Mellman I. MHC class II distribution in dendritic cells and B cells is determined by ubiquitin chain length. *Proc Natl Acad Sci U S A* 2012;109:8820–7. doi:10.1073/pnas.1202977109.
- 151 Burgdorf S, Schölz C, Kautz A, Tampé R, Kurts C. Spatial and mechanistic separation of cross-presentation and endogenous antigen presentation. *Nat Immunol* 2008;9:558–66. doi:10.1038/ni.1601.
- 152 Ackerman AL, Kyritsis C, Tampé R, Cresswell P. Early phagosomes in dendritic cells form a cellular compartment sufficient for cross presentation of exogenous antigens. *Proc Natl Acad Sci U S A* 2003;100:12889–94. doi:10.1073/pnas.1735556100.
- 153 Houde M, Bertholet S, Gagnon E, Brunet S, Goyette G, Laplante A, et al. Phagosomes are competent organelles for antigen cross-presentation. *Nature* 2003;425:402–6. doi:10.1038/nature01912.
- 154 Guermónprez P, Saveanu L, Kleijmeer M, Davoust J, Van Endert P, Amigorena S. ER-phagosome fusion defines an MHC class I cross-presentation compartment in dendritic cells. *Nature* 2003;425:397–402. doi:10.1038/nature01911.
- 155 Ackerman AL, Giodini A, Cresswell P. A role for the endoplasmic reticulum protein retrotranslocation machinery during cross-presentation by dendritic cells. *Immunity* 2006;25:607–17. doi:10.1016/j.immuni.2006.08.017.
- 156 Touret N, Paroutis P, Terebiznik M, Harrison RE, Trombetta S, Pypaert M, et al. Quantitative and dynamic assessment of the contribution of the ER to phagosome formation. *Cell* 2005;123:157–70. doi:10.1016/j.cell.2005.08.018.
- 157 Lencer WI, Tsai B. The intracellular voyage of cholera toxin: going retro. *Trends Biochem Sci* 2003;28:639–45. doi:10.1016/j.tibs.2003.10.002.
- 158 Lord JM, Spooner RA. Ricin trafficking in plant and mammalian cells. *Toxins (Basel)* 2011;3:787–801. doi:10.3390/toxins3070787.
- 159 Ackerman AL, Kyritsis C, Tampé R, Cresswell P. Access of soluble antigens to the endoplasmic reticulum can explain cross-presentation by dendritic cells. *Nat Immunol* 2005;6:107–13. doi:10.1038/ni1147.
- 160 Koopmann JO, Albring J, Hüter E, Bulbuc N, Spee P, Neefjes J, et al. Export of antigenic peptides from the endoplasmic reticulum intersects with retrograde protein translocation through the Sec61p channel. *Immunity* 2000;13:117–27.
- 161 Ménager J, Ebstein F, Oger R, Hulin P, Nedellec S, Duverger E, et al. Cross-presentation of synthetic long peptides by human dendritic cells: a process dependent on ERAD component p97/VCP but Not sec61 and/or Derlin-1. *PLoS One* 2014;9:e89897. doi:10.1371/journal.pone.0089897.
- 162 Kaufmann SH, Schaible UE. Antigen presentation and recognition in bacterial infections. *Curr Opin Immunol* 2005;17:79–87. doi:10.1016/j.coi.2004.12.004.
- 163 Bomberger JM, Ely KH, Bangia N, Ye S, Green KA, Green WR, et al. *Pseudomonas aeruginosa* Cif protein enhances the ubiquitination and proteasomal degradation of the transporter associated with antigen processing (TAP) and reduces major histocompatibility complex (MHC) class I antigen presentation. *J Biol Chem* 2014;289:152–62. doi:10.1074/jbc.M113.459271.
- 164 Albaghdadi H, Robinson N, Finlay B, Krishnan L, Sad S. Selectively reduced intracellular proliferation of *Salmonella enterica* serovar typhimurium within APCs limits antigen presentation and development of a rapid CD8 T cell response. *J Immunol* 2009;183:3778–87. doi:10.4049/jimmunol.0900843.

- 165 Maman Y, Nir-Paz R, Louzoun Y. Bacteria modulate the CD8+ T cell epitope repertoire of host cytosol-exposed proteins to manipulate the host immune response. *PLoS Comput Biol* 2011;7:e1002220. doi:10.1371/journal.pcbi.1002220.
- 166 Smiley JR. Herpes simplex virus virion host shutoff protein: immune evasion mediated by a viral RNase? *J Virol* 2004;78:1063–8.
- 167 Abendroth A, Lin I, Slobedman B, Ploegh H, Arvin AM. Varicella-zoster virus retains major histocompatibility complex class I proteins in the Golgi compartment of infected cells. *J Virol* 2001;75:4878–88. doi:10.1128/JVI.75.10.4878-4888.2001.
- 168 Eisfeld AJ, Yee MB, Erazo A, Abendroth A, Kinchington PR. Downregulation of class I major histocompatibility complex surface expression by varicella-zoster virus involves open reading frame 66 protein kinase-dependent and -independent mechanisms. *J Virol* 2007;81:9034–49. doi:10.1128/JVI.00711-07.
- 169 Zuo J, Thomas W, van Leeuwen D, Middeldorp JM, Wiertz EJHJ, Rensing ME, et al. The DNase of gammaherpesviruses impairs recognition by virus-specific CD8+ T cells through an additional host shutoff function. *J Virol* 2008;82:2385–93. doi:10.1128/JVI.01946-07.
- 170 Rowe M, Glaunsinger B, van Leeuwen D, Zuo J, Sweetman D, Ganem D, et al. Host shutoff during productive Epstein-Barr virus infection is mediated by BGLF5 and may contribute to immune evasion. *Proc Natl Acad Sci U S A* 2007;104:3366–71. doi:10.1073/pnas.0611128104.
- 171 Zuo J, Currin A, Griffin BD, Shannon-Lowe C, Thomas WA, Rensing ME, et al. The Epstein-Barr virus G-protein-coupled receptor contributes to immune evasion by targeting MHC class I molecules for degradation. *PLoS Pathog* 2009;5:e1000255. doi:10.1371/journal.ppat.1000255.
- 172 Park B, Spooner E, Houser BL, Strominger JL, Ploegh HL. The HCMV membrane glycoprotein US10 selectively targets HLA-G for degradation. *J Exp Med* 2010;207:2033–41. doi:10.1084/jem.20091793.
- 173 Kleijnen MF, Huppa JB, Lucin P, Mukherjee S, Farrell H, Campbell AE, et al. A mouse cytomegalovirus glycoprotein, gp34, forms a complex with folded class I MHC molecules in the ER which is not retained but is transported to the cell surface. *EMBO J* 1997;16:685–94. doi:10.1093/emboj/16.4.685.
- 174 Babić M, Pyzik M, Zafirova B, Mitrović M, Butorac V, Lanier LL, et al. Cytomegalovirus immunoevasin reveals the physiological role of “missing self” recognition in natural killer cell dependent virus control in vivo. *J Exp Med* 2010;207:2663–73. doi:10.1084/jem.20100921.
- 175 Reusch U, Muranyi W, Lucin P, Burgert HG, Hengel H, Koszinowski UH. A cytomegalovirus glycoprotein re-routes MHC class I complexes to lysosomes for degradation. *EMBO J* 1999;18:1081–91. doi:10.1093/emboj/18.4.1081.
- 176 Khan S, Zimmermann A, Basler M, Groettrup M, Hengel H. A cytomegalovirus inhibitor of gamma interferon signaling controls immunoproteasome induction. *J Virol* 2004;78:1831–42.
- 177 Ziegler H, Thale R, Lucin P, Muranyi W, Flohr T, Hengel H, et al. A mouse cytomegalovirus glycoprotein retains MHC class I complexes in the ERGIC/cis-Golgi compartments. *Immunity* 1997;6:57–66.
- 178 Hudson AW, Howley PM, Ploegh HL. A human herpesvirus 7 glycoprotein, U21, diverts major histocompatibility complex class I molecules to lysosomes. *J Virol* 2001;75:12347–58. doi:10.1128/JVI.75.24.12347-12358.2001.
- 179 Hudson AW, Blom D, Howley PM, Ploegh HL. The ER-luminal domain of the HHV-7 immunoevasin U21 directs class I MHC molecules to lysosomes. *Traffic* 2003;4:824–37.
- 180 Glosson NL, Hudson AW. Human herpesvirus-6A and -6B encode viral immunoevasins that downregulate class I MHC molecules. *Virology* 2007;365:125–35. doi:10.1016/j.virol.2007.03.048.
- 181 Glosson NL, Gonyo P, May NA, Schneider CL, Ristow LC, Wang Q, et al. Insight into the mechanism of human herpesvirus 7 U21-mediated diversion of class I MHC molecules to lysosomes. *J Biol Chem* 2010;285:37016–29. doi:10.1074/jbc.M110.125849.
- 182 May NA, Glosson NL, Hudson AW. Human herpesvirus 7 u21 downregulates classical and nonclassical class I major histocompatibility complex molecules from the cell surface. *J Virol* 2010;84:3738–51. doi:10.1128/

## Chapter 2

---

JVI.01782-09.

- 183 Glaunsinger B, Ganem D. Lytic KSHV infection inhibits host gene expression by accelerating global mRNA turnover. *Mol Cell* 2004;13:713–23.
- 184 Glaunsinger B, Chavez L, Ganem D. The exonuclease and host shutoff functions of the SOX protein of Kaposi's sarcoma-associated herpesvirus are genetically separable. *J Virol* 2005;79:7396–401. doi:10.1128/JVI.79.12.7396-7401.2005.





## CHAPTER 3

# A high-complexity shRNA library screen identifies TMEM129 as E3 ligase involved in ER-associated protein degradation

Michael L. van de Weijer<sup>1</sup>, Michael C. Bassik<sup>2,7</sup>, Rutger D. Luteijn<sup>1</sup>, Cornelia M. Voorburg<sup>1</sup>, Mirjam A.M. Lohuis<sup>1</sup>, Elisabeth Kremmer<sup>3</sup>, Rob C. Hoeben<sup>4</sup>, Emily M. LeProust<sup>5,7</sup>, Siyuan Chen<sup>5,7</sup>, Hanneke Hoelen<sup>1</sup>, Maaïke E. Ressing<sup>1,4</sup>, Weronika Patena<sup>2,6,7</sup>, Jonathan S. Weissman<sup>2</sup>, Michael T. McManus<sup>6,\*</sup>, Emmanuel J.H.J. Wiertz<sup>1,\*</sup>, Robert Jan Lebbink<sup>1,\*</sup>

<sup>1</sup>Medical Microbiology, University Medical Center Utrecht, Utrecht 3584CX, The Netherlands

<sup>2</sup>Department of Cellular and Molecular Pharmacology, California Institute for Quantitative Biomedical Research, and Howard Hughes Medical Institute, University of California, San Francisco, California 94158, USA

<sup>3</sup>Helmholtz Zentrum München, German Research Center for Environmental Health, Institute of Molecular Immunology, 81377 Munich, Germany

<sup>4</sup>Department of Molecular Cell Biology, Leiden University Medical Center, Leiden 2333ZC, The Netherlands

<sup>5</sup>Genomics Solution Unit, Agilent Technologies Inc., Santa Clara, California 95051, USA <sup>6</sup>Department of Microbiology and Immunology, University of California, San Francisco, California 94143, USA

<sup>7</sup>Present address: M.C.B., Department of Genetics, Stanford University, California 94305, USA; E.M.L. and S.C., Twist Bioscience, San Francisco, CA 94158, USA; W.P., Carnegie Institution for Science, Department of Plant Biology, Stanford, California 94305, USA

\*These authors contributed equally to this work

Published in:

Nature Communications 5 (2014) 3832. doi:10.1038/ncomms4832

## **ABSTRACT**

Misfolded ER proteins are retrotranslocated into the cytosol for degradation via the ubiquitin-proteasome system. The human cytomegalovirus protein US11 exploits this ER-associated protein degradation (ERAD) pathway to downregulate HLA class I molecules in virus-infected cells, thereby evading elimination by cytotoxic T-lymphocytes. US11-mediated degradation of HLA class I has been instrumental in the identification of key components of mammalian ERAD, including Derlin1, p97, VIMP, and SEL1L. Despite this, the process governing retrotranslocation of the substrate is still poorly understood. Here, using a high-coverage genome-wide shRNA library, we identify the uncharacterized protein TMEM129 and the ubiquitin-conjugating E2 enzyme UBE2J2 to be essential for US11-mediated HLA class I downregulation. TMEM129 is an unconventional C4C4-type RING finger E3 ubiquitin ligase that resides within a complex containing various other ERAD components, including Derlin-1, Derlin-2, VIMP, and p97, indicating that TMEM129 is an integral part of the ER-resident dislocation complex mediating US11-induced HLA class I degradation.



## INTRODUCTION

In the ER, newly synthesized proteins undergo a quality check by chaperones, which attempt to induce proper folding [1]. Failure to do so may result in protein accumulation and aggregation in the ER, thereby compromising protein and cellular homeostasis [2,3]. To prevent this, terminally misfolded luminal and transmembrane ER proteins are targeted for ubiquitin-dependent degradation by the proteasome in the cytosol [4], a process called ER-associated protein degradation (ERAD) [5,6]. This process depends on retrograde transport, or dislocation, of proteins into the cytosol via a reaction that is facilitated by a multiprotein complex that combines several functions essential for ERAD, such as recognition, guidance, ubiquitination, dislocation, and deglycosylation of the substrate [7,8]. ERAD is not only used for removal of misfolded proteins, but also for physiologically regulated proteolysis of ER-resident proteins [9,10].

Human cytomegalovirus (HCMV) encodes several proteins that impair the HLA class I antigen presentation pathway [11], thus avoiding detection of infected cells by cytotoxic T lymphocytes [12]. In particular, HCMV US11 exploits ERAD to induce rapid dislocation of newly synthesized HLA class I heavy chains (HCs) from the ER into the cytosol, where the HCs are subsequently degraded via the ubiquitin-proteasome system [13]. The ER luminal domain of US11 is required for interaction with HLA class I, while the transmembrane domain of US11 is essential for interaction with Derlin-1 [14–16]. In this way, US11 recruits the HLA class I molecule to the dislocation complex, which besides Derlin-1 [14,17] contains VIMP [17], the AAA ATPase p97 [17,18], Derlin-2 [19], and SEL1L [19]. HLA class I is then ubiquitinated, dislocated, and subsequently directed towards the proteasome for degradation [13,17–21].

The US11-mediated degradation of HLA class I has been instrumental in the identification of key components of mammalian ERAD, such as Derlin-1 [15,17], p97 [18], VIMP [17], and SEL1L [22]. However, a complete understanding of the dislocation complex and its modes of action is currently lacking. Most known pathways of ERAD rely on multispansing transmembrane E3 ubiquitin ligases containing a cytosolic RING domain [23], such as the yeast Hrd1p [24] and Doa10 [25], and the mammalian HRD1 (mammalian homolog of yeast Hrd1p) [26], AMFR/gp78 [27], TEB4 (mammalian homolog of yeast Doa10) [28], and TRC8 [29]. The RING domain of the E3 ubiquitin ligase forms a docking site for an E2 ubiquitin-conjugating enzyme, which in turn catalyzes polyubiquitination of target substrates [30]. In the context of US11-induced HLA class I degradation, the E3 ubiquitin ligase responsible has remained elusive.

Functional genomics in mammalian cells has been greatly aided by the use of silencing techniques to study loss-of-function phenotypes. Long term silencing and analysis of non-transfectable cell lines can be achieved by genomic integration of short-hairpin RNAs (shRNAs) through the use of viral vectors for delivery [31]. As with other RNAi-based approaches, the shRNA utility is limited by the low efficacy of many shRNAs, resulting in

high false-negative rates, and by off-target effects, leading to high false-positive rates [32]. To overcome these issues, we recently reported on the use of pooled ultracomplex shRNA libraries where each gene is targeted by many different shRNA sequences [33,34]. When combined with deep-sequencing-based readouts [33,35], such pooled shRNA library screens allow accurate massive multiplexing in a controlled, identical environment for all cells.

Here, we construct a novel high-complexity shRNA library targeting all known human protein-encoding genes and subsequently perform a genome-wide screen to identify novel proteins that are essential for US11-mediated HLA class I degradation. Besides known players, we identify the previously uncharacterized TMEM129 and the ubiquitin-conjugating E2 enzyme UBE2J2 as essential components for US11-mediated HLA class I downregulation. We demonstrate that TMEM129 is a C4C4-type RING E3 ubiquitin ligase, of which its RING domain is essential for US11-mediated HLA class I downregulation. Co-immunoprecipitation studies indicate that TMEM129 is present in US11-containing dislocation complexes. Besides the previously reported UBE2K, also UBE2J2 is essential for US11-mediated HLA class I downregulation and it is part of TMEM129-containing dislocation complexes. Notably, TMEM129 is associated with various dislocation components independently of US11, suggesting that TMEM129 might be involved in ERAD of proteins outside the context of HCMV-mediated HLA class I degradation.

## MATERIALS & METHODS

**Cell culture and lentiviral infection.** U937 human monocytic cells, 293T human embryonic kidney cells, and MeJuSo (MJS) human melanoma cells were obtained from ATCC (American Type Culture Collection) and grown in RPMI medium supplemented with glutamine, penicillin/streptomycin, and 10% FCS. For individual gene infections using lentiviruses, virus was produced in 24-well plates using standard lentiviral production protocols and 3<sup>rd</sup> generation packaging vectors, and 50ul viral supernatant adjusted to 8 mg/ml polybrene was used to infect approximately 20,000 cells by spin infection at 1,000 x g for 2 hrs at 33°C.

**Plasmids.** Several different lentiviral vectors were used in the present studies. The N-terminally eGFP and Myc-tagged human HLA-A2 vector present in the lentiviral pHRsincPPT-SGW vector was kindly provided by Dr. Paul Lehner and Dr. Louise Boyle (University of Cambridge, Cambridge UK). The pooled shRNA library vector is described in the 'genome-wide shRNA screen' paragraph in the Methods section. Individual shRNAs were derived from the Mission shRNA library (Sigma-Aldrich, St. Louis, MO). Typically, we tested 5 different shRNAs per gene. The ones that were used for figures in this manuscript are presented in Supplementary Table 1. For rescue and overexpression experiments, we cloned tagged and untagged cDNAs from TMEM129, UBE2J1, UBE2J2, HRD1 and US11 in a dual promoter lentiviral vector (#2025.pCCLsin.PPT.pA.CTE.4x-scrT.eGFP.mCMV.hPGK.NGFR.

pre, kindly provided by Dr. Luigi Naldini, San Raffaele Scientific Institute, Milan, Italy). This vector was altered to: replace the minimal CMV promoter with the human EF1A promoter to facilitate potent expression in immune cells; replace the eGFP with a cassette containing several unique restriction sites facilitating DNA cloning (NheI, PaeI, PmeI, AfeI, SphI, SphI, and NsiI); and replace the NGFR gene with various combinations of fluorescent proteins (mCherry, mAmetrine) and selection markers (PuroR, BlastR, ZeoR, and HygroR), which were fused together by means of the ribosomal skipping peptide T2A. The choice of vector used was dictated by the presence of other fluorescent and selection markers in the cell lines in question. For confocal co-localization studies, we used the same dual promoter lentiviral vectors described above in which we either cloned TMEM129 C-terminally fused to a FLAG-epitope and eGFP (TMEM129-eGFP), mCherry alone (mCherry), mCherry N-terminally tagged to amino acids 1-60 of the human galactosyltransferase (GalT-mCherry), or mCherry fused to a C-terminal BiP-leader and N-terminal KDEL-sequence (mCherry-KDEL).

RING-less TMEM129 was generated by removing amino acids 285-362. Dominant-negative UBE2J2 was generated by mutating the cysteine of the active site at position 94 into a serine, as described previously [44]. When indicated, we used the following (epitope) tags: HA-tag (YPYDVPDYA), Myc-tag (EQKLISEEDL), FLAG-tag (DYKDDDDK), and triple Strep-Tag II (ST2; WSHQPFEKGSWSHPQFEKGSWSHPQFEKGS). For CRISPR/Cas experiments, we obtained vectors from the Church lab [48] via Addgene (Addgene plasmid 41824: gRNA\_Cloning Vector, and Addgene plasmid 41815: Cas9 expression vector). Additionally, we constructed a selectable lentiviral CRISPR/Cas vector (which will be described elsewhere, manuscript in preparation) to facilitate efficient and selectable expression of Cas9 and gRNAs in target cells: briefly, the lentiviral pSicoR vector (Jacks lab, MIT) was altered to express a nuclear localized Cas9 gene which was N-terminally fused to puroR and a T2A sequence. Additionally, the region immediately downstream of the U6 promoter was replaced by a cassette consisting of two unique restriction sites (BsmBI) to allow cloning of gRNA target sites followed by the gRNA scaffold and a terminator consisting of 5 T-residues.

**Pooled shRNA libraries.** We designed shRNAs targeting all protein-encoding transcripts in human cells using the shRNA retriever program [49], which generates shRNAs with 22-nucleotide guide strands. We designed oligos consisting of the shRNA hairpin (fully complementary 22bp arms, and a 9bp loop) surrounded by 3' and 5' primer binding sites. The shRNAs include an initial G before the sense arm, for correct expression by the U6 promoter, a complementary C after the antisense arm, and a TTTT (UUUUU in the RNA sequence) terminator to end transcription immediately after the hairpin. Oligonucleotides encoding shRNAs in a sub-library of 55,000 sequences were synthesized by Agilent, and used to generate shRNA libraries as previously described [33]. 12 sub-libraries were generated where genes were organized into functionally related groups, using GO annotation, curated localization, and data from various proteomic surveys of organelles. ShRNAs were cloned

into our vector MP-177, for which a detailed map will be provided on request. This vector was derived from the lentiviral pSicoR vector (Jacks lab, MIT) in which the U6 promoter was altered to allow for sticky cloning of shRNAs in between a BstXI and XhoI site, and in which the CMV promoter was used to drive expression a cassette encoding a puromycin resistance marker, the ribosomal skipping peptide T2A, and mCherry. Library quality was evaluated by sequencing 96 colonies from each sub-library, the percentage of perfect sequences ranged from 58 to 76% with an average of 66%. The coverage of each library ranged from 31 to 128 fold with an average of 50 fold, as assessed by bacterial colony counts.

**Genome-wide shRNA screen.** U937 monocytic cells co-expressing eGFP-Myc-HLA-A2 and US11 were grown in RPMI medium supplemented with glutamine, penicillin/streptomycin, and 10% FCS. Virus was produced in 15cm plates of 293T cells using standard lentivirus production protocols. For each screen, approximately  $160 \times 10^6$  cells were infected with the entire genome-wide shRNA library in 320 ml virus supernatant supplemented with 8 mg/ml polybrene, divided into wells of a 6-well plate, and spin-infected at  $1,000 \times g$  for 2 hrs at  $33^\circ C$  to reach a target infection of approximately 80%. 6 days after infection, approximately  $800 \times 10^6$  cells were harvested and subjected to cell sorting via a two-step sort-protocol using a Becton Dickinson Influx cell sorter. First, eGFP-upregulated cells were sorted using an 'enrichment-protocol', which allowed for high-speed cell sorting of the entire population of cells in a short timeframe. Next, the selected cells were sorted for purity selecting mCherry-positive cells (cells transduced with an shRNA lentivector) and eGFP-bright cells. The top 0.75% of eGFP<sup>bright</sup> cells was selected, which resulted in a total of approximately  $2.8 \times 10^6$  cells/screen. As control, approximately  $115 \times 10^6$  mCherry-positive, eGFP<sup>dim</sup> cells were sorted. Subsequently, genomic DNA was isolated from the selected cells using standard phenol-chloroform extractions. Next, the lentiviral shRNA inserts were PCR amplified for 23 cycles using primers AATGATACGGCGACCACCGACTCTTTCCacaaaaggaaactcacctaac and CAAGCAGAAGACGGCATAACGAgcggtatacggttatccacg and Phusion polymerase (NEB) in the presence of buffer GC supplemented with DMSO. These primers contain Illumina adapter sequences (displayed in capital letters) that allow direct loading on an Illumina HiSeq2000 sequencer. As input we PCR'd from genomic DNA equivalent to approximately  $2.8 \times 10^6$  cells for the selected eGFP<sup>bright</sup> cells, and  $20 \times 10^6$  cells for the eGFP<sup>dim</sup> control cells. This resulted in approximately 35 and 250 50ul PCR reactions for the selected and control cells respectively. The PCR products were pooled and purified/concentrated using a PCR purification kit (Qiagen), and subsequently loaded on a 20% polyacrylamide gel in 0.5X TBE. Bands of the correct size were excised, electro-eluted, purified by phenol-chloroform extraction, and subsequently quantitated using a Nanodrop quantification device (Nanodrop, Rockland, DE) and an Agilent bioanalyzer (Agilent Technologies, Palo Alto, CA, USA). Deep sequencing was carried out on an Illumina HiSeq2000 (performed by BGI, Hong Kong) using the sequencing primer GAGACTATAAGTATCCCTTGAGAACACCTTGTGG, in which the guide strands of the

shRNA-encoding constructs were detected. Sequences were aligned to the known library sequences using Bowtie [50] and the counts per shRNA were calculated. On average we obtained approximately  $78 \times 10^6$  aligned sequences per sample, which ranged from  $56 \times 10^6$  cells to  $106 \times 10^6$  reads/sample. To identify hit genes in the genome-wide screen, we calculated a P-value for each gene in our library using a Mann-Whitney U test as described previously [34]. The genome-wide screen was carried out in two independent replicates and the overlap between the top 100 genes with the lowest p-values from both screens was selected as hit list. These hits were assessed for enrichment of GO terms using DAVID [51,52] and network analysis was performed using Ingenuity pathway analysis (Ingenuity Systems, Redwood City, CA).

**Generation of CRISPR/Cas-mediated knockout cells.** U937 cells co-expressing eGFP-Myc-HLA-A2 and US11 were transfected twice on subsequent days using the Neon Transfection System (Life technologies, Breda, The Netherlands) with a Cas9-encoding vector and a gRNA expression vector targeting human TMEM129. Typically, we obtained approximately 10% knockout cells as determined by flow-cytometry assessment of upregulated total eGFP-Myc-HLA-A2 (eGFP) levels. Cells were sorted by flow cytometry (FACS AriaII, BD Biosciences) and single-cell cloned by limiting dilution.

Later on, we moved to a lentiviral CRISPR/Cas system (see 'Plasmids' section) in which a single lentiviral vector co-expresses a Cas9, puromycin and a gRNA sequence. Virus was produced and cells were infected as described in the 'Cell Culture and Lentiviral Infection' section. Two days post-infection, infected cells were selected by using  $2 \mu\text{g/ml}$  puromycin and allowed to recover. Typically, we observed 30-90% of selected cells to display a full knockout phenotype as assessed by flow cytometry. See also Supplementary Table 2 for gRNA sequences used in this study and Supplementary Figure 8 for a visualization of the genomic target sites of these gRNAs.

**Antibodies.** Primary antibodies used in our studies were: mouse  $\alpha$ -HLA class I HC HC10 mAb; mouse  $\alpha$ -HLA class I HC HCA2 mAb; human  $\alpha$ -HLA-A3 OK2F3 mAb (kindly provided by Dr. Arend Mulder and Dr. Frans Claas (LUMC), 1:40); rabbit  $\alpha$ -VIMP pAb (1:500, kindly provided by Y. Ye, NIH, Bethesda, MD) [17]; rabbit  $\alpha$ -US11 pAb (1:1000) [20]; rabbit  $\alpha$ -Derlin-1 pAb (#PM018, MBL, 1:1000); rabbit  $\alpha$ -Derlin-2 pAb (#PM019, MBL, 1:1000); mouse  $\alpha$ -VCP/p97 18/VCP mAb (#612183, BD Transduction laboratories, 1:1000); rabbit  $\alpha$ -SEL1L pAb (#S3699, Sigma-Aldrich, 1/1000), rabbit  $\alpha$ -HRD1 pAb (#AP2184a, Abgent, 1:1000), mouse  $\alpha$ -Ub P4D1 mAb (#SC-8017, Santa Cruz Biotechnology, 1:400); mouse  $\alpha$ -Actin C4 mAb (#MAB1501R, Millipore, 1:10000); mouse  $\alpha$ -TfR H68.4 mAb (#13-68xx, Invitrogen, 1:2000); mouse  $\alpha$ -FLAG-M2 mAb (#F1804, Sigma-Aldrich, 1:50000); rat  $\alpha$ -HA 3F10 mAb (#11867423001, Roche, 1:1000); mouse  $\alpha$ -Myc 9E10 mAb (UCSF hybridoma core, 1:200); mouse  $\alpha$ -Myc 9E10-biotin mAb (UCSF hybridoma core, 1:200); rat  $\alpha$ -TMEM129 4G10 and 13E2 mAbs (E.

Kremmer, Helmholtz Zentrum München, 1:5); mouse  $\alpha$ -TMEM129 8D7 and 8G9 mAbs (E. Kremmer, Helmholtz Zentrum München, 1:5).

Secondary antibodies used in our studies were: F(ab')<sub>2</sub> fragment goat  $\alpha$ -human IgG+IgM(H+L)-PE (#109-116-127, Jackson ImmunoResearch, 1:160); streptavidin-BV421 (#405226, BioLegend, 1:160); goat  $\alpha$ -mouse IgG(H+L)-HRP (#170-6516, Bio-Rad, 1:10000); goat  $\alpha$ -rabbit IgG(H+L)-HRP (#4030-05, Southern Biotech, 1:10000); mouse  $\alpha$ -rabbit IgG(L)-HRP (#211-032-171, Jackson Immunoresearch, 1:10000); goat  $\alpha$ -mouse IgG(L)-HRP (#115-035-174, Jackson Immunoresearch, 1:10000); Goat  $\alpha$ -rat IgG(L)-HRP (#112-035-175, Jackson Immunoresearch, 1:10000); mouse  $\alpha$ -rat IgG1-HRP (E. Kremmer, Helmholtz Zentrum München, 1:1000); mouse  $\alpha$ -rat IgG2c-HRP (E. Kremmer, Helmholtz Zentrum München, 1:1000); rat  $\alpha$ -mouse IgG2a-HRP (E. Kremmer, Helmholtz Zentrum München, 1:1000).

**Generation of TMEM129-specific mAbs.** TMEM129-specific rat and mouse monoclonal Abs were prepared by immunizing respectively Lou/C rats and CBL mice with OVA-coupled peptides encompassing TMEM129 amino acids 191-204 (VTESRQHELSPDSN). Hybridomas were subsequently generated using standard hybridoma culturing techniques. The following TMEM129-specific mAbs were used: 4G10 of rat subclass IgG1, 13E2 of isotype IgG2c, and 8D7 and 8G9 mAbs both of mouse subclass IgG2a. TMEM129-specificity of these mAbs in immunoblotting and immunoprecipitation experiments is shown in Supplementary Figure 9a-d.

**Flow cytometry.** To assess HLA class I expression levels, cells were first fixed in 0.5% PFA and subsequently washed in FACS buffer (PBS, 0.5% BSA, 0.02% sodium azide). All subsequent staining protocols and washings were performed in FACS buffer. Endogenous HLA-A3 surface expression and eGFP-Myc-HLA-A2 surface expression were assessed by staining with human  $\alpha$ -HLA-A3 OK2F3 mAb and mouse  $\alpha$ -Myc 9E10-biotin mAb, respectively. Secondary antibodies used were F(ab')<sub>2</sub> fragment goat  $\alpha$ -human IgG+IgM(H+L)-PE and streptavidin-BV421, respectively. Afterwards, cells were subjected to flow cytometry acquisition on a FACSCantoll (BD Bioscience). Flow cytometry data were analyzed using FlowJo software.

**Immunoprecipitations.** Cells were lysed in 1% Triton X-100 lysis buffer (1.0% Triton X-100, 20 mM MES, 100 mM NaCl, 30 mM Tris, pH 7.5) containing 1 mM Pefabloc SC (Roche) and 10  $\mu$ M Leupeptin (Roche). Cell fragments were pelleted at 12,000g for 20 min at 4°C. Postnuclear supernatants were incubated for at least 2 hrs with Protein A or G Sepharose beads (GE Healthcare) and indicated antibodies. After four washes in IP washing buffer (1.0% Triton X-100, 100 mM NaCl; 30 mM Tris, pH 7.5), proteins were eluted in Laemmli sample buffer. Immunoblotting was performed as described below.

**Co-immunoprecipitations.** Cells were lysed in 1% Digitonin lysis buffer (1% Digitonin

(Calbiochem), 50 mM TrisHCl, 5 mM MgCl<sub>2</sub>, 150 mM NaCl; pH 7.5) containing 1 mM Pefabloc SC (Roche) and 10 μM Leupeptin (Roche). Lysates were incubated for 90 minutes at 4°C. Cell fragments were pelleted 12,000 x g for 20 min at 4°C. Postnuclear supernatants were incubated overnight with StrepTactin beads (GE Healthcare), or FLAG-M2-coupled beads (Sigma). After four washes in 1% digitonin lysis buffer, proteins were eluted in elution buffer (For StrepTactin beads: 2.5 mM desthiobiotin, 150 mM NaCl, 100 mM Tris-HCl, 1 mM EDTA, pH 8; For FLAG-M2-coupled beads: 500 μg/mL FLAG peptide, 150 mM NaCl, 100 mM Tris-HCl, pH 7.5) for 30 minutes on ice. Beads were pelleted, the supernatant was transferred to a new tube, and subsequently denatured in Laemmli sample buffer containing DTT. Immunoblotting was performed as described below.

**Immunoblotting.** Samples were incubated at 95°C for 5 min, separated by SDS-PAGE, and proteins were transferred to PVDF membranes (Immobilon-P, Millipore). Membranes were probed with indicated antibodies. Reactive bands were detected by ECL (Thermo Scientific Pierce), and exposed to Amersham Hyperfilm ECL films (GE Healthcare).

***In vitro* ubiquitination assay.** Cells were lysed in 1% Triton X-100 lysis buffer (1.0% Triton X-100, 20 mM MES, 100 mM NaCl, 30 mM Tris, pH 7.5) containing 1 mM Pefabloc SC (Roche) and 10 μM Leupeptin (Roche). Cell fragments were pelleted at 12,000 x g for 20 min at 4°C. Postnuclear supernatants were incubated overnight with StrepTactin beads (GE Healthcare). After four washes in stringent IP washing buffer (1.0% Triton X-100, 400 mM NaCl, 20 μM ZnSO<sub>4</sub>, 30 mM Tris, pH 7.5), proteins were eluted in elution buffer (2.5 mM desthiobiotin, 150 mM NaCl, 20 μM ZnSO<sub>4</sub>, 100 mM Tris-HCl, pH 8) for 30 minutes on ice. Beads were pelleted, and the supernatant was directly used in the *in vitro* ubiquitination assay. The MuRF1/S5a ubiquitination kit (#K-102) was purchased from Boston Biochem, and reactions were performed as described by the manufacturer. To test the E3 ubiquitin ligase activity of TMEM129, GST-MuRF1 was replaced by immunoprecipitated TMEM129(ΔRING)-FLAG-ST2. Immunoblotting was performed as described above.

**Pulse-chase analysis.** To study HLA class I dislocation, cells were pre-incubated with 20 μM MG132 (Sigma-Aldrich) for 4 hrs. All subsequent steps were performed in the presence of 20 μM MG132. To study HLA class I degradation, cells were not treated with a proteasome inhibitor. Cells were starved for 30 min in Met- and Cys-free medium, and pulsed for 10 min with EasyTag™ EXPRESS [<sup>35</sup>S] Protein Labeling Mix (20 Mbq/10<sup>6</sup> cells/mL; Perkin-Elmer). Cells were chased for the indicated time periods and lysed in 1% Triton X-100 lysis buffer. HLA class I HCs were immunoprecipitated as described above. Samples were incubated at 95°C for 5 min, separated by SDS-PAGE (12%), and bands were visualized by exposure to a BioMAX MR High Resolution film (Kodak).

**Fluorescence confocal microscopy.** MelJuSo cells were grown overnight on 12mm circular glass coverslips. Attached cells were washed with PBS supplemented with 0.5mM MgCl<sub>2</sub> and 1mM CaCl<sub>2</sub> (PBS++) and fixed in 3% paraformaldehyde for 15 min at room temperature. Coverslips were washed again in PBS++ and embedded on microscope slides with Mowiol 4-88 (Carl Roth, Germany). Slides were air-dried overnight at room temperature and imaged using a Leica TCS SP5 confocal microscope equipped with a HCX PL APO CS 63×/1.40-0.60 OIL objective (Leica Microsystems, the Netherlands). eGFP and mCherry fluorescent signals were detected with PMTs set at the appropriate bandwidth after excitation using the 488nm argon laser for eGFP and the 543 nm helium neon laser for mCherry. Images were processed and analyzed using Leica SP5 software.

**UPR assessment.** Cells were either incubated with Thapsigargin (50 μM) or DMSO. After 6 hours of incubation, cells were harvested, and mRNA was isolated using standard Trizol RNA isolation procedures. Possible genomic DNA contamination was removed using a TURBO DNase kit (Life Technologies) according to the manufacturer's protocol. Using oligo dT primers, mRNA was specifically reverse transcribed into cDNA (SuperScriptIII, Invitrogen) according to the manufacturer's protocol. GAPDH and XBP-1 were then amplified using specific primers (Supplementary Table 3) and DreamTaq Green (Fermentas). PCR products were separated in SYBRsafe (Life Technologies)-containing 2.5% agarose.



## RESULTS

### An shRNA screen identifies TMEM129 as player in HLA-I ERAD

We have previously established a screening platform in which pooled shRNA library screens were coupled to deep-sequencing as a means to perform large RNAi screens in a single population of cells [33,34,36]. Here, we constructed a new pooled lentiviral shRNA library targeting each annotated human protein-coding gene with approximately 30 independent shRNAs (see Methods section for details). We exploited this new resource to identify proteins that are essential for US11-mediated HLA class I downregulation in human cells. To this end, U937 monocytic cells were generated expressing a chimeric HLA-A2 molecule that was N-terminally tagged with eGFP and a Myc-epitope (eGFP-Myc-HLA-A2). In this way, relative total HLA class I expression can be measured by assessing the eGFP signal and surface display can be visualized by flow cytometry using a Myc-specific antibody. As expected, introduction of the HCMV US11 protein into these cells induced potent downregulation of the chimeric HLA-A2 molecule as well as that of endogenously expressed HLA-A3 (Supplementary Fig. 1a).

A single population of U937 cells co-expressing eGFP-Myc-HLA-A2 and US11 was infected with the pooled shRNA library and the cells were divided into eGFP-bright and -dim populations by FACS sorting. Subsequently, we assessed which shRNAs were enriched in the eGFP-bright population as compared to the eGFP-dim population and performed statistical analysis on these (Fig. 1a). Two independent screens were executed and the overlap of the top 100 enriched genes from both screens is presented as our primary hit list in Table 1. GO-term enrichment analysis of the hits showed a strong enrichment for genes involved in Golgi vesicle transport and proteasome-dependent catabolic processes (Fig. 1b). Indeed, network analysis of the hits revealed two clear clusters comprising most members of the coat protein complex involved in retrograde transport of proteins from the Golgi complex back to the rough ER [37] (Fig. 1c), and numerous proteasome subunits (Fig. 1d). Since it is known that US11-mediated ERAD of HLA class I relies on ubiquitin-dependent proteasomal degradation of the HLA class I substrate [13], we expected to identify proteasome subunits in our screen. Additionally, the valosin-containing protein (VCP, commonly referred to as p97) was a clear hit. p97 is an AAA ATPase responsible for extracting and shuttling dislocated substrates from the ER environment towards the proteasome for degradation [18]. Besides these, there were numerous genes involved in ubiquitin biology that were clearly enriched in both screens but which did not meet our strict cut-off requirements; these genes included ubiquitin B (UBB), ubiquitin C (UBC), Ubiquitin-Activating Enzyme E1 (UBA1), the E2 conjugating enzyme UBE2J2, the p97-interacting proteins UFD1L and NPLOC4, as well as multiple additional proteasome subunits.

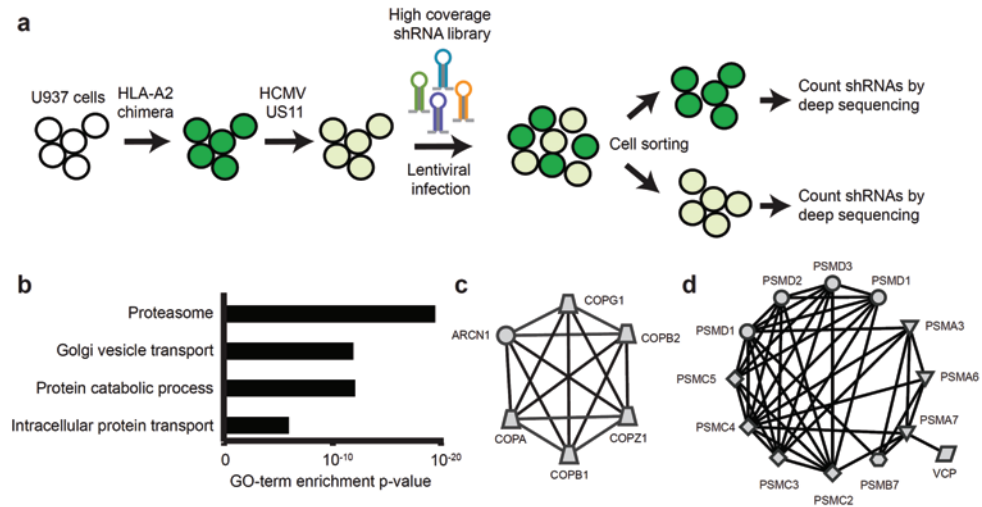


**Figure 1: Pooled high-coverage RNAi screen for players involved in US11-mediated ERAD of HLA class I molecules.**

**(a)** Experimental strategy: U937 cells were transduced with an eGFP-Myc-HLA-A2 chimera and subsequently transduced with an HCMV US11-expression vector. The resulting cells were cloned and displayed low total eGFP-Myc-HLA-A2 expression as assessed by eGFP expression, and low cell-surface expression of the chimeric (as assessed by anti-Myc cell-surface stain) and endogenous HLA class I alleles. The cells were infected with the pooled genome-wide high-coverage shRNA library and subjected to flow cytometry sorting 6 dpi to select for eGFP<sup>bright</sup> cells and eGFP<sup>dim</sup> control cells. The frequency of shRNA-encoding constructs in each subpopulation was determined by deep sequencing. **(b)** GO-term enrichment analysis for hits from the screen was assessed using the Database for Annotation, Visualization and Integrated Discovery (DAVID). Based on the frequency in the treated and untreated **Figure 1 (continued)**: subpopulations, a hit list was established covering genes that were shared among the top 100 enriched genes from two independent screens (see Table 1). **(c,d)** Network analysis on the selected genes identified two clusters consisting of genes present in the COPI complex **(c)** and proteasome associated genes **(d)**.

### TMEM129 is essential for HLA class I dislocation by US11

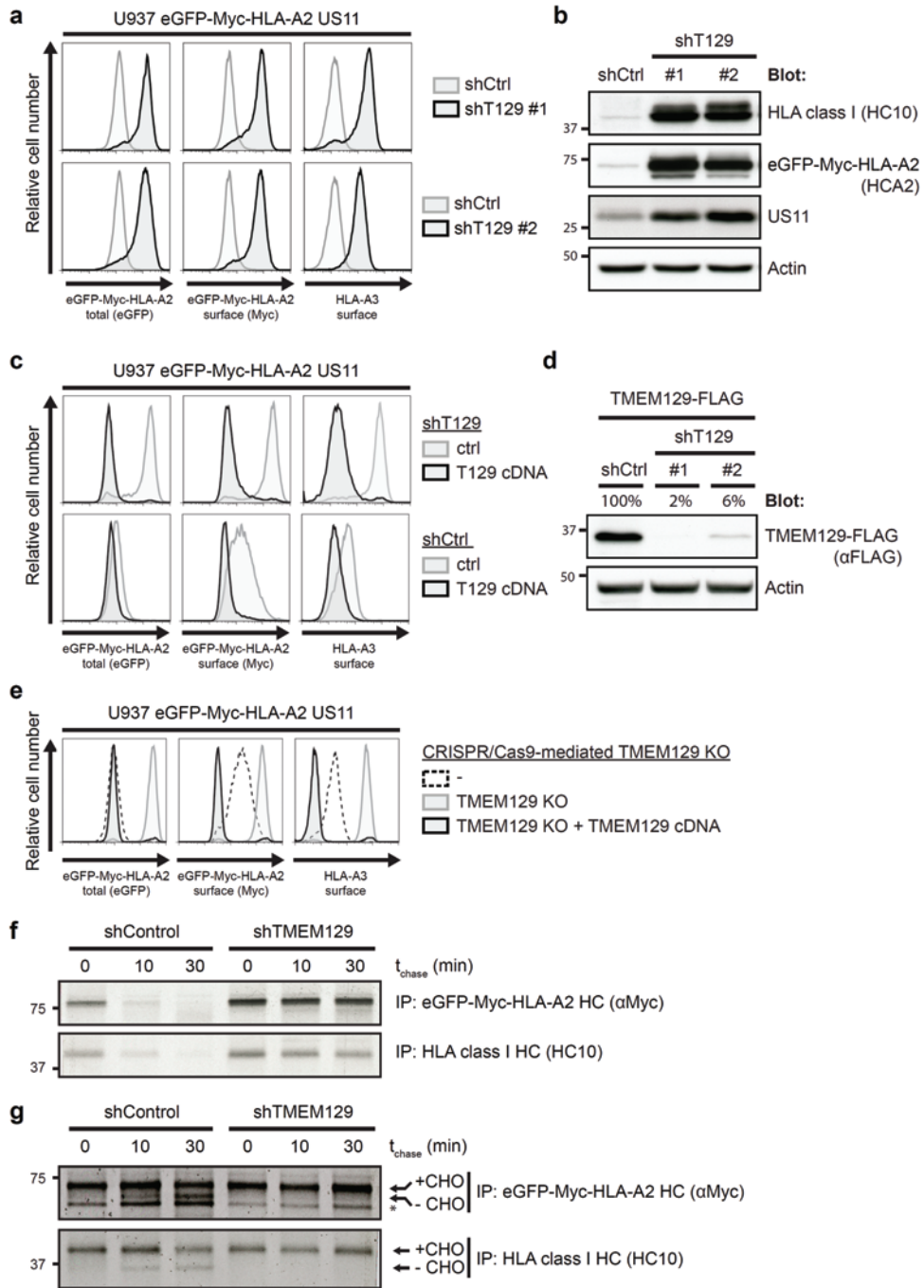
We focused our validation analysis on the uncharacterized protein TMEM129. Depletion of TMEM129 by using independent shRNAs induced potent rescue of both the chimeric HLA-A2 and the endogenous HLA-A3 expression in U937 cells co-expressing US11 (Fig. 2a, Supplementary Fig. 1b). Consistent with the flow cytometry data, immunoblot analysis for HLA class I expression revealed increased protein levels in the presence of TMEM129 shRNAs (Fig. 2b, Supplementary Figure 1c). Intriguingly, US11 protein levels were upregulated upon TMEM129 depletion as well. The impaired HLA class I downregulation in TMEM129-depleted cells was restored upon overexpression of TMEM129 (Fig. 2c, upper panels), which excludes the possibility that HLA class I rescue was caused by off-targeting effects of the used shRNAs. Notably, overexpression of TMEM129 even enhanced HLA class I downregulation in both TMEM129- and mock-depleted cells (Fig. 2c, lower panels). The efficiency of shRNA-mediated TMEM129 depletion is depicted in Figure 2d. Similar results were obtained for additional TMEM129-targeting shRNAs (Supplementary Fig. 1b-d).

Gene ID	Gene Symbol	Full name
372	ARCN1	archain 1
1314	COPA	coatomer protein complex, subunit alpha
1315	COPB1	coatomer protein complex, subunit beta 1
1939	EIF2D	eukaryotic translation initiation factor 2D
5684	PSMA3	proteasome (prosome, macropain) subunit, alpha type, 3
5687	PSMA6	proteasome (prosome, macropain) subunit, alpha type, 6
5688	PSMA7	proteasome (prosome, macropain) subunit, alpha type, 7
5695	PSMB7	proteasome (prosome, macropain) subunit, beta type, 7
5701	PSMC2	proteasome (prosome, macropain) 26S subunit, ATPase, 2
5702	PSMC3	proteasome (prosome, macropain) 26S subunit, ATPase, 3
5704	PSMC4	proteasome (prosome, macropain) 26S subunit, ATPase, 4
5705	PSMC5	proteasome (prosome, macropain) 26S subunit, ATPase, 5
5707	PSMD1	proteasome (prosome, macropain) 26S subunit, non-ATPase, 1
5708	PSMD2	proteasome (prosome, macropain) 26S subunit, non-ATPase, 2
5709	PSMD3	proteasome (prosome, macropain) 26S subunit, non-ATPase, 3
6633	SNRPD2	small nuclear ribonucleoprotein D2 polypeptide 16.5kDa
7415	VCP	valosin containing protein
9276	COPB2	coatomer protein complex, subunit beta 2 (beta prime)
22818	COPZ1	coatomer protein complex, subunit zeta 1
22820	COPG	coatomer protein complex, subunit gamma
92305	TMEM129	transmembrane protein 129

**Table 1: Overlapping genes in top 100 from duplicate screens.** Entrez gene Ids, Gene symbols and full names of genes present in the top 100 of two independent screens are presented. All genes validated in subsequent shRNA validation experiments, except for EIF2D and SNRPD2. Genes are ranked according gene ID number.

Besides validating TMEM129 by using RNAi, we employed the recently established CRISPR/Cas genome engineering system to generate TMEM129-null cells. Expression of a *TMEM129*-targeting guideRNA (gRNA) induced potent rescue of both chimeric and endogenous HLA class I molecules to levels comparable to those in US11-negative cells (Fig. 2e and Supplementary Fig. 2a-b). Loss of the TMEM129 protein was confirmed by TMEM129 immunoprecipitation experiments (Supplementary Fig. 9d). Subsequent reconstitution of TMEM129 restored US11-mediated HLA class I downregulation in TMEM129-null cells, and even reduced HLA class I protein levels to almost undetectable levels (Fig. 2e and Supplementary Fig. 2b, lower panels).

US11 induces rapid dislocation of HLA class I molecules from the ER to the cytosol, where HLA class I is subsequently degraded by the proteasome (Supplementary Fig. 3) [13]. Upon dislocation into the cytosol, HLA class I HCs are deglycosylated, and these species can be visualized upon proteasome inhibition [13]. We performed pulse chase experiments to



< **Figure 2: TMEM129 is crucial for US11-mediated HLA class I downregulation.** (a) Depletion of endogenous TMEM129 by shRNAs induces potent rescue of eGFP-Myc-HLA-A2 and endogenous HLA-A3 in U937 eGFP-Myc-HLA-A2 US11 cells. ShRNAs targeting TMEM129 (black histograms) or control shRNAs (gray histograms) were introduced. 7 d p.i surface endogenous HLA-A3 and surface (Myc) and total (eGFP) eGFP-Myc-HLA-A2 were assessed by flow cytometry. An assessment of TMEM129 levels upon shRNA depletion is presented in Figure 2d. (b) Immunoblot analysis of endogenous HLA class I, eGFP-Myc-HLA-A2, US11, and loading control actin in mock- (shCtrl) and TMEM129-depleted cells (shTMEM129 #1-2). (c) Rescue of HLA class I upon TMEM129 depletion is reversed upon overexpression of TMEM129. A TMEM129-expressing vector (black-lined histograms) or an empty vector (gray-lined histograms) were stably introduced in TMEM129- (shT129, upper panels) or mock-depleted (shCtrl, lower panels) cells, after which surface endogenous HLA-A3, and surface (Myc) and total (eGFP) eGFP-Myc-HLA-A2 were assessed by flow cytometry. (d) Immunoblot analysis of shRNA-mediated downregulation of overexpressed TMEM129-FLAG. Percentages indicate expression levels compared to mock (shCtrl) depletion normalized against actin levels. Similar results were obtained for additional TMEM129-targeting shRNAs (Supplementary Figure 1b-d). Depletion of endogenous TMEM129 by the first shRNA is depicted in Supplementary Figure 9c). (e) CRISPR/Cas-mediated knockout of endogenous TMEM129 induces potent rescue of HLA class I. Surface endogenous HLA-A3, and surface (Myc) plus total (eGFP) expression of eGFP-Myc-HLA-A2 were assessed by flow cytometry in control cells (dashed histogram), TMEM129-null cells (gray-lined histograms), and TMEM129-null cells with reconstituted TMEM129 expression (black histograms). A clonal TMEM129-null cell line was established and stained; additional clones are depicted in Supplementary Figure 2a-b. (f) Mock- (shControl) and TMEM129-depleted U937 eGFP-Myc-HLA-A2 US11 cells were subjected to a pulse chase analysis. Cells were radioactively labeled for 10 min, and chased for the indicated timeframes. Subsequently, HLA class I HCs were immunoprecipitated from lysates using indicated antibodies. (g) TMEM129 depletion in the presence of a proteasome inhibitor abrogates dislocation of HLA class I. Similar experiment as in (f), albeit in the presence of the proteasome inhibitor MG132 (20 μM) immediately prior and during the experiment. N-linked glycosylated (+CHO) and deglycosylated (-CHO) HLA class I HCs are indicated. The asterisk indicates a non-specific background band.

determine if TMEM129 depletion impairs HLA class I HC dislocation and/or its subsequent degradation by the proteasome. As expected, TMEM129 depletion greatly stabilized HLA class I in the presence of US11 (Fig. 2f). Upon proteasome inhibition, we observed accumulation of deglycosylated HCs in control cells, whereas these species were completely absent in cells depleted for TMEM129 (Fig. 2g). Results were comparable for eGFP-Myc-HLA-A2 and endogenous HLA class I HCs (compare upper and lower panels in Fig. 2f and 2g). These data show that TMEM129 is critically involved in US11-mediated HLA class I dislocation and degradation.

### TMEM129 is a novel E3 ubiquitin ligase

TMEM129 is an uncharacterized transmembrane protein of 362 amino acids that is predicted to have 3 transmembrane domains (TOPCONS; Fig. 3a), and is localized to the ER (Fig. 3b). The protein contains a putative unconventional C4C4 RING domain, suggesting that TMEM129 might be an E3 ubiquitin ligase. To test this, FLAG- and Strep-tag II-tagged versions of TMEM129 and RING-less TMEM129 were immunoprecipitated from U937 cell lysates and used in *in vitro* ubiquitination assays. Incubation of TMEM129 with E1 UBA1, the promiscuous E2 UBE2D3, S5a (Rpn10) protein substrate, ubiquitin, and ATP resulted in the

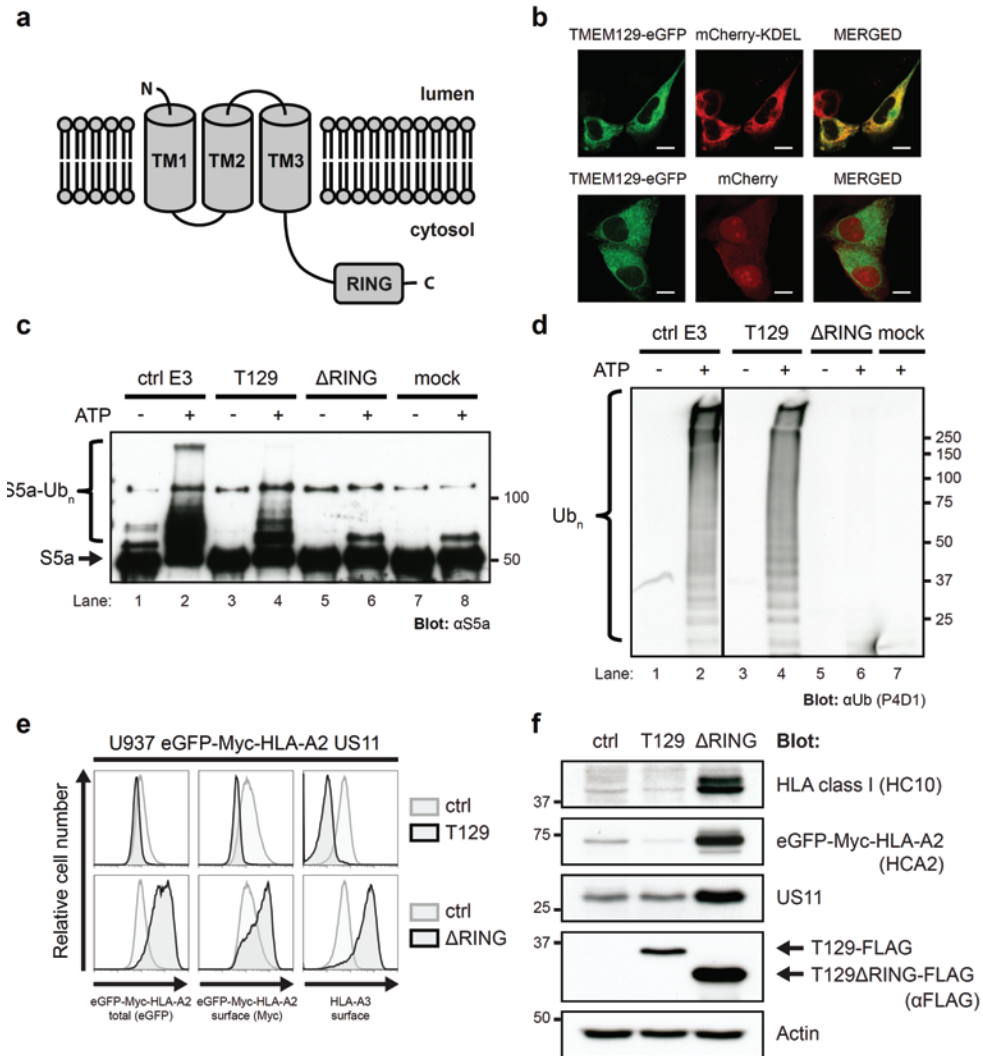


**Figure 3: TMEM129 is an E3 ubiquitin ligase essential for US11-mediated HLA class I downregulation. (a)** Predicted topology of TMEM129 using the TOPCONS prediction server. TM: transmembrane domain; RING: RING domain. The N- and C-terminus of the protein are depicted. **(b)** TMEM129 localizes to the ER. MeJuSo cells stably co-expressing TMEM129-eGFP with either mCherry (cytosolic and nuclear) or mCherry-KDEL (ER-localized) were subjected to fluorescent confocal microscopy to assess co-localization of TMEM129-eGFP with either marker. White bars represent 10  $\mu\text{m}$ . **(c)** TMEM129 is an E3 ubiquitin ligase. *In vitro* ubiquitination assays were performed by using purified ubiquitin, E1 enzyme UBA1, E2 enzyme UBE2D3, and E3 enzyme MuRF1 (ctrl E3), immunoprecipitated TMEM129-FLAG-ST2 (T129) or TMEM129 $\Delta$ RING-FLAG-ST2 ( $\Delta$ RING), in the absence or presence of ATP. Purified S5a was used as a substrate. Immunoblot analysis was performed using an anti-S5a antibody to visualize polyubiquitinated S5a. Addition of the tags did not interfere with TMEM129 function (see Supplementary Figure 10c). **(d)** The experiment was performed as in Figure 3c, although a specific substrate was omitted from the reaction. Immunoblot analysis was performed using the anti-ubiquitin P4D1 mAb to visualize polyubiquitin ( $\text{Ub}_n$ ). **(e)** The TMEM129 RING domain is essential for US11-mediated HLA class I downregulation.

**Figure 3 (continued):** Flow cytometry analysis of endogenous surface HLA-A3, and surface (Myc) and total (eGFP) eGFP-Myc-HLA-A2 in U937 eGFP-Myc-HLA-A2 cells expressing US11 and co-expressing either TMEM129 (T129), TMEM129 $\Delta$ RING ( $\Delta$ RING), or an empty vector (ctrl). **(f)** Same cells as in Figure 3e, now analyzed by immunoblotting for the indicated proteins. TMEM129-FLAG retained its ability to enhance HLA class I downregulation (Supplementary Figure 10a).

formation of poly-ubiquitinated S5a species (Fig. 3c, lane 4), whereas removal of the RING domain completely abrogated this activity (lane 6). Also, in the absence of S5a substrate, TMEM129 induced the formation of polyubiquitin chains (Fig. 3d, lane 4), whereas the RING-less mutant did not (lane 6).

Next, we investigated whether the RING domain of TMEM129 is required for US11-mediated HLA class I downregulation. Expression of the full-length TMEM129 enhanced HLA class I downregulation (Fig. 3e, upper panels), whereas expression of RING-less TMEM129 in U937 eGFP-Myc-HLA-A2 US11 cells resulted in a dominant-negative phenotype, i.e. rescue of surface HLA-A3, and total and surface eGFP-Myc-HLA-A2 (Fig. 3e, lower panels). These results were confirmed by immunoblotting experiments (Fig. 3f), in which increased levels of HLA class I HCs were observed in the presence of RING-less TMEM129. Again, increased US11 protein levels were observed, this time upon RING deletion. The RING-less TMEM129 data recapitulate our findings obtained by TMEM129 depletion via shRNAs and CRISPR gRNAs. In conclusion, these findings identify TMEM129 as an E3 ubiquitin ligase with a C4C4 RING domain, removal of which results in a dominant-negative phenotype rescuing HLA class I from US11-mediated dislocation.

### **TMEM129 is part of the US11 dislocation complex**

To assess whether TMEM129 is present in the US11-containing dislocation complex, we generated N-terminally Strep-tag II and HA-tagged US11 molecules (ST2-HA-US11) and subjected these to co-immunoprecipitation experiments. Endogenous TMEM129 coprecipitated with ST2-HA-US11 in control cells (Fig. 4, lanes 2 and 4), but not in TMEM129-depleted cells (lane 3). High levels of overexpressed TMEM129 and TMEM129 $\Delta$ RING (lanes 5 and 6) were coprecipitated with US11, together with Derlin-1, Derlin-2, VIMP, p97, SEL1L and HRD1. Depletion of TMEM129 using shRNAs (lane 3) or removal of the RING domain (lane 6) did not abrogate association of Derlin-1, Derlin-2, VIMP, p97, SEL1L and HRD1. Notably, HLA class I HCs were exclusively detectable in complexes isolated from TMEM129-depleted (lane 3) or TMEM129 $\Delta$ RING-expressing (lane 6) cells. Taken together, our data show that TMEM129 is part of the US11-containing dislocation complex.

### **UBE2J2 is essential for US11-mediated HLA class I ERAD**

Ubiquitination of a target substrate is often facilitated by more than one E2 ubiquitin-conjugating enzyme [38]. Currently, the identity of one E2 ubiquitin-conjugating enzyme contributing to US11-mediated HLA class I downregulation is known, namely UBE2K/E2-25K

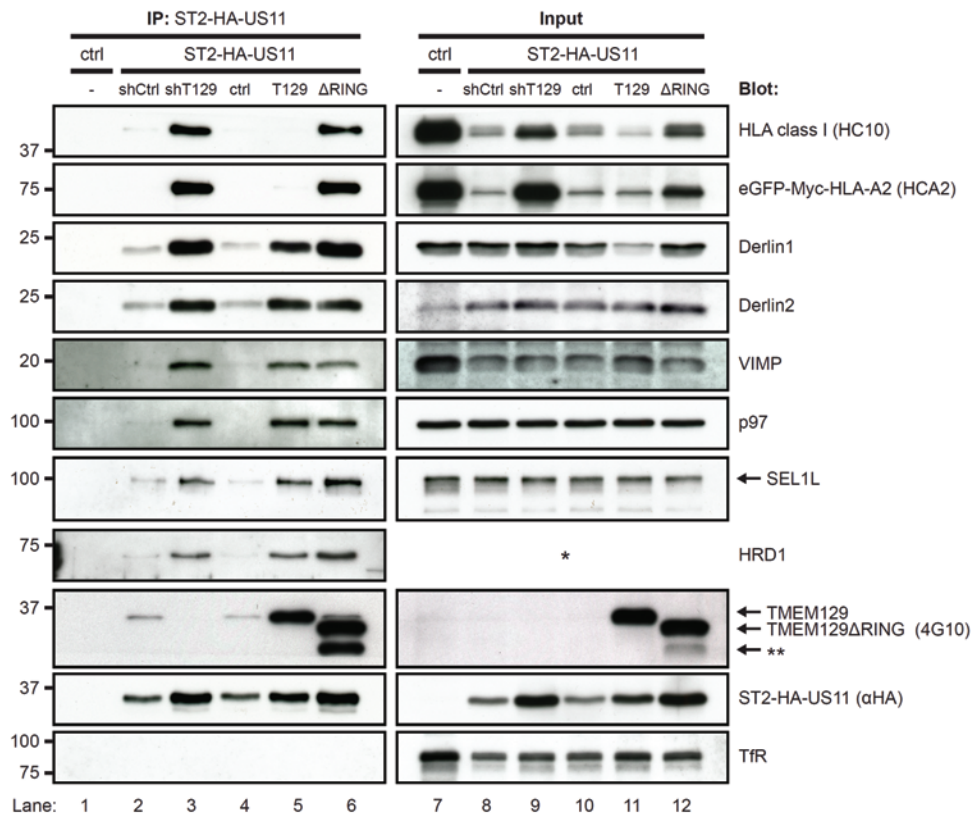


**Figure 4: TMEM129 is part of the US11 dislocation complex.** Strep-tag II- and HA-tagged US11 was immunoprecipitated using StrepTactin beads from 1.0% digitonin lysates of US11-negative (lane 1) and positive (lanes 2-6) U937 eGFP-Myc-HLA-A2 cells. The US11-expressing cells were co-expressing a control shRNA (shCtrl, lane 2), an shRNA targeting TMEM129 (shT129, lane 3), an empty vector (ctrl, lane 4), TMEM129 (T129, lane 5), or TMEM129 $\Delta$ RING ( $\Delta$ RING, lane 6). Immunoprecipitated proteins were eluted using d-Desthiobiotin, after which immunoblot analysis was performed for proteins indicated. The right panels (lanes 7-12) indicate loading controls to analyze input of the indicated proteins prior immunoprecipitation. The Strep-tag II- and HA-tagged US11 retained its ability to downregulate HLA class I molecules (Supplementary Figure 10b). The HRD1 antibody could not detect HRD1 in digitonin cell lysates, indicated by the asterisk. The double asterisk indicates an additional unspecified truncated form of TMEM129 $\Delta$ RING.

[39]. The combined results of our two genome-wide shRNA screens did not identify any additional candidates. However, one of the two screens did show clear enrichment for the E2 UBE2J2. We therefore tested UBE2J2-targeting shRNAs which indeed rescued endogenous and chimeric HLA class I molecules in US11-expressing cells (Fig. 5a, upper two panels). This rescue was completely abolished upon co-expression of an UBE2J2 cDNA, showing that these effects were caused by on-target effects of the UBE2J2-targeting shRNAs. These results were confirmed by the generation of UBE2J2-null cells using the CRISPR/Cas system



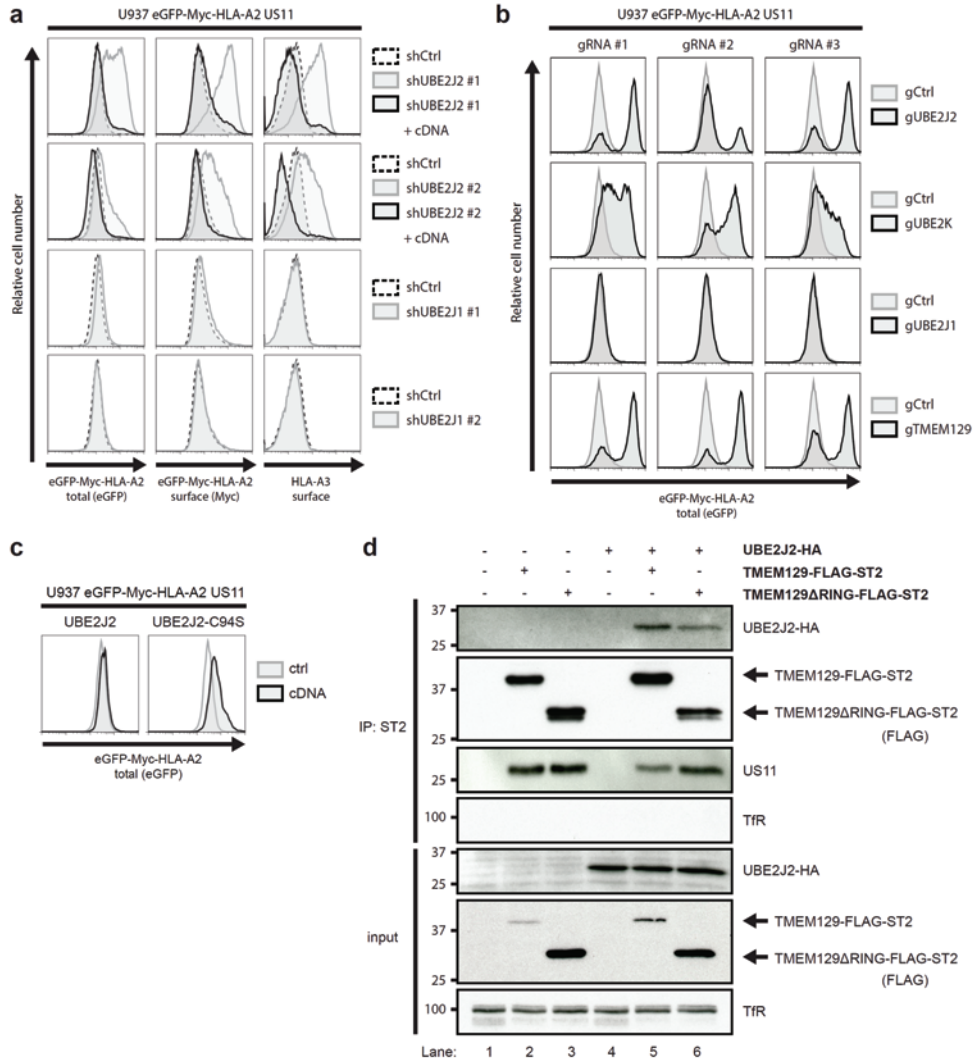


**Figure 5: UBE2J2 is essential for US11-mediated HLA class I downregulation.** (a) UBE2J2 depletion by shRNAs induces rescue of HLA class I in US11-expressing cells. Two individual UBE2J2- and UBE2J1-targeting shRNAs (gray-lined histograms), two individual UBE2J2-targeting shRNAs together with UBE2J2 cDNA (black-lined histograms), or one control shRNA (dashed histograms) were introduced in U937 eGFP-Myc-HLA-A2 US11 cells. Flow cytometry analysis was performed of endogenous surface HLA-A3, and surface (Myc) and total (eGFP) eGFP-Myc-HLA-A2 expression 7 dpi. (b) CRISPR/Cas-mediated knockout of UBE2J2 and UBE2K induce potent rescue of HLA class I. Total (eGFP) expression of eGFP-Myc-HLA-A2 were assessed by flow cytometry in U937 eGFP-Myc-HLA-A2 US11 control cells (gray histogram) and cells knocked out for either UBE2J2 (black histograms, upper panels), UBE2K (black histograms; second panels), UBE2J1 (black histograms, third panels), or TMEM129 (black histograms, lower panels) using three individual CRISPR gRNAs. (c) Dominant negative UBE2J2 (C94S) causes rescue of HLA class I. Total (eGFP) expression of eGFP-Myc-HLA-A2 was assessed by flow cytometry in U937 eGFP-Myc-HLA-A2 US11 control cells (gray histogram) and cells expressing either wildtype UBE2J2 (black histogram, left panel) or dominant

**Figure 5 (Continued):** negative UBE2J2-C94S (black histogram, right panel). **(d)** UBE2J2 associates with TMEM129. Strep-tag II- and FLAG-tagged TMEM129 was immunoprecipitated using StrepTactin beads from 1.0% digitonin lysates of U937 eGFP-Myc-HLA-A2 US11 cells expressing indicated constructs. The Strep-tag II- and FLAG-tagged TMEM129 retained its ability to enhance HLA class I downregulation (Supplementary Figure 10c, left panels). Immunoprecipitated proteins were eluted using d-Desthiobiotin, after which immunoblot analysis was performed for the proteins indicated.

(Fig. 5b, upper panel). ShRNAs (Fig. 5a, lower two panels) and CRISPR gRNAs (Fig. 5b, third row) targeting the homologous UBE2J1 did not have any effect on HLA class I expression. Expression of a dominant negative UBE2J2 (C94S) increased HLA class I expression in US11-expressing cells (Fig. 5c). Co-immunoprecipitation experiments showed that UBE2J2 is in the same complex as the E3 ubiquitin ligase TMEM129 (Fig. 5d). RING-removal of TMEM129 does not affect association of UBE2J2 with the complex. Intriguingly, UBE2K-null cells showed a clear rescue of HLA class I molecules (Fig. 5b, second row), suggesting that both UBE2J2 and UBE2K are essential for HLA class I downregulation by US11.

#### **TMEM129 is an integral component of dislocation complexes**

We next assessed whether TMEM129 is part of ER-resident dislocation complexes independent of US11, which might indicate that TMEM129 plays a role in general ERAD. Co-immunoprecipitation experiments were performed using C-terminal Strep-tag II- and FLAG-tagged TMEM129 and TMEM129 $\Delta$ RING. Both proteins were found to be associated with Derlin-1, Derlin-2, VIMP, p97, SEL1L and HRD1 to similar levels in both US11-expressing and US11-negative cells (Fig. 6a). In the absence of US11, no or very low levels of HLA class I and eGFP-Myc-HLA-A2 associated with TMEM129, despite the presence of considerable amounts of HLA class I molecules in these cells (compare upper two panels, lanes 2 and 8, and lanes 3 and 9). In the presence of US11, again increased levels of HLA class I were found in association with TMEM129 $\Delta$ RING as compared to wildtype TMEM129 (compare lanes 5 and 6 upper two panels).

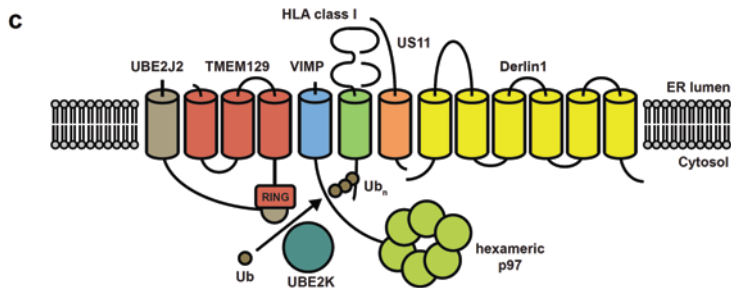
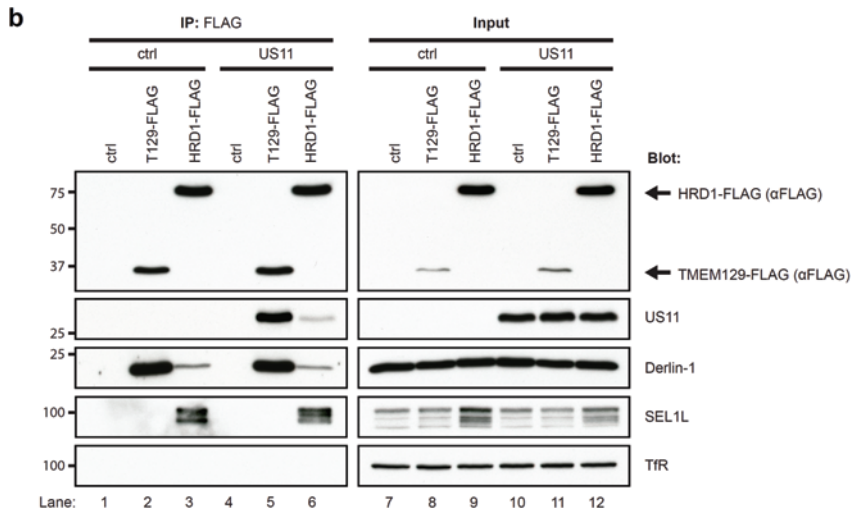
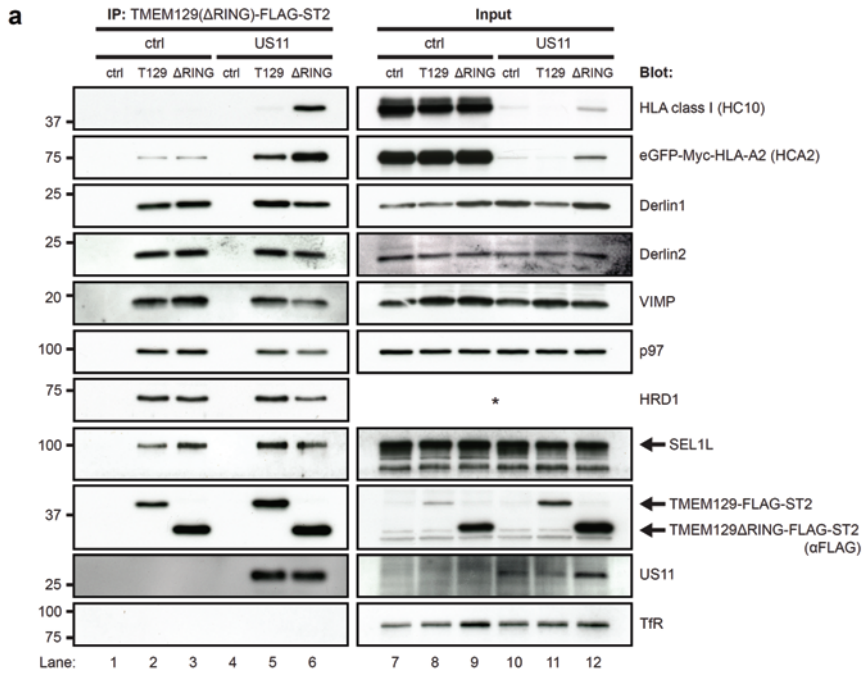
Because HRD1 and SEL1L co-precipitated together with US11 (Fig. 4) and TMEM129 (Fig. 6a), we compared overexpressed TMEM129 and HRD1 in their ability to associate with US11, Derlin-1, and SEL1L (Fig. 6b). Immunoprecipitation of TMEM129 recovered higher quantities of US11 and Derlin-1 compared to immunoprecipitation of HRD1-FLAG (compare Fig. 6b, lanes 5 and 6). In addition, immunoprecipitation of HRD1 recovered SEL1L (lane 6), which was not observed upon TMEM129 pull-down (lane 5). The same results were observed when US11 was absent (lanes 1-3). Thus, TMEM129, and not HRD1, preferentially associates with US11 and Derlin-1. SEL1L preferentially interacts with HRD1 and not with TMEM129. These results demonstrate that TMEM129 is an integral constituent of the ER-resident dislocation complexes, suggesting that this E3 ubiquitin ligase might play a role in physiological ERAD, independently of US11. A model of the US11 dislocation complex is depicted in Figure 6c.

## DISCUSSION

HCMV US11-mediated degradation of HLA class I molecules serves as a paradigm for ERAD and has facilitated the identification of multiple essential components of this important degradation pathway. In this study, we identified additional essential players of US11-mediated HLA class I downregulation by performing a pooled genome-wide shRNA library screen in human cells expressing the US11 protein. To this end, we constructed a new high-complexity genome-wide shRNA library consisting of approximately 550,000 different shRNAs. We assessed whether we could successfully conduct a genome-wide screen using the entire library in a single population of cells. This approach proved successful, as we identified known players, such as p97 and a large compendium of proteasome subunits. Besides this, we identified multiple new genes potentially involved, such as subunits of the COPI retrograde trafficking machinery and the uncharacterized TMEM129. We chose a strict cut-off for our validation experiments and only allowed the overlap of the top 100 enriched genes from two independent screens in our hit list. This screen is the first to show that ultra-complex libraries with over 550,000 different shRNAs can be successfully applied in genetic screens using deep-sequencing as a read-out for library complexity and dynamics.

Our hit list contained multiple genes of the COPI retrograde transport system. In agreement with this, we observed a moderate rescue of eGFP-Myc-HLA-A2 expression in COPI-depleted cells co-expressing the chimeric molecule and US11 (Supplementary Fig. 4a). Since immature HLA class I molecules that escape to the Golgi complex, are efficiently recruited back to the ER in a COPI-dependent manner [40], depletion of COPI subunits would theoretically cause accumulation of these HCs in the Golgi, which could protect these from US11-induced ERAD initiated in the ER. Indeed, we observed accumulation of both endogenous and chimeric HLA class I molecules in a post-ER compartment upon COPI depletion, as EndoH resistant HCs became apparent in immunoblot analysis (Supplementary Fig. 4b). Additionally, confocal studies clearly demonstrated a relocalization of chimeric HLA class I molecules to the Golgi upon COPI depletion (Supplementary Fig. 4c). Rescue of HLA class I in COPI-depleted cells could be related to the inability of ER-localized US11 to initiate degradation of Golgi-localized HCs, or by a lack of ERAD components in the ER due to an impaired retrieval of membrane proteins from the Golgi to the ER upon blockage of the retrograde transport system. We therefore believe that the COPI complex is not specifically involved in US11-mediated HLA class I ERAD, but that the identification of these subunits in the screen is likely caused by an indirect effect.

Our hit list contained the previously uncharacterized protein TMEM129. Subsequent validation experiments, including shRNA-mediated knockdown, CRISPR/Cas-mediated knockout and overexpression of TMEM129, showed that TMEM129 is crucial for US11-mediated HLA class I downregulation. Sequence analysis revealed that TMEM129 contains a putative non-classical RING domain. Whereas a conventional RING domain contains three



< **Figure 6: TMEM129 is present in ERAD complexes in the absence of US11.** (a) C-terminally Strep-tag-II- and FLAG-tagged TMEM129 or TMEM129 $\Delta$ RING were immunoprecipitated using StrepTactin beads from 1.0% digitonin lysates of US11-negative (lanes 1-3) and US11-positive (lanes 4-6) U937 eGFP-Myc-HLA-A2 cells. The cells were co-expressing a control vector (ctrl, lanes 1 and 4), TMEM129-FLAG-ST2 (T129, lanes 2 and 5), and TMEM129 $\Delta$ RING-FLAG-ST2 ( $\Delta$ RING, lane 3 and 6). Immunoprecipitated proteins were eluted using d-Desthiobiotin, after which immunoblot analysis was performed for the proteins indicated. The right panels (lanes 7-12) indicate loading controls to analyze input of the indicated proteins prior to immunoprecipitation. The C-terminally Strep-tag-II- and FLAG-tagged TMEM129 construct retained its ability to enhance US11-mediated HLA class I downregulation (Supplementary Figure 10c, left panels), whereas the C-terminally tagged TMEM129 $\Delta$ RING retained its dominant-negative phenotype (Supplementary Figure 10c, right panels). The HRD1 antibody could not detect HRD1 in digitonin cell lysates, indicated by the asterisk. (b) C-terminally FLAG-tagged TMEM129 and HRD1 were immunoprecipitated using FLAG-M2-coupled beads from 1.0% digitonin lysates of US11-negative (lanes 1-3) and US11-positive (lanes 4-6) U937 eGFP-Myc-HLA-A2 cells. Immunoprecipitated proteins were eluted using FLAG peptides, after which immunoblot analysis was performed for the proteins indicated. (c) Schematic overview of the US11 dislocation complex. The depicted location of the proteins is not accurate.

zinc-coordinating cysteine pairs and one cysteine-histidine pair, the RING domain of TMEM129 possesses four zinc-coordinating cysteine pairs (C4C4) that are fully conserved among a wide range of TMEM129 orthologs (Supplementary Fig. 5). Thus far, only a single mammalian E3 ubiquitin ligase (CNOT4) has been described to contain a C4C4 RING domain [41]. We show that TMEM129 is a bona-fide E3 ubiquitin ligase as it possesses such activity *in vitro*, and removal of the RING domain completely abrogated this activity. In line with this, expression of RING-less TMEM129 in US11-expressing cells caused a dominant-negative phenotype of increased HLA class I levels. Not only HLA class I levels were found to be elevated, but also US11 protein levels were increased upon expression of RING-less TMEM129, an observation also made upon shRNA-mediated depletion of TMEM129. However, when TMEM129 was overexpressed in US11-expressing cells, US11 levels remained unchanged, whereas HLA class I levels decreased to almost undetectable levels. Thus, while we cannot rule out that US11 is a substrate for TMEM129 to some extent, we show that TMEM129 primarily mediates dislocation of HLA class I molecules. Immunoprecipitation of US11 and TMEM129 demonstrated that TMEM129 is an integral part of the US11 dislocation complex. Depletion of TMEM129 and expression of RING-less TMEM129 appear to lock the dislocation complex in a dislocation-incompetent state, indicated by high levels of HLA class I in complex with US11, while normally, association of HLA class I with US11 is transient [15]. The presence of TMEM129 in ERAD complexes independently of US11 suggests that the protein may also be involved in dislocation of other cellular substrates. Among these substrates may be cellular proteins destined for degradation in the context of ER quality control and/or alleviation of ER stress through the unfolded protein response (UPR). CRISPR/Cas-mediated TMEM129 knockout results in a slight induction of the UPR as assessed by XBP-1 splicing analysis (Supplementary Fig. 6), suggesting that TMEM129 might play a role in this process.

The identification of the E3 ubiquitin ligase crucial for US11-mediated HLA class I downregulation has been a subject of intense investigation. Currently, only a few E3

ubiquitin ligases involved in human ERAD are known, of which HRD1 is the most studied. However, previous attempts to link HRD1 to US11-mediated HLA class I degradation have not been successful, as HRD1 depletion studies did not rescue HLA class I from US11-mediated degradation [42]. In line with this, we did not observe increased US11-mediated HLA class I downregulation upon HRD1 overexpression (Supplementary Fig. 7a), nor did we see rescue of HLA class I from US11-mediated degradation upon either shRNA-mediated HRD1 depletion or gRNA-mediated *HRD1* gene disruption (Supplementary Fig. 7c and 7e respectively). Nevertheless, HRD1 was present in US11 and TMEM129-containing dislocation complexes (Figure 4 and 6a). A subsequent immunoprecipitation experiment to compare the binding of HRD1 and TMEM129 to other dislocation components revealed that US11 and Derlin-1 associated more strongly with TMEM129, compared to HRD1 (Figure 6b). In this context, SEL1L was preferentially associated with HRD1, and not with TMEM129, even though both E3 ligases were immunoprecipitated to similar quantities. Hence, SEL1L may thus be recruited to the dislocation complex through its association with HRD1, which is also present in the complex, albeit in small amounts. We therefore propose that TMEM129 is the E3 ubiquitin ligase that is essential for US11-mediated HLA class I degradation.

The fact that TMEM129 has escaped identification thus far [43] is likely due to its low endogenous expression levels, which complicates its identification via standard biochemical approaches. Additionally, TMEM129 was a previously uncharacterized protein, which prevented including TMEM129 as a candidate in focused E3 ubiquitin ligase screening approaches by e.g. RNAi. Our strategy involved the use of an unbiased genome-wide shRNA library screen in which all protein-encoding genes were included, thereby eliminating these hurdles and illustrating the advantages of genome-wide pooled shRNA library screens.

E3 ubiquitin ligases collaborate with E2 enzymes to facilitate polyubiquitination of a target substrate [30]. Previously, the E2 UBE2J1 was implicated to be involved in US11-mediated HLA class I dislocation [43]. Unexpectedly, not only the dominant-negative UBE2J1, but also the wildtype E2 protein was found to impair US11-mediated HLA class I dislocation [43]. We now show that UBE2J2, and not UBE2J1, is essential for HLA class I degradation by US11, since depletion or knockout of UBE2J2, but not UBE2J1, causes a dramatic rescue of HLA class I from US11-mediated degradation. Considering that mammalian UBE2J1 and UBE2J2 are highly homologous [44], UBE2J1 might compete with UBE2J2 for binding to certain E3 ubiquitin ligases; when present in excess, UBE2J1 might prevent UBE2J2 from binding, which could explain the earlier observations. Additionally, co-immunoprecipitation experiments confirmed that UBE2J2 is present in complexes with TMEM129. Also, the E2 UBE2K/E2-25K has been reported to facilitate ubiquitination of HLA class I in permeabilized US11-expressing cells [39]. In this experimental setup however, membrane-anchored E2 enzymes (e.g. UBE2J2) remained uninvestigated since the usurped semi-permeabilized system only allowed removal and addition of cytosolic E2 enzymes. Using CRISPR/Cas-mediated gene disruption, we show that UBE2K is also essential for US11-mediated HLA class I downregulation, thereby confirming the previous

findings for UBE2K. UBE2J2- and UBE2K-null cells expressing US11 both show high levels of rescued HLA class I, which indicates that these two E2 enzymes are not interchangeable and catalyze two different ubiquitination steps essential for the dislocation process.

The processivity of polyubiquitin formation is often orchestrated by at least two different E2 enzymes, one of which is responsible for ubiquitin chain initiation, while the other E2 promotes ubiquitin chain elongation [38]. Mono-ubiquitination of HLA class I is not sufficient to induce US11-mediated dislocation; completion of this reaction requires Lys48-linked polyubiquitination [21,45]. While UBE2K is known to catalyze Lys48-linked ubiquitin chain elongation, and not chain initiation [46], it is unknown what type of ubiquitin chain formation is catalyzed by UBE2J2. However, in the context of US11-mediated HLA class I degradation, the membrane-bound UBE2J2 may promote mono-ubiquitination of HLA class I, thereby enabling the cytosolic UBE2K to catalyze Lys48-linked ubiquitin chain elongation. Removal of either UBE2J2 or UBE2K would prevent polyubiquitination of HLA class I and thereby inhibit its dislocation. This hypothesis would also be in line with the results previously obtained for UBE2K using the semi-permeabilized cells [39]; in this system, the membrane-bound UBE2J2, which was not removed, would enable the supplied UBE2K to catalyze ubiquitin chain elongation.

Besides US11, the HCMV-encoded protein US2 also mediates dislocation of HLA class I. Whereas US11 uses the E3 ubiquitin ligase TMEM129, US2 relies on the activity of TRC8 [29]. The ERAD pathway exploited by US2 differs from US11-mediated HLA class I degradation in several other ways, including the lack of Derlin-1 involvement. When the degradation of HLA class I HCs is accelerated via depletion of  $\beta_2m$ , yet another E3 ubiquitin ligase, HRD1, catalyzes the degradation of HLA class I HCs [42,47]. It is notable that the dislocation of a single degradation substrate may be catalyzed by at least three different E3 ubiquitin ligases, depending on its context. This observation testifies to the versatility of ER-associated protein degradation and underscores the essential role that E3 ubiquitin ligases play in regulating the dislocation of substrates into the cytosol for degradation by the ubiquitin-proteasome system.

## ACKNOWLEDGEMENTS

We would like to thank Gerrit Spierenburg from the Laboratory of Translational Immunology (UMC Utrecht, The Netherlands) and Ger Arkesteijn from the Department of Veterinary Medicine (Utrecht University, The Netherlands) for technical assistance with cell sorting. We would like to thank Dr. Hidde Ploegh (Whitehead Institute / MIT, Cambridge, MA) for generously sharing reagents and valuable advice, Dr. Paul Lehner and Dr. Louise Boyle (University of Cambridge, Cambridge, UK) for generously sharing reagents, and Dr. Tom Rapoport (Harvard Medical School, Boston, MA) for valuable advice. We would like to acknowledge Martijn Rabelink from the Department of Molecular Cell Biology (LUMC,

Leiden, The Netherlands) for providing lentivirus vectors. We are grateful to Dr. Arend Mulder and Dr. Frans Claas (LUMC, Leiden, The Netherlands) for providing the human  $\alpha$ -HLA-A3 OK2F3 mAb. We thank the members of the Wiertz, McManus, and Weissman labs for helpful discussions and critical reading of the manuscript.

This work was supported by Veni grant 916.10.138 from The Netherlands Organisation for Scientific Research (NWO) and Marie Curie Career Integration Grant PCIG-GA-2011-294196 to R.J.L.. E.J.H.J.W. was supported by a grant from the Dutch Diabetes Research Foundation. M.C.B. was funded by a career development award from the Leukemia and Lymphoma Society. M.T.M. was funded by the UCSF Program for Breakthrough Biomedical Research and the NIH (1U01CA168370-01 and RO1 GM80783).

## CONTRIBUTIONS

The work presented here was carried out in collaboration between all authors. M.L.W., R.J.L., and E.J.H.J.W. designed the project, organized the research and wrote the manuscript. M.L.W. performed all experiments, except for the genome-wide shRNA library screen and the COPI validation experiments. R.J.L. designed the CRISPR/Cas-mediated genome engineering experiments, and R.J.L. and M.L.W. performed these experiments. R.J.L. designed and performed DNA cloning experiments. R.J.L. and C.M.V. performed the genome-wide shRNA library screen. R.J.L., M.C.B., J.W., and M.T.M. designed the genome-wide shRNA library and R.J.L., M.C.B. and W.P. cloned and QCed the shRNA library. E.M.L. and S.C. provided essential reagents to construct the shRNA library. M.C.B. analyzed the data from the shRNA library screen. M.A.M. performed the COPI validation experiments and R.D.L. performed the fluorescence microscopy experiments. H.H. provided technical assistance with the pulse-chase experiments. E.K. generated the TMEM129 monoclonal antibodies. R.C.H. provided essential shRNA expression vectors. M.E.R. gave conceptual advice.

## COMPETING FINANCIAL INTERESTS STATEMENT

E.M.L. and S.C. are employed by Agilent Technologies, Inc., and Agilent reagents are used in the research presented in this article. All other authors declare that there are no conflicts of interest.

## REFERENCES

- [1] Y.E. Kim, M.S. Hipp, A. Bracher, M. Hayer-Hartl, F.U. Hartl, Molecular chaperone functions in protein folding and proteostasis., *Annu. Rev. Biochem.* 82 (2013) 323–55. doi:10.1146/annurev-biochem-060208-092442.
- [2] R.Y. Hampton, ER-associated degradation in protein quality control and cellular regulation., *Curr. Opin. Cell Biol.* 14 (2002) 476–82. <http://www.ncbi.nlm.nih.gov/pubmed/12383799> (accessed September 28, 2013).
- [3] I. Amm, T. Sommer, D.H. Wolf, Protein quality control and elimination of protein waste: The role of the



- ubiquitin-proteasome system., *Biochim. Biophys. Acta.* (2013). doi:10.1016/j.bbamcr.2013.06.031.
- [4] D. Finley, Recognition and processing of ubiquitin-protein conjugates by the proteasome., *Annu. Rev. Biochem.* 78 (2009) 477–513. doi:10.1146/annurev.biochem.78.081507.101607.
- [5] J. Merulla, E. Fasana, T. Soldà, M. Molinari, Specificity and regulation of the endoplasmic reticulum-associated degradation machinery., *Traffic.* 14 (2013) 767–77. doi:10.1111/tra.12068.
- [6] P.G. Needham, J.L. Brodsky, How early studies on secreted and membrane protein quality control gave rise to the ER associated degradation (ERAD) pathway: the early history of ERAD., *Biochim. Biophys. Acta.* 1833 (2013) 2447–57. doi:10.1016/j.bbamcr.2013.03.018.
- [7] M.H. Smith, H.L. Ploegh, J.S. Weissman, Road to ruin: targeting proteins for degradation in the endoplasmic reticulum., *Science* (80-. ). 334 (2011) 1086–90. doi:10.1126/science.1209235.
- [8] J.C. Christianson, J. a Olzmann, T. a Shaler, M.E. Sowa, E.J. Bennett, C.M. Richter, R.E. Tyler, E.J. Greenblatt, J.W. Harper, R.R. Kopito, Defining human ERAD networks through an integrative mapping strategy., *Nat. Cell Biol.* 14 (2011) 93–105. doi:10.1038/ncb2383.
- [9] R.Y. Hampton, J. Rine, Regulated degradation of HMG-CoA reductase, an integral membrane protein of the endoplasmic reticulum, in yeast, *J. Cell Biol.* 125 (1994) 299–312.
- [10] R.Y. Hampton, H. Bhakta, Ubiquitin-mediated regulation of 3-hydroxy-3-methylglutaryl-CoA reductase., *Proc. Natl. Acad. Sci. U. S. A.* 94 (1997) 12944–8. <http://www.pubmedcentral.nih.gov/articlerender.fcgi?artid=24243&tool=pmcentrez&rendertype=abstract> (accessed July 9, 2013).
- [11] T.H. Hansen, M. Bouvier, MHC class I antigen presentation: learning from viral evasion strategies., *Nat. Rev. Immunol.* 9 (2009) 503–13. doi:10.1038/nri2575.
- [12] A.K. Pinto, A.B. Hill, Viral interference with antigen presentation to CD8+ T cells: lessons from cytomegalovirus., *Viral Immunol.* 18 (2005) 434–44. doi:10.1089/vim.2005.18.434.
- [13] E.J. Wiertz, T.R. Jones, L. Sun, M. Bogyo, H.J. Geuze, H.L. Ploegh, The human cytomegalovirus US11 gene product dislocates MHC class I heavy chains from the endoplasmic reticulum to the cytosol., *Cell.* 84 (1996) 769–79. <http://www.ncbi.nlm.nih.gov/pubmed/8625414> (accessed October 30, 2014).
- [14] B.N. Lilley, D. Tortorella, H.L. Ploegh, Dislocation of a type I membrane protein requires interactions between membrane-spanning segments within the lipid bilayer., *Mol. Biol. Cell.* 14 (2003) 3690–8. doi:10.1091/mbc.E03-03-0192.
- [15] B.N. Lilley, H.L. Ploegh, A membrane protein required for dislocation of misfolded proteins from the ER., *Nature.* 429 (2004) 834–40. doi:10.1038/nature02592.
- [16] S. Cho, M. Lee, Y. Jun, Forced interaction of cell surface proteins with Derlin-1 in the endoplasmic reticulum is sufficient to induce their dislocation into the cytosol for degradation., *Biochem. Biophys. Res. Commun.* 430 (2013) 787–92. doi:10.1016/j.bbrc.2012.11.068.
- [17] Y. Ye, Y. Shibata, C. Yun, D. Ron, T. a Rapoport, A membrane protein complex mediates retro-translocation from the ER lumen into the cytosol., *Nature.* 429 (2004) 841–7. doi:10.1038/nature02656.
- [18] Y. Ye, H.H. Meyer, T.A. Rapoport, The AAA ATPase Cdc48/p97 and its partners transport proteins from the ER into the cytosol., *Nature.* 414 (2001) 652–6. doi:10.1038/414652a.
- [19] B.N. Lilley, H.L. Ploegh, Multiprotein complexes that link dislocation, ubiquitination, and extraction of misfolded proteins from the endoplasmic reticulum membrane., *Proc. Natl. Acad. Sci. U. S. A.* 102 (2005) 14296–301. doi:10.1073/pnas.0505014102.
- [20] M. Kikkert, G. Hassink, M. Barel, C. Hirsch, F.J. van der Wal, E. Wiertz, Ubiquitination is essential for human cytomegalovirus US11-mediated dislocation of MHC class I molecules from the endoplasmic reticulum to the cytosol., *Biochem. J.* 358 (2001) 369–77. <http://www.pubmedcentral.nih.gov/articlerender.fcgi?artid=1222069&tool=pmcentrez&rendertype=abstract> (accessed September 7, 2013).
- [21] C.E. Shamu, D. Flierman, H.L. Ploegh, T.A. Rapoport, V. Chau, Polyubiquitination is required for US11-dependent movement of MHC class I heavy chain from endoplasmic reticulum into

- cytosol., *Mol. Biol. Cell.* 12 (2001) 2546–55. <http://www.pubmedcentral.nih.gov/articlerender.fcgi?artid=58612&tool=pmcentrez&rendertype=abstract> (accessed September 7, 2013).
- [22] B. Mueller, B.N. Lilley, H.L. Ploegh, SEL1L, the homologue of yeast Hrd3p, is involved in protein dislocation from the mammalian ER., *J. Cell Biol.* 175 (2006) 261–70. doi:10.1083/jcb.200605196.
- [23] J.H.L. Claessen, L. Kundrat, H.L. Ploegh, Protein quality control in the ER: balancing the ubiquitin checkbook., *Trends Cell Biol.* 22 (2012) 22–32. doi:10.1016/j.tcb.2011.09.010.
- [24] N.W. Bays, R.G. Gardner, L.P. Seelig, C.A. Joazeiro, R.Y. Hampton, Hrd1p/Der3p is a membrane-anchored ubiquitin ligase required for ER-associated degradation., *Nat. Cell Biol.* 3 (2001) 24–9. doi:10.1038/35050524.
- [25] R. Swanson, M. Locher, M. Hochstrasser, A conserved ubiquitin ligase of the nuclear envelope/endoplasmic reticulum that functions in both ER-associated and Matalpha2 repressor degradation., *Genes Dev.* 15 (2001) 2660–74. doi:10.1101/gad.933301.
- [26] M. Kikkert, R. Doolman, M. Dai, R. Avner, G. Hassink, S. van Voorden, S. Thanedar, J. Roitelman, V. Chau, E. Wiertz, Human HRD1 is an E3 ubiquitin ligase involved in degradation of proteins from the endoplasmic reticulum., *J. Biol. Chem.* 279 (2004) 3525–34. doi:10.1074/jbc.M307453200.
- [27] S. Fang, M. Ferrone, C. Yang, J.P. Jensen, S. Tiwari, A.M. Weissman, The tumor autocrine motility factor receptor, gp78, is a ubiquitin protein ligase implicated in degradation from the endoplasmic reticulum., *Proc. Natl. Acad. Sci. U. S. A.* 98 (2001) 14422–7. doi:10.1073/pnas.251401598.
- [28] G. Hassink, M. Kikkert, S. van Voorden, S.-J. Lee, R. Spaapen, T. van Laar, C.S. Coleman, E. Barteel, K. Früh, V. Chau, E. Wiertz, TEB4 is a C4HC3 RING finger-containing ubiquitin ligase of the endoplasmic reticulum., *Biochem. J.* 388 (2005) 647–55. doi:10.1042/BJ20041241.
- [29] H.R. Stagg, M. Thomas, D. van den Boomen, E.J.H.J. Wiertz, H. a Drabkin, R.M. Gemmill, P.J. Lehner, The TRC8 E3 ligase ubiquitinates MHC class I molecules before dislocation from the ER., *J. Cell Biol.* 186 (2009) 685–92. doi:10.1083/jcb.200906110.
- [30] R.J. Deshaies, C.A.P. Joazeiro, RING domain E3 ubiquitin ligases., *Annu. Rev. Biochem.* 78 (2009) 399–434. doi:10.1146/annurev.biochem.78.101807.093809.
- [31] K. Chang, S.J. Elledge, G.J. Hannon, Lessons from Nature: microRNA-based shRNA libraries., *Nat. Methods.* 3 (2006) 707–14. doi:10.1038/nmeth923.
- [32] A. Reynolds, D. Leake, Q. Boese, S. Scaringe, W.S. Marshall, A. Khvorova, Rational siRNA design for RNA interference., *Nat. Biotechnol.* 22 (2004) 326–30. doi:10.1038/nbt936.
- [33] M.C. Bassik, R.J. Lebbink, L.S. Churchman, N.T. Ingolia, W. Patena, E.M. LeProust, M. Schuldiner, J.S. Weissman, M.T. McManus, Rapid creation and quantitative monitoring of high coverage shRNA libraries., *Nat. Methods.* 6 (2009) 443–5. doi:10.1038/nmeth.1330.
- [34] M.C. Bassik, M. Kampmann, R.J. Lebbink, S. Wang, M.Y. Hein, I. Poser, J. Weibezahn, M.A. Horlbeck, S. Chen, M. Mann, A.A. Hyman, E.M. Leproust, M.T. McManus, J.S. Weissman, A systematic mammalian genetic interaction map reveals pathways underlying ricin susceptibility., *Cell.* 152 (2013) 909–22. doi:10.1016/j.cell.2013.01.030.
- [35] J.M. Silva, K. Marran, J.S. Parker, J. Silva, M. Golding, M.R. Schlabach, S.J. Elledge, G.J. Hannon, K. Chang, Profiling essential genes in human mammary cells by multiplex RNAi screening., *Science* (80-. ). 319 (2008) 617–20. doi:10.1126/science.1149185.
- [36] C.J. Matheny, M.C. Wei, M.C. Bassik, A.J. Donnelly, M. Kampmann, M. Iwasaki, O. Piloto, D.E. Solow-Cordero, D.M. Bouley, R. Rau, P. Brown, M.T. McManus, J.S. Weissman, M.L. Cleary, Next-Generation NAMPT Inhibitors Identified by Sequential High-Throughput Phenotypic Chemical and Functional Genomic Screens., *Chem. Biol.* 20 (2013) 1352–63. doi:10.1016/j.chembiol.2013.09.014.
- [37] R. Schekman, L. Orci, Coat proteins and vesicle budding., *Science* (80-. ). 271 (1996) 1526–33. <http://www.ncbi.nlm.nih.gov/pubmed/8599108> (accessed September 28, 2013).

- [38] Y. Ye, M. Rape, Building ubiquitin chains: E2 enzymes at work., *Nat. Rev. Mol. Cell Biol.* 10 (2009) 755–64. doi:10.1038/nrm2780.
- [39] D. Flierman, C.S. Coleman, C.M. Pickart, T.A. Rapoport, V. Chau, E2-25K mediates US11-triggered retrotranslocation of MHC class I heavy chains in a permeabilized cell system., *Proc. Natl. Acad. Sci. U. S. A.* 103 (2006) 11589–94. doi:10.1073/pnas.0605215103.
- [40] K.M. Paulsson, M.J. Kleijmeer, J. Griffith, M. Jevon, S. Chen, P.O. Anderson, H.-O. Sjogren, S. Li, P. Wang, Association of tapasin and COPI provides a mechanism for the retrograde transport of major histocompatibility complex (MHC) class I molecules from the Golgi complex to the endoplasmic reticulum., *J. Biol. Chem.* 277 (2002) 18266–71. doi:10.1074/jbc.M201388200.
- [41] H. Hanzawa, M.J. de Ruwe, T.K. Albert, P.C. van Der Vliet, H.T. Timmers, R. Boelens, The structure of the C4C4 ring finger of human NOT4 reveals features distinct from those of C3HC4 RING fingers., *J. Biol. Chem.* 276 (2001) 10185–90. doi:10.1074/jbc.M009298200.
- [42] M.L. Burr, F. Cano, S. Svobodova, L.H. Boyle, J.M. Boname, P.J. Lehner, HRD1 and UBE2J1 target misfolded MHC class I heavy chains for endoplasmic reticulum-associated degradation., *Proc. Natl. Acad. Sci. U. S. A.* 108 (2011) 2034–9. doi:10.1073/pnas.1016229108.
- [43] B. Mueller, E.J. Klemm, E. Spooner, J.H. Claessen, H.L. Ploegh, SEL1L nucleates a protein complex required for dislocation of misfolded glycoproteins., *Proc. Natl. Acad. Sci. U. S. A.* 105 (2008) 12325–30. doi:10.1073/pnas.0805371105.
- [44] U. Lenk, H. Yu, J. Walter, M.S. Gelman, E. Hartmann, R.R. Kopito, T. Sommer, A role for mammalian Ubc6 homologues in ER-associated protein degradation., *J. Cell Sci.* 115 (2002) 3007–14. <http://www.ncbi.nlm.nih.gov/pubmed/12082160> (accessed August 16, 2013).
- [45] D. Flierman, Y. Ye, M. Dai, V. Chau, T.A. Rapoport, Polyubiquitin serves as a recognition signal, rather than a ratcheting molecule, during retrotranslocation of proteins across the endoplasmic reticulum membrane., *J. Biol. Chem.* 278 (2003) 34774–82. doi:10.1074/jbc.M303360200.
- [46] D.E. Christensen, P.S. Brzovic, R.E. Klevit, E2-BRCA1 RING interactions dictate synthesis of mono- or specific polyubiquitin chain linkages., *Nat. Struct. Mol. Biol.* 14 (2007) 941–8. doi:10.1038/nsmb1295.
- [47] M.L. Burr, D.J.H. van den Boomen, H. Bye, R. Antrobus, E.J. Wiertz, P.J. Lehner, MHC class I molecules are preferentially ubiquitinated on endoplasmic reticulum luminal residues during HRD1 ubiquitin E3 ligase-mediated dislocation., *Proc. Natl. Acad. Sci. U. S. A.* 110 (2013) 14290–5. doi:10.1073/pnas.1303380110.
- [48] P. Mali, L. Yang, K.M. Esvelt, J. Aach, M. Guell, J.E. DiCarlo, J.E. Norville, G.M. Church, RNA-guided human genome engineering via Cas9., *Science* (80-. ). 339 (2013) 823–6. doi:10.1126/science.1232033.
- [49] P.J. Paddison, M. Cleary, J.M. Silva, K. Chang, N. Sheth, R. Sachidanandam, G.J. Hannon, Cloning of short hairpin RNAs for gene knockdown in mammalian cells., *Nat. Methods.* 1 (2004) 163–167.
- [50] B. Langmead, C. Trapnell, M. Pop, S.L. Salzberg, Ultrafast and memory-efficient alignment of short DNA sequences to the human genome., *Genome Biol.* 10 (2009) R25. doi:10.1186/gb-2009-10-3-r25.
- [51] D.W. Huang, B.T. Sherman, R.A. Lempicki, Systematic and integrative analysis of large gene lists using DAVID bioinformatics resources., *Nat. Protoc.* 4 (2009) 44–57. doi:10.1038/nprot.2008.211.
- [52] D.W. Huang, B.T. Sherman, R.A. Lempicki, Bioinformatics enrichment tools: paths toward the comprehensive functional analysis of large gene lists., *Nucleic Acids Res.* 37 (2009) 1–13. doi:10.1093/nar/gkn923.

# Supplementary Information

Supplementary Information provides 11 Supplementary Figures and 3 Supplementary Tables; a brief description for each element is given below.

**Supplementary Figure 1** shows the extended results for all four TMEM129-targeting shRNAs used throughout this study.

**Supplementary Figure 2** provides a detailed flow cytometry analysis of TMEM129-null cell clones generated via CRISPR/Cas genome engineering.

**Supplementary Figure 3** shows a pulse-chase analysis of HLA class I in the absence or presence of HCMV US11.

**Supplementary Figure 4** provides analysis of the COPI hits.

**Supplementary Figure 5** shows the evolutionary conservation of TMEM129.

**Supplementary Figure 6** shows the state of the UPR in TMEM129-null cells.

**Supplementary Figure 7** provides a functional assessment of HRD1 in US11-mediated HLA class I downregulation.

**Supplementary Figure 8** provides an overview of genomic target sites for the gRNAs used throughout this study.

**Supplementary Figure 9** shows the validation of generated TMEM129-specific mAbs.

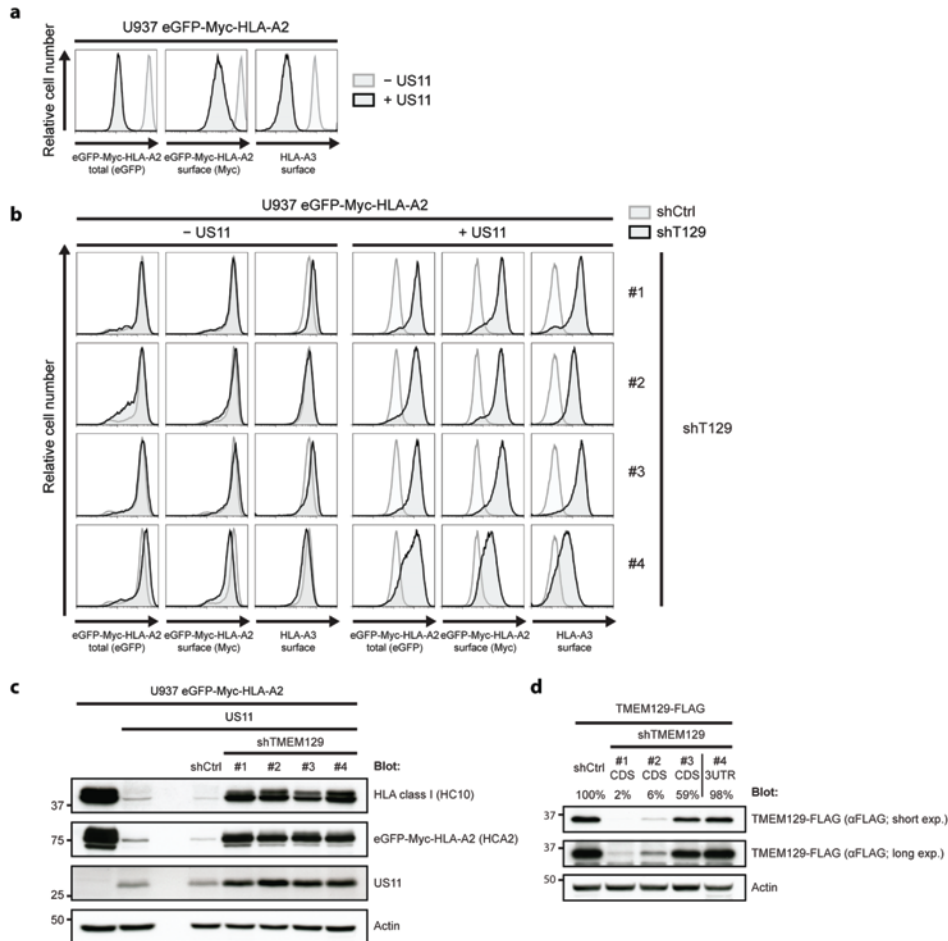
**Supplementary Figure 10** shows the functionality of the TMEM129 and US11 constructs used throughout this study.

**Supplementary Figure 11** shows the full scans of the Western blots.

**Supplementary Table 1** shows sequences of shRNAs used for independent validation experiments.

**Supplementary Table 2** shows gRNA sequences used for CRISPR/Cas-mediated gene disruption.

**Supplementary Table 3** shows primer sequences used for UPR assessment.

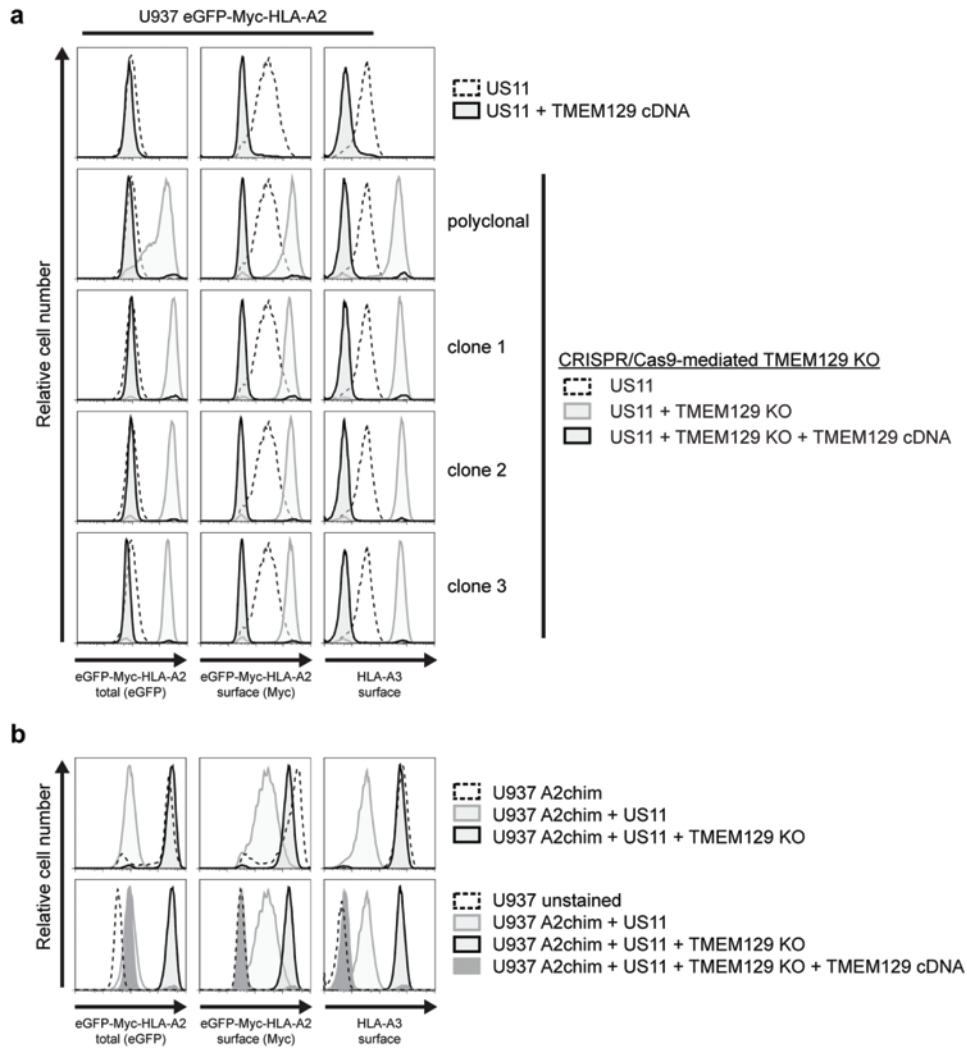


**Supplementary Figure 1: TMEM129 is crucial for US11-mediated HLA class I downregulation.** (a) HCMV US11 induces downregulation of the eGFP-Myc-HLA-A2 chimera and endogenous HLA class I in U937 cells. Flow cytometry analysis of total (eGFP) and surface (Myc) expression of eGFP-Myc HLA-A2 and surface expression of endogenous HLA-A3 in U937 eGFP-Myc-HLA-A2 cells with (black histogram) and without expression of HCMV US11 (gray histogram). (b) Depletion of endogenous TMEM129 by shRNAs induces potent rescue of eGFP-Myc-HLA-A2 and endogenous HLA-A3 expression in U937 eGFP-Myc-HLA-A2 US11 cells. Four shRNAs targeting TMEM129 (black histograms) or one control shRNA (gray histogram) were introduced in U937 eGFP-Myc-HLA-A2 cells and U937 eGFP-Myc-HLA-A2 US11 cells. 7 dpi flow cytometry analysis was performed of endogenous surface HLA-A3, and surface (Myc) and total (eGFP) eGFP-Myc-HLA-A2. (c) Immunoblot analysis of endogenous HLA class I, eGFP-Myc-HLA-A2, US11, and loading control actin in U937 eGFP-Myc-HLA-A2 US11 cells after mock (shCtrl) or TMEM129 (shTMEM129 #1-4) depletion. (d) Downregulation of ectopically expressed tagged TMEM129 using shRNAs. Immunoblot analysis of TMEM129-FLAG levels and loading control actin in U937 cells after mock (shCtrl) or TMEM129 (shT129 #1-4) depletion 7 dpi. Percentages indicate expression levels compared to mock (shCtrl) depletion normalized to actin levels. Of note, effective shRNA-mediated depletion was confirmed in cells ectopically expressing TMEM129-FLAG, as endogenous protein levels of TMEM129 could not be assessed via immunoblotting. Therefore, in this experimental setup, the fourth shRNA had no effect on TMEM129-FLAG expression levels (lane

### An shRNA library screen identifies TMEM129 as E3 ligase involved in ERAD

5), because this shRNA targets the 3'-UTR, which is absent in the ectopic TMEM129-FLAG construct. In all further experiments, where TMEM129 is depleted, the most efficient and stable TMEM129-targeting shRNA (shTMEM129 #1) was used. CDS, coding sequence; 3UTR, 3' untranslated region.

3

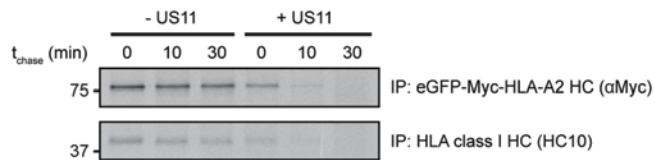


**Supplementary Figure 2: Generation and analysis of CRISPR/Cas-mediated TMEM129-null lines.** (a) CRISPR/Cas-mediated knockout of TMEM129 induces potent rescue of HLA class I. U937 eGFP-Myc-HLA-A2 US11 cells were transiently transfected with Cas9- and gTMEM129-expressing plasmids. Cells with increased eGFP signal were sorted (polyclonal), and subsequently clonally expanded, which resulted in the generation of 3 individual clones (clone 1-3). TMEM129 was re-introduced in these cells. Cells were then subjected to flow cytometry analysis of surface endogenous HLA-A3, and surface (Myc) and total (eGFP) eGFP-Myc-HLA-A2. (b, upper panel) TMEM129-null US11 cells show completely restored HLA class I expression. Surface endogenous HLA-A3, and surface (Myc) and total (eGFP) eGFP-Myc-HLA-A2 comparison between U937 eGFP-Myc-HLA-A2 (dashed histograms), U937 eGFP-Myc-HLA-A2 US11 (gray-lined histograms), and U937 eGFP-Myc-HLA-A2 US11 TMEM129-null cells (black-lined histograms). (b, lower panel) TMEM129-overexpressing TMEM129-null US11 cells are almost devoid of HLA class I molecules. Surface endogenous HLA-A3, and surface (Myc) and total (eGFP) eGFP-Myc-HLA-A2 comparison between unstained U937 (dashed histograms), U937 eGFP-Myc-HLA-A2 US11 (gray-lined histograms), and



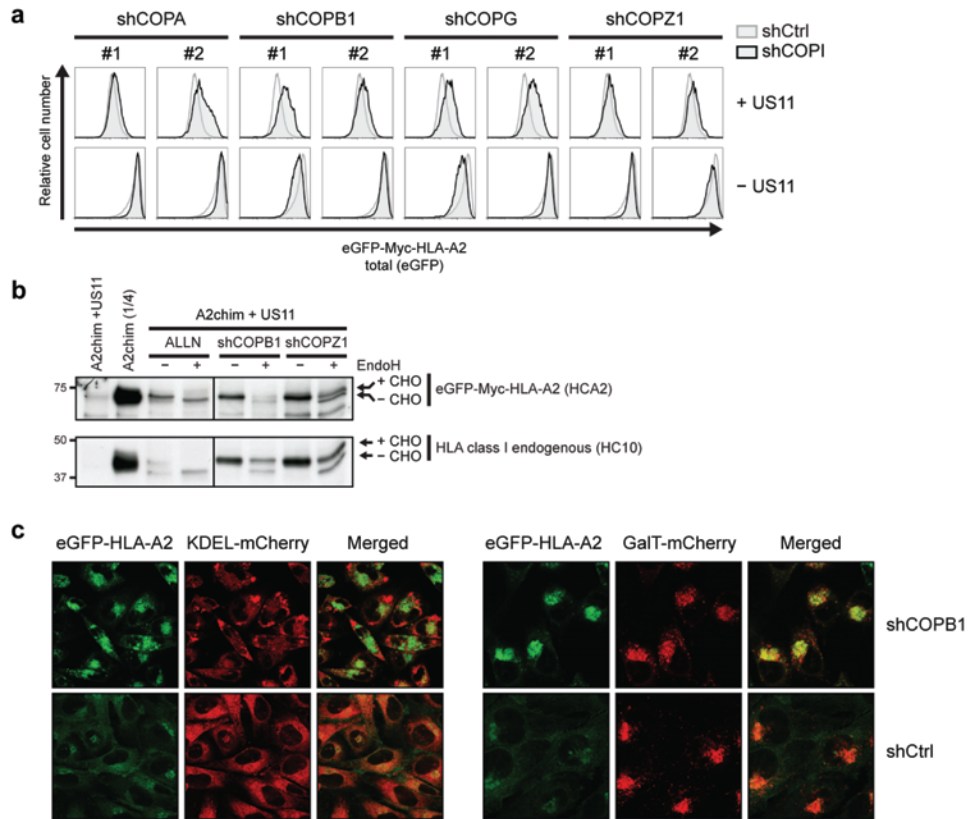
An shRNA library screen identifies TMEM129 as E3 ligase involved in ERAD

U937 eGFP-Myc-HLA-A2 US11 TMEM129-null cells (black-lined histograms), and U937 eGFP-Myc-HLA-A2 US11 TMEM129-null cells overexpressing TMEM129 cDNA (gray-filled histograms).



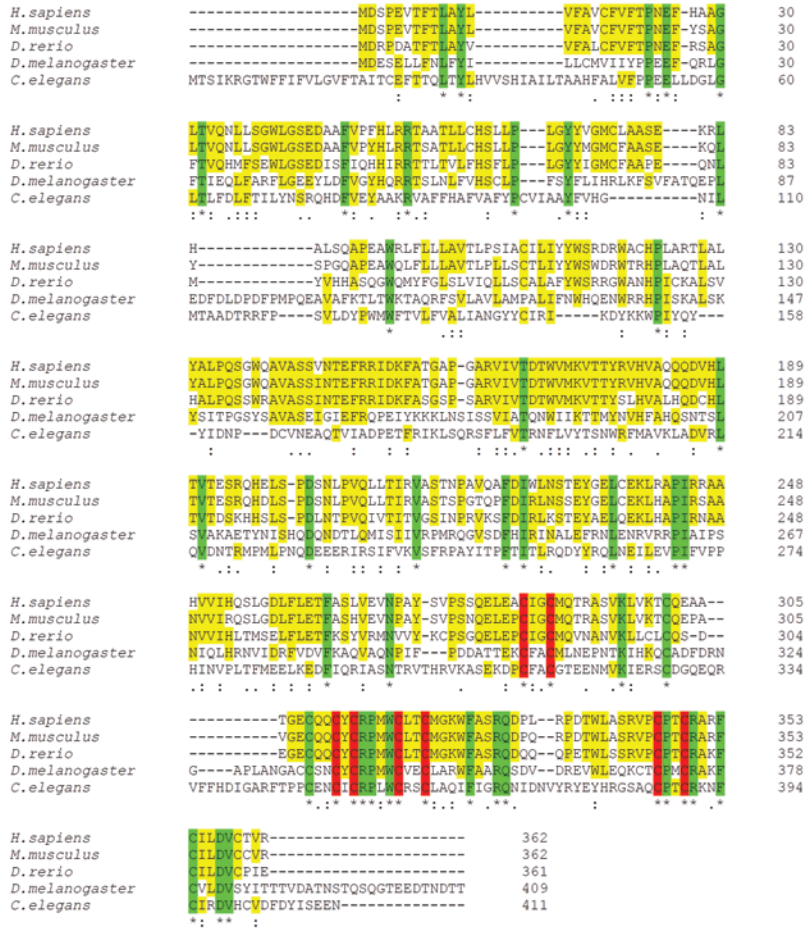
**Supplementary Figure 3: US11 induces rapid degradation of HLA class I in U937 cells.** U937 eGFP-Myc-HLA-A2 cells with and without US11 were subjected to pulse chase analysis, for which cells were radioactively labeled for 10 min, and chased for the indicated timeframes. Subsequently, eGFP-Myc-HLA-A2 and HLA class I HCs were immunoprecipitated from lysates using respectively the Myc-specific 9E10 mAb and the HLA class I HC-specific HC10 mAb.

3



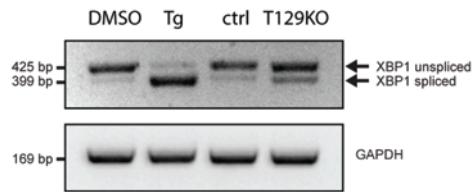
**Supplementary Figure 4: COPI depletion causes accumulation of HLA class I in the Golgi.** (a) COPI subunit depletion by shRNAs induces rescue of chimeric HLA-A2 expression in U937 cells co-expressing eGFP-Myc-HLA-A2 and US11. shRNAs targeting indicated COPI subunits (black histograms) or control shRNAs (gray histogram) were introduced in U937 eGFP-Myc-HLA-A2 and U937 eGFP-Myc-HLA-A2 US11 cells, and total expression of eGFP-Myc-HLA-A2 was assessed by measuring eGFP expression 4 dpi. by flow cytometry, whereas surface expression of eGFP-Myc-HLA-A2 and endogenous HLA-A3 were assessed by specific antibody stainings (anti-Myc and anti-A3 respectively). Of note, as COPI subunit depletion induced rapid cell death (approximately 4 dpi), the full effect of COPI depletion could not be assessed since optimal protein target knockdown is often only reached after approximately 6 d p.i. [1]. (b) COPI subunit depletion by shRNAs induces rescue of HLA class I to post-ER compartments in U937 cells co-expressing eGFP-Myc-HLA-A2 and US11. Lysates of U937 eGFP-Myc-HLA-A2 US11 cells incubated with either DMSO or ALLN, or U937 eGFP-Myc-HLA-A2 US11 cells expressing an shRNA targeting either COPB1 or COPZ1, were mock- or EndoH-treated, after which immunoblot analysis was performed to detect endogenous HLA class I and eGFP-Myc-HLA-A2. One-fourth of U937 eGFP-Myc-HLA-A2 lysate as compared to other lanes is loaded as a reference. (c) COPI subunit depletion causes accumulation of eGFP-Myc-HLA-A2 in the Golgi-compartment. MJS GFP-HLA-A2 cells stably expressing either mCherry-KDEL (ER-localized) or GAIT-mCherry (Golgi-localized) were either mock- or COPI-subunit-depleted and fixed, after which immunofluorescence analysis for eGFP-HLA-A2 and mCherry-KDEL or GAIT-mCherry was performed. Individual images were merged to assess co-localization.

An shRNA library screen identifies TMEM129 as E3 ligase involved in ERAD



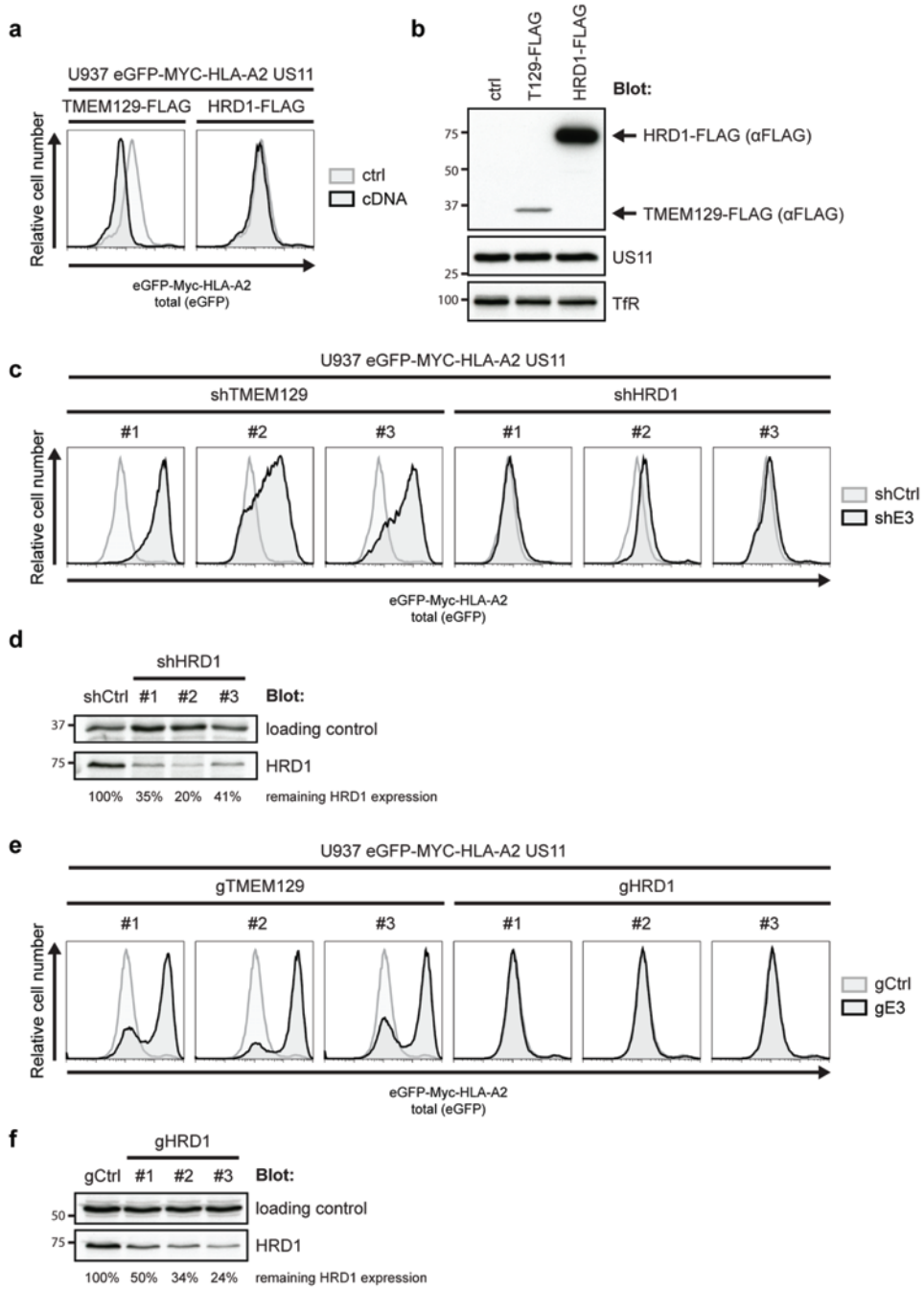
% identity					
<b>Hs</b>	100				
<b>Mm</b>	89.2	100			
<b>Dr</b>	64.8	66.5	100		
<b>Dm</b>	32.8	33.6	34.7	100	
<b>Ce</b>	24.7	25	22.7	23.9	100
	<b>Hs</b>	<b>Mm</b>	<b>Dr</b>	<b>Dm</b>	<b>Ce</b>

**Supplementary Figure 5: Multiple sequence alignment of TMEM129.** Amino acid sequences of TMEM129 from *H. sapiens* (UniProt: A0AVI4), *M. musculus* (UniProt: Q8K304), *D. rerio* (UniProt: Q6PD82), *D. melanogaster* (UniProt: Q9VN16), and *C. elegans* (UniProt: O17638) were aligned using ClustalO software, and conserved residues were visualized using JalView. Identity percentages were calculated using Clustal software. Green: fully conserved residue; Yellow, 50% or more residues with similar identity; Red: fully conserved zinc-coordinating cysteine as part of the RING domain. An '\*' (asterisk) indicates a single, fully conserved residue. A ':' (colon) indicates conservation between groups of strongly similar properties with a scoring of > 0.5 in the Gonnet PAM 250 matrix. A '.' (period) indicates conservation between groups of weakly similar properties with a scoring of ≤ 0.5 in the Gonnet PAM 250 matrix

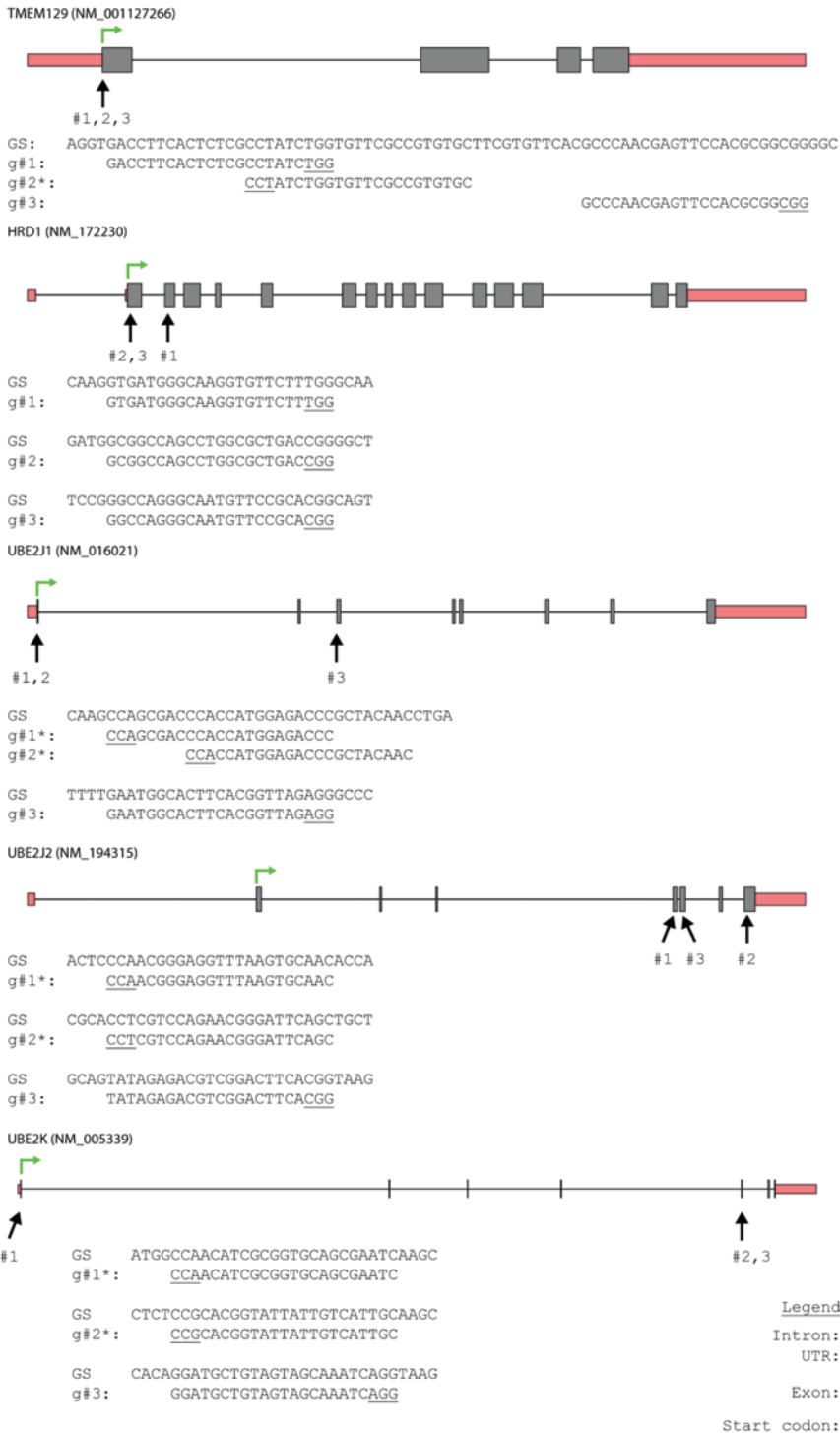


**Supplementary Figure 6: TMEM129 knockout does not induce a strong UPR response.** RNA was isolated from TMEM129-null cells (T129KO), generated via the CRISPR/Cas9 system, or from control cells (ctrl). From the RNA, mRNA was specifically converted to cDNA, after which levels of spliced and unspliced XBP-1 were detected via semi-quantitative PCR as a marker for UPR activation. GAPDH was included as a loading control. As a positive UPR control, cells were incubated with Thapsigargin (50  $\mu$ M) for 6 hours, or, as a negative control, with DMSO.

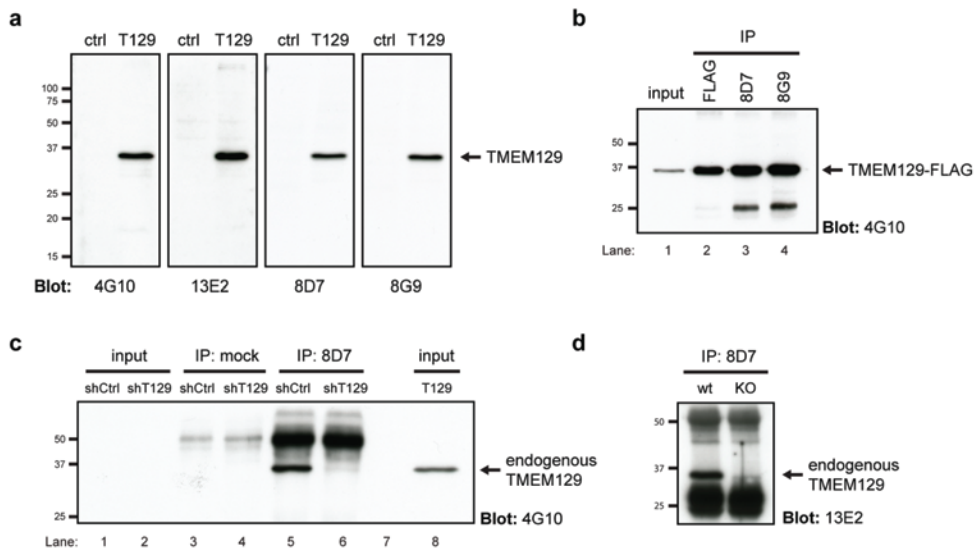
> **Supplementary Figure 7: Functional assessment of HRD1 in US11-mediated HLA class I downregulation.** (a) HRD1 overexpression does not enhance US11-mediated HLA class I downregulation. Flow cytometry analysis of total (eGFP) eGFP-Myc-HLA-A2 in U937 eGFP-Myc-HLA-A2 US11 cells overexpressing TMEM129-FLAG (black-lined histogram, left panels), HRD1-FLAG (black-lined histogram, right panels), or a control vector (gray-lined histograms, both panels). (b) Immunoblot analysis of TMEM129-FLAG and HRD1-FLAG expression levels in cells used in (a). US11 expression levels are indicated as well, along with transferrin receptor used as a loading control. (c) ShRNA-mediated HRD1 depletion does not rescue HLA class I from US11-mediated downregulation. Flow cytometry analysis of total (eGFP) eGFP-Myc-HLA-A2 in U937 eGFP-Myc-HLA-A2 US11 cells expressing shRNAs targeting TMEM129 (black-lined histograms, left three panels) or HRD1 (black-lined histograms, right three panels), or a control shRNA (gray-lined histograms). (d) Assessment of knockdown efficiency of HRD1-targeting shRNAs. A background band was used as a loading control. Percentages indicate HRD1 expression levels as compared to mock (shCtrl) depletion normalized against loading control levels. (e) CRISPR/Cas-mediated HRD1 gene disruption does not rescue HLA class I from US11-mediated downregulation. Same experimental setup as in C, but instead of shRNAs, CRISPR/Cas gRNAs were lentivirally introduced. (f) Validation of HRD1-targeting gRNAs. Western blots depict the expression level of HRD1 in the indicated polyclonal CRISPR/Cas-mediated HRD1 knock-out or control cells. The lentiviral delivery of the CRISPR/Cas system results in a mixed population of cells in which either no, one or both HRD1 alleles are knocked-out. Typically, we observe approximately 30-90% of full knock-out phenotypes upon CRISPR/Cas mediated genome editing. Indicated percentages show HRD1 expression levels in these polyclonal lines as compared to control gRNA treated cells normalized to a loading control.



Chapter 3

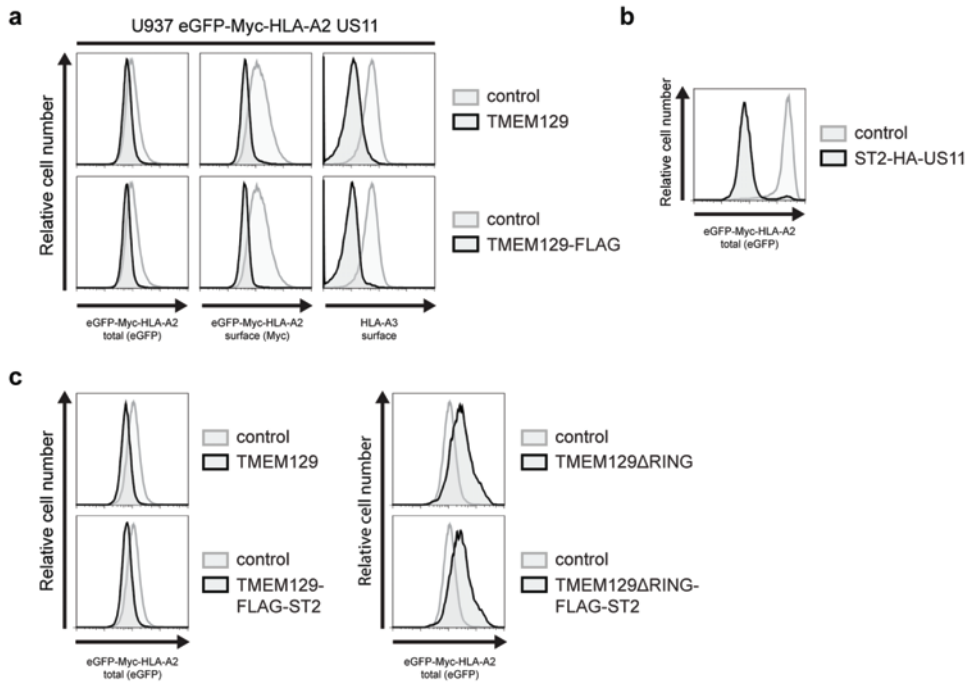


**Supplementary Figure 8: Genomic target sites of gRNAs for CRISPR/Cas-mediated genome engineering.** gRNAs were designed to target coding regions of TMEM129, HRD1, UBE2J1, UBE2J2, and UBE2K that lie as close to the start codon as possible to minimize potential expression of truncated gene products. However, gRNA target sites were limited by the presence of the PAM motive (underlined) and were designed to be uniquely present in the human genome to limit the impact of potential off-targeting effects [2]. gRNA target sites that are indicated with an asterisk, are reverse complement to gRNA sequences used. Gene structures including UTRs, introns and exons have been visualized using FancyGene [3]. See Supplementary Table 2 for more information on the gRNAs that were used in this study. GS, Genomic Sequence; PAM, protospacer adjacent motive; g#, gRNA number.



**Supplementary Figure 9: TMEM129-specific monoclonal antibodies.** (a) The rat 4G10 and 13E2 mAbs, and the mouse 8D7 and 8G9 mAbs were tested for their TMEM129 specificity using lysates of wildtype U937 cells and TMEM129-overexpressing U937 cells. (b) The mouse 8D7 and 8G9 mAbs were tested for their ability to immunoprecipitate TMEM129 from lysates of U937 TMEM129-FLAG cells (lane 3, 4). As a positive immunoprecipitation control, an anti-FLAG immunoprecipitation was included (lane 2). Immunoprecipitated samples were subjected to immunoblotting using the TMEM129-specific 4G10 mAb to visualize TMEM129-FLAG. (c) Endogenous TMEM129 can be visualized by immunoprecipitation and subsequent immunoblotting using a TMEM129-specific mAb. Lysates of U937 cells that were either mock- (shCtrl) or TMEM129-depleted (shT129), were subjected to immunoprecipitation using empty beads (mock; lane 3 and 4) or the TMEM129-specific 8D7 mAb (lane 5 and 6), after which immunoblotting was performed using the TMEM129-specific 4G10 mAb. Each IP lane corresponds to 20\*10<sup>6</sup> cells, while each input lane corresponds to 0.2\*10<sup>6</sup> cells. As a size reference, lysate of TMEM129-overexpressing U937 cells was included (lane 8). (d) CRISPR/Cas-mediated TMEM129 knockout. Lysates of U937 cells (wt, lane 1) and TMEM129-null cells (KO, lane 2) were subjected to immunoprecipitation using the TMEM129-specific 8D7 mAb, after which immunoblotting was performed using the TMEM129-specific 13E2 mAb.

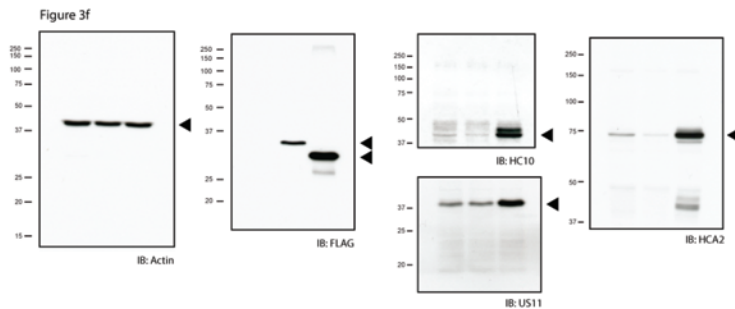
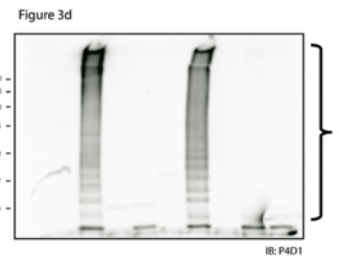
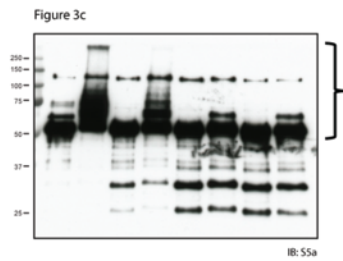
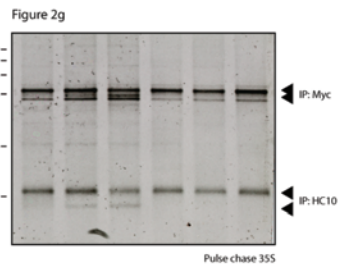
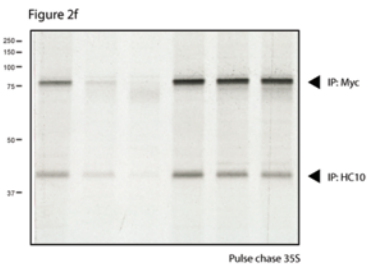
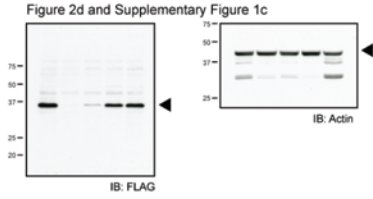
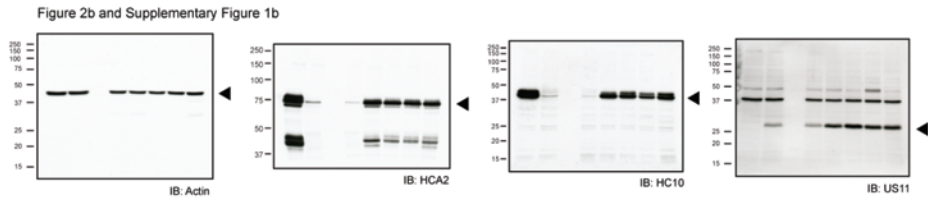
3



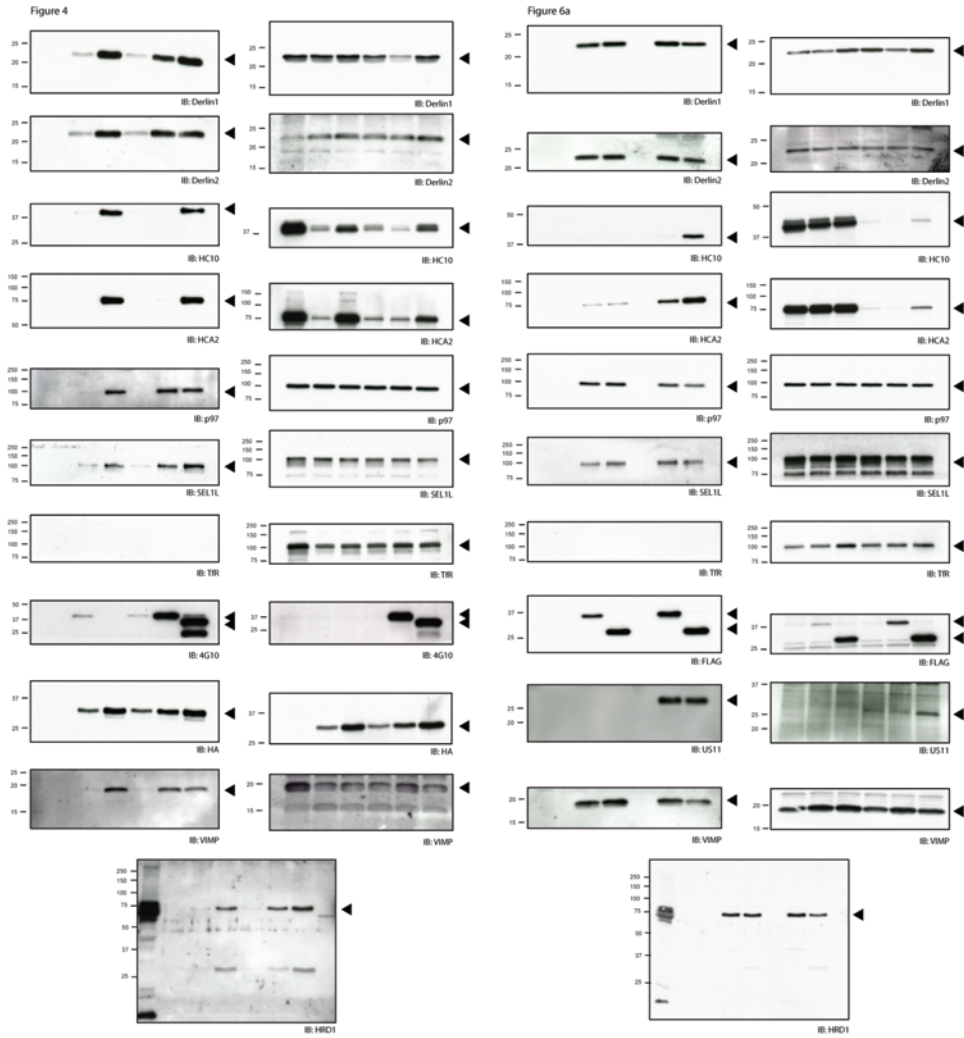
**Supplementary Figure 10: Tagged TMEM129 and US11 constructs are functional.** (a) FLAG-tagged TMEM129 retains activity. Flow cytometry analysis of surface endogenous HLA-A3, and surface (Myc) and total (eGFP) eGFP-Myc-HLA-A2 in U937 eGFP-Myc-HLA-A2 US11 cells overexpressing TMEM129 (black-lined histograms, upper panels), TMEM129-FLAG (black-lined histograms, lower panels), or a control vector (gray-lined histograms, upper and lower panels). (b) Strep-II-HA-tagged US11 retains activity. Flow cytometry analysis of total eGFP-Myc-HLA-A2 in U937 eGFP-Myc-HLA-A2 cells expressing ST2-HA-US11 (black-lined histogram), or a control vector (gray-lined histogram). (c) Strep-II-HA-tagged TMEM129 retains activity. Flow cytometry analysis of total eGFP-Myc-HLA-A2 in U937 eGFP-Myc-HLA-A2 US11 cells expressing TMEM129 (black-lined histogram, left-upper panel), TMEM129-FLAG-ST2 (black-lined histogram, left-lower panel), TMEM129 $\Delta$ RING (black-lined histogram, right-upper panel), TMEM129 $\Delta$ RING-FLAG-ST2 (black-lined histogram, right-lower panel), or an empty vector (gray-lined histogram).

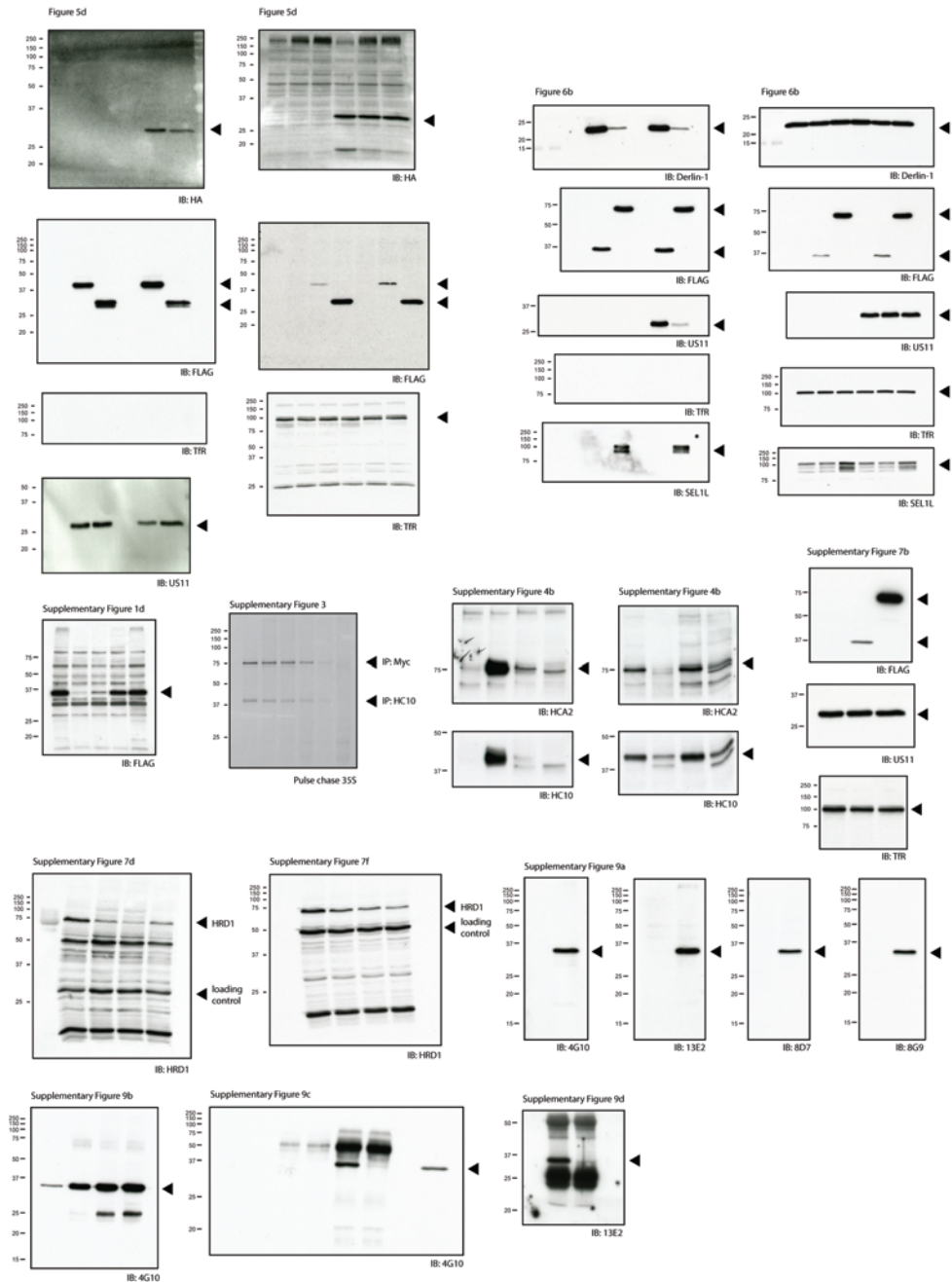


An shRNA library screen identifies TMEM129 as E3 ligase involved in ERAD



3





3

**Supplementary Figure 11. Full scans Western blots.** Molecular weight marker (kDa) is included on the left side of each blot. Specific bands are depicted with an arrow on the right side.

Supplementary Table 1: Sequences of shRNAs used for independent validation experiments

Name	Target	Target site in <sup>1</sup>	Sigma TRC number	Sigma Clone ID	Sequence shRNA	Comments
shCtrl	-	-	SHC002	Non-target shRNA Control Vector	-	
shMEM129 #1	TMEM129	CDS	TRCN0000042616	NM_138385.3-837s1c1	CGGTTCCCTGCACTCCGATCTACTCTCGAAGGTAAGTCCAGATCCAGGCGAATTTT	
shMEM129 #2	TMEM129	CDS	TRCN0000042617	NM_138385.3-942s2c1	CGGTTGCTCTCCCTGTCGAAATGTCCTCGAGCCAGTGTGTGACAGGAGGAGCAATTTT	
shMEM129 #3	TMEM129	CDS	TRCN0000042618	NM_138385.3-1025s1c1	CGGAGCTGTGGGTGATGAAAGGTAACCTCCAGAGGATTAACCTTCATCAACCCAGCTTTT	
shMEM129 #4	TMEM129	3'UTR	TRCN0000042619	NM_138385.3-1528s1c1	CGGAGCTGGACAAAGGAGCTGTAATTAAGTCCGAGGTGAAGTCAAGCCCTTTGACAGTTT	
shHRD1 #1	HRD1	3'UTR	TRCN0000034004	NM_032431.1-2804s1c1	CGGATGATAGCTTAATCCCGGAGAAATCGAGGATTTCCCGGAGATTAAGCAATGATTTT	
shHRD1 #2	HRD1	CDS	TRCN0000034006	NM_032431.1-152s1c1	CGGAGCTCAGCCCTACTACTCCAGACTCGAGGCTTGGAGGTGGAGAGGAGAGCCCTTTT	
shHRD1 #3	HRD1	CDS	TRCN0000034007	NM_032431.1-458s1c1	CGGAGCCCGTGTGGACTTTATGGAGACTCGAGGTTCCATTAAGGTCACAGCGGCTTTT	
shUBC2J1 #1	UBC2J1	3'UTR	TRCN0000004131	NM_016021.X-315s1c1	CGGAGCTGAGATTTGTTGTGCTAGGAGACTCGAGGTTCCAGCCAGCACTCCAGCTTTT	
shUBC2J1 #2	UBC2J1	CDS	TRCN0000004134	NM_016021.X-1227s1c1	CGGATGACTCTTATATATTCGAGCGAGACTCGAGGTTCCGTTGGAGATTAAGGACTGTTT	
shUBC2J1 #1	UBC2J2	CDS	TRCN00000034096	NM_058167.2-408s1c1	CGGATCAACCTCCAGATCTATATATTCGAGGATTAAGATTAAGATTAAGATTAAGATTTT	
shUBC2J2 #2	UBC2J2	CDS	TRCN00000034087	NM_058167.2-358s1c1	CGGAGAGGTTGAGTATATCATCGAGACTCGAGGTTCCATTAAGATTAAGCACTTTT	
shCOP1 #1	COP1	CDS	TRCN0000065289	NM_004371.2-404s1c1	CGGAGCCCTGAGGTTCAAAAGGTTCAATTCGAGAAATTTGACTTTGAACTCAAGGTTT	
shCOP1 #2	COP1	CDS	TRCN0000065271	NM_004371.2-2890s1c1	CGGAGCCTTATATTAATGACTGATCCAGACTCGAGGTTGGATGACAGTCAATTAAGGCTTT	
shCOP1 #1	COP1	CDS	TRCN00000151483	NM_016451.3-2636s1c1	CGGAGCCCTCATGACTTCGCAAAATATCTTCGAGAAATTTTCGAGAAATCATGAGGTTT	
shCOP1 #2	COP1	CDS	TRCN00000151067	NM_016451.3-3110s1c1	CGGAGCCCTTAAGTTCTGAGAGATAGAACTCGAGGTTTACTCCAGGCTTAAGGCTTTT	Used in Suppl. Fig. 4b and 4c
shCOP6 #1	COP6	3'UTR	TRCN00000149699	NM_016128.3-2940s1c1	CGGAGCTTGTCTTAATATCTTGGCTGTGCTCGAGAGCAGCCAGAAATTAAGGCAAGCTTTT	
shCOP6 #2	COP6	CDS	TRCN00000146530	NM_016128.3-1730s1c1	CGGAGCAAGGCTTATATATCCTAAGTGGTTCGAGAGCCATTTAGGATTAAGTCCCTTTT	
shCOP1 #1	COP1	CDS	TRCN0000064998	NM_016057.1-193s1c1	CGGAGCCATGAGATTAAGATTAAGTATGAGAAATTCGAGAAATTTTCAGTGTCCAGTGTGTT	
shCOP1 #2	COP1	CDS	TRCN0000065002	NM_016057.1-249s1c1	CGGAGCAATTAAGATCTCTAATTTCTTCGAGAGAAATTAAGAAATTAAGATTAAGATTTT	Used in Suppl. Figure 4b

<sup>1</sup>CDS, Coding sequence; 3'UTR, 3'-untranslated region.

Name	Gene targeted	CRISPR target site (without PAM <sup>1</sup> )
TMEM129-gRNA#1	<i>TMEM129</i>	GACCTTCACTCTCGCCTATC
TMEM129-gRNA#2	<i>TMEM129</i>	GCACACGGCGAACACCAGAT
TMEM129-gRNA#3	<i>TMEM129</i>	GCCCAACGAGTTCCACGCGG
HRD1-gRNA#1	<i>HRD1</i>	GTGATGGGCAAGGTGTTCTT
HRD1-gRNA#2	<i>HRD1</i>	GCGGCCAGCCTGGCGCTGAC
HRD1-gRNA#3	<i>HRD1</i>	GGCCAGGGCAATGTTCCGCA
UBE2J1-gRNA#1	<i>UBE2J1</i>	GGGTCTCCATGGTGGGTCCG
UBE2J1-gRNA#2	<i>UBE2J1</i>	GTTGTAGCGGGTCTCCATGG
UBE2J1-gRNA#3	<i>UBE2J1</i>	GAATGGCACTTCACGGTTAG
UBE2J2-gRNA#1	<i>UBE2J2</i>	GTTGCACTTAAACCTCCCGT
UBE2J2-gRNA#2	<i>UBE2J2</i>	GCTGAATCCCGTTCTGGACG
UBE2J2-gRNA#3	<i>UBE2J2</i>	TATAGAGACGTCGGACTTCA
UBE2K-gRNA#1	<i>UBE2K</i>	GATTGCTGCACCGCGATGT
UBE2K-gRNA#2	<i>UBE2K</i>	GCAATGACAATAATACCGTG
UBE2K-gRNA#3	<i>UBE2K</i>	GGATGCTGTAGTAGCAAATC

<sup>1</sup>PAM, protospacer adjacent motif.

Supplementary Table 2: gRNA sequences used for CRISPR/Cas-mediated gene disruption.

Primer Name	Primer sequence	RefSeq	Expected band size (bp)
XBP-1 fw	CTGGAACAGCAAGTGGTAGA	NM_005080	Unspliced: 425 Spliced: 399
XBP-1 rev	ACTGGGTCCTTCTGGGTAGA		
GAPDH fw	CATCACCATCTTCCAGGAGC	NM_002046	404
GAPDH rev	GGCTCTCCAGAACATCATCC		

Supplementary Table 3: Primer sequences used for UPR assessment.

## REFERENCES

- [1] Lebbink, R. J. et al. Polymerase II promoter strength determines efficacy of microRNA adapted shRNAs. *PLoS One* 6, e26213 (2011).
- [2] Mali, P. et al. RNA-guided human genome engineering via Cas9. *Science* 339, 823–6 (2013).
- [3] Rambaldi, D. & Ciccarelli, F. D. FancyGene: dynamic visualization of gene structures and protein domain architectures on genomic loci. *Bioinformatics* 25, 2281–2 (2009).



## CHAPTER 4

# The E3 Ubiquitin Ligase TMEM129 Is a Tri-Spanning Transmembrane Protein

Michael L. van de Weijer, Guus H. van Muijlwijk, Linda J. Visser, Ana I. Costa, Emmanuel J.H.J. Wiertz\*, Robert Jan Lebbink\*

Medical Microbiology, University Medical Center Utrecht, 3584CX Utrecht, The Netherlands;

\*These authors contributed equally to this work

Published in:  
Viruses 8 (2016). doi:10.3390/v8110309

## ABSTRACT

Misfolded proteins from the endoplasmic reticulum (ER) are transported back into the cytosol for degradation via the ubiquitin-proteasome system. The human cytomegalovirus protein US11 hijacks this ER-associated protein degradation (ERAD) pathway to downregulate human leukocyte antigen (HLA) class I molecules in virus-infected cells, thereby evading elimination by cytotoxic T-lymphocytes. Recently, we identified the E3 ubiquitin ligase transmembrane protein 129 (TMEM129) as a key player in this process, where interference with TMEM129 activity in human cells completely abrogates US11-mediated class I degradation. Here, we set out to further characterize TMEM129. We show that TMEM129 is a non-glycosylated protein containing a non-cleaved signal anchor sequence. By glycosylation scanning mutagenesis, we show that TMEM129 is a tri-spanning ER-membrane protein that adopts a  $N_{\text{exo}}-C_{\text{cyto}}$  orientation. This insertion in the ER membrane positions the C-terminal really interesting new gene (RING) domain of TMEM129 in the cytosol, making it available to catalyze ubiquitination reactions that are required for cytosolic degradation of secretory proteins.



## INTRODUCTION

The endoplasmic reticulum (ER) is the nexus for translation of proteins destined for the secretory pathway. It is estimated that around 30% of all proteins produced in the human cell are directed towards the secretory route. The oxidative environment and folding machinery present in the ER are responsible for the proper folding of these proteins [1]. Proteins that become terminally misfolded need to be removed, as these can form larger aggregates and as such may compromise cell homeostasis and survival [2]. ER quality control mechanisms recognize misfolded proteins and redirect these towards the ubiquitin–proteasome system for degradation [3]. To this end, ER-resident proteins destined for degradation have to cross the ER membrane to reach the cytosol for proteolysis by the proteasome. This retrograde movement of proteins, called retrotranslocation or dislocation, is a key step in ER-associated protein degradation (ERAD) [4,5]. At the center of the ERAD process are multiprotein complexes that combine the various essential functions in a defined manner, namely recognition, dislocation, ubiquitination, and degradation of substrates [6].

The multiprotein complexes that facilitate ERAD generally contain multipass transmembrane E3 ubiquitin ligases harboring a really interesting new gene (RING) domain [7–10]. The RING domain of these E3 ubiquitin ligases is situated in the cytosol and serves as a docking site for an E2 ubiquitin-conjugating enzyme, which in turn catalyzes polyubiquitination of the target substrates [11]. In yeast, the main ER-resident transmembrane E3 ubiquitin ligases involved in ERAD are Hrd1p [12] and Doa10 [13]. In addition, multiprotein ERAD complexes were recently discovered to be present in the inner nuclear membrane of yeast, centered around the E3 enzymes Asi1 and Asi3 [14,15]. In contrast to yeast ERAD, mammalian ERAD shows an expansion of E3 ubiquitin ligases. Currently, ten mammalian transmembrane E3 enzymes involved in ERAD have been identified [16]: mammalian homologue of yeast Hrd1p (HRD1) [17], gp78/autocrine motility factor receptor (AMFR) [18], mammalian homologue of yeast Doa10 (TEB4/MARCHVI) [19,20], transmembrane protein 129 (TMEM129) [21,22], translocation in renal carcinoma on chromosome 8 protein (TRC8) [23,24], ring finger protein 5 (RNF5)/RMA-1 [25,26], ring finger protein 103 (RNF103)/Kf-1 [27], ring finger protein 170 (RNF170) [28], ret finger protein 2 (RFP2)/tripartite motif containing 13 (TRIM13) [29,30], and Nixin [31]. Whereas several E3 ligases, such as HRD1 and gp78/AMFR, can process many different protein substrates, other mammalian ERAD E3 enzymes have a narrower substrate range.

Several viruses exploit the ERAD pathway for the purpose of immune evasion. For example, human cytomegalovirus (HCMV) encodes the proteins US2 and US11 that exploit ERAD to induce proteasomal degradation of the antigen-presenting human leukocyte antigen (HLA) class I molecules in order to evade cytotoxic T cell responses [32–34]. US2 and US11 use different mechanisms to target HLA class I molecules for degradation. Whereas US2 uses TRC8 to catalyze ubiquitination [23], TMEM129 has recently been identified as

the ER-resident E3 ubiquitin ligase essential for HLA class I degradation by US11 [21,22]. Prediction of membrane topology of TMEM129 suggests a N<sub>exo</sub>-C<sub>cyto</sub> orientation with three transmembrane domains. However, predictions of membrane protein topology are not always accurate. Experimental validation of the membrane topology of ERAD E3 enzymes is key to understanding their function. Here, we experimentally map the membrane topology of the ER-resident TMEM129 using in vitro translation, truncation scanning, and glycosylation scanning mutagenesis. We demonstrate that TMEM129 is not glycosylated, does not contain disulphide bonds, and contains a non-cleaved signal-anchor sequence. In addition, we show that TMEM129 contains three transmembrane domains with an overall N<sub>exo</sub>-C<sub>cyto</sub> orientation, thereby positioning the C-terminal RING domain in the cytosol.

## MATERIALS & METHODS

### 2.1. Cell Culture and Lentiviral Infection

U937 human monocytic cells and 293T human embryonic kidney cells were obtained from American Type Culture Collection (ATCC, Manassas, Virginia, USA) and grown in RPMI medium (Lonza, Breda, The Netherlands) supplemented with glutamine (Thermo Fischer Scientific Gibco, Waltham, Massachusetts, USA), penicillin/streptomycin (Gibco), and 10% fetal calf serum (FCS) (GE Healthcare PAA Laboratories, Eindhoven, The Netherlands). For individual gene infections using lentiviruses, the virus was produced in 293T human embryonic kidney cells seeded in 24-well plates using standard lentiviral production protocols and third-generation packaging vectors. The viral supernatant was harvested after three days post-transfection and stored at -80 °C. If required, the virus was concentrated using the Lenti-X Concentrator kit (Takara Bio Europe Clontech, Saint-Germain-en-Laye, France). For lentiviral gene infections, 50 µL of viral supernatant supplemented with 8 µg/mL polybrene (Santa Cruz Biotechnology, Heidelberg, Germany) was used to transduce approximately 20,000 U937 cells by spin infection at 1000 g for 2 h at 33 °C. Complete medium was added after centrifugation to reduce polybrene concentration.

### 2.2. Antibodies

Primary antibodies used in our studies were: mouse anti-CD74/li PIN.1 monoclonal antibody (mAb) (1/500; no. ab22603; Abcam, Cambridge, UK); mouse anti-Calnexin AF8 mAb (1/10,000; kindly provided by Michael Brenner, Harvard Medical School, Boston, Massachusetts, USA); mouse anti-transferrin receptor (TfR) H68.4 mAb (1/2500; no. 13-68xx; Thermo Fischer Scientific Invitrogen, Waltham, Massachusetts, USA); mouse anti-FLAG-M2 mAb (1/5000; no. F1804; Sigma-Aldrich, Zwijndrecht, Netherlands); rat anti-HA 3F10 mAb (1/1000; no. 11867423001; Sigma-Aldrich Roche, Zwijndrecht, Netherlands).

Secondary antibodies used in our studies were: F(ab)<sub>2</sub> goat-α-mouse IgG(H+L)-PE (1/1000; no. R0480; Agilent Dako, Middelburg, The Netherlands), goat anti-rat IgG(H+L)-PE

(1/200; no. 112-116-143; Jackson ImmunoResearch, Suffolk UK), goat anti-mouse IgG(H+L)-HRP (1/10,000; no. 170-6516; Bio-Rad, Veenendaal, The Netherlands); goat anti-mouse IgG(L)-HRP (1/10,000; no. 115-035-174; Jackson ImmunoResearch).

### 2.3. Plasmids

The N-terminally enhanced green fluorescent protein (eGFP)- and Myc-tagged human HLA-A2 present in the lentiviral pHRsincPPT-SGW vector was kindly provided by Dr. Paul Lehner and Dr. Louise Boyle (University of Cambridge, Cambridge, UK). For rescue and overexpression experiments, we cloned FLAG-tagged TMEM129 in a dual promoter lentiviral vector as previously described [21]. In general, the vectors carrying the cDNA used in this study also expressed ZeoR-T2A-mAmetrine under control of the human phosphoglycerate kinase (hPGK) promoter. Generation of TMEM129-FLAG and TMEM129-RING-FLAG vectors have been described previously [21]. Introduction of the glycosylation motifs and generation of truncation mutants was achieved by polymerase chain reaction (PCR) amplification of one or two TMEM129 fragments carrying the desired alterations and assembling these into the lentiviral ZeoR-T2A-mAmetrine vector by means of Gibson assembly (see Tables 1 and 2 for sequence information). All constructs were verified by Sanger sequencing.

### 2.4. Flow Cytometry

For surface stainings, cells were washed in fluorescence-activated cell sorting (FACS) buffer (phosphate buffered saline (PBS), 0.5% bovine serum albumin (BSA), 0.02% sodium azide), fixed in 0.5% paraformaldehyde (PFA), and subsequently washed in FACS buffer. All subsequent staining protocols and washings were performed in FACS buffer. Afterwards, cells were subjected to flow cytometry acquisition on a FACSCanto II flow cytometer (BD Bioscience, Breda, The Netherlands). Flow cytometry data were analyzed using FlowJo software (FlowJo LLC, Ashland, Oregon, USA).

For intracellular stainings, two different permeabilization methods were used: Streptolysin-O (SLO) for plasma membrane permeabilization (semi-permeabilization), and saponin for full permeabilization.

**Streptolysin-O permeabilization:** SLO was activated by adding 4 mM dithiothreitol (DTT; Roche) and 1 mM CaCl<sub>2</sub> followed by incubation at 37 °C for 10 min. Cells were kept on ice and washed once in ice-cold PBS. After resuspension in PBS, cells were incubated with SLO for 10 min. Cells were washed twice with PBS, after which cells were kept at room temperature (RT) for 20 min. Permeabilization was analyzed using Trypan Blue staining. After sufficient permeabilization, cells were fixed in 0.25% PFA and stained according to the surface staining protocol, except the washing buffer consisted of PBS supplemented with 2% fetal calf serum (FCS).

**Saponin permeabilization:** Cells were washed once in PBS prior to fixing in 3.7% PFA for 15 min at RT. After fixation, cells were washed once with PBS and permeabilized at RT

for 10 min by adding permeabilization buffer (PBS, 2% FCS, 0.5% saponin (Sigma-Aldrich)). Subsequently, cells were stained according to the surface staining protocol, except all subsequent stainings and washings were performed in permeabilization buffer. After antibody staining, cells were washed and resuspended in PBS + 2% FCS before analysis by flow cytometry.

**Table 1.** Primer sequences for glycosylation mutants.

Glyc Mutant	Forward or Reverse	Sequence 5'–3'
Backbone	Forward	TGAGCTAGCAGTATTAATTAACCAC
	Reverse	ATGACTAAGCTAGTACCGGTTAG
#1 Ser43 NAT	Forward	GTCGGGCTGGCTGGGCAGCA <u>AACGCAAC</u> AGAGGACGCCCTTCGTG
	Reverse	CACGAAGCGCGCTCCTCTGTTGCGTTGCTGCCAGCCAGCCCGAC
#2 Ala85 GAAGGAANATE GAEGAAGG	Forward	<u>ACCGCCAGCTGCACCTCCTGCCGCGCC</u> <b><u>CTCTGTTGCGTT</u></b> AGCTGCACCTCCTGCCGCGCGGCGTGGAGCC GCTTTTCTG
	Reverse	<u>GGCGCGGCAGGAGGTGCAGCT</u> <b><u>AACGCAACAGAG</u></b> GGCGCGGCAGAAGGTGCAGCTGGCGGTCTCAGCCA GGCCCTGAG
#3 Asp117 NATE	Forward	CTACTACTGGTCCCCTGAC <u>AACGCAACAGAG</u> CGGTGGGCTGCCACC
	Reverse	GGGTGGCAGGCCACCCTCTGTTGCGTTGTCACGGGACCAGTAGTAG
#4 Ala125 NATE	Forward	GCCTGCCACCCACTGGCG <u>AACGCAACAGAG</u> CGCACCCCTGCCCTCTACG
	Reverse	CGTAGAGGGCCAGGGTGCCTCTGTTGCGTTCCGCCAGTGGGTGGCAGGC
#5 Ala140 NATE	Forward	CACAGTCTGGTGGCAGGCT <u>AACGCAACAGAG</u> GTTGCTCCTCTGTCAACAC
	Reverse	GTGTTGACAGAGGAGGCAACTCTGTTGCGTTAGCCTGCCAGCCAGACTGTG
#6 Ile152 NAT	Forward	CACTGAGTCCGGCGGATT <u>AACGCAACAGAG</u> GACAAGTTTGCCACCCGGT
	Reverse	CACCGGTGGCAAACCTTGCTCTGTTGCGTTAATCCGCGGAACACTAGT
#7 Trp170 NATE	Forward	GTGATTGTGACAGACACGTGG <u>AACGCAACAGAG</u> GTGATGAAGGTAACCACCTAC
	Reverse	GTAGGTGGTTACCTTCATCACCTCTGTTGCGTTCCACGTGTCTGTCAACAATAC
#8 Val191 NA	Forward	GGACGTGCACCTGACTGTG <u>AACGCAACAGAG</u> TACGGCAGCATG
	Reverse	CATGCTGCCGAGACTCCGTTGCGTTCCACAGTCAAGTGCACGTCC
#9 Ser230 NA	Forward	CTTTGACATCTGGTGAACCTC <u>AACGCAACAGAG</u> TACGGGAGCTCTG
	Reverse	CAGAGCTCCCCGACTACTCAGTTGCGTTGGAGTTCAGCCAGATGTCAAAG
#10 Ser275 NATE	Forward	GAGGTCAACCCGGCCTACTC <u>AACGCAACAGAG</u> TGCCAGCAGCCAGGAG
	Reverse	CTCCTGGCTGTGGGCACCTCTGTTGCGTTGAGTAGGCCGGTTGACCTC
#11 Phe363 NATE	Reverse	ATGACTAAGCTAGTACCGGTTAGGATGCATTCACTTGTGTCATCGCTTTGTAGTCTCCTCTGTTGCGTTG AAGCGCACGGTGCACAC

This table contains the sequences of primers used with TMEM129-FLAG as a template. The 'Glyc Mutant' column displays the glycosylation mutant number, the amino acid (aa) residue immediately preceding the glycosylation acceptor sequence that was inserted, and the inserted amino acids. In the 'Sequence 5'–3'' column, the inserted nucleotides encoding for these are underlined. In mutant #2, the sequence highlighted in bold is the inserted glycosylation consensus sequence.

Truncation Mutant	Forward or Reverse	Sequence 5'-3'
#1	Reverse	ATGACTAAGCTAGTACCGGTTAGGATGCATTCACTTGTCGTCATCGTCTTTGTAGTCTTCGAAGGCAAATGCTCCAGG
#2	Reverse	ATGACTAAGCTAGTACCGGTTAGGATGCATTCACTTGTCGTCATCGTCTTTGTAGTCTTCGAACCTGCGGATGGTGCCCG
#3	Reverse	ATGACTAAGCTAGTACCGGTTAGGATGCATTCACTTGTCGTCATCGTCTTTGTAGTCTTCGAATGGCGAGAGCTCATGCTGC
#4	Reverse	ATGACTAAGCTAGTACCGGTTAGGATGCATTCACTTGTCGTCATCGTCTTTGTAGTCTTCGAAGCGGCCAGTGGTGCC

**Table 2. Primer sequences for truncation mutants.** This table contains the sequences of primers used for generation of truncation mutants (#1–4, 'Truncation Mutant' column), with TMEM129-FLAG as a template.

## 2.5. Immunoblotting

Cells were lysed in 1% Triton X-100 lysis buffer (1.0% Triton X-100, 20 mM MES (2-(N-morpholino)ethanesulfonic acid), 100 mM NaCl, 30 mM Tris; pH 7.5) containing 1 mM Pefabloc SC (Roche) and 10  $\mu$ M Leupeptin (Roche). Nuclei and cell debris were pelleted at 12,000 g for 20 min at 4 °C. Post-nuclear samples were denatured by adding Laemmli sample buffer and incubated at RT for 30 min. Proteins were separated by sodium dodecyl sulfate polyacrylamide gel electrophoresis (SDS-PAGE) and transferred to Immobilon-P polyvinylidene difluoride (PVDF) membranes (Merck Millipore, Amsterdam, The Netherlands). Membranes were probed with indicated antibodies. Reactive bands were detected by enhanced chemiluminescence (ECL; Thermo Fischer Scientific Pierce, Rockford, Illinois, USA), and exposed to Amersham Hyperfilm ECL films (GE Healthcare, Eindhoven, The Netherlands).

## 2.6. Immunoprecipitation

Cells were lysed in 1% Triton X-100 lysis buffer containing 1 mM Pefabloc SC (Roche) and 10  $\mu$ M Leupeptin (Roche). Cell fragments were pelleted at 12,000 g for 20 min at 4 °C. FLAG-M2-coupled beads (Sigma-Aldrich) were pre-washed four times with lysis buffer. Next, the post-nuclear lysate was added to the beads and incubated overnight at 4 °C. Samples were then washed four times with immunoprecipitation (IP) washing buffer (1.0% Triton X-100, 100 mM NaCl, 30 mM Tris; pH 7.5). Proteins were eluted from the beads upon incubation with elution buffer (500  $\mu$ g/mL FLAG-peptide (Sigma-Aldrich) in 1x Tris-buffered saline (TBS)) for 30 min on ice. Eluate was separated from the beads using a 0.45  $\mu$ m Spin-X filter column (Corning Costar, Amsterdam, The Netherlands). One fraction of the eluate was used for Endo H<sub>f</sub>/PNGase F digestion; the other was denatured using Laemmli sample buffer containing DTT for direct SDS-PAGE analysis.

## 2.7. Deglycosylation Studies

Endo H<sub>f</sub>: Post-nuclear lysate or eluate was denatured by adding Laemmli sample buffer and incubated at RT for 30 min, after which Endo H<sub>f</sub> (New England Biolabs, Bioké, Leiden, The Netherlands) was added and incubated at 37 °C for 1 h prior to immunoblotting.

PNGase F: Eluted immunoprecipitated proteins were deglycosylated by adding G7

Reaction Buffer (New England Biolabs) and Remove-iT PNGase F (New England Biolabs), followed by incubation at 37 °C for 2 h. Note: the molecular weight of PNGase F (approximately 36 kDa) is approximately the same as that of TMEM129. To prevent distortion of the apparent molecular size of TMEM129 and putative glycosylated forms to occur, we used a removable PNGase F. Chitin Magnetic Beads (New England Biolabs) were pre-washed two times in TBS, added to the deglycosylated sample and incubated for 10 min at RT. PNGase F was removed by pelleting the beads and recovering the supernatant. Isolated proteins were denatured by adding Laemmli sample buffer, and then subjected to SDS-PAGE.

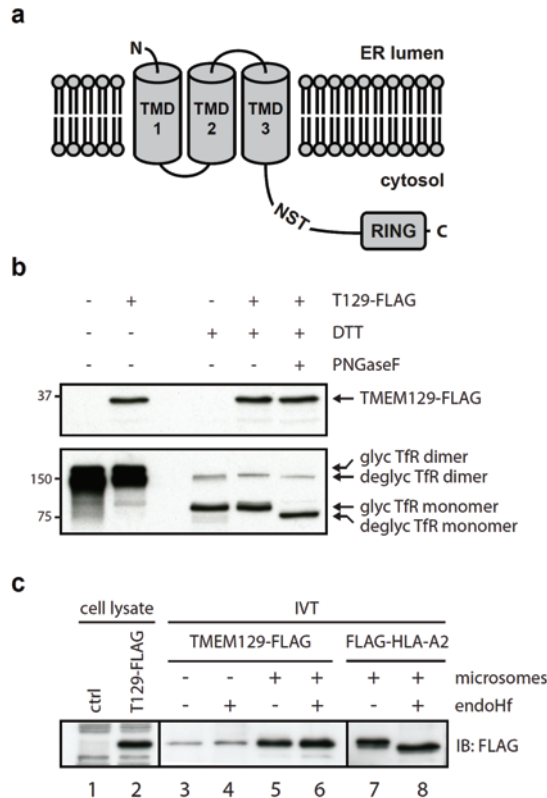
## RESULTS

### **TMEM129 Is a Non-Glycosylated Protein Lacking a Cleavable Signal Sequence and Disulphide Bonds**

TMEM129 is a transmembrane protein of 362 amino acid residues, localized to the ER [21,22], and has been predicted to contain three transmembrane domains according to the TOPCONS membrane protein topology prediction server (Figure 1a) [35]. One putative glycosylation site consisting of the amino acid residues NST is present at amino acid position 229–231. According to membrane topology predictions, this putative glycosylation site is expected to reside in the cytosol. Hence, the glycosylation machinery should not have access to this site, and glycosylation will probably not occur. To verify this, lysates were prepared from U937 cells expressing TMEM129-FLAG and subjected to deglycosylation using PNGase F (Figure 1b). No shift in molecular size was observed for TMEM129, indicating that TMEM129 is a non-glycosylated protein (Figure 1b, compare lanes 4 and 5). Transferrin receptor was successfully deglycosylated. Also, the mobility of TMEM129 was similar in non-reducing and reducing conditions, indicating that TMEM129 does not contain intermolecular disulphide bonds (Figure 1b, lanes 2 and 4).

The first transmembrane domain is predicted to span amino acid residues 7 through 28, but whether these residues represent a cleavable signal sequence (aa 1–28) or a non-cleavable signal anchor (aa 7–28) remains unknown. To study this, TMEM129-FLAG was translated in vitro in the absence (Figure 1c, lane 3 and 4) or presence (lane 5 and 6) of microsomes. As we did not observe a difference in the apparent TMEM129-FLAG molecular size between both conditions, the E3 ligase appears to contain a non-cleavable signal anchor (Figure 1c, lanes 3 and 5). Also, endo Hf-mediated digestion of the samples did not alter the molecular size of TMEM129, again showing that TMEM129 is not glycosylated and hence likely correctly inserted into the microsomes (Figure 1c, lanes 5 and 6). As a positive control for insertion into the microsomes, HLA-A2 was translated in vitro in the presence of microsomes (Figure 1c, compare lanes 7 and 8). Upon endo Hf-mediated digestion (lane 8), a lower molecular size species became apparent, showing that HLA-A2 was efficiently and correctly inserted into the microsomes. These findings indicate that TMEM129 lacks

N-linked glycans and intermolecular disulphide bonds, and is inserted into the membrane through a non-cleaved signal anchor.



4

**Figure 1. Transmembrane protein 129 (TMEM129) does not contain disulphide bonds, N-linked glycans, nor a cleavable signal sequence.** (a) Predicted TMEM129 topology according to the TOPCONS membrane protein topology prediction program. Indicated are the predicted transmembrane domains (TMD) 1–3 and a putative endogenous glycosylation site (NST). ER, endoplasmic reticulum; (b) TMEM129 does not contain intermolecular disulphide bonds and is not glycosylated. Lysate of U937 cells expressing TMEM129-FLAG were subjected to non-reducing and reducing conditions. Reduced lysates were subjected to PNGase F digestion. Transferrin receptor (Tfr) served as a control for both reducing and deglycosylating conditions. TMEM129 and Tfr were visualized by immunoblotting with specific antibodies. Glycosylated and deglycosylated proteins are indicated; (c) In vitro translation of TMEM129-FLAG in the absence and presence of microsomes shows that TMEM129 does not contain a cleavable signal peptide. Simultaneous deglycosylation revealed that TMEM129 is not glycosylated. As a positive control, HLA-A2 was translated in vitro in the presence of microsomes and subjected to endo Hf treatment. TMEM129 and HLA-A2 were visualized by immunoblotting with a FLAG-reactive antibody. Experiments were performed three times, of which one representative experiment is shown.

**TMEM129 Is Localized in the Endoplasmic Reticulum Membrane in a N<sub>exo</sub>-C<sub>cyto</sub> Orientation**

Next, we set out to experimentally map the orientation of TMEM129 by determining the subcellular localization of its N- and C-termini. As the N-terminus of TMEM129 contains a non-cleaved signal-anchor sequence, an epitope tag could be inserted at both the N- and C-terminus (HA and FLAG tag respectively) to allow assessment of the orientation of TMEM129 within the ER membrane. Upon stable introduction of HA-TMEM129-FLAG in U937 cells, cells were subjected to selective permeabilization using the pore-forming toxin SLO, or the detergent saponin. Through carefully timed application, activation, and washing, SLO was used to selectively permeabilize the plasma membrane, leaving the ER membrane intact. The detergent saponin was used to permeabilize both the plasma membrane and the ER membrane. By using both permeabilization methods prior to staining with HA- and FLAG-specific antibodies, the exact subcellular localization of the N- and C-terminus can be assessed. As a positive control for proper membrane permeabilization, monoclonal antibodies were used that recognize either a cytosolic epitope of the invariant chain (Ii) or an ER-luminal epitope of the ER-resident calnexin. Indeed, cells were properly permeabilized, as anti-calnexin antibodies only stained saponin-treated cells, but not SLO-treated cells, whereas anti-Ii antibodies did react with SLO-treated cells (Figure 2, left panels). Flow cytometric analysis of HA-TMEM129-FLAG revealed that anti-HA antibodies recognized saponin-treated, but not SLO-treated, cells (Figure 2). This indicates that the N-terminus is located in the ER lumen (Figure 2). On the other hand, the FLAG-reactive antibody reacted in both SLO- and saponin-permeabilized cells, suggesting that the C-terminus is present in the cytosol. These data show that TMEM129 adopts an overall N<sub>exo</sub>-C<sub>cyto</sub> orientation.

**The Cytosolic Tail of TMEM129 Is Essential for Activity**

We next generated TMEM129-FLAG truncation mutants to assess which regions of the protein are important for its activity. We generated multiple truncation variants, in which increasing parts of the predicted cytosolic domain of TMEM129 were deleted. Although several deletion variants were not expressed (data not shown), four mutants (Figure 3a) were readily detected upon stable transduction in U937 cells (Figure 3b). To assess whether these proteins were properly inserted in the ER membrane, the localization of their C-termini were assessed by selective permeabilization followed by anti-FLAG antibody stains. In both SLO- and saponin-permeabilized cells, the C-terminal FLAG-tagged truncation mutants #1–4 were detected, indicating that their C-termini were indeed still present in the cytosol (Figure 3c).

We previously showed that expression of full-length TMEM129 enhanced HLA class I downregulation in eGFP-Myc-HLA-A2 and US11 expressing cells ([21] and Figure 3d, left panel), whereas expression of a RING-less TMEM129 mutant (truncation mutant #4) resulted in a dominant-negative phenotype, efficiently rescuing eGFP-Myc-HLA-A2 expression ([21] and Figure 3d right panel). Correspondingly, deletion of the RING domain



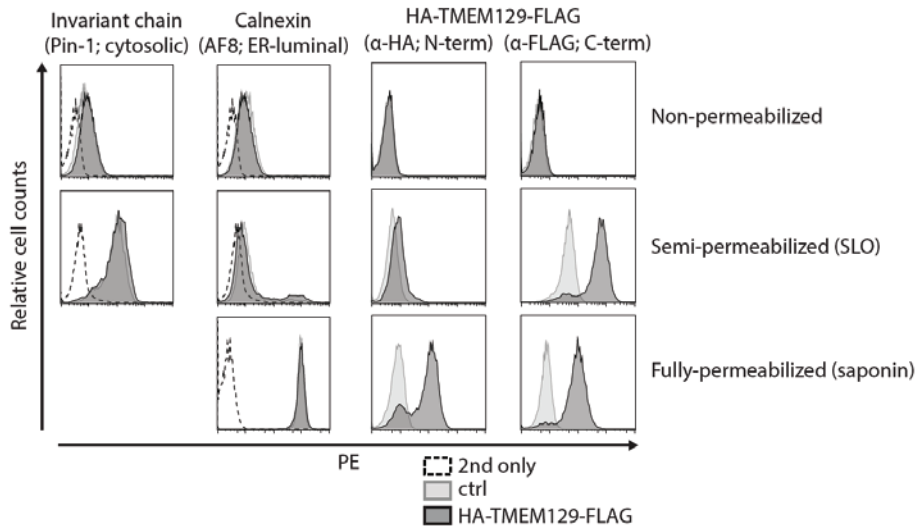


**Figure 2. The N-terminus of TMEM129 is localized in the ER lumen, the C-terminus in the cytosol.** U937 cells transduced with either HA-TMEM129-FLAG or vector control (ctrl) were either left untreated (non-permeabilized), semi-permeabilized using streptolysin-O (SLO), or fully-permeabilized using saponin. The termini of HA-TMEM129-FLAG were detected using HA- or FLAG-reactive antibodies respectively, after which flow cytometric analysis was performed. As a control for semi-permeabilization, cells were stained with a monoclonal antibody directed against a cytosolic epitope of the invariant chain (Ii) or were incubated with the secondary antibody only (2nd only). As a control for full-permeabilization, cells were stained with a monoclonal antibody directed against an ER-luminal epitope of calnexin or they were incubated with the secondary antibody only. Experiments were performed three times, of which one representative experiment is shown.

4

in truncation mutants #2 and #3 resulted in a dominant-negative phenotype. Truncation mutant #1, however, completely lost E3 ligase activity and also did not act as a dominant-negative variant. Hence, the region between amino acids 126–246 is responsible for the switch to the dominant-negative phenotype, and it is therefore suggestive that this area is involved in the recruitment of interaction partners to aid in the US11-mediated HLA class I dislocation event.

### TMEM129 Contains Three Transmembrane Domains

To study the topology of TMEM129 in more detail, N-linked glycosylation acceptor sequences were inserted at various sites throughout the protein. As N-glycosylation only occurs in the ER lumen, evaluation of the glycosylation status of these mutants allows for an accurate assessment of the subcellular localization of these motifs which aids in determining the number of transmembrane domains for TMEM129. We constructed 11 different TMEM129 glycosylation mutants, in which the NATE glycosylation consensus motif was introduced (Figure 4a). In addition, these TMEM129 glycosylation mutants were C-terminally fused to a FLAG-tag to facilitate detection by flow cytometry and immunoblotting experiments. The

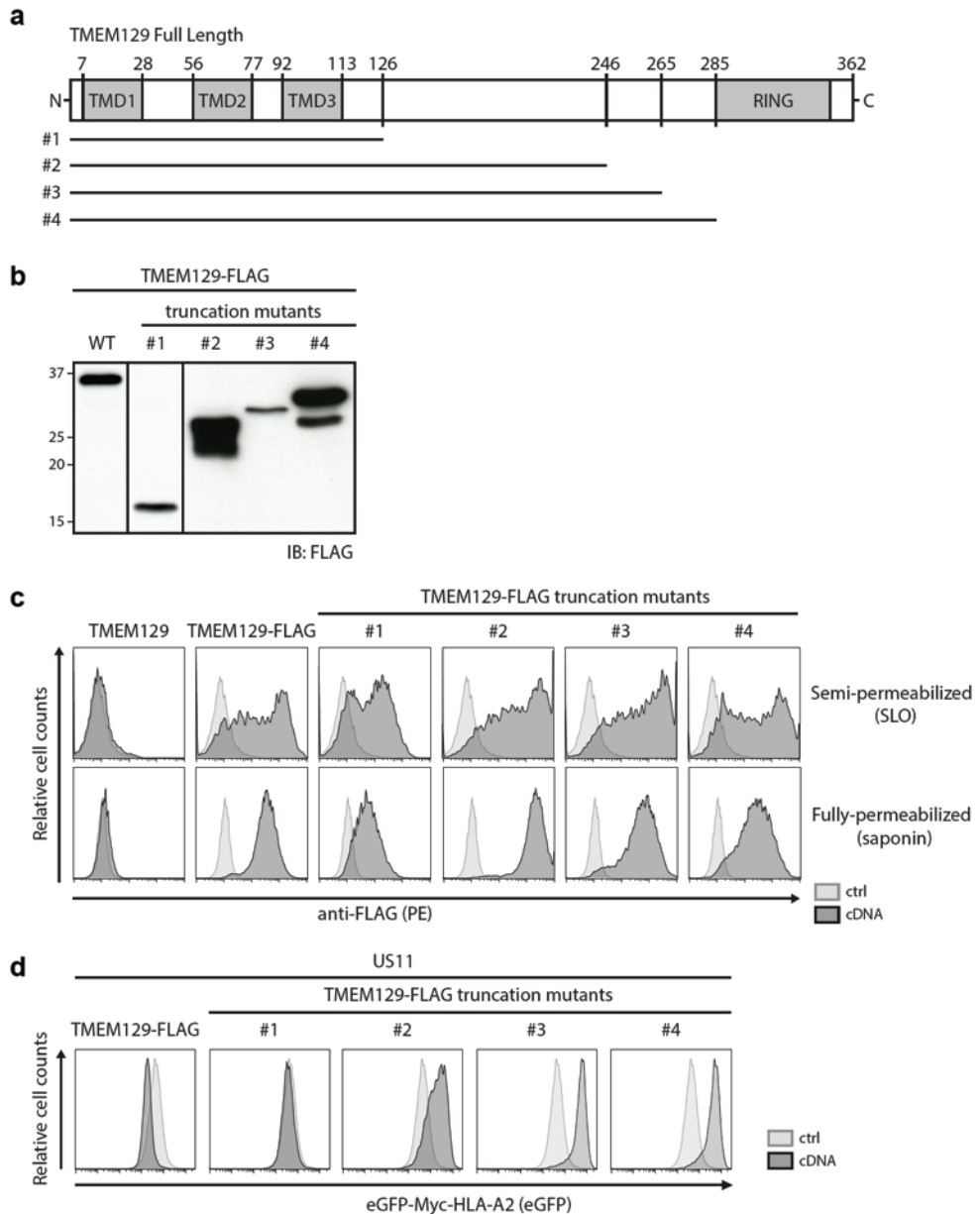


**Figure 3. The cytosolic tail of TMEM129 is essential for activity.** (a) Schematic representation of TMEM129 truncation mutants; (b) Truncation mutants of TMEM129 were expressed in U937 cells, after which the lysate was prepared and subjected to immunoblotting using a FLAG-reactive antibody. The full-length TMEM129-FLAG protein is indicated as wild-type (WT); (c) TMEM129 truncation mutants are properly inserted in the ER membrane. U937 cells expressing TMEM129-FLAG truncation mutants were semi-permeabilized using SLO, or fully-permeabilized using saponin. The C-terminus of the truncation mutants was detected using a FLAG-reactive antibody, after which flow cytometric analysis was performed;

**Figure 3 (continued).** (d) Deletion of the entire TMEM129 cytosolic tail interfered with US11-mediated HLA class I downregulation whereas deletion of the RING domain resulted in a dominant-negative phenotype. Indicated truncation mutants of TMEM129-FLAG were expressed in U937 cells, co-expressing eGFP-Myc-HLA-A2 and HCMV US11. Flow cytometric analysis was performed to assess the total levels of eGFP-Myc-HLA-A2. Experiments were performed three times, of which one representative experiment is shown.

mutants, stably expressed in U937 cells, were immunoprecipitated using anti-FLAG coupled beads. Next, immunoprecipitates were left untreated or were incubated with PNGase F to cleave all N-linked glycans. Upon Western blotting for TMEM129-FLAG, only mutant #2 was sensitive to PNGase F treatment resulting in a shift in apparent molecular weight, whereas the other mutants were non-reactive (Figure 4b). As the putative ER-luminal loop between the predicted transmembrane domain 2 and 3 was rather short, we introduced the NATE consensus sequence as part of a 16-amino acid insertion, explaining the increased size of the protein as compared to the other mutants. Importantly, the TMEM129-FLAG mutant #2 was correctly inserted into the ER membrane, as the C-terminal FLAG-sequence was present in the cytosol (Figure 4c).

We next assessed the functionality of the TMEM129 glycosylation mutants in US11-expressing cells (Figure 4d). The TMEM129 glycosylation mutants were stably expressed in U937 TMEM129-null cells co-expressing eGFP-Myc-HLA-A2 and the HCMV protein US11. Reconstitution of a functional TMEM129 protein restored US11-mediated HLA class I downregulation in TMEM129-null cells, as measured by flow cytometry (Figure 4d, top left panel). Glycosylation mutant #2 was still functional, as it could rescue the TMEM129-null phenotype, suggesting that the topology of TMEM129 mutant #2 is unaltered. Only glycosylation mutants #4 and #7 did not rescue the TMEM129-null phenotype, indicating that insertion of the glycosylation acceptor sequence either disrupts protein topology or interferes with TMEM129 activity by altering an essential domain of the E3 ligase. In conclusion, our data show that the N-terminus of TMEM129 resides in the ER, the glycosylation site of mutant #1 is present in the cytosol, the glycosylation site of mutant #2 is localized to the ER lumen, and the glycosylation sites for mutants #3 through #11 together with the C-terminus reside in the cytosol. Hence, our data support a model in which TMEM129 is inserted in the ER membrane by three transmembrane domains.

## DISCUSSION

The topology of many proteins involved in ERAD is poorly studied and current models are often based on prediction software that may be incorrect. Therefore, experimental validation of protein topology is essential for understanding their function. Indeed, the multipass transmembrane protein Derlin-1 was predicted to contain four transmembrane domains [36–38], although later studies showed that this important ERAD factor contains six transmembrane domains, consistent with its homology to rhomboid family members [39]. Additionally, the topology and number of transmembrane domains of gp78/AMFR

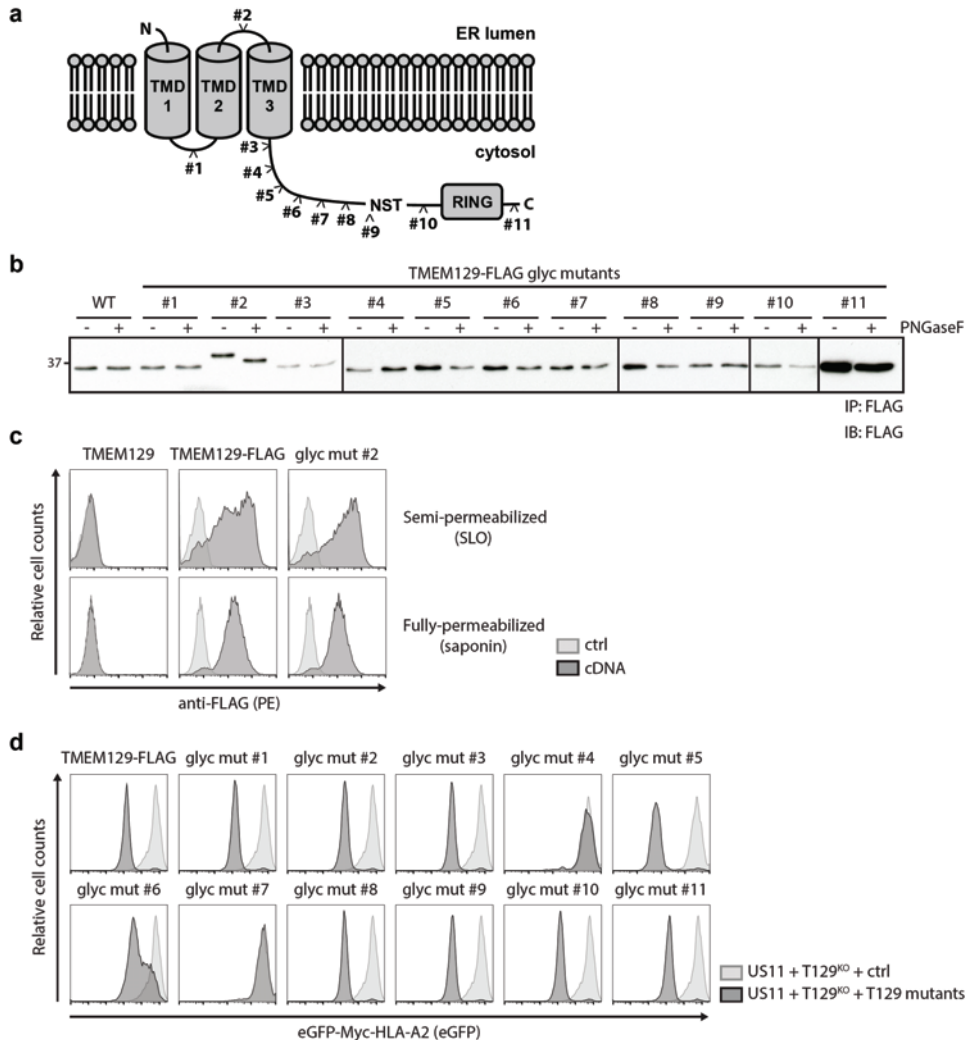


**Figure 4. TMEM129 is a tri-spanning ER membrane protein.** (a) Glycosylation motif insertion mutants of TMEM129 (#1–11) were generated as indicated; (b) The loop between transmembrane domain (TMD) 2 and TMD3 is located inside the ER lumen. TMEM129-FLAG glycosylation mutants were expressed in U937 cells, and subjected to immunoprecipitation using anti-FLAG-coupled beads. Eluted proteins were then subjected to PNGase F digestion. After PNGase F was removed, TMEM129-FLAG mutants were detected using a FLAG-reactive antibody. This experiment was performed two times, of which one representative experiment is shown; (c) The C-terminal orientation of glycosylation mutant #2 is unaltered. U937 cells expressing TMEM129-FLAG or glycosylation mutant #2 were semi-permeabilized using SLO, or fully-permeabilized using saponin. The respective C-termini were detected using a FLAG-reactive antibody, after which the flow cytometric analysis was performed; (d) Most, but not all, glycosylation insertions did not affect TMEM129 activity. TMEM129-FLAG glycosylation mutants were expressed in TMEM129-null U937 cells, co-expressing eGFP-Myc-HLA-A2 and HCMV US11. Flow cytometric analysis was performed to assess the total levels of eGFP-Myc-HLA-A2. Experiments were performed three times, of which one representative experiment is shown.

is still a matter of debate as, depending on the algorithm used, the estimated number of transmembrane domains ranges from five to seven [40]. Using HCMV US11-mediated HLA class I downregulation as a model [21,22], TMEM129 has been recently identified as an ER-resident E3 ubiquitin ligase. In the present study, we have determined the general characteristics and the topology of TMEM129.

Our data show that TMEM129 does not contain N-linked glycans, or disulphide bonds. Moreover, TMEM129 does not contain a cleavable signal peptide, suggesting that the first transmembrane domain functions as a signal-anchor sequence. Topological analysis of the N- and C-termini using flow cytometry revealed that the N-terminus is in the ER-lumen and the C-terminus in the cytosol. Hence, the subcellular location of the C-terminus is consistent with the presence of a functional RING domain in the cytosolic C-terminus that catalyzes the ubiquitination reaction.

We have constructed a set of C-terminal truncation mutants to map the ligase activity of TMEM129. We inferred that all mutants were properly inserted into the ER membrane, as no changes were made to the TMDs and their C-terminal FLAG-tags were localized in the cytosol (Figure 3c). However, besides the expected full-length products, cells transduced with mutants #2 and #4 also expressed a smaller, less abundant, species (Figure 3b). As the TMEM129 truncation mutants were tagged at the C-terminus, and the Western blot was stained with a monoclonal antibody directed against this tag, it is possible that the lower molecular weight species were N-terminal truncation variants that may (partially) lack the first TMD. As this TMD could function as an anchor sequence, these proteins may not have been properly inserted into the ER membrane, which could have affected their activity. However, as the majority of TMEM129 in cells transduced with these two mutants migrated at the correct molecular weight, and no apparent altered staining patterns were observed between these mutants and the full-length FLAG-tagged TMEM129 (Figure 3b), we assume that the impact of these smaller TMEM129 proteins are limited.

Using the TOPCONS webserver, TMEM129 was predicted to have three transmembrane domains which was confirmed in our study. The predicted transmembrane regions are located at amino acid positions 6–26 (TMD1), 56–76 (TMD2), and 95–115 (TMD3). Based on this prediction, the loop between TMD1 and TMD2 (loop 1) would span 28 amino acids and the loop between TMD2 and TMD3 (loop 2) would span 17 amino acids. In general, luminal loops containing N-linked oligosaccharides have a minimum size of  $\pm 25$ –30 residues, with the glycosylation acceptor site located at least 10 residues away from a predicted transmembrane domain [41,42] due to steric hindrance constraint of the oligosaccharyltransferase with the ER membrane and the glycosylation acceptor sequence during translation [43]. Hence, glycosylation consensus motifs present in short loops might fail to be glycosylated which can be prevented by artificially extending the length of the loop [42]. Thus, for putative glycosylation to occur in glycosylation mutant #2 (containing an inserted glycosylation acceptor sequence in loop 2), the NATE consensus sequence was

flanked by eight additional amino acid residues on both sides. The resulting protein is 18 amino acids longer, which was reflected by immunoblotting data. The extension of loop 2 did not influence the functionality of the mutant, as it could still rescue US11-mediated HLA class I downregulation in TMEM129-null cells. However, two other glycosylation mutants, #4 and #7, could not rescue US11-mediated HLA class I downregulation. These mutants were not glycosylated; hence it is likely that the insertion of a glycosylation site disrupted TMEM129 function or a protein–protein interaction essential for US11-mediated HLA class I downregulation.

Although it has been established that TMEM129 is essentially involved in retrograde transport and degradation of HLA class I molecules [21,22], its exact role in this process remains to be determined. An important, yet unresolved, question is how ER-resident degradation substrates cross the ER membrane. This pertains to membrane proteins such as HLA class I molecules, but also to soluble ER proteins destined for degradation in the cytoplasm. Most likely, these proteins migrate back into the cytosol through a channel [44]. Using US2-mediated degradation of HLA class I molecules as a model, a role has been proposed for the Sec61 channel, generally involved in protein import into the ER [32]. This possibility is supported by studies using other proteins as dislocation substrates [45–54].

For US11-mediated degradation of HLA class I molecules, no indications were found for a role of the Sec61 channel in dislocation of the substrate; several other multipass membrane proteins have been proposed to fulfill this function. These include the Derlins, multipass membrane proteins widely involved in ERAD [37–39,55–57]. Derlin-1 has been shown to contain six transmembrane domains [39] and the protein is involved in the degradation of HLA class I molecules in the context of US11, but not US2 [37,38]. In addition, several E3 ligases that are involved in ERAD are multipass membrane proteins and may therefore be part of the dislocation channel. Yeast Hrd1p, for example, contains six transmembrane domains [58]. Human HRD1 likely has an identical topology [59] and is involved in degradation of misfolded HLA class I molecules in the absence of US2 and US11 [60,61]. Experiments involving the *in vitro* reconstitution of retrotranslocation using proteoliposomes and purified *Saccharomyces cerevisiae* proteins suggest that Hrd1p forms a ubiquitin-gated protein-conducting channel [62,63]. TEB4 and its yeast homolog Doa10 have been reported to encompass fourteen TMDs [64]. For gp78/AMFR, the number of TMDs has been predicted to be between five and seven [40]. Although TMEM129 only contains three TMDs, this E3 ligase may still form part of the dislocation channel, especially if TMEM129 forms multimers. If TMEM129 indeed occurs as a multimeric complex, our experiments indicate that this does not rely on the formation of disulfide bonds.

In conclusion, TMEM129 adopts an N<sub>exo</sub>–C<sub>cyto</sub> orientation with three transmembrane domains and a C-terminal cytosolic RING domain. This topology is in agreement with its function as an E3 ubiquitin ligase involved in the degradation of ER-resident proteins.

## Acknowledgments

We are grateful to Michael Brenner (Harvard Medical School, Boston, MA, USA), and Paul Lehner and Louise Boyle (University of Cambridge, Cambridge, UK) for generously sharing reagents and vectors. We thank the members of the Wiertz lab for helpful discussions. R.J.L. was supported by a Veni grant 916.10.138 from The Netherlands Organisation for Scientific Research (NWO, <http://www.nwo.nl/en>). R.J.L. and E.J.H.W. were supported by grant UU 2012-5667 from the Dutch Cancer Society (KWF, <http://www.kwf.nl/english>).

Author Contributions: M.L.v.d.W., E.J.H.J.W., and R.J.L. conceived and designed the experiments. M.L.v.d.W., G.v.M., and L.J.V. performed the experiments. M.L.v.d.W., G.v.M., and L.J.V. analyzed the data. M.L.v.d.W., A.I.C., E.J.H.J.W., and R.J.L. wrote the paper.

Conflicts of Interest: The authors declare that there is no conflict of interest.

## REFERENCES

1. Kim, Y.E.; Hipp, M.S.; Bracher, A.; Hayer-Hartl, M.; Hartl, F.U. Molecular chaperone functions in protein folding and proteostasis. *Ann. Rev. Biochem.* 2013, 82, 323–355.
2. Hampton, R.Y. ER-associated degradation in protein quality control and cellular regulation. *Curr. Opin. Cell Biol.* 2002, 14, 476–482.
3. Amm, I.; Sommer, T.; Wolf, D.H. Protein quality control and elimination of protein waste: The role of the ubiquitin-proteasome system. *Biochim. Biophys. Acta* 2014, 1843, 182–196.
4. Needham, P.G.; Brodsky, J.L. How early studies on secreted and membrane protein quality control gave rise to the ER associated degradation (ERAD) pathway: The early history of ERAD. *Biochim. Biophys. Acta* 2013, 1833, 2447–2457.
5. Olzmann, J.A.; Kopito, R.R.; Christianson, J.C. The mammalian endoplasmic reticulum-associated degradation system. *Cold Spring Harb. Perspect. Biol.* 2013, 5, doi:10.1101/cshperspect.a013185.
6. Christianson, J.C.; Olzmann, J.A.; Shaler, T.A.; Sowa, M.E.; Bennett, E.J.; Richter, C.M.; Tyler, R.E.; Greenblatt, E.J.; Harper, J.W.; Kopito, R.R. Defining human ERAD networks through an integrative mapping strategy. *Nat. Cell Biol.* 2012, 14, 93–105.
7. Denic, V.; Quan, E.M.; Weissman, J.S. A luminal surveillance complex that selects misfolded glycoproteins for ER-associated degradation. *Cell* 2006, 126, 349–359.
8. Gauss, R.; Sommer, T.; Jarosch, E. The Hrd1p ligase complex forms a linchpin between ER-luminal substrate selection and Cdc48p recruitment. *EMBO J.* 2006, 25, 1827–1835.
9. Carvalho, P.; Goder, V.; Rapoport, T.A. Distinct ubiquitin-ligase complexes define convergent pathways for the degradation of ER proteins. *Cell* 2006, 126, 361–373.
10. Carvalho, P.; Stanley, A.M.; Rapoport, T.A. Retrotranslocation of a misfolded luminal ER protein by the ubiquitin-ligase Hrd1p. *Cell* 2010, 143, 579–591.
11. Ye, Y.; Rape, M. Building ubiquitin chains: E2 enzymes at work. *Nat. Rev. Mol. Cell Biol.* 2009, 10, 755–764.
12. Bays, N.W.; Gardner, R.G.; Seelig, L.P.; Joazeiro, C.A.; Hampton, R.Y. Hrd1p/Der3p is a membrane-anchored ubiquitin ligase required for ER-associated degradation. *Nat. Cell Biol.* 2001, 3, 24–29.
13. Swanson, R.; Locher, M.; Hochstrasser, M. A conserved ubiquitin ligase of the nuclear envelope/endoplasmic reticulum that functions in both ER-associated and Matalpha2 repressor degradation. *Genes. Dev.* 2001, 15, 2660–2674.

14. Foresti, O.; Rodriguez-Vaello, V.; Funaya, C.; Carvalho, P. Quality control of inner nuclear membrane proteins by the Asi complex. *Science* 2014, 346, 751–755.
15. Khmelinskii, A.; Blaszczak, E.; Pantazopoulou, M.; Fischer, B.; Omnus, D.J.; Le Dez, G.; Brossard, A.; Gunnarsson, A.; Barry, J.D.; Meurer, M.; et al. Protein quality control at the inner nuclear membrane. *Nature* 2014, 516, 410–413.
16. Claessen, J.H.; Kundrat, L.; Ploegh, H.L. Protein quality control in the ER: Balancing the ubiquitin checkbook. *Trends Cell Biol.* 2012, 22, 22–32.
17. Kikkert, M.; Doolman, R.; Dai, M.; Avner, R.; Hassink, G.; van Voorden, S.; Thanedar, S.; Roitelman, J.; Chau, V.; Wiertz, E. Human HRD1 is an E3 ubiquitin ligase involved in degradation of proteins from the endoplasmic reticulum. *J. Biol. Chem.* 2004, 279, 3525–3534.
18. Fang, S.; Ferrone, M.; Yang, C.; Jensen, J.P.; Tiwari, S.; Weissman, A.M. The tumor autocrine motility factor receptor, gp78, is a ubiquitin protein ligase implicated in degradation from the endoplasmic reticulum. *Proc. Natl. Acad. Sci. USA* 2001, 98, 14422–14427.
19. Bartee, E.; Mansouri, M.; Hovey Nerenberg, B.T.; Gouveia, K.; Fruh, K. Downregulation of major histocompatibility complex class I by human ubiquitin ligases related to viral immune evasion proteins. *J. Virol.* 2004, 78, 1109–1120.
20. Hassink, G.; Kikkert, M.; van Voorden, S.; Lee, S.J.; Spaapen, R.; van Laar, T.; Coleman, C.S.; Bartee, E.; Fruh, K.; Chau, V.; et al. TEB4 is a C4HC3 RING finger-containing ubiquitin ligase of the endoplasmic reticulum. *Biochem. J.* 2005, 388, 647–655.
21. Van de Weijer, M.L.; Bassik, M.C.; Luteijn, R.D.; Voorburg, C.M.; Lohuis, M.A.; Kremmer, E.; Hoeben, R.C.; LeProust, E.M.; Chen, S.; Hoelen, H.; et al. A high-coverage shRNA screen identifies TMEM129 as an E3 ligase involved in ER-associated protein degradation. *Nat. Commun.* 2014, 5, 3832.
22. van den Boomen, D.J.; Timms, R.T.; Grice, G.L.; Stagg, H.R.; Skodt, K.; Dougan, G.; Nathan, J.A.; Lehner, P.J. TMEM129 is a Derlin-1 associated ERAD E3 ligase essential for virus-induced degradation of MHC-I. *Proc. Natl. Acad. Sci. USA* 2014, 111, 11425–11430.
23. Stagg, H.R.; Thomas, M.; van den Boomen, D.; Wiertz, E.J.; Drabkin, H.A.; Gemmill, R.M.; Lehner, P.J. The TRC8 E3 ligase ubiquitinates MHC class I molecules before dislocation from the ER. *J. Cell Biol.* 2009, 186, 685–692.
24. Lin, P.H.; Lan, W.M.; Chau, L.Y. TRC8 suppresses tumorigenesis through targeting heme oxygenase-1 for ubiquitination and degradation. *Oncogene* 2013, 32, 2325–2334.
25. Younger, J.M.; Chen, L.; Ren, H.Y.; Rosser, M.F.; Turnbull, E.L.; Fan, C.Y.; Patterson, C.; Cyr, D.M. Sequential quality-control checkpoints triage misfolded cystic fibrosis transmembrane conductance regulator. *Cell* 2006, 126, 571–582.
26. Morito, D.; Hirao, K.; Oda, Y.; Hosokawa, N.; Tokunaga, F.; Cyr, D.M.; Tanaka, K.; Iwai, K.; Nagata, K. Gp78 cooperates with RMA1 in endoplasmic reticulum-associated degradation of CFTRDeltaF508. *Mol. Biol. Cell* 2008, 19, 1328–1336.
27. Maruyama, Y.; Yamada, M.; Takahashi, K.; Yamada, M. Ubiquitin ligase Kf-1 is involved in the endoplasmic reticulum-associated degradation pathway. *Biochem. Biophys. Res. Commun.* 2008, 374, 737–741.
28. Lu, J.P.; Wang, Y.; Sliter, D.A.; Pearce, M.M.; Wojcikiewicz, R.J. RNF170 protein, an endoplasmic reticulum membrane ubiquitin ligase, mediates inositol 1,4,5-trisphosphate receptor ubiquitination and degradation. *J. Biol. Chem.* 2011, 286, 24426–24433.
29. Lerner, M.; Corcoran, M.; Cepeda, D.; Nielsen, M.L.; Zubarev, R.; Ponten, F.; Uhlen, M.; Hober, S.; Grander, D.; Sangfelt, O. The RBCC gene RFP2 (Leu5) encodes a novel transmembrane E3 ubiquitin ligase involved in ERAD. *Mol. Biol. Cell* 2007, 18, 1670–1682.
30. Altier, C.; Garcia-Caballero, A.; Simms, B.; You, H.; Chen, L.; Walcher, J.; Tedford, H.W.; Hermosilla, T.; Zamponi, G.W. The Cavbeta subunit prevents RFP2-mediated ubiquitination and proteasomal degradation of L-type



- channels. *Nat. Neurosci.* 2011, 14, 173–180.
31. Neutzner, A.; Neutzner, M.; Benischke, A.S.; Ryu, S.W.; Frank, S.; Youle, R.J.; Karbowski, M. A systematic search for endoplasmic reticulum (ER) membrane-associated RING finger proteins identifies Nixin/ZNF4 as a regulator of calnexin stability and ER homeostasis. *J. Biol. Chem.* 2011, 286, 8633–8643.
  32. Wiertz, E.J.; Jones, T.R.; Sun, L.; Bogyo, M.; Geuze, H.J.; Ploegh, H.L. The human cytomegalovirus US11 gene product dislocates MHC class I heavy chains from the endoplasmic reticulum to the cytosol. *Cell* 1996, 84, 769–779.
  33. Wiertz, E.J.; Tortorella, D.; Bogyo, M.; Yu, J.; Mothes, W.; Jones, T.R.; Rapoport, T.A.; Ploegh, H.L. Sec61-mediated transfer of a membrane protein from the endoplasmic reticulum to the proteasome for destruction. *Nature* 1996, 384, 432–438.
  34. van de Weijer, M.L.; Luteijn, R.D.; Wiertz, E.J. Viral immune evasion: Lessons in MHC class I antigen presentation. *Semin. Immunol.* 2015, 27, 125–137.
  35. Tsirigos, K.D.; Peters, C.; Shu, N.; Kall, L.; Elofsson, A. The TOPCONS web server for consensus prediction of membrane protein topology and signal peptides. *Nucleic Acids Res.* 2015, 43, W401–W407.
  36. Hitt, R.; Wolf, D.H. Der1p, a protein required for degradation of malformed soluble proteins of the endoplasmic reticulum: Topology and Der1-like proteins. *FEMS Yeast Res.* 2004, 4, 721–729.
  37. Lilley, B.N.; Ploegh, H.L. A membrane protein required for dislocation of misfolded proteins from the ER. *Nature* 2004, 429, 834–840.
  38. Ye, Y.; Shibata, Y.; Yun, C.; Ron, D.; Rapoport, T.A. A membrane protein complex mediates retro-translocation from the ER lumen into the cytosol. *Nature* 2004, 429, 841–847.
  39. Greenblatt, E.J.; Olzmann, J.A.; Kopito, R.R. Derlin-1 is a rhomboid pseudoprotease required for the dislocation of mutant alpha-1 antitrypsin from the endoplasmic reticulum. *Nat. Struct. Mol. Biol.* 2011, 18, 1147–1152.
  40. Fairbank, M.; St-Pierre, P.; Nabi, I.R. The complex biology of autocrine motility factor/phosphoglucose isomerase (AMF/PGI) and its receptor, the gp78/AMFR E3 ubiquitin ligase. *Mol. Biosyst.* 2009, 5, 793–801.
  41. Landolt-Marticorena, C.; Reithmeier, R.A. Asparagine-linked oligosaccharides are localized to single extracytosolic segments in multi-span membrane glycoproteins. *Biochem. J.* 1994, 302, 253–260.
  42. Popov, M.; Tam, L.Y.; Li, J.; Reithmeier, R.A. Mapping the ends of transmembrane segments in a polytopic membrane protein. Scanning N-glycosylation mutagenesis of extracytosolic loops in the anion exchanger, band 3. *J. Biol. Chem.* 1997, 272, 18325–18332.
  43. Nilsson, I.M.; von Heijne, G. Determination of the distance between the oligosaccharyltransferase active site and the endoplasmic reticulum membrane. *J. Biol. Chem.* 1993, 268, 5798–5801.
  44. Christianson, J.C.; Ye, Y. Cleaning up in the endoplasmic reticulum: Ubiquitin in charge. *Nat. Struct. Mol. Biol.* 2014, 21, 325–335.
  45. Plemper, R.K.; Bohmler, S.; Bordallo, J.; Sommer, T.; Wolf, D.H. Mutant analysis links the translocon and BiP to retrograde protein transport for ER degradation. *Nature* 1997, 388, 891–895.
  46. Pilon, M.; Schekman, R.; Romisch, K. Sec61p mediates export of a misfolded secretory protein from the endoplasmic reticulum to the cytosol for degradation. *EMBO J.* 1997, 16, 4540–4548.
  47. Plemper, R.K.; Bordallo, J.; Deak, P.M.; Taxis, C.; Hitt, R.; Wolf, D.H. Genetic interactions of Hrd3p and Der3p/Hrd1p with Sec61p suggest a retro-translocation complex mediating protein transport for ER degradation. *J. Cell Sci.* 1999, 112, 4123–4134.
  48. Zhou, M.; Schekman, R. The engagement of Sec61p in the ER dislocation process. *Mol. Cell* 1999, 4, 925–934.
  49. Gillece, P.; Pilon, M.; Romisch, K. The protein translocation channel mediates glycopeptide export across the endoplasmic reticulum membrane. *Proc. Natl. Acad. Sci. USA* 2000, 97, 4609–4614.
  50. Wilkinson, B.M.; Tyson, J.R.; Reid, P.J.; Stirling, C.J. Distinct domains within yeast Sec61p involved in post-translational translocation and protein dislocation. *J. Biol. Chem.* 2000, 275, 521–529.

51. Schmitz, A.; Herrgen, H.; Winkler, A.; Herzog, V. Cholera toxin is exported from microsomes by the Sec61p complex. *J. Cell Biol.* 2000, 148, 1203–1212.
52. Scott, D.C.; Schekman, R. Role of Sec61p in the ER-associated degradation of short-lived transmembrane proteins. *J. Cell Biol.* 2008, 181, 1095–1105.
53. Willer, M.; Forte, G.M.; Stirling, C.J. Sec61p is required for ERAD-L: Genetic dissection of the translocation and ERAD-L functions of Sec61P using novel derivatives of CPY. *J. Biol. Chem.* 2008, 283, 33883–33888.
54. Schafer, A.; Wolf, D.H. Sec61p is part of the endoplasmic reticulum-associated degradation machinery. *EMBO J.* 2009, 28, 2874–2884.
55. Wahlman, J.; DeMartino, G.N.; Skach, W.R.; Bulleid, N.J.; Brodsky, J.L.; Johnson, A.E. Real-time fluorescence detection of ERAD substrate retrotranslocation in a mammalian in vitro system. *Cell* 2007, 129, 943–955.
56. Huang, C.H.; Hsiao, H.T.; Chu, Y.R.; Ye, Y.; Chen, X. Derlin2 protein facilitates HRD1-mediated retro-translocation of sonic hedgehog at the endoplasmic reticulum. *J. Biol. Chem.* 2013, 288, 25330–25339.
57. Hoelen, H.; Zaldumbide, A.; van Leeuwen, W.F.; Torfs, E.C.; Engelse, M.A.; Hassan, C.; Lebbink, R.J.; de Koning, E.J.; Ressing, M.E.; de Ru, A.H.; et al. Proteasomal Degradation of Proinsulin Requires Derlin-2, HRD1 and p97. *PLoS ONE* 2015, 10, e0128206.
58. Deak, P.M.; Wolf, D.H. Membrane topology and function of Der3/Hrd1p as a ubiquitin-protein ligase (E3) involved in endoplasmic reticulum degradation. *J. Biol. Chem.* 2001, 276, 10663–10669.
59. Nadav, E.; Shmueli, A.; Barr, H.; Gonen, H.; Ciechanover, A.; Reiss, Y. A novel mammalian endoplasmic reticulum ubiquitin ligase homologous to the yeast Hrd1. *Biochem. Biophys. Res. Commun.* 2003, 303, 91–97.
60. Burr, M.L.; Cano, F.; Svobodova, S.; Boyle, L.H.; Boname, J.M.; Lehner, P.J. HRD1 and UBE2J1 target misfolded MHC class I heavy chains for endoplasmic reticulum-associated degradation. *Proc. Natl. Acad. Sci. USA* 2011, 108, 2034–2039.
61. Burr, M.L.; van den Boomen, D.J.; Bye, H.; Antrobus, R.; Wiertz, E.J.; Lehner, P.J. MHC class I molecules are preferentially ubiquitinated on endoplasmic reticulum luminal residues during HRD1 ubiquitin E3 ligase-mediated dislocation. *Proc. Natl. Acad. Sci. USA* 2013, 110, 14290–14295.
62. Stein, A.; Ruggiano, A.; Carvalho, P.; Rapoport, T.A. Key steps in ERAD of luminal ER proteins reconstituted with purified components. *Cell* 2014, 158, 1375–1388.
63. Baldrige, R.D.; Rapoport, T.A. Autoubiquitination of the Hrd1 Ligase Triggers Protein Retrotranslocation in ERAD. *Cell* 2016, 166, 394–407.
64. Kreft, S.G.; Wang, L.; Hochstrasser, M. Membrane topology of the yeast endoplasmic reticulum-localized ubiquitin ligase Doa10 and comparison with its human ortholog TEB4 (MARCH-VI). *J. Biol. Chem.* 2006, 281, 4646–4653.





## CHAPTER 5

# The p97-cofactor UBXD8 is essential for HCMV US11-mediated HLA class I degradation

Michael L. van de Weijer, Robert Jan Lebbink\*, Emmanuel J.H.J. Wiertz\*

Department of Medical Microbiology, University Medical Center Utrecht, 3584CX Utrecht, The Netherlands

\*These authors contributed equally to this work

Manuscript in preparation

## **ABSTRACT**

Misfolded ER proteins are dislocated to the cytosol and degraded by the ubiquitin–proteasome system in a process called ER-associated protein degradation. During infection with human cytomegalovirus, the viral protein US11 efficiently downregulates HLA-I molecules via ERAD to avoid recognition and elimination of infected cells by the host’s immune system. Using this model system, p97 was previously identified as critical factor for ERAD. However, the mode of p97 recruitment has remained elusive to this date. In this study, we generated a lentiviral CRISPR/Cas9 library targeting all known human p97-cofactors and assessed their contribution to HLA-I downregulation. We identified UBXD8 to be critically involved in US11-mediated HLA-I degradation. Although the UBA domain of UBXD8 was dispensable for HLA-I downregulation, the UBX domain was essential. However, UBXD8 appeared not to be primarily responsible for p97 recruitment to the dislocation complex. Instead, UBXD8 may function as an ERAD scaffolding coordinator, mediating proper spatial and/or temporal arrangement of p97 complexes. Our findings illustrate the complexity of p97 recruitment and positioning during the dislocation process.

## INTRODUCTION

Human cytomegalovirus (HCMV) is a member of the  $\beta$ -herpesviridae and is a common virus with a seroprevalence of 40–100%, depending on the socioeconomic status of the host population. Although primary HCMV infection usually occurs asymptomatic in healthy individuals, the virus is the most common infectious cause of congenital disease and severe opportunistic infections in the immunocompromised host [1]. HCMV has the largest genome of the human herpesviruses and carries a large collection of immunomodulatory genes that facilitate interference with the host's immune system. As a result, HCMV persists in infected individuals for life [2–4].

The HLA class I antigen presentation pathway is a major target for the immune-evasive strategies of HCMV resulting in effective elusion of CD8-positive cytotoxic T cells [5]. The HCMV type 1 ER-glycoproteins US2 and US11 induce retrograde transport of newly synthesized HLA class I (HLA-I) heavy chains (HCs) from the ER into the cytosol for proteasomal degradation. This process of retrograde transport coupled to proteasomal degradation is called ER-associated protein degradation [6,7]. At the center of the ERAD process are multiprotein complexes that combine the functions essential to this reaction, namely substrate recognition, dislocation, ubiquitination, and degradation [8,9]. Although US2 and US11 both target HLA-I for degradation, they employ distinct protein complexes to this cause. US2 co-opts the E3 ubiquitin ligase TRC8 [10] and the E2 enzyme UBE2G2 (Chapter 6), whereas US11 relies on Derlin-1 and the E3 ubiquitin ligase TMEM129. The tri-spanning TMEM129 acts in conjunction with the E2 ubiquitin-conjugating enzymes UBE2J2 and UBE2K to target HLA-I molecules for degradation [11–15]. On the cytosolic side, both US2 and US11 require the AAA-ATPase p97 (also known as VCP) to shuttle HLA-I to the proteasome for degradation [16].

P97 contains an N-terminal domain, two ATPase domains D1 and D2, and an unstructured carboxy-terminal extension. The ATPase domains form a stable homo-hexameric ring with a central pore. It is believed that p97 extracts polyubiquitinated substrates from the ER membrane to the proteasome through ATP hydrolysis [17,18]. p97 may be recruited to the ER-membrane with the aid of various proteins, such as E3 ubiquitin ligases [19], Derlins [20], and/or dedicated p97-cofactors [21]. Despite the evident contribution of p97 to US11-mediated HLA-I degradation [18], the mechanism of p97 recruitment remains unknown. Here, we constructed a lentiviral CRISPR/Cas9-based library targeting known human p97-cofactors and used this resource to screen for p97-cofactors essential for US11-mediated HLA-I downregulation. We identify UBXD8 (also known as ETEA or FAF2) as an essential p97-cofactor for downregulation of HLA-I by US11. UBXD8 depletion rescues HLA class I from US11-mediated degradation and retains HLA class I in the US11-TMEM129 complex. We show that UBXD8 is present in a complex with both US11 and TMEM129. Moreover, the UBX domain of UBXD8 is essential for US11-mediated HLA-I downregulation, whereas the UBA

domain is dispensable. Nevertheless, UBXD8 is not essential for p97 recruitment, as p97 recruitment is not diminished in UBXD8 knockout cells. We hypothesize that UBXD8 and its UBX domain are required for the correct positioning of p97 during the dislocation process.

## **MATERIALS & METHODS**

### **Cell culture and lentiviral infection**

U937 human monocytic cells and 293T human embryonic kidney cells were obtained from ATCC (American Type Culture Collection) and grown in RPMI medium (Lonza) supplemented with glutamine (Gibco), penicillin/streptomycin (Gibco) and 10% fetal bovine serum (Biowest). For individual transductions using lentiviruses, virus was produced in 293T cells in 24-well plates using standard lentiviral production protocols and third-generation packaging vectors. The supernatant containing virus was harvested 3 days post transfection and stored at -80°C. For lentiviral transductions, 50 µl supernatant containing virus supplemented with 8 µg/mL polybrene (Santa Cruz Biotechnology) was used to infect approximately 20,000 U937 cells by spin infection at 1,000 g for 2 h at 33 °C. Complete medium was added after centrifugation to reduce polybrene concentration.

### **Generation of clonal CRISPR/Cas9-mediated knockout cells**

U937 cells stably co-expressing eGFP-Myc-HLA-A2 and HA-US11 or 3xST2-HA-US11 were transduced with a lentiviral CRISPR/Cas9 system, in which a single lentiviral vector co-expresses a Cas9, puromycin and a guide RNA (gRNA) sequence [12]. Two days post infection (d p.i.), transduced cells were selected by using 2 µg/mL puromycin and allowed to recover. Cells were single-cell sorted by fluorescence-activated cell sorting (FACS Aria III, BD Biosciences). The knockout status of the clonal cell lines was confirmed by flow cytometry and immunoblotting.

### **Antibodies**

Primary antibodies used in our studies were: mouse α-HLA class I HC HCA2 mAb; mouse α-TfR H68.4 mAb (no. 13-68xx, Invitrogen); mouse α-FLAG-M2 mAb (no. F1804, Sigma-Aldrich); rat α-HA 3F10 mAb (no. 11867423001, Roche); rabbit α-ETEA/UBXD8 (D8H6D) mAb (no. 34945, Cell Signaling Technology); mouse α-TMEM129 8D7 mAb (E. Kremmer, Helmholtz Zentrum München); rabbit α-Derlin-1 pAb (no. PM018, MBL); mouse α-VCP/p97 18/VCP mAb (no. 612183, BD Transduction laboratories); rabbit α-VIMP (D1D1M) mAb (no. 15160, Cell Signaling Technology).

Secondary antibodies used in our studies were: goat α-mouse IgG(H+L)-HRP (no. 170-6516, Bio-Rad); goat α-rabbit IgG(H+L)-HRP (no. 4030-05, Southern Biotech); mouse α-rabbit IgG(L)-HRP (no. 211-032-171, Jackson ImmunoResearch); goat α-mouse IgG(L)-HRP (no. 115-035-174, Jackson ImmunoResearch); goat α-rat IgG(L)-HRP (no. 112-035-175, Jackson ImmunoResearch).



### Plasmids and cDNAs

Several different lentiviral vectors were used in the present studies. The N-terminally eGFP and Myc-tagged human HLA-A2 vector present in the lentiviral pHSincPPT-SGW vector was kindly provided by Dr Paul Lehner and Dr Louise Boyle (University of Cambridge, Cambridge, UK). HCMV US11 was N-terminally tagged with either an HA-tag only, or three Strep(II) tags followed by an HA-tag. The original leader was replaced by the hCD8 leader sequence in the tagged US11 constructs. US11 and tagged variants were expressed from a dual promoter lentiviral vector, which also included expression of BlastR-T2A-mAmetrine via the hPGK promoter. For rescue and ectopic expression experiments, gRNA-resistant N-terminally FLAG-tagged UBXD8 was generated and cloned into a dual promoter lentiviral vector, which also included expression of ZeoR-T2A-mAmetrine via the hPGK promoter, as described previously [12]. UBXD8 deletion mutants UBXD8 $\Delta$ UBA and UBXD8 $\Delta$ UBX were generated by respectively deleting amino acids 12-48 and 357-439. UBXD8 and mutants were N-terminally tagged with either a FLAG tag or a Strep(II)-tag followed by a FLAG tag. Derlin-1 $\Delta$ SHP was generated by deleting the last 11 amino acids. gRNA-resistant Derlin-1 and Derlin-1 $\Delta$ SHP were cloned into a dual promoter lentiviral vector, which also included expression of ZeoR-T2A-mAmetrine via the hPGK promoter.

### Generation of CRISPR/Cas9-based screen targeting known p97-cofactors

A lentiviral CRISPR/Cas9 vector carrying a puromycin resistance cassette was used to facilitate efficient and selectable expression of a nuclear-localized Cas9 gene that was N-terminally fused to puroR using a T2A sequence, and a gRNA regulated by a U6 promoter, as described previously [12]. Additionally, the region immediately downstream of the U6 promoter contains a cassette with a BsmBI restriction site on each side to allow cloning of gRNA target sites followed by the gRNA scaffold and a terminator consisting of 5 T-residues. gRNAs targeting all known human E2s were designed using an online CRISPR Design Tool (<http://crispr.mit.edu/>). gRNA sequences are listed in Supplementary Information S1. The genomic target site for the gRNAs used in the validation studies and/or in the generation of clonal knockout cell lines are listed in Table 1.

gRNA	Genomic target site incl. PAM
gUBXD8_1	GGGTTAGATCCCGCTCCTC <u>AGG</u>
gDerlin1_3	AGGCCGAGTTTGCCGACCA <u>AGG</u>
gTMEM129_2	GCACACGGCGAACACCAGAT <u>AGG</u>

**Table 1:** Genomic target sites for gRNAs used in the validation studies and/or in the generation of clonal knockout cell lines. PAM sites are underlined.

### **Flow cytometry**

Cells were washed in FACS buffer (PBS containing 0.5% BSA and 0.02% sodium azide). Total eGFP-Myc-HLA-A2 expression was analyzed by assessment of the eGFP signal via flow cytometry acquisition on a FACSCanto II (BD Bioscience). Flow cytometry data were analyzed using FlowJo software.

### **Immunoblotting**

Cells were lysed in 1% Triton X-100 lysis buffer (1.0% Triton X-100, 100 mM NaCl, 50 mM Tris, pH 7.5) containing 1 mM Pefabloc SC (Roche) and 10  $\mu$ M Leupeptin (Roche). Nuclei and cell debris were pelleted at 12,000g for 20 min at 4 °C. Post-nuclear lysates were denatured in Laemmli sample buffer and incubated at RT for 30 minutes. Proteins were separated by SDS-PAGE and transferred to PVDF membranes (Immobilon-P, Millipore). Membranes were probed with indicated antibodies. Reactive bands were detected by ECL (Thermo Scientific Pierce), and exposed to Amersham Hyperfilm ECL films (GE Healthcare).

### **Co-immunoprecipitations**

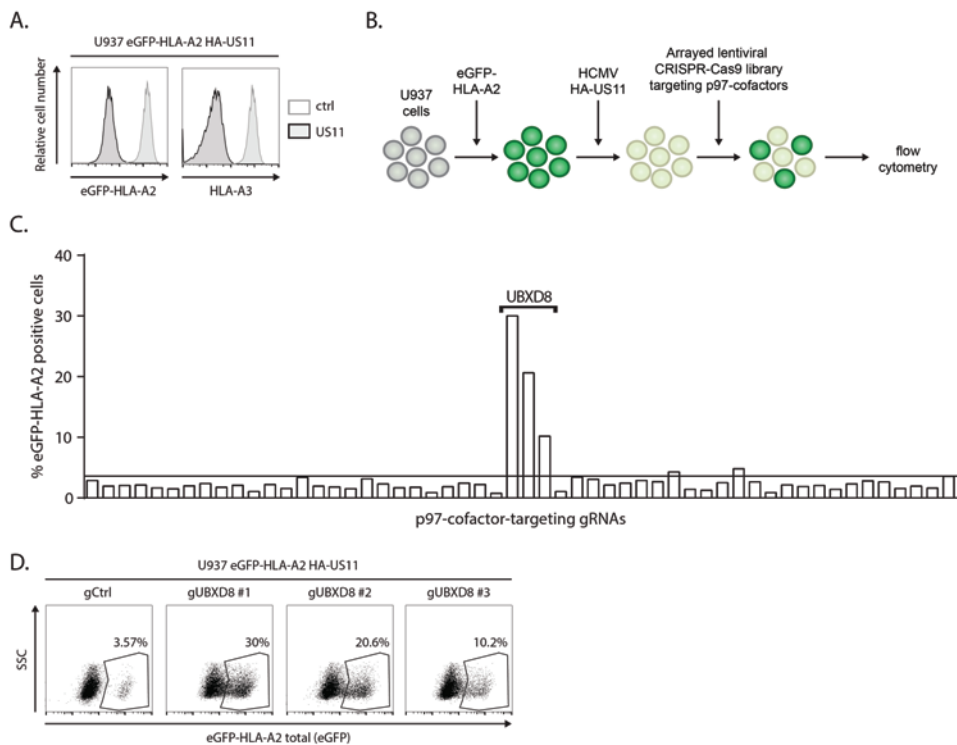
Cells were lysed in Digitonin lysis buffer (1% Digitonin (Calbiochem), 50 mM Tris-HCl, 5 mM MgCl<sub>2</sub>, 150 mM NaCl; pH 7.5) containing 1 mM Pefabloc SC (Roche) and 10  $\mu$ M Leupeptin (Roche). Lysates were incubated for 90 min at 4 °C. Nuclei and cell debris were pelleted 12,000g for 20 min at 4 °C. Post-nuclear supernatants were incubated overnight with StrepTactin beads (GE Healthcare). After four washes in 0.1% digitonin lysis buffer, proteins were eluted in elution buffer (2.5 mM desthiobiotin, 150 mM NaCl, 100 mM Tris-HCl, 1 mM EDTA, pH 8) for 30 min on ice. The eluate was separated from the beads using 0.45  $\mu$ m Spin-X filter column (Corning Costar), and subsequently denatured in Laemmli sample buffer containing DTT. Immunoblotting was performed as described above.

## **RESULTS**

### **A CRISPR/Cas9 library screen identifies UBXD8/FAF2 as essential player in US11-mediated HLA-I downregulation**

To identify p97-cofactors required for US11-mediated degradation of HLA-I molecules, we constructed an arrayed lentiviral CRISPR/Cas9-based library targeting 17 known p97-cofactors using approximately three gRNAs per gene (Supplementary Information S1). U937 monocytic cells stably expressing an HLA-A2 molecule with an N-terminal eGFP tag were generated to allow monitoring of total HLA-I expression levels by flow cytometry. Upon stable introduction of HCMV US11, the chimeric HLA-I molecule was efficiently degraded (Fig. 1A). These cells were then transduced with the lentiviral CRISPR/Cas9 library. Disruption of an essential p97-cofactor would rescue eGFP-HLA-A2 from degradation and thus increase eGFP fluorescence, which was evaluated by flow cytometry (Fig. 1B).

Of all gRNAs tested, only anti-UBXD8 gRNAs induced rescue of eGFP-HLA-A2 in  $\pm 10$  to 30% of US11-expressing cells (Fig. 1C and D). We established three clonal UBXD8 knockout lines from this polyclonal population, which all displayed abrogated US11-mediated HLA-I downregulation as indicated by increased eGFP-HLA-A2 levels (Fig. 1E). US11-mediated HLA-I downregulation was not affected in control clonal VIMP knockout cells (Fig. 1E). In addition to increased eGFP-HLA-A2 levels, endogenous HLA-I expression was upregulated in UBXD8 knockout cells (Fig. 1F). Besides regulation of HLA-I, US11 levels were increased in UBXD8-null cells, an effect often observed upon knockout of genes essential for US11 functioning. This increase in US11 levels may be caused by stabilization of dislocation complexes in the absence of UBXD8 [12]. To validate the involvement of UBXD8 in US11-mediated HLA-I degradation, expression of UBXD8 in the clonal UBXD8 knockout cells was restored by introduction of a gRNA-resistant UBXD8 cDNA which resulted in restoration of US11-mediated HLA-I downregulation (Fig. 1G). Our results show that UBXD8 is essential for US11-mediated HLA-I downregulation



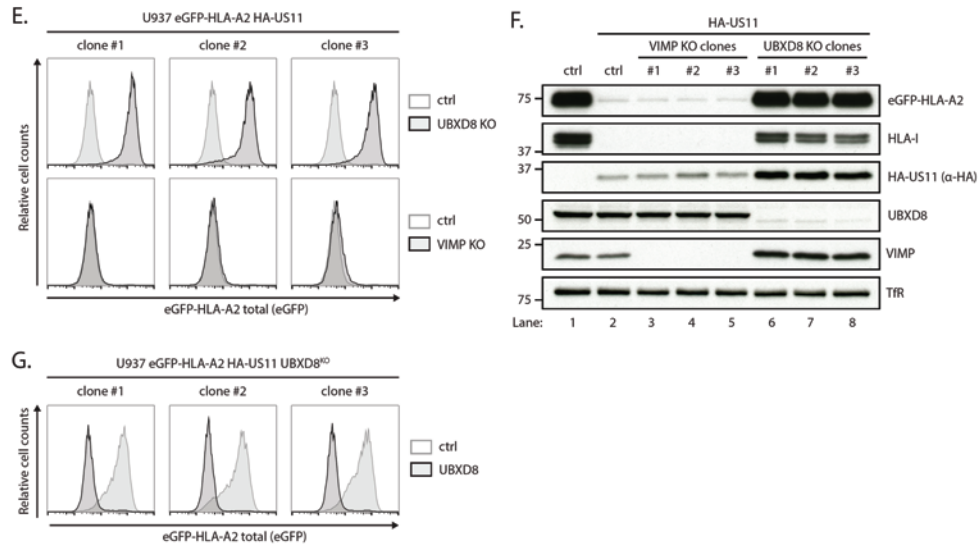


**Figure 1. A lentiviral CRISPR/Cas9 library screen identifies the p97 cofactors UBXD8 as essential for US11-mediated HLA-I downregulation.** (A) Downregulation of eGFP-HLA-A2 and endogenous HLA-A3 by HA-US11 in U937 cells expressing eGFP-HLA-A2 as assessed by flow cytometry. (B) Schematic overview of the lentiviral CRISPR/Cas9-based screen focused on p97 cofactors. U937 cells were transduced with a chimeric eGFP-HLA-A2 and subsequently transduced with an HCMV US11-expression vector. As a result, cells displayed low total eGFP-HLA-A2 expression levels as assessed by quantification of the eGFP signal. Cells were subsequently transduced with lentiviral CRISPR/Cas9 constructs targeting individual p97 cofactors. Two days after infection, cells were selected using puromycin. Next, flow cytometry analysis was performed 12 d p.i. to analyze total eGFP-HLA-A2 levels. All experiments have been performed three times, if not indicated otherwise, of which one representative figure is shown. (C) Quantification of the percentage eGFP-HLA-A2-positive cells after transduction with CRISPR/Cas9 constructs targeting individual p97-cofactors (see also Supplementary Information S1). (D) CRISPR/Cas9-mediated knockout of UBXD8 using three distinct gRNAs induces rescue of eGFP-HLA-A2 in US11-expressing cells. eGFP-HLA-A2 levels were assessed by flow cytometry 12 d p.i.. Percentages of eGFP-HLA-A2-positive cells are indicated. (E) Three independent knockout clones of either UBXD8 or VIMP were established from a polyclonal population, after which flow cytometry analysis was performed to assess eGFP-HLA-A2 levels. (F) Triton X-100 lysates of UBXD8 and VIMP knockout clones were prepared and subjected to immunoblot analysis to assess expression levels of indicated proteins. (G) To validate the involvement of UBXD8 in US11-induced HLA-I degradation, UBXD8 was reintroduced into the UBXD8 knockout clones used in (D), after which flow cytometry analysis was performed to assess eGFP-HLA-A2.

### UBXD8 is in complex with US11 and TMEM129

To assess whether UBXD8 is present in the US11-exploited dislocation complex, we generated N-terminally Strep(II)-tag and HA-tagged US11 molecules (ST2-HA-US11) and subjected these to co-immunoprecipitation experiments. Upon pull-down of ST2-HA-US11, endogenous UBXD8 was co-isolated. In agreement with previous findings, endogenous Derlin-1 and TMEM129 co-precipitated with ST2-HA-US11 as well (Fig. 2A, lane 4). To test if UBXD8 is part of dislocation complexes centered around the E3 TMEM129, TMEM129

complexes were isolated from cells. Upon TMEM129-FLAG-ST2 pulldown in the absence and presence of US11, UBXD8 was co-precipitated (Fig. 2B, lane 6 and 8 respectively). In agreement with previous findings, Derlin-1 (lane 6 and 8) and US11 (lane 8) were co-precipitated as well. These data show that UBXD8 associates with US11-exploited and TMEM129-centered dislocation complexes.

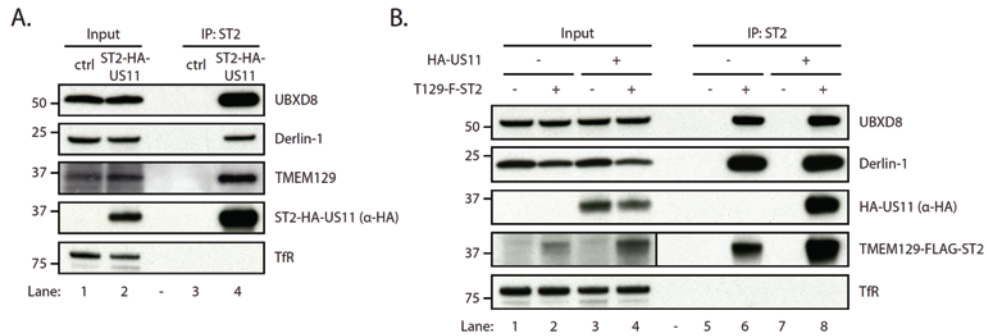


**Figure 2. UBXD8 is present in US11-exploited and TMEM129-centered dislocation complexes.** (A) UBXD8 is part of US11-exploited dislocation complexes. Strep(II)-HA-tagged US11 was immunoprecipitated using StrepTactin beads from 1.0% digitonin lysates of ST2-HA-US11-negative and -positive U937 eGFP- HLA-A2 cells. Immunoprecipitated proteins were eluted using d-Desthiobiotin. Immunoblot analysis was performed on post-nuclear cell lysate (Input) and immunoprecipitated material (IP) for the indicated proteins. (B) UBXD8 is part of TMEM129-containing dislocation complexes. Strep(II)-FLAG-tagged TMEM129 was immunoprecipitated using StrepTactin beads from 1.0% digitonin lysates of HA-US11-negative and -positive U937 eGFP-HLA-A2 cells. Immunoprecipitated proteins were eluted using d-Desthiobiotin. Immunoblot analysis was performed on post-nuclear cell lysate (Input) and immunoprecipitated material (IP) for the indicated proteins. Immunoblot analysis of TMEM129-FLAG-ST2 input and immunoprecipitated levels is respectively composed of a long and a shorter exposure

5

**The UBX domain of UBXD8 is essential for HCMV US11-mediated HLA-I downregulation**

Next, we investigated which domains of UBXD8 are essential for US11-mediated HLA-I degradation. UBXD8 is inserted into the outer leaflet of the ER lipid bilayer via a hydrophobic patch (HP), thereby exposing both the N- and C-terminus of the protein to the cytosol [22,23]. The N-terminal part of UBXD8 contains a UBA domain, responsible for the interaction with poly-ubiquitinated proteins, whereas the C-terminal part contains a UBX domain, facilitating interaction with p97 and cofactors [24].

To investigate the requirement of the UBA and UBX domain in US11-mediated HLA-I degradation, we generated UBA- and UBX-deletion mutants of UBXD8 (Fig. 3A). These deletion mutants were introduced into clonal UBXD8 knockout US11-expressing cells. Next, eGFP-HLA-A2 levels were assessed by flow cytometry (Fig.3B). Introduction of the UBA-deletion mutant (ΔUBA) restored HLA-I degradation by US11 comparable to introduction of full length (FL) UBXD8, whereas introduction of the UBX-deletion mutant (ΔUBX) did not restore HLA-I degradation. Thus, the UBA domain of UBXD8 is dispensable for US11-mediated HLA-I degradation, whereas the UBX domain is essential.

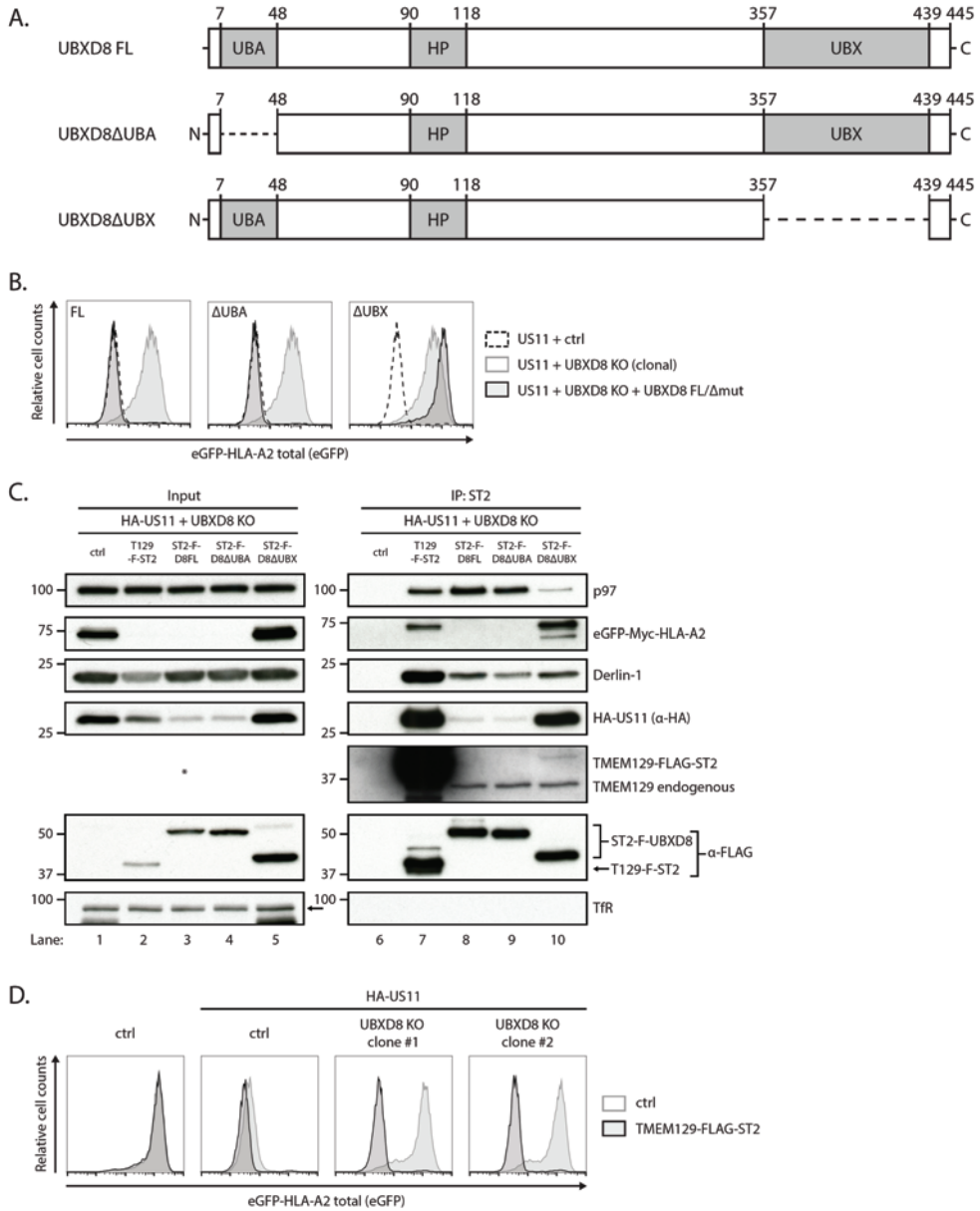


**Figure 3. The p97-recruiting UBX-domain of UBXD8 is essential for US11-mediated HLA-I degradation.** (A) Domain organization of human UBXD8, and domain-deletion mutants  $\Delta$ UBA and  $\Delta$ UBX. FL, Full length; UBA, ubiquitin-associated; HP, hydrophobic patch; UBX, ubiquitin regulatory X. (B) The p97-recruiting UBX-domain of UBXD8 is essential for US11-mediated HLA class I degradation. Full length of UBXD8 (FL) and domain-deletion mutants UBXD8 $\Delta$ UBA and UBXD8 $\Delta$ UBX were lentivirally introduced into UBXD8-knockout cells expressing US11 and eGFP-HLA-A2. eGFP-HLA-A2 levels were assessed by flow cytometry 7 days post transduction. (C) Deletion of the UBX domain impairs p97 recruitment by UBXD8. Strep(II)-FLAG-tagged UBXD8 and domain-deletion mutants

**Figure 3 (continued):** UBXD8 $\Delta$ UBA and UBXD8 $\Delta$ UBX were immunoprecipitated using StrepTactin beads from 1.0% digitonin lysates of UBXD8-knockout U937 cells co-expressing HA-US11 and eGFP-HLA-A2. As a positive control, TMEM129-FLAG-ST2 was immunoprecipitated. Immunoprecipitated proteins were eluted using d-Desthiobiotin. Immunoblot analysis was performed on post-nuclear cell lysate (input) and immunoprecipitated material (IP) for the indicated proteins. This experiment has been performed two times, of which one representative figure is shown. \*The TMEM129 antibody could not detect endogenous TMEM129 in digitonin cell lysates. (D) TMEM129-FLAG-ST2 was lentivirally introduced in UBXD8-knockout clones or control cells expressing US11 and eGFP-HLA-A2. eGFP-HLA-A2 levels were assessed by flow cytometry 12 days post transduction.

We next subjected these deletion mutants to co-immunoprecipitation experiments to investigate their association to p97, US11, Derlin-1, and TMEM129 (Fig. 3C). Pull-down of UBXD8 complexes showed reduced p97 association to UBXD8 $\Delta$ UBX (lane 10) compared to full length UBXD8 (lane 8) and the UBA deletion mutant (lane 9). Both UBXD8 mutants (lane 9,10) showed similar association with TMEM129 and Derlin-1 as compared to full length wt UBXD8 (lane 8). Full length UBXD8 (lane 8) and UBXD8 $\Delta$ UBA (lane 9) associated with equal amounts of US11, while UBXD8 $\Delta$ UBX (lane 10) showed increased association with US11. HLA-I was only co-precipitated with the UBXD8 $\Delta$ UBX deletion mutant (lane 10) likely due to stalling of the US11-exploited dislocation complexes.

As a positive control, TMEM129-FLAG-ST2 was expressed (Fig. 3C, lane 2) and immunoprecipitated (lane 7) in these cells. Surprisingly, TMEM129-FLAG-ST2 expression bypassed the requirement of UBXD8 in US11-mediated HLA-I degradation, as no HLA-I expression was detected in TMEM129-FLAG-ST2-expressing UBXD8 knockout cells (lane 2). This observation was confirmed by flow cytometry which displayed restored HLA-I degradation by US11 in UBXD8 KO cells upon overexpression of the TMEM129-FLAG-ST2 (Fig. 3D).

### **UBXD8 knockout does not abolish p97 recruitment to US11-exploited dislocation complexes**

We next investigated whether UBXD8 is responsible for p97 recruitment to US11-exploited dislocation complexes. To this end, we performed co-immunoprecipitation experiments on ST2-HA-US11 in either Derlin-1, TMEM129 or UBXD8 knockout cells (Fig. 4A). The knockout of these genes completely disrupted HLA-I degradation by US11 (Fig. 4A, lanes 3-5). As often seen for genes essential for US11-mediated HLA-I degradation, the knockout of Derlin-1, TMEM129, and UBXD8 resulted in increased US11 levels (lane 3-5) compared to control cells (lane 2). This resulted in different levels of precipitated US11. If the differences in the amount of precipitated US11 are taken into account, the knockout of Derlin-1 caused decreased association of p97 and TMEM129 (lane 8) compared to control cells (lane 7). A knockout of either TMEM129 (lane 9) or UBXD8 (lane 10) did not decrease p97 association, indicating that Derlin-1, and not TMEM129 and UBXD8, might contribute to recruitment of p97 to the complex.

Derlin-1 contains a C-terminal SHP domain which is able to recruit p97 [20]. To test the

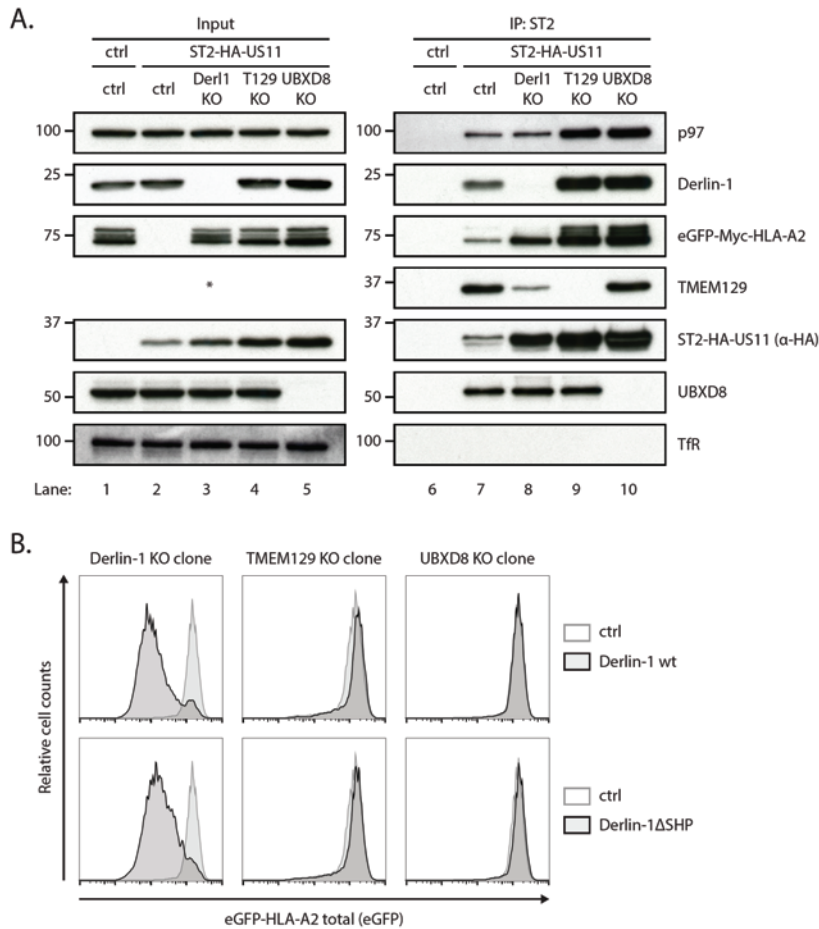


**Figure 4. Derlin-1 is involved in p97 recruitment.** (A) UBXD8 knockout does not diminish p97 recruitment to US11-exploited dislocation complexes. Strep(II)-HA-tagged US11 was immunoprecipitated using StrepTactin beads from 1.0% digitonin lysates of mock- (lane 1) or US11-expressing U937 eGFP-HLA-A2 cells (lane 2), in which either Derlin-1 (lane 3), TMEM129 (lane 4), or UBXD8 (lane 5) was knocked out. Immunoprecipitated proteins were eluted using d-Desthiobiotin. Immunoblot analysis was performed on post-nuclear cell lysate (input) and immunoprecipitated material (IP) for the indicated proteins. This experiment has been performed two times, of which one representative figure is shown. \*The TMEM129 antibody could not detect endogenous TMEM129 in digitonin cell lysates. (B) The p97-recruiting SHP domain of Derlin-1 is not essential for US11-mediated HLA class I downregulation. Full length Derlin-1 (FL) and SHP-deletion mutant Derlin-1 $\Delta$ SHP were lentivirally introduced into Derlin-1-, TMEM129-, and UBXD8-knockout cells co-expressing US11 and eGFP-HLA-A2. Flow cytometry analysis was performed to assess total eGFP-HLA-A2 levels.



involvement of Derlin-1 and its SHP domain in p97 recruitment during US11-mediated HLA-I degradation, a Derlin-1 SHP-deletion mutant was expressed in clonal Derlin-1 knockout US11-expressing cells. Surprisingly, both full length Derlin-1 and Derlin-1 $\Delta$ SHP restored HLA-I degradation by US11 as assessed by flow cytometry (Fig. 4B), suggesting that p97 is indirectly recruited via Derlin-1 to the dislocation complex in an SHP-independent manner. Moreover, US11-mediated HLA-I degradation in TMEM129 or UBXD8 knockout cells could not be restored through overexpression of Derlin-1 or Derlin-1 $\Delta$ SHP, indicating that Derlin-1 does not provide redundant TMEM129 and UBXD8 functionality during US11-mediated HLA-I degradation.

## DISCUSSION

The ATPase P97 is indispensable for US11-mediated HLA-I degradation, although the mechanism of its recruitment to the dislocation complex remains elusive. It has previously been suggested that either VIMP [25] or UBXD8 [26] are responsible for p97 recruitment during US11-mediated HLA-I degradation, but convincing evidence confirming their essential involvement in US11-mediated HLA-I degradation, is lacking. Using a focused lentiviral CRISPR/Cas9 screen, we identified the p97-cofactor UBXD8, but not VIMP, to be essential for US11-mediated HLA-I degradation. Pull-down experiments on US11 revealed that UBXD8 is present in dislocation complexes in the presence of US11. In the absence of US11, pull-down experiments on TMEM129 showed that UBXD8 is also in complex with TMEM129, that TMEM129 plays a more general role in ER-associated protein degradation.

p97 cofactors use various domains to associate with p97. Where UBX, UBX-like, SHP, VBM, and VIM domains can interact with the N-terminus of p97, PUB and PUL domains interact with its C-terminal tail [27]. E3 ubiquitin ligases and the Derlin proteins can also directly recruit p97 [19,20,27]. This plethora of p97 recruitment possibilities may reflect a requirement for different p97 configurations at different steps of the dislocation complex.

The UBA domain of UBXD8 is dispensable for US11-mediated HLA-I degradation. UBA domains in general interact with polyubiquitinated proteins [24]. In addition, the UBA domain of UBXD8 is able to recruit BAG6, a cytosolic chaperone involved in ERAD, through the UBL domain of BAG6 [28]. While BAG6 is essential for US11-mediated HLA-I degradation [29], the UBA domain of UBXD8 domain is not suggesting that the UBA domain of UBXD8 is not responsible for BAG6 recruitment during US11-mediated HLA-I degradation, or that some form of redundancy exists for recruiting BAG6.

The UBX domain of UBXD8 is required for p97 recruitment [26,30,31] and for the degradation of at least one ERAD substrate, i.e. lipidated ApoB-100 [30]. Here we found that the UBX domain of UBXD8 is also essential for degradation of HLA-I by US11. UBXD8 pull-down experiments showed that the UBX-deletion mutant has severely impaired p97 recruitment. Surprisingly, however, the amount of recruited p97 to US11-exploited

complexes was unaffected upon UBXD8 knockout, indicating that UBXD8 is not primarily responsible for the recruitment of p97 to the dislocation complex.

Surprisingly, TMEM129 overexpression bypassed the requirement of UBXD8 in US11-mediated HLA-I degradation. TMEM129 does not contain any known p97 recruitment domains. In addition, direct immunoprecipitation of TMEM129 in Triton X-100 does not co-precipitate p97 (data not shown). Also, a knockout of TMEM129 did not diminish p97 recruitment to the US11 complex. Thus, it is unlikely that TMEM129 can directly recruit p97. It has been postulated that oligomers of ERAD E3 ubiquitin ligases may comprise the protein-conducting channel, as has been suggested for yeast Hrd1p from *in vitro* dislocation assays [17,32]. UBXD8 may be involved in the oligomerization of TMEM129 to allow the formation of the protein-conducting channel. By overexpressing TMEM129, oligomerization may occur in the absence of UBXD8. In analogy, yeast Hrd1p overexpression induces aspecific oligomerization and bypasses the need for accessory factors, such as Der1p and Sel1p, in ERAD [33].

Interestingly, only a Derlin-1 knockout resulted in decreased p97 recruitment. Derlin-1 contains a C-terminal SHP domain which is essential for p97 recruitment and subsequent extraction of the soluble ERAD substrate NHK, a constitutively degraded truncated variant of  $\alpha$ -1 antitrypsin, from the ER membrane [20]. Surprisingly, the SHP-deletion mutant of Derlin-1 was still able to drive US11-mediated HLA-I degradation in Derlin-1 knockout cells. We thus hypothesize that Derlin-1 recruits p97 indirectly via a yet unknown factor. Additionally, we think that in the context of US11-mediated HLA-I degradation, UBXD8 mediates proper spatial and/or temporal arrangement of p97 complexes. Alternatively, UBXD8 may prevent the binding of cofactors negatively affecting the dislocation process.

## REFERENCES

- [1] P. Griffiths, I. Baraniak, M. Reeves, The pathogenesis of human cytomegalovirus., *J. Pathol.* 235 (2015) 288–97. doi:10.1002/path.4437.
- [2] W. Dunn, C. Chou, H. Li, R. Hai, D. Patterson, V. Stolc, H. Zhu, F. Liu, Functional profiling of a human cytomegalovirus genome., *Proc. Natl. Acad. Sci. U. S. A.* 100 (2003) 14223–8. doi:10.1073/pnas.2334032100.
- [3] E.S. Mocarski, Immunomodulation by cytomegaloviruses: manipulative strategies beyond evasion., *Trends Microbiol.* 10 (2002) 332–9. <http://www.ncbi.nlm.nih.gov/pubmed/12110212> (accessed January 17, 2016).
- [4] S.G. Hansen, C.J. Powers, R. Richards, A.B. Ventura, J.C. Ford, D. Siess, M.K. Axthelm, J.A. Nelson, M.A. Jarvis, L.J. Picker, K. Früh, Evasion of CD8+ T cells is critical for superinfection by cytomegalovirus., *Science.* 328 (2010) 102–6. doi:10.1126/science.1185350.
- [5] M.L. van de Weijer, R.D. Luteijn, E.J.H.J. Wiertz, Viral immune evasion: Lessons in MHC class I antigen presentation., *Semin. Immunol.* 27 (2015) 125–37. doi:10.1016/j.smim.2015.03.010.
- [6] E.J. Wiertz, D. Tortorella, M. Bogyo, J. Yu, W. Mothes, T.R. Jones, T.A. Rapoport, H.L. Ploegh, Sec61-mediated transfer of a membrane protein from the endoplasmic reticulum to the proteasome for destruction., *Nature.* 384 (1996) 432–8. doi:10.1038/384432a0.
- [7] E.J. Wiertz, T.R. Jones, L. Sun, M. Bogyo, H.J. Geuze, H.L. Ploegh, The human cytomegalovirus US11 gene product dislocates MHC class I heavy chains from the endoplasmic reticulum to the cytosol., *Cell.* 84 (1996)

- 769–79. <http://www.ncbi.nlm.nih.gov/pubmed/8625414> (accessed October 30, 2014).
- [8] J.A. Olzmann, R.R. Kopito, J.C. Christianson, The mammalian endoplasmic reticulum-associated degradation system., *Cold Spring Harb. Perspect. Biol.* 5 (2013). doi:10.1101/cshperspect.a013185.
- [9] J.C. Christianson, J. a Olzmann, T. a Shaler, M.E. Sowa, E.J. Bennett, C.M. Richter, R.E. Tyler, E.J. Greenblatt, J.W. Harper, R.R. Kopito, Defining human ERAD networks through an integrative mapping strategy., *Nat. Cell Biol.* 14 (2011) 93–105. doi:10.1038/ncb2383.
- [10] H.R. Stagg, M. Thomas, D. van den Boomen, E.J.H.J. Wiertz, H. a Drabkin, R.M. Gemmill, P.J. Lehner, The TRC8 E3 ligase ubiquitinates MHC class I molecules before dislocation from the ER., *J. Cell Biol.* 186 (2009) 685–92. doi:10.1083/jcb.200906110.
- [11] B.N. Lilley, H.L. Ploegh, A membrane protein required for dislocation of misfolded proteins from the ER., *Nature.* 429 (2004) 834–40. doi:10.1038/nature02592.
- [12] M.L. van de Weijer, M.C. Bassik, R.D. Luteijn, C.M. Voorburg, M.A.M. Lohuis, E. Kremmer, R.C. Hoeben, E.M. LeProust, S. Chen, H. Hoelen, M.E. Ressing, W. Patena, J.S. Weissman, M.T. McManus, E.J.H.J. Wiertz, R.J. Lebbink, A high-coverage shRNA screen identifies TMEM129 as an E3 ligase involved in ER-associated protein degradation., *Nat. Commun.* 5 (2014) 3832. doi:10.1038/ncomms4832.
- [13] D.J.H. van den Boomen, R.T. Timms, G.L. Grice, H.R. Stagg, K. Skødt, G. Dougan, J.A. Nathan, P.J. Lehner, TMEM129 is a Derlin-1 associated ERAD E3 ligase essential for virus-induced degradation of MHC-I., *Proc. Natl. Acad. Sci. U. S. A.* 111 (2014) 11425–30. doi:10.1073/pnas.1409099111.
- [14] D. Flierman, C.S. Coleman, C.M. Pickart, T.A. Rapoport, V. Chau, E2-25K mediates US11-triggered retrotranslocation of MHC class I heavy chains in a permeabilized cell system., *Proc. Natl. Acad. Sci. U. S. A.* 103 (2006) 11589–94. doi:10.1073/pnas.0605215103.
- [15] M.L. Van De Weijer, G.H. Van Muijlwijk, L.J. Visser, A.I. Costa, E.J.H.J. Wiertz, R.J. Lebbink, The E3 ubiquitin ligase TMEM129 is a tri-spanning transmembrane protein, *Viruses.* 8 (2016). doi:10.3390/v8110309.
- [16] N. Soetandyo, Y. Ye, The p97 ATPase dislocates MHC class I heavy chain in US2-expressing cells via a Ufd1-Npl4-independent mechanism., *J. Biol. Chem.* 285 (2010) 32352–9. doi:10.1074/jbc.M110.131649.
- [17] R.D. Baldrige, T.A. Rapoport, Autoubiquitination of the Hrd1 Ligase Triggers Protein Retrotranslocation in ERAD., *Cell.* 166 (2016) 394–407. doi:10.1016/j.cell.2016.05.048.
- [18] Y. Ye, H.H. Meyer, T.A. Rapoport, The AAA ATPase Cdc48/p97 and its partners transport proteins from the ER into the cytosol., *Nature.* 414 (2001) 652–6. doi:10.1038/414652a.
- [19] Y. Ye, Y. Shibata, M. Kikkert, S. van Voorden, E. Wiertz, T.A. Rapoport, Recruitment of the p97 ATPase and ubiquitin ligases to the site of retrotranslocation at the endoplasmic reticulum membrane., *Proc. Natl. Acad. Sci. U. S. A.* 102 (2005) 14132–8. doi:10.1073/pnas.0505006102.
- [20] E.J. Greenblatt, J.A. Olzmann, R.R. Kopito, Derlin-1 is a rhomboid pseudoprotease required for the dislocation of mutant  $\alpha$ -1 antitrypsin from the endoplasmic reticulum., *Nat. Struct. Mol. Biol.* 18 (2011) 1147–52. doi:10.1038/nsmb.2111.
- [21] A. Buchberger, H. Schindelin, P. Hänzelmann, Control of p97 function by cofactor binding, *FEBS Lett.* 589 (2015) 2578–2589. doi:10.1016/j.febslet.2015.08.028.
- [22] J.N. Lee, H. Kim, H. Yao, Y. Chen, K. Weng, J. Ye, Identification of Ubx8 protein as a sensor for unsaturated fatty acids and regulator of triglyceride synthesis., *Proc. Natl. Acad. Sci. U. S. A.* 107 (2010) 21424–9. doi:10.1073/pnas.1011859107.
- [23] B. Schrul, R.R. Kopito, Peroxin-dependent targeting of a lipid-droplet-destined membrane protein to ER subdomains, *Nat. Cell Biol.* 18 (2016) 740–51. doi:10.1038/ncb3373.
- [24] A. Buchberger, From UBA to UBX: new words in the ubiquitin vocabulary., *Trends Cell Biol.* 12 (2002) 216–21. <http://www.ncbi.nlm.nih.gov/pubmed/12062168> (accessed December 7, 2016).
- [25] Y. Ye, Y. Shibata, C. Yun, D. Ron, T. a Rapoport, A membrane protein complex mediates retro-translocation from the ER lumen into the cytosol., *Nature.* 429 (2004) 841–7. doi:10.1038/nature02656.

- [26] B. Mueller, E.J. Klemm, E. Spooner, J.H. Claessen, H.L. Ploegh, SEL1L nucleates a protein complex required for dislocation of misfolded glycoproteins., *Proc. Natl. Acad. Sci. U. S. A.* 105 (2008) 12325–30. doi:10.1073/pnas.0805371105.
- [27] A. Stolz, W. Hilt, A. Buchberger, D.H. Wolf, Cdc48: a power machine in protein degradation, *Trends Biochem. Sci.* 36 (2011) 515–523. doi:10.1016/j.tibs.2011.06.001.
- [28] Y. Xu, Y. Liu, J. -g. Lee, Y. Ye, A Ubiquitin-like Domain Recruits an Oligomeric Chaperone to a Retrotranslocation Complex in Endoplasmic Reticulum-associated Degradation, *J. Biol. Chem.* 288 (2013) 18068–18076. doi:10.1074/jbc.M112.449199.
- [29] Q. Wang, Y. Liu, N. Soetandyo, K. Baek, R. Hegde, Y. Ye, A ubiquitin ligase-associated chaperone holdase maintains polypeptides in soluble states for proteasome degradation., *Mol. Cell.* 42 (2011) 758–70. doi:10.1016/j.molcel.2011.05.010.
- [30] M. Suzuki, T. Otsuka, Y. Ohsaki, J. Cheng, T. Taniguchi, H. Hashimoto, H. Taniguchi, T. Fujimoto, Derlin-1 and UBXD8 are engaged in dislocation and degradation of lipidated ApoB-100 at lipid droplets., *Mol. Biol. Cell.* 23 (2012) 800–10. doi:10.1091/mbc.E11-11-0950.
- [31] G. Alexandru, J. Graumann, G.T. Smith, N.J. Kolawa, R. Fang, R.J. Deshaies, UBXD7 binds multiple ubiquitin ligases and implicates p97 in HIF1alpha turnover., *Cell.* 134 (2008) 804–16. doi:10.1016/j.cell.2008.06.048.
- [32] A. Stein, A. Ruggiano, P. Carvalho, T.A. Rapoport, Key steps in ERAD of luminal ER proteins reconstituted with purified components., *Cell.* 158 (2014) 1375–88. doi:10.1016/j.cell.2014.07.050.
- [33] P. Carvalho, A.M. Stanley, T.A. Rapoport, Retrotranslocation of a misfolded luminal ER protein by the ubiquitin-ligase Hrd1p., *Cell.* 143 (2010) 579–91. doi:10.1016/j.cell.2010.10.028.

UBXD8 is essential for HCMV US11-mediated HLA class I degradation

5



## CHAPTER 6

# Multiple E2 ubiquitin-conjugating enzymes regulate human cytomegalovirus US2-mediated immunoreceptor downregulation

Michael L van de Weijer<sup>1,\*</sup>, Anouk BC Schuren<sup>1,\*</sup>, Dick JH van den Boomen<sup>2</sup>, Arend Mulder<sup>3</sup>, Frans HJ Claas<sup>3</sup>, Paul J Lehner<sup>2</sup>, Robert Jan Lebbink<sup>1,#</sup>, Emmanuel JHJ Wiertz<sup>1,#</sup>

<sup>1</sup>Dept. Medical Microbiology, University Medical Center Utrecht, 3584CX Utrecht, The Netherlands

<sup>2</sup>Cambridge Institute for Medical Research, University of Cambridge, Cambridge, United Kingdom

<sup>3</sup>Dept. Immunohematology and blood transfusion, Leiden University Medical Center, 2333 ZA Leiden, The Netherlands

\*,#These authors contributed equally to this work

Manuscript submitted

## **ABSTRACT**

Misfolded ER proteins are dislocated towards the cytosol and degraded by the ubiquitin–proteasome system in a process called ER-associated protein degradation (ERAD). During infection with human cytomegalovirus (HCMV), the viral US2 protein targets HLA class I molecules (HLA-I) for degradation via ERAD to avoid elimination by the immune system. US2-mediated degradation of HLA-I serves as a paradigm of ERAD and has facilitated the identification of TRC8 as an E3 ubiquitin ligase. To date, no specific E2 enzymes had been described for cooperation with TRC8. In this study, we used a lentiviral CRISPR/Cas9 library targeting all known human E2 enzymes to assess their involvement in US2-mediated HLA-I downregulation. We identified multiple E2 enzymes involved in this process, of which UBE2G2 was crucial for the degradation of various immunoreceptors. UBE2J2, on the other hand, counteracted US2-induced ERAD by downregulating TRC8 expression. These findings indicate the complexity of cellular quality control mechanisms, which are elegantly exploited by HCMV to elude the immune system.



## INTRODUCTION

Human cytomegalovirus (HCMV) is a member of the  $\beta$ -herpesviridae and carries the largest dsDNA genome of the human herpesviruses (McGeoch et al., 2006). HCMV is a common virus with a seroprevalence of 40–100%, depending on the socioeconomic status of the host population. Primary infection of healthy individuals usually is asymptomatic, but in pregnant women and immunocompromised patients, HCMV infection can cause serious disease (Griffiths et al., 2015). HCMV encodes multiple immunomodulatory proteins that facilitate interference with the host's immune system, thereby facilitating HCMV to establish a lifelong infection (Dunn et al., 2003; Mocarski, 2002; Hansen et al., 2010).

The HLA-I antigen presentation pathway is a major target for immune-evasive strategies of HCMV, resulting in effective elusion of CD8-positive cytotoxic T cells (Schuren et al., 2016; Noriega et al., 2012a). At least five unique short (US) regions in the HCMV genome are known to encode proteins that specifically interfere with the expression of HLA-I molecules (van de Weijer et al., 2015). US3 retains newly synthesized HLA-I proteins in the ER and blocks tapasin-dependent peptide loading (Jones et al., 1996; Park et al., 2004; Noriega et al., 2012b). US6 interacts with the Transporter associated with Antigen Processing (TAP) and induces conformational changes of TAP that prevent ATP binding, thereby inhibiting TAP-mediated peptide translocation into the ER (Ahn et al., 1997; Hengel et al., 1997; Lehner et al., 1997; Hewitt et al., 2001). US10 specifically targets HLA-G molecules for degradation (Park et al., 2010). US2 and US11 are type 1 transmembrane ER-glycoproteins that cause retrograde transport, or dislocation, of newly synthesized HLA-I heavy chains from the ER into the cytosol for proteasomal degradation (Wiertz et al., 1996b; a; Oresic et al., 2009).

In doing so, US2 and US11 hijack the cellular protein quality control pathway in the ER that recognizes misfolded proteins and targets them for degradation via the ubiquitin-proteasome system. This reaction is referred to as ER-associated protein degradation (ERAD). At the center of this process are multiprotein complexes that combine the various functions essential to this reaction, namely substrate recognition, dislocation, ubiquitination, and degradation (Olzmann et al., 2013; Christianson et al., 2011; Preston and Brodsky, 2017; Ye et al., 2001, 2004). Although US2 and US11 both target HLA-I for degradation, they utilize distinct protein complexes. US11 uses Derlin-1 and the E3 ubiquitin ligase TMEM129 in cooperation with the E2 ubiquitin-conjugating enzymes UBE2J2 and UBE2K to dislocate HLA-I (Lilley and Ploegh, 2004; Van De Weijer et al., 2014; van den Boomen et al., 2014; Flierman et al., 2006). US2, however, does not depend on these proteins but usurps the E3 ubiquitin ligase TRC8 to mediate HLA-I downregulation (Stagg et al., 2009). On the cytosolic side, both US2 and US11 rely on the ATPase p97/VCP to shuttle HLA-I to the proteasome for degradation (Ye et al., 2005; Soetandyo and Ye, 2010). Besides HLA-I, US2 induces downregulation of multiple immunoreceptors to modulate cellular migration and immune signaling, whereas US11-mediated degradation is restricted to HLA-I (Hsu et al., 2015).

In US2-mediated degradation of HLA-I, the function of TRC8 as E3 ligase is well documented (Stagg et al., 2009; Hsu et al., 2015). However, no specific E2 ubiquitin-conjugating enzymes have been implicated in this process. Here, we constructed a lentiviral CRISPR/Cas9-based library targeting all known human E2 enzymes and used this resource to screen for E2 enzymes that regulate US2-mediated HLA-I downregulation. We identify UBE2G2 as an essential E2 enzyme for this process. Upon UBE2G2 depletion, HLA-I molecules are detected in an ER-resident US2- and TRC8-containing complex, possibly because ubiquitination may be required for extraction of the class I molecules from the ER and their subsequent degradation. Interestingly, our screen also identifies UBE2J2 as a counteracting E2 enzyme, depletion of which further downregulates HLA-I in US2-expressing cells. In line with our findings for HLA-I, the immunoreceptors integrin- $\alpha$ 1,  $\alpha$ 2 and  $\alpha$ 4, the IL12 receptor  $\beta$ 1-subunit, and thrombomodulin are also degraded by US2 in a UBE2G2-dependent manner, whereas UBE2J2 counteracts this effect. In conclusion, we show that the E2 ubiquitin-conjugating enzymes UBE2G2 and UBE2J2 are broadly involved in regulating the downregulation of immunoreceptors targeted by HCMV US2.

## **MATERIALS & METHODS**

### **Cell culture and lentiviral infection**

U937 human monocytic cells and 293T human embryonic kidney cells were obtained from ATCC (American Type Culture Collection) and grown in RPMI medium (Lonza) supplemented with glutamine (Gibco), penicillin/streptomycin (Gibco) and 10% fetal bovine serum (Biowest). For individual transductions using lentiviruses, virus was produced in 24-well plates using standard lentiviral production protocols and third-generation packaging vectors. The supernatant containing virus was harvested 3 days post transfection and stored at -80°C. For lentiviral transductions, 50  $\mu$ l supernatant containing virus supplemented with 8  $\mu$ g/mL polybrene (Santa Cruz Biotechnology) was used to infect approximately 20,000 U937 cells by spin infection at 1,000g for 2 h at 33 °C. Complete medium was added after centrifugation to reduce polybrene concentration.

### **Generation of CRISPR/Cas9-based library and selection of clonal E2 knockout cell lines**

CRISPR gRNAs and Cas9 were expressed from a lentiviral vector, as described previously (Van De Weijer et al., 2014). In short, this vector carried a CRISPR gRNA under control of a U6 promoter as well as a Cas9 gene that was N-terminally fused to a puromycin resistance cassette by means of a T2A sequence. The region immediately downstream of the U6 promoter contains a cassette with a BsmBI restriction site on each side to allow cloning of gRNA target sites followed by the gRNA scaffold and a terminator consisting of 5 T-residues. gRNAs targeting all known human E2s were designed using an online CRISPR Design Tool (<http://crispr.mit.edu/>). gRNA sequences are listed in **Supplementary Information S1**. The

genomic target site for the gRNAs used in the validation studies and/or in the generation of clonal knockout cell lines are listed in **Table 1**.

U937 cells stably co-expressing eGFP-Myc-HLA-A2 and HA-US2 or 3xST2-HA-US2 were transduced with this CRISPR/Cas9 system. Two days post infection (d p.i.), transduced cells were selected by using 2 µg/mL puromycin and allowed to recover. Additional CRISPR gRNAs targeting UBE2G2 were expressed from a pKLV lentiviral backbone containing a U6 sgRNA as well as a pGK Puro-2A-BFP cassette. This vector was expressed in THP1 cells already containing US2-IRES-mCherry with hygromycin resistance as well as Cas9 under blasticidin resistance.

Cells were single-cell sorted by fluorescence-activated cell sorting (FACS AriaII, BD Biosciences). The knockout status of the clonal cell lines was confirmed by flow cytometry and immunoblotting (UBE2G2) or genomic target site sequencing (UBE2J2). For genomic target site sequencing of UBE2J2, genomic DNA was isolated using the Quick-DNA Miniprep kit (Zymo Research), and the specific region containing the gRNA-target site was amplified by PCR using primers 5'-CCGACGTCTCTATACTGCC-3' and 5'-GGCCCTTCTGTTTTGTTCC-3'. Subsequently a nested PCR was performed using primers 5'-CCGACGTCTCTATACTGCC-3' and 5'-GACACAGCTGCAAAACGGG-3' to generate more specific PCR products. PCR products were prepared according to manufacturer's guidelines, and subjected to deep-sequencing using the MiSeq Reagent Nano Kit v2, 500 cycles. Deep sequencing data was analyzed using the Varscan algorithm and is presented in Figure S2.

gRNA	Genomic target site incl. PAM
gUBE2D3_3	GGTTGAAGGGTAGTCTGTAGG
gUBE2G2_1	GGAGAAGATCCTGCTGTCGGTGG
gUBE2J2_1	GTTGCACTTAAACCTCCCGTTGG
gTRC8	GAGGAAGATGACAGGCGTCTGG

**Table 1: Genomic target sites for gRNAs used in the validation studies and/or in the generation of clonal knockout cell lines.** PAM sites are underlined.

### Antibodies

Primary antibodies used in our studies were: mouse  $\alpha$ -HLA-I HC HC10 mAb; mouse  $\alpha$ -HLA-I HC HCA2 mAb; PE-conjugated mouse  $\alpha$ -HLA-A2 (clone BB7.2, no. 558570, BD Pharmingen); human  $\alpha$ -HLA-A3 OK2F3 mAb (LUMC, Leiden, the Netherlands); mouse  $\alpha$ -TfR H68.4 mAb (no. 13-68xx, Invitrogen); mouse  $\alpha$ -FLAG-M2 mAb (no. F1804, Sigma-Aldrich); rat  $\alpha$ -HA 3F10 mAb (no. 11867423001, Roche) rabbit anti-UBE2G2 mAb (EPR9248, no. ab174296, Abcam), rabbit anti-TRC8 pAb (H89, no. sc-68373, Santa Cruz Biotechnology), mouse  $\alpha$ -CD141 (THBD) mAb (clone 1A4, no. 559780, BD Pharmingen), mouse  $\alpha$ -CD49b (ITGA2) mAb (clone 12F1, no. 555668, BD Pharmingen), mouse  $\alpha$ -CD49d (ITGA4) mAb (clone 9F10, no. 555502, BD Pharmingen), rabbit  $\alpha$ -ITGA4 mAb (EPR1355Y, no. ab81280, Abcam), rabbit  $\alpha$ -ITGA2 mAb (EPR17338, no. ab181548, Abcam).

Secondary antibodies used were: F(ab')<sub>2</sub> goat  $\alpha$ -human IgG+IgM(H+L)-PE (no. 109-116-127, Jackson ImmunoResearch); F(ab')<sub>2</sub> goat  $\alpha$ -mouse IgG-PE (no. R0480, Dako); goat-anti-mouse-AlexaFluor647 (no. A21236, Invitrogen/Thermo); goat  $\alpha$ -mouse IgG(H+L)-HRP (no. 170-6516, Bio-Rad); goat  $\alpha$ -rabbit IgG(H+L)-HRP (no. 4030-05, Southern Biotech); mouse  $\alpha$ -rabbit IgG(L)-HRP (no. 211-032-171, Jackson ImmunoResearch); goat  $\alpha$ -mouse IgG(L)-HRP (no. 115-035-174, Jackson ImmunoResearch); goat  $\alpha$ -rat IgG(L)-HRP (no. 112-035-175, Jackson ImmunoResearch).

### **Plasmids and cDNAs**

Several different lentiviral vectors were used in the present studies. The N-terminally eGFP and Myc-tagged human HLA-A2 vector present in the lentiviral pHRSincPPT-SGW vector was kindly provided by Dr. Paul Lehner and Dr. Louise Boyle (University of Cambridge, Cambridge, UK). HCMV US2 was N-terminally tagged with either an HA-tag only, or three Strep(II) tags followed by an HA-tag. The original leader was replaced by the hCD8 leader sequence in the tagged US2 constructs. US2 and tagged variants were expressed from a dual promoter lentiviral vector, which also included expression of BlastR-T2A-mAmetrine via the hPGK promoter. For E2 rescue and overexpression experiments, gRNA-resistant HA-tagged E2 ubiquitin-conjugating enzymes were generated and cloned into a dual promoter lentiviral vector, which also included expression of ZeoR-T2A-mAmetrine via the hPGK promoter, as described previously (Van De Weijer et al., 2014). UBE2D3 and UBE2G2 were tagged N-terminally, UBE2J2 was tagged C-terminally. Catalytically inactive E2 mutants were generated using PCR-based site directed mutagenesis with primers carrying the mutation desired: UBE2D3 C85S, UBE2G2 C89S, UBE2J2 C94S. TRC8 was tagged C-terminally with a FLAG and ST2-tag. The resulting TRC8-FLAG-ST2 was still functional (Fig. S3). All constructs were verified by standard Sanger sequencing (Macrogen, The Netherlands).

### **Flow cytometry**

Cells were washed in FACS buffer (PBS containing 0.5% BSA and 0.02% sodium azide) and analyzed on a FACSCanto II (BD Bioscience). Flow cytometry data were analyzed using FlowJo software.

### **Immunoblotting**

Cells were lysed in 1% Triton X-100 lysis buffer (1.0% Triton X-100, 20 mM MES, 100 mM NaCl, 30 mM Tris, pH 7.5) containing 1 mM Pefabloc SC (Roche) and 10  $\mu$ M Leupeptin (Roche). Nuclei and cell debris were pelleted at 12,000g for 20 min at 4 °C. Post-nuclear lysates were denatured in Laemmli sample buffer and incubated at RT for 30 minutes. Proteins were separated by SDS-PAGE and transferred to PVDF membranes (Immobilon-P, Millipore). Membranes were probed with indicated antibodies. Reactive bands were detected by ECL (Thermo Scientific Pierce), and exposed to Amersham Hyperfilm ECL films (GE Healthcare).

### Co-immunoprecipitations

Cells were lysed in Digitonin lysis buffer (1% Digitonin (Calbiochem), 50 mM Tris-HCl, 5 mM MgCl<sub>2</sub>, 150 mM NaCl; pH 7.5) containing 1 mM Pefabloc SC (Roche) and 10  $\mu$ M Leupeptin (Roche). Lysates were incubated for 90 min at 4 °C. Nuclei and cell debris were pelleted 12,000g for 20 min at 4 °C. Post-nuclear supernatants were incubated overnight with StrepTactin beads (GE Healthcare). After four washes in 0.1% digitonin lysis buffer, proteins were eluted in elution buffer (2.5 mM desthiobiotin, 150 mM NaCl, 100 mM Tris-HCl, 1 mM EDTA, pH 8) for 30 min on ice. The eluate was separated from the beads using 0.45  $\mu$ m Spin-X filter column (Corning Costar), and subsequently denatured in Laemmli sample buffer containing DTT. Immunoblotting was performed as described above.

## RESULTS

### A CRISPR/Cas9 library screen identifies the E2 ubiquitin-conjugating enzyme UBE2G2 to be essential for US2-mediated HLA-I downregulation

To identify E2 ubiquitin-conjugating enzymes required for US2-mediated degradation of HLA-I molecules, we established a lentiviral CRISPR/Cas9-based library targeting all known human E2 ubiquitin-conjugating enzymes. Approximately three gRNAs were used per E2 gene. U937 monocytic cells stably expressing an HLA-A2 molecule with an N-terminal eGFP tag were generated to allow monitoring of HLA-I expression levels by flow cytometry. Upon stable introduction of HCMV US2, the chimeric HLA-I molecules as well as endogenous HLA-I proteins were degraded efficiently (Fig. 1A). These cells were then transduced with the lentiviral E2-targeting CRISPR/Cas9 library, after which eGFP-HLA-A2 expression was evaluated by flow cytometry. Disruption of an E2 gene essential for US2 activity would rescue eGFP-HLA-A2 from degradation and thus increase eGFP-HLA-A2 levels (Fig. 1B).

CRISPR gRNAs targeting UBE2D3 and UBE2G2 induced rescue of eGFP-HLA-A2 expression in US2-expressing cells (Fig. 1C). Expression of gRNAs targeting UBE2G2 induced the strongest rescue of eGFP-HLA-A2. The anti-UBE2G2 and anti-UBE2D3 gRNAs also increased the levels of endogenous HLA-A3 in these US2-expressing cells (Fig. 1D). By contrast, targeting the UBE2G2 homologue UBE2G1 with CRISPR gRNAs did not affect eGFP-HLA-A2 expression. To validate the involvement of UBE2G2 and UBE2D3, their expression was restored by introduction of gRNA-resistant E2 cDNA constructs into the gRNA-expressing cells (Fig. 1E). For both UBE2G2 and UBE2D3, reconstitution of protein expression restored US2-mediated HLA-A2-eGFP downregulation. For UBE2G2, a similar pattern was also observed for endogenous HLA-A3. On the other hand, introduction of catalytically inactive E2 mutants, in which the active cysteine was replaced with a serine, did not result in restoration of US2-mediated HLA-I downregulation. Expression of the HA-tagged wildtype (wt) and catalytically inactive (ci) E2 enzymes was confirmed by immunoblotting (Fig. 1F).

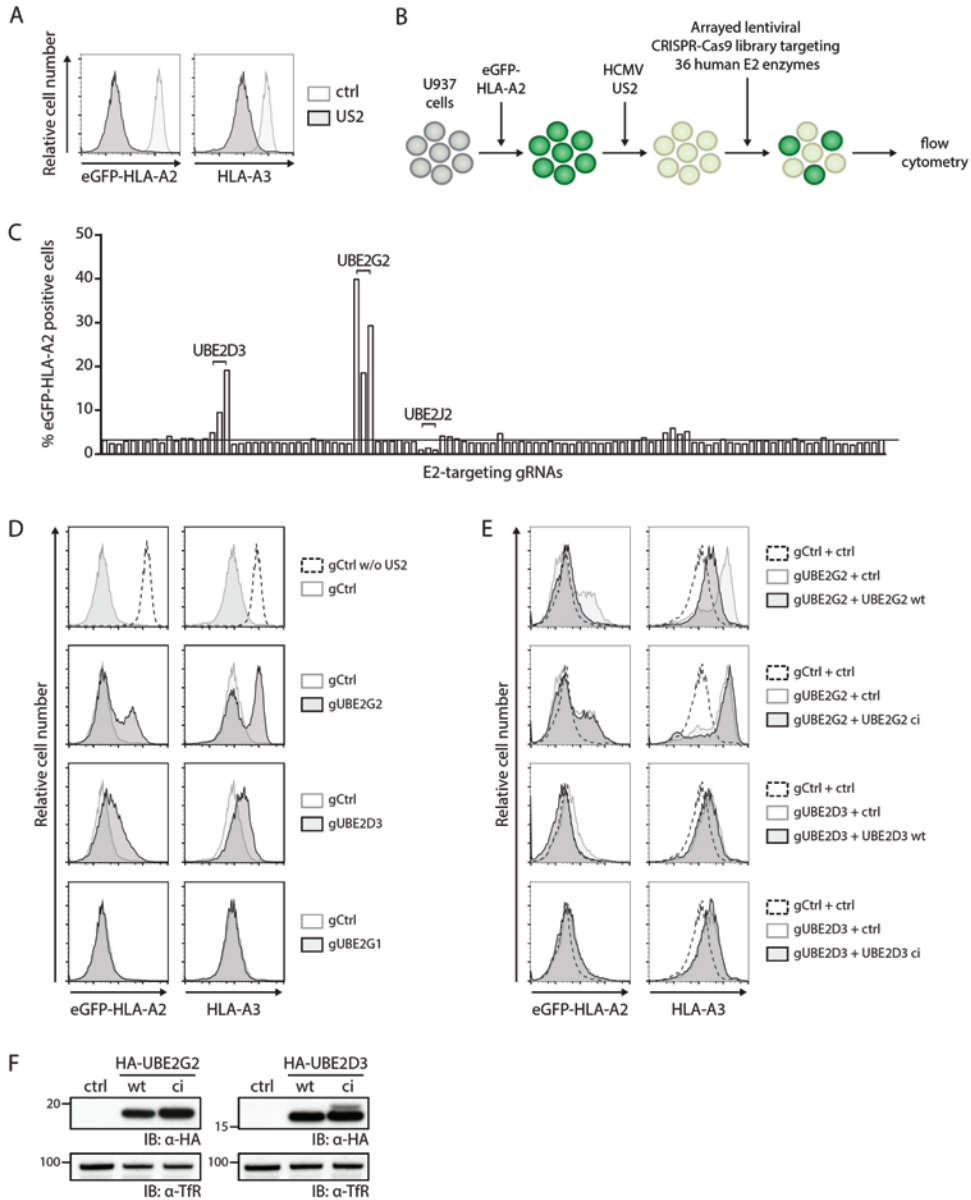


**Figure 1. A CRISPR/Cas9 library screen for E2 ubiquitin-conjugating enzymes identifies UBE2G2 and UBE2D3 as essential players in US2-mediated HLA-I downregulation.** (A) Downregulation of eGFP-HLA-A2 and endogenous HLA-A3 by US2 in U937 cells expressing eGFP-HLA-A2. (B) Schematic overview of the CRISPR/Cas9 library screen to identify E2 ubiquitin-conjugating enzymes essential for US2-mediated HLA-I downregulation. U937 cells are transduced with eGFP-HLA-A2 and subsequently transduced with an HCMV US2-expression vector. As a result, cells display low total eGFP-HLA-A2 expression levels which can be monitored by means of the eGFP tag. Subsequently, cells are lentivirally transduced with CRISPR/Cas9 constructs targeting individual E2 ubiquitin-conjugating enzymes and selected to purity using puromycin. Cells are analyzed by flow cytometry 10 d p.i. to assess total eGFP-HLA-A2

**Figure 1 (continued):** levels. (C) Quantification of the percentage eGFP-HLA-A2-positive US2-expressing cells upon transduction with CRISPR/Cas9 constructs targeting individual E2 ubiquitin-conjugating enzymes. gRNAs targeting UBE2D3, UBE2G2, and UBE2J2 are indicated. (D) CRISPR/Cas9-mediated knockout of E2 ubiquitin-conjugating enzymes UBE2G2 (gRNA #1) and UBE2D3 (gRNA #3) rescues expression of chimeric eGFP-HLA-A2 and endogenous HLA-A3 from US2-expressing cells. gRNAs targeting UBE2G1 (gRNA #1) were used as a negative control. eGFP-HLA-A2 and endogenous HLA-A3 surface levels were assessed 10 d p.i. by flow cytometry. (E) Reconstitution of UBE2G2 or UBE2D3 expression in E2 knock-out cells rescues US2-mediated downregulation of HLA-class I. Wildtype E2 (E2 wt) or a catalytically inactive E2 (E2 ci) was introduced in the corresponding polyclonal E2 knock-out cells from C), after which flow cytometry analysis was performed to assess eGFP-HLA-A2 total levels and endogenous HLA-A3 surface levels at 7 days post infection. (F) Expression of wildtype and catalytically inactive E2 ubiquitin-conjugating enzyme used in (D) was assessed via immunoblotting. Transferrin receptor (Tfr) was used as a loading control.

These results indicate that UBE2G2 and UBE2D3 affect US2-mediated degradation of HLA-I. Compared to UBE2G2, the effects of UBE2D3 depletion and reconstitution were limited, especially for the endogenous HLA-A3 molecule. Because UBE2G2 has a stronger effect on HLA-I rescue, mechanistic experiments in this study will focus on this E2 enzyme.

#### **The E2 ubiquitin conjugase UBE2J2 counteracts US2-mediated HLA-I downregulation**

In contrast to UBE2G2 and UBE2D3, we noticed that targeting UBE2J2 with CRISPR gRNAs resulted in a further downregulation of eGFP-HLA-A2 (Fig. 1C) and endogenous HLA-A3 expression (Fig. 2A). The window to assess reduced eGFP-HLA-A2 levels was low, as US2 downregulates the chimeric eGFP-HLA-A2 molecule to near background levels (Fig. 1A). Downregulation of the endogenous HLA-A3 by US2 was less potent (Fig. 1A), allowing us to study the effect of UBE2J2 depletion in more detail. Indeed, gRNAs targeting UBE2J2 further decreased HLA-A3 levels (Fig. 2B). Depletion of the UBE2J2 homologue UBE2J1 did not affect HLA-A3 expression (Fig. 2B). Reconstitution of wildtype UBE2J2 (wt) expression abolished the enhanced downregulation of HLA-A3 molecules (Fig. 2C, left panel), showing that the gRNA effect was specific for UBE2J2. Expression of the exogenous UBE2J2 even resulted in slightly less downregulation of HLA-A3 by US2 (Fig. 2C, left panel), which could be due to overexpression of the cDNA. In US2-expressing cells with intact endogenous UBE2J2, introduction of this UBE2J2 cDNA increased HLA-A3 expression in a similar manner (Fig. 2D, left panel). These findings indicate that UBE2J2 counteracts US2-mediated downregulation of HLA-I.

Reconstitution with a catalytically inactive UBE2J2 (ci) or a UBE2J2 mutant lacking its transmembrane domain ( $\Delta$ TMD) did not counteract the enhanced HLA-I downregulation (Fig. 2C, middle and right panels). These results indicated that catalytic activity is required for this phenotype. Expression of the catalytically inactive mutant in the absence of gRNAs further stimulated US2-mediated HLA-A3 downregulation (Fig. 2D, middle panel), mimicking the phenotype of CRISPR/Cas9-mediated UBE2J2 disruption. This indicates that the catalytically inactive UBE2J2 acts as a dominant negative mutant. Expression of the soluble mutant ( $\Delta$ TMD) did not affect HLA-A3 expression levels (Fig. 2D, right panel). The expression levels

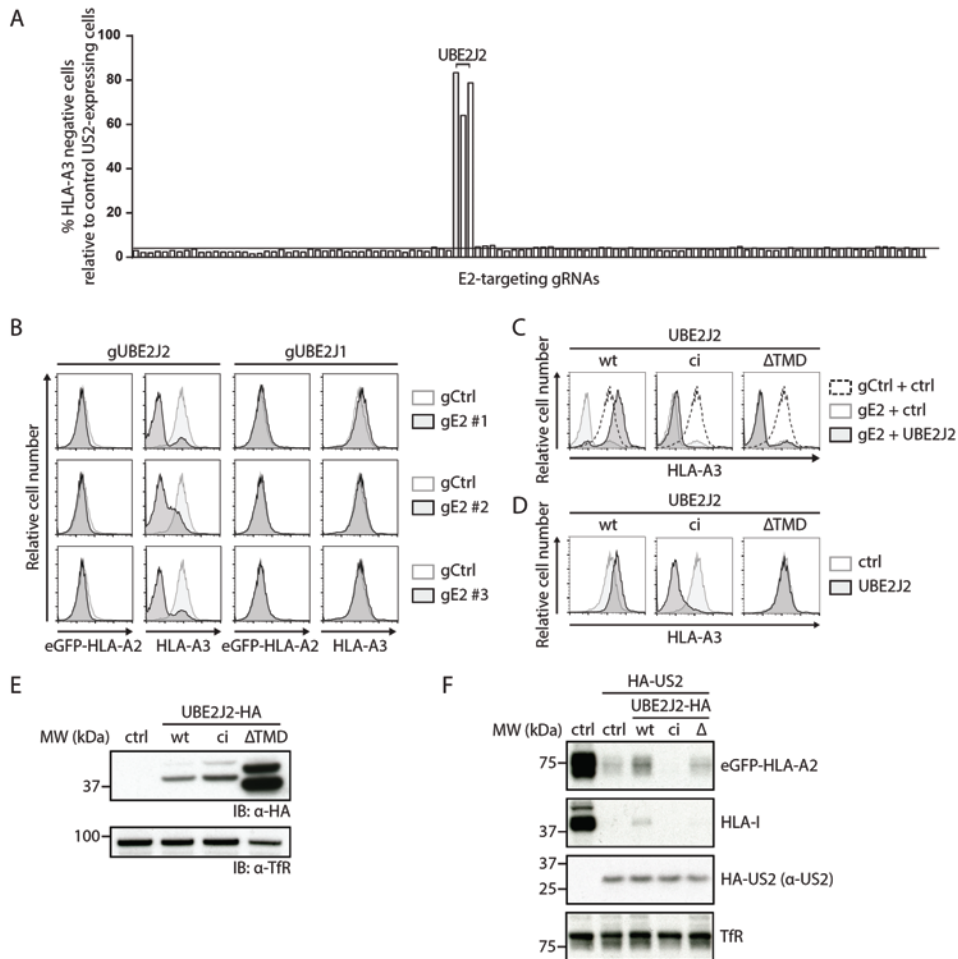


**Figure 2. UBE2J2 counteracts US2-mediated HLA-I downregulation.** (A) Quantification of the percentage of cells expressing enhanced downregulation of HLA-A3 upon transduction with CRISPR/Cas9 constructs targeting individual E2 ubiquitin-conjugating enzymes. gRNAs targeting UBE2J2 are indicated. (B) CRISPR/Cas9-mediated knockout of UBE2J2 decreases endogenous HLA-A3 surface expression in US2-expressing cells. The homologues UBE2J1 is shown as a negative control. Endogenous HLA-A3 surface levels were assessed 10 d p.i. by flow cytometry. (C) Reconstitution of UBE2J2 expression in UBE2J2 knock-out cells rescues HLA-I from enhanced US2-mediated downregulation. Wildtype UBE2J2 (E2 wt), catalytically inactive UBE2J2 (E2 ci), or soluble UBE2J2 (E2 ΔTMD) was introduced in knock-out cells from B) (gRNA #1), after which flow cytometry analysis was performed to assess endogenous HLA-A3 surface levels at 7 days post-infection. (D) Ectopic expression of UBE2J2 increases HLA-A3 expression. Wildtype UBE2J2 (E2 wt), catalytically inactive UBE2J2 (E2 ci), or soluble UBE2J2 (E2 ΔTMD) was ectopically expressed in cells similar to those from B), but lacking a gRNA targeting UBE2J2. Endogenous HLA-A3 surface levels were assessed using flow cytometry. (E) Expression of wildtype, catalytically inactive, and TMD-less UBE2J2 used in (C) and (D) as assessed by immunoblotting. Transferrin receptor was used as a loading control. (F) Lysates of U937 cells expressing either wildtype UBE2J2 (wt), catalytically inactive UBE2J2 (ci), or soluble UBE2J2 (Δ) were prepared and immunoblotted for the indicated proteins.



of wt, ci and soluble UBE2J2 were confirmed by immunoblotting (Fig. 2E). The effect of UBE2J2 counteracting US2-mediated HLA-I degradation was not caused by directly affecting US2 expression, as introduction of wildtype, catalytically inactive, or TMD-less UBE2J2 did not alter US2 levels (Fig. 2F). Taken together, our data indicate that UBE2J2 counteracts US2-mediated downregulation of HLA-I through a mechanism that relies on its catalytic activity.

### **Depletion of UBE2G2 accumulates HLA-I in the US2-TRC8 complex**

Next, we investigated the effect of UBE2G2 and UBE2J2 depletion on the composition of the US2 ERAD complex. To this end, clonal UBE2G2- and UBE2J2-null cell lines were established (Fig. S1). Removal of UBE2G2 in these cells caused a growth defect, but was not lethal. HLA-I levels were increased in UBE2G2-null cells as compared to control cells (Fig. 3A, lane 1 and 2 vs lane 5), which was in agreement with the flow cytometry results from Fig. 1C. Also, US2 protein levels were increased, likely due to the stabilization of the US2 ERAD complex in the absence of UBE2G2.

In line with our previous results, immunoblot analysis for UBE2J2-null cells revealed that HLA-I levels were further decreased as compared to control cells (Fig. 3A, lanes 3 and 4 vs lane 5). US2 protein levels were comparable to control conditions (lane 3) or slightly elevated (lane 4), suggesting that the strong increase in HLA-I degradation upon UBE2J2 knockout was not caused by increased US2 levels.

To investigate the effects of UBE2G2 and UBE2J2 depletion on the composition of the US2 ERAD complex, US2 was immunoprecipitated from cell lysates prepared using digitonin, which preserves most membrane protein complexes. The E3 ubiquitin ligase TRC8 is part of this ERAD complex and is essential for HLA-I downregulation by US2 (Stagg et al., 2009). Knocking out TRC8 rescues US2-associated HLA-I (Fig. 3B, lanes 1-3 vs 10). In UBE2G2-null cells, HLA-I co-precipitated with US2 as well (lanes 4-6). Also, increased amounts of TRC8 were co-precipitated from UBE2G2-null cells as compared to control cells (lane 10). Overall US2 expression varied slightly per condition and seemed higher in UBE2G2-null cells. Our data suggest that the US2-TRC8 ERAD complex is stabilized in the absence of UBE2G2, accumulating HLA-I prior to their dislocation from the ER membrane.

### **UBE2J2 counteracts HLA-I degradation by US2 via downregulation of TRC8**

Upon UBE2J2 knockout (Fig. 3B, lanes 7-9), HLA-I was not detectable in the US2-TRC8 complex, consistent with the observation that HLA-I degradation is enhanced in these cells. Intriguingly, the amount of TRC8 present in the complex was increased upon UBE2J2 knockout (Fig. 3B, lanes 7-9) compared to control cells (lane 10), while US2 levels were elevated only slightly. This suggests that depletion of UBE2J2 may increase TRC8 levels. Because TRC8 is the rate-limiting factor for US2-mediated HLA-I degradation (Van den Boomen and Lehner, 2015), this TRC8 increase would explain the enhanced HLA-I downregulation. To investigate this, we assessed TRC8 levels in UBE2J2 KO cells by direct quantitative immunoprecipitation

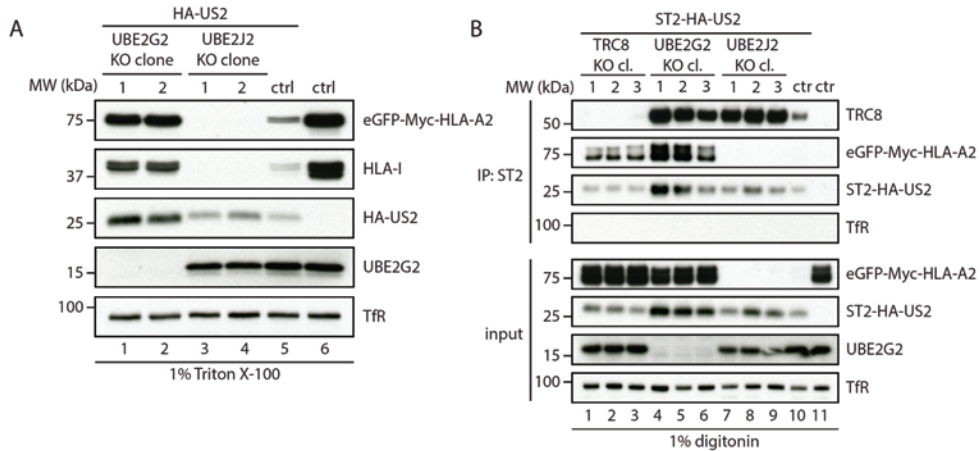


**Figure 3. Loss of UBE2G2 locks the US2-TRC8 complex in a dislocation-incompetent state.** (A) Two independent knockout clones of either UBE2G2 or UBE2J2 were established in U937 cells co-expressing eGFP-HLA-A2 and HA-US2. These clones were subjected to immunoblot analysis to assess expression levels of the indicated proteins. (B) Strep(II)-HA-tagged US2 was immunoprecipitated by using StrepTactin beads from 1.0% digitonin lysates of TRC8 (lane 1-3), UBE2G2 (lane 4-6) or UBE2J2 (lane 7-9) were knocked out. US2-expressing U937 eGFP-HLA-A2 cells without knockout (lane 9) and cells without US2 (lane 10) were used as controls. Immunoprecipitated complexes were eluted using d-Desthiobiotin, after which immunoblot analysis was performed to detect the indicated proteins.

of TRC8 (Fig. 4A), as the ligase could not be detected in lysate directly. Indeed, in US2-expressing cells, TRC8 expression levels were increased upon UBE2J2 knockout compared to control conditions (Fig. 4A). A minor increase in TRC8 expression could be observed in cells without US2 as well (Fig. S4A, lane 3 vs 4).

We observed a similar increase in TRC8 expression in US2 cells expressing catalytically inactive UBE2J2 (Fig. 4B). These cells show stronger HLA-I downregulation compared to US2 alone (Fig. 2C). Again, TRC8 expression was also elevated in cells without US2 (Fig. S4B, lane 4 vs 2), indicating that the effect of UBE2J2 on TRC8 is independent of US2. Expression levels of US2 (Fig. S4A and S4B) and UBE2G2 (Fig. 4C, S4A and S4B) were not clearly affected by expression of catalytically inactive or wildtype UBE2J2 constructs.

Catalytically inactive UBE2J2 not only raised total TRC8 expression, but also resulted in increased TRC8 levels present in the ERAD complex immunoprecipitated via US2 (Fig. 4C, lane 12 vs 10). On the contrary, exogenous expression of wildtype UBE2J2 (lane 11 vs 10) caused decreased TRC8 association. Thus, UBE2J2 depletion or the expression of catalytically inactive UBE2J2 increases TRC8 expression levels, which in turn enhances US2-mediated HLA-I downregulation.

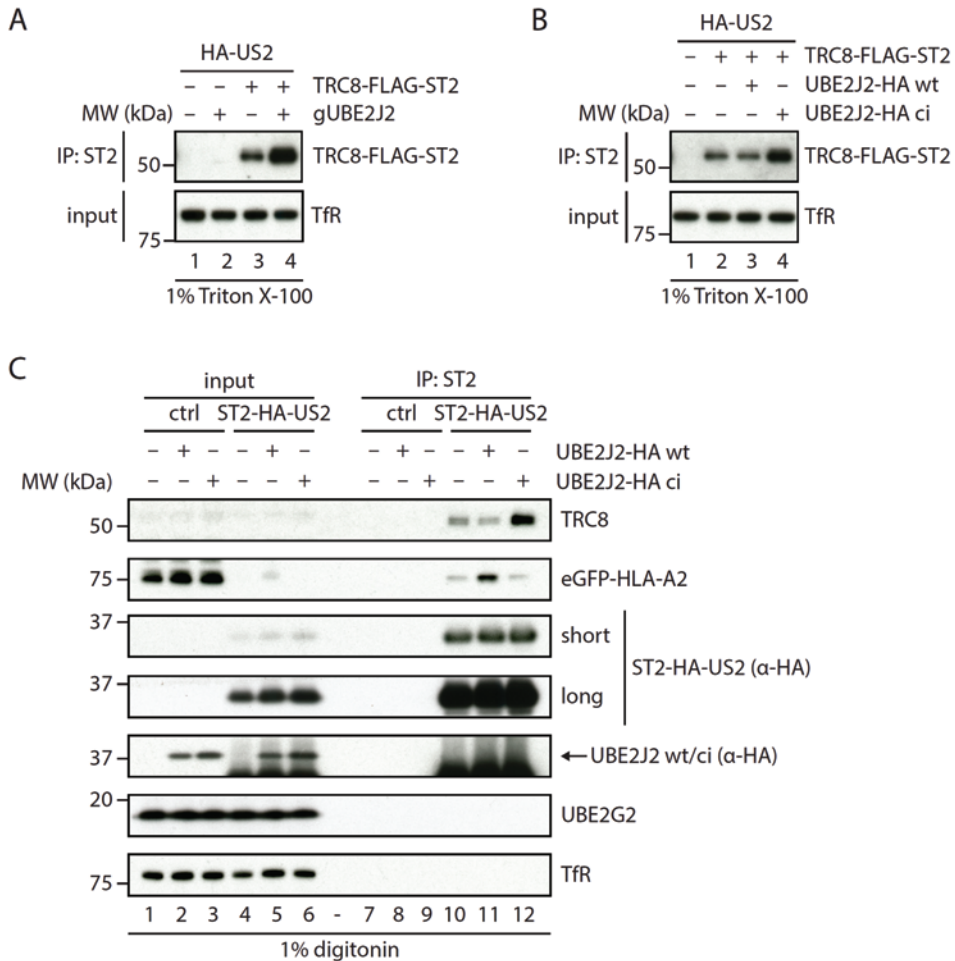


**Figure 4. Impaired UBE2J2 function enhances HLA-I downregulation by US2 via upregulation of TRC8.** (A) US2-expressing TRC8 KO cells were transduced with TRC8-Flag-ST2 or a control vector. To these cells, UBE2J2-targeting CRISPR gRNAs or empty vector were added. TRC8 levels were assessed by direct immunoprecipitation. Upon UBE2J2 knockout, the expression of TRC8 increases. (B) US2-expressing TRC8 KO cells were transduced with TRC8-Flag-ST2 or a control vector. To these cells, cDNA of wildtype (wt) or catalytically inactive (ci) HA-tagged UBE2J2 or a control vector were added. TRC8 levels were assessed by direct immunoprecipitation. Upon expression of ci UBE2J2, the expression of TRC8 increases compared to control cells without HA-UBE2J2 or cells with wildtype HA-UBE2J2. (C) Catalytically inactive UBE2J2 increases TRC8 levels in the US2 ERAD complex. A control vector, a vector expressing wildtype UBE2J2 (wt) or catalytically inactive UBE2J2 (ci) was transduced in U937 cells expressing eGFP-HLA-A2 and ST2-HA-US2. After G418 selection, cells were lysed in 1.0% digitonin lysis buffer, after which ST2-HA-US2 was immunoprecipitated using StrepTactin beads. Immunoprecipitated complexes were eluted using d-Desthiobiotin, after which immunoblot analysis was performed for the proteins indicated.

**Degradation of immunoreceptors by US2 is dependent on UBE2G2 and counteracted by UBE2J2**

HCMV US2-mediated protein degradation is not limited to HLA-I; US2 also modulates the expression of various other cell surface receptors, including integrin- $\alpha$ 2 (ITGA2), integrin- $\alpha$ 4 (ITGA4) and thrombomodulin (THBD) (Hsu et al., 2015). Similar to HLA-I, the degradation of these cell surface receptors is catalyzed by the E3 ubiquitin ligase TRC8 (Hsu et al., 2015). We tested whether the degradation of these cell surface receptors by US2 is also dependent on UBE2G2, and whether their downregulation can be counteracted by UBE2J2. Indeed, TRC8 and UBE2G2 depletion restored the surface expression of these receptors in US2-expressing U937 and THP-1 cells (Fig. 5A and 5B), whereas UBE2J2 depletion further decreased the expression compared to control US2-expressing cells (Fig 5A and 5B). When looking at HLA-I downregulation, we noticed a difference between the two cell lines used. In contrast to U937 cells, which express the HLA-A3 allele, the HLA-A2-expressing THP-1 cells displayed only partial rescue of this HLA-A protein upon introduction of anti-UBE2G2 gRNAs. Other US2 substrates, including integrin  $\alpha$ 1 (ITGA1), ITGA2, ITGA4, the IL12 receptor  $\beta$ 1-subunit (IL12R-B1), and thrombomodulin were upregulated more potently in the THP-1 cells (Fig. 5B and C). The elevated expression of HLA class I, ITGA2, ITGA4 and THBD upon UBE2G2 knockout was confirmed by immunoblotting (Fig. 5D). Thus, UBE2G2 and UBE2J2 not only regulate US2-induced downregulation of HLA-I, but also of other cell surface receptors, including several integrins and thrombomodulin.

**DISCUSSION**

HCMV US2 facilitates proteasomal degradation of HLA-I and various other immunoreceptors through a pathway that is poorly characterized (Wiertz et al., 1996b; Stagg et al., 2009; Hsu et al., 2015). Here, we identify multiple E2 ubiquitin-conjugating enzymes involved in US2-mediated immunoreceptor downregulation. Knocking out UBE2G2 in US2-expressing cells using the CRISPR/Cas9 system rescues HLA-I expression. Loss of UBE2G2 stabilizes HLA-I in a complex also containing US2 and TRC8, suggesting that UBE2G2 is required for dislocation to occur. We were unable to show association of UBE2G2 with the US2-TRC8 complex, possibly due to the weak and transient nature of the interaction between E2 ubiquitin-conjugating enzymes and the E3 ubiquitin ligases *in vivo*, as has been reported for other E2-E3 interactions (Duncan et al., 2010; Kleiger et al., 2009; Yin et al., 2009).

In our CRISPR/Cas9 screen we noticed that the knockout of a second E2 enzyme, UBE2D3, also rescued HLA-I. UBE2D3 appears to be an essential gene for U937 cell survival, as we were not able to establish clonal knockout cell lines. UBE2D3 depletion only moderately counteracted US2-mediated HLA-I downregulation in U937 cells, although this low rescue may have been impacted by the lethality of knocking out this E2 enzyme.

Our studies consistently demonstrated a partial rescue of HLA-A2 upon depletion of

UBE2G2; HLA-A3, as well as other US2 substrates were rescued more strongly. Especially when HLA-A-specific antibodies were used in cell lines that carry a single HLA-A locus product, this difference was apparent. The weaker rescue phenotype observed for HLA-A2 suggests that another E2 enzyme, possibly UBE2D3, may contribute to the downregulation of this HLA protein.

Previous functional studies have associated UBE2G2 with several ER-resident E3 ubiquitin ligases. For example, UBE2G2 interacts with HRD1 (Kikkert et al., 2004) and TEB4 (Hassink et al., 2005) to promote K48-linked polyubiquitination *in vitro*. The E3 ligase gp78

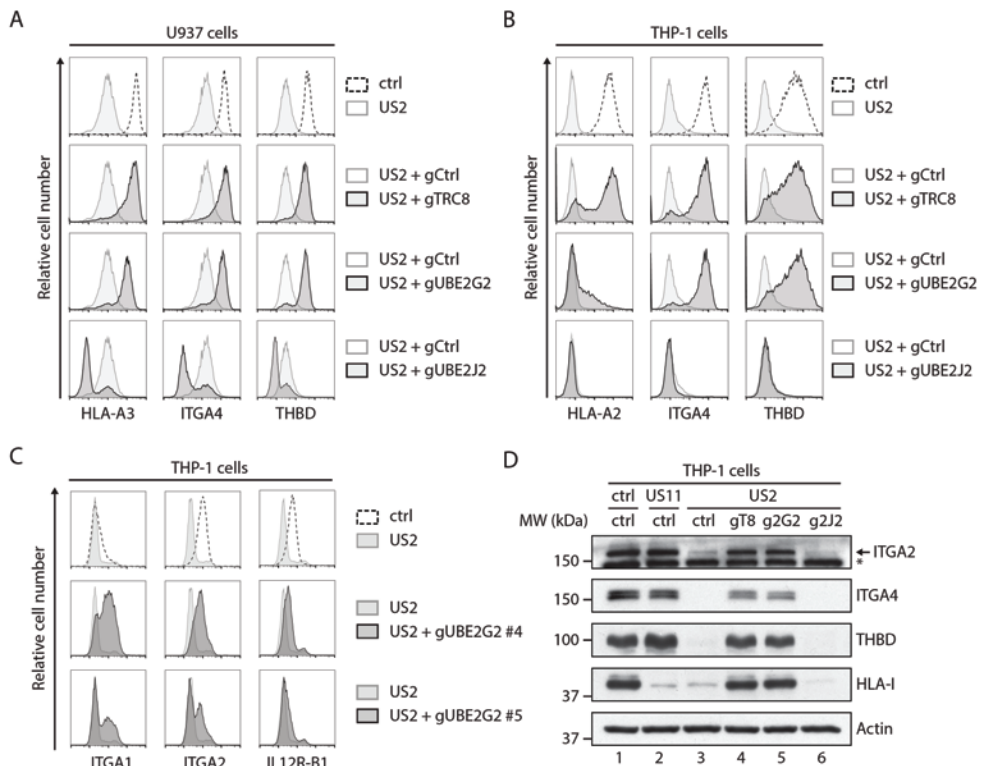


**Figure 5. UBE2G2 and UBE2J2 regulate US2-induced immunoreceptor downregulation.** (A&B) U937 (A) or THP-1 (B) cells expressing US2 were lentivirally transduced with a CRISPR/Cas9 vector targeting TRC8 (gRNA #1), UBE2G2 (gRNA #1) and UBE2J2 (gRNA #1). Two days after infection, gRNA-expressing cells were selected using puromycin. Cell surface expression of integrin-alpha4 (ITGA4), thrombomodulin (THBD), and HLA-I (HLA-A2 for THP-1 cells, HLA-A3 for U937 cells) was assessed by flow cytometry at 10 days (U937) or 15 days (THP-1) post infection. (C) THP-1 cells expressing US2 were lentivirally transduced with two CRISPR gRNAs (#4 and #5) targeting UBE2G2. 2 days after infection, gRNA-expressing cells were selected using Puromycin, and expression of integrin  $\alpha$ 1 (ITGA1), integrin  $\alpha$ 2 (ITGA2) or IL12 receptor  $\beta$ 1-subunit (IL12R-B1) was assessed by flow cytometry at 7 days post infection. (D) Lysates from cells used in (B) were prepared and subjected to immunoblotting analysis for total protein expression levels of ITGA2, ITGA4, thrombomodulin, and HLA-I (HCA2). US11-expressing cells were included as a control. Actin was used as a loading control. The asterisk marks an unspecific band.

also cooperates with UBE2G2 (Liu et al., 2014). A dedicated UBE2G2-binding region (G2BR) has been identified for gp78 that increases its affinity for UBE2G2 by approximately 50-fold. The strong interaction between gp78 and UBE2G2 allows for efficient ubiquitination and degradation of the CD3 $\delta$  subunit (Das et al., 2009; Chen et al., 2006). Both gp78 and HRD1 act with UBE2G2 to catalyze cholera toxin dislocation (Bernardi et al., 2010). UBE2G2 has also been proposed to be involved in the turnover of HMGCR (Miao et al., 2010). HMGCR degradation is facilitated by the E3 ligases gp78 (Jo et al., 2013, 2011) and TRC8 (Chen et al., 2006; Jo et al., 2011) as well as the UBE2G2-recruiting protein AUP1 (Jo et al., 2013). Although this suggests that UBE2G2 cooperates with the E3s TRC8 and gp78 to facilitate degradation of HMGCR, a direct role for UBE2G2 has not been established in these studies. Our data show that UBE2G2 is a crucial player in US2-induced dislocation of HLA-I as well as degradation of other immunoreceptors, all of which also require the E3 ubiquitin ligase TRC8 (Stagg et al., 2009). We therefore propose that TRC8 and UBE2G2 indeed cooperate in ubiquitinating ERAD substrates.

Surprisingly, we identify UBE2J2 to counteract US2-induced HLA-I degradation. When knocking out UBE2J2, we observed an unexpected further downregulation of eGFP-HLA-A2 as well as endogenous HLA-A3. This phenotype is reverted upon reconstitution of UBE2J2 expression by means of cDNA expression. In contrast to UBE2G2, little is known on the tail-anchored E2 ubiquitin-conjugating enzyme UBE2J2 and its role in protein degradation. Its murine homologue plays a role in ERAD of unassembled T-cell receptor subunits (Tiwari and Weissman, 2001).

Interestingly, UBE2J2 has previously been described to be involved in MHC class I downregulation in the context of herpesviral infection. During infection with gamma-herpesvirus 68 ( $\gamma$ -HV68), UBE2J2 is recruited by the viral murine K3 (mK3) E3 ubiquitin ligase and facilitates the degradation of murine MHC class I molecules (Wang et al., 2009). The HCMV protein US11 also cooperates with UBE2J2 to downregulate HLA-I. Similar to US2, US11 causes accelerated ER-associated degradation of HLA-I, but the proteins do so by different degradation pathways. US11 acts in concert with the cellular E3 ubiquitin ligase TMEM129 and recruits UBE2J2 to ubiquitinate and dislocate HLA-I from the ER membrane (Van De Weijer et al., 2014; van den Boomen et al., 2014). How UBE2J2 balances HLA-I downregulation during HCMV infection, in which both the UBE2J2-dependent US11 as well as the UBE2J2-counteracted US2 are present, is currently unknown.

The counteracting effect of UBE2J2 on US2-mediated HLA-I degradation may be related to downregulation of the ubiquitin E3 ligase TRC8. We observe increased levels of TRC8 in both clonal UBE2J2 knockout cells and cells expressing catalytically inactive UBE2J2. TRC8 is a crucial player in US2-mediated ERAD, not only for HLA-I degradation (Stagg et al., 2009), but also for degradation of other cell surface receptors, including  $\alpha$ - and  $\beta$ -integrins, the NK cell activating receptor CD112, trombosmodulin, and the IL-12 receptor  $\beta$ 1 subunit (Hsu et al., 2015). In the absence of US2, UBE2J2 depletion or expression of a catalytically inactive

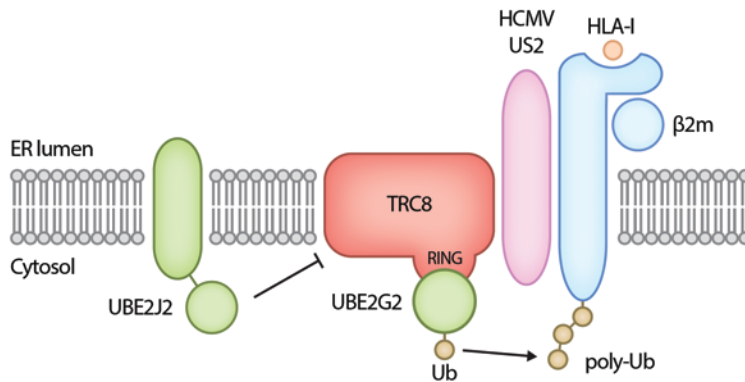


**Figure 6. Schematic overview of the ubiquitination step in US2-mediated HLA-I downregulation.** US2 engages  $\beta$ 2m-associated HLA-I and directs it to the E3 ubiquitin ligase TRC8. In cooperation with UBE2G2, TRC8 facilitates polyubiquitination of HLA-I. Next, p97 catalyzes the extraction from the ER-membrane into the cytosol for proteasomal degradation. UBE2J2 depletion increases TRC8 expression levels in the presence of US2, and in this way enhances US2-mediated HLA-I downregulation.

UBE2J2 also results in increased TRC8 expression levels, indicating that UBE2J2 might play a general role in the turnover of TRC8. We thus propose that the increased downregulation of HLA-I upon UBE2J2 depletion is primarily caused by increased TRC8 levels in these cells (Fig. 6). Expression of a catalytically inactive UBE2J2 mutant also enhances HLA-I downregulation, mimicking the UBE2J2 knockout phenotype. These results suggest that the catalytic activity of UBE2J2 is required for the downregulation of TRC8 and hence for the increased HLA-I downregulation.

Remarkably, expression of US2 alone was sufficient to induce a dramatic decrease in TRC8 levels. This observation suggests that US2 also induces degradation of TRC8. This reaction is potentially aided by UBE2J2. Why US2 limits TRC8 expression while it relies on this E3 ligase to dispose of HLA-I and other immunoreceptors remains to be determined.

Counteracting mechanisms such as TRC8 downregulation by UBE2J2 and US2 highlight an interesting regulatory pathway in which ERAD factors themselves influence turnover of the ERAD- and ER stress machinery. A similar phenomenon has been described for HERP, a key organizer of ERAD complexes in the ER (Leitman et al., 2014). HERP is upregulated under ER stress, when the unfolded protein response (UPR) is activated. Once stress is relieved, HERP levels are reduced again via ERAD, in this case via UBE2G2- and gp78-mediated ubiquitination (Yan et al., 2014). IRE1 $\alpha$ , a sensor for the unfolded protein response, is also upregulated under conditions of ER stress. This ER-resident transmembrane protein is degraded by an ERAD complex centered around the E3 ubiquitin ligase HRD1, in complex with SEL1L (Sun et al., 2015). For TRC8, no such downregulation has been described to date, although this E3 ligase is known to catalyze auto-ubiquitination and cause its own

downregulation upon sterol abundance (Lee et al., 2010). The existence of negative feedback loops in the life cycle of ERAD- and ER stress-related factors underlines the complexity of these protein turnover pathways. The present study sheds light on the regulation of HCMV-induced immunoreceptor degradation, as well as a feedback loop within this ERAD pathway, a process that involves a multitude of acting and counteracting E2 ubiquitin conjugating enzymes.

## ACKNOWLEDGEMENTS

We thank Jasper Soppe, Ferdy van Diemen and Luan Nguyen from the Medical Microbiology department at UMC Utrecht for their assistance in deep sequencing. A.B.C.S. is funded by the Graduate Programme of the Netherlands Organisation for Scientific Research (NWO) with project number 022.004.018, and by a Wellcome Trust PRF (Principal Research Fellowship) to P.J.L. with grant no. 101835/Z/13/Z. The authors declare no competing financial interests.

Author contributions: M.L. van de Weijer and A.B.C. Schuren conceived the project, designed experiments, analyzed data, wrote, and edited the paper. D.J.H. van den Boomen performed experiments and analyzed data. A. Mulder and F.H.J. Claas designed and generated reagents. P.J. Lehner analyzed data. R.J. Lebbink and E.J.H.J. Wiertz analyzed data and edited the paper.

## ABBREVIATIONS

CRISPR = clustered regularly interspaced palindromic repeats

ERAD = ER-associated protein degradation

HCMV = human cytomegalovirus

HLA = human leukocyte antigen

ITGA = integrin alpha

THBD = thrombomodulin

TMD = transmembrane domain

US = unique short

## REFERENCES

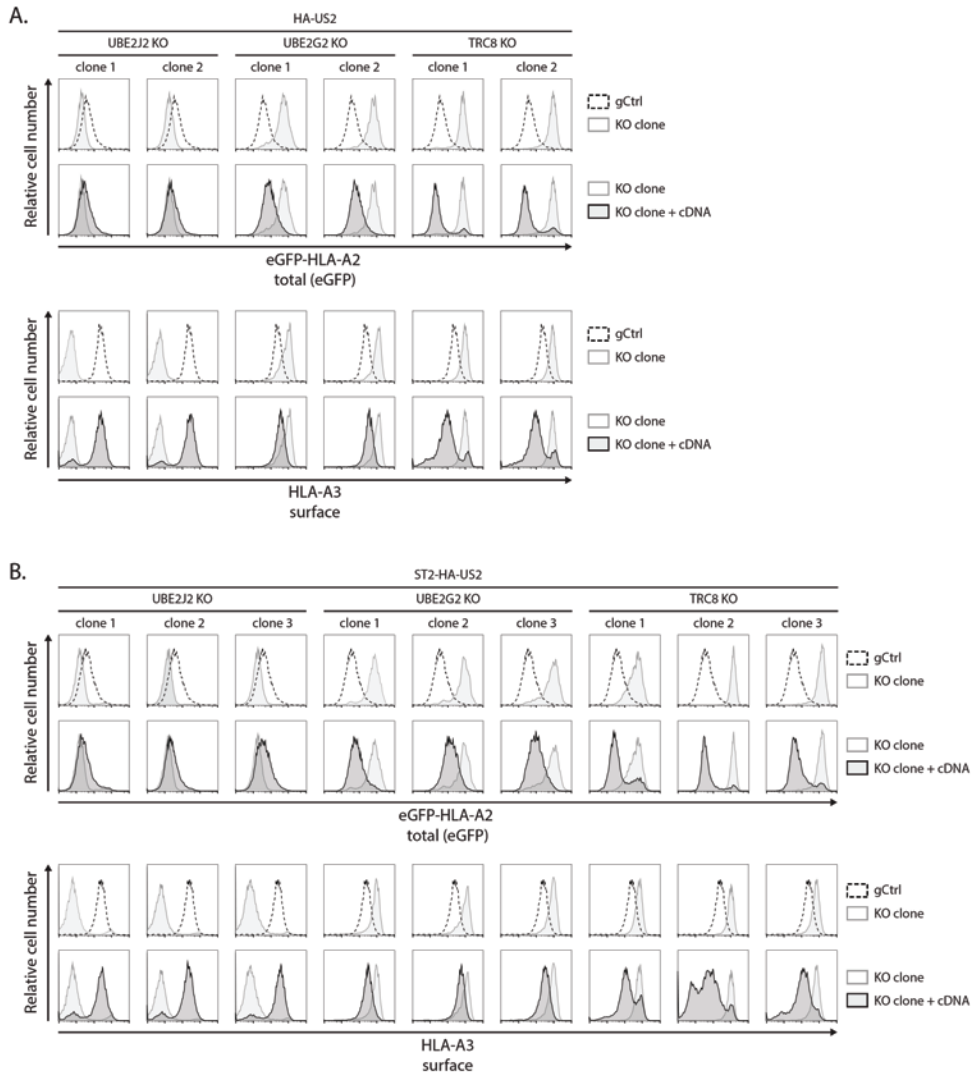
- Ahn, K., A. Gruhler, B. Galocha, T.R. Jones, E.J. Wiertz, H.L. Ploegh, P.A. Peterson, Y. Yang, and K. Früh. 1997. The ER-luminal domain of the HCMV glycoprotein US6 inhibits peptide translocation by TAP. *Immunity*. 6:613–21.
- Bernardi, K.M., J.M. Williams, M. Kikkert, S. van Voorden, E.J. Wiertz, Y. Ye, and B. Tsai. 2010. The E3 ubiquitin ligases Hrd1 and gp78 bind to and promote cholera toxin retro-translocation. *Mol. Biol. Cell*. 21:140–51. doi:10.1091/mbc.E09-07-0586.
- Van den Boomen, D.J.H., and P.J. Lehner. 2015. Identifying the ERAD ubiquitin E3 ligases for viral and cellular targeting of MHC class I. *Mol. Immunol.* 68:106–111. doi:10.1016/j.molimm.2015.07.005.



- van den Boomen, D.J.H., R.T. Timms, G.L. Grice, H.R. Stagg, K. Skødt, G. Dougan, J.A. Nathan, and P.J. Lehner. 2014. TMEM129 is a Derlin-1 associated ERAD E3 ligase essential for virus-induced degradation of MHC-I. *Proc. Natl. Acad. Sci. U. S. A.* 111:11425–30. doi:10.1073/pnas.1409099111.
- Chen, B., J. Mariano, Y.C. Tsai, A.H. Chan, M. Cohen, and A.M. Weissman. 2006. The activity of a human endoplasmic reticulum-associated degradation E3, gp78, requires its Cue domain, RING finger, and an E2-binding site. *Proc. Natl. Acad. Sci. U. S. A.* 103:341–6. doi:10.1073/pnas.0506618103.
- Christianson, J.C., J. a Olzmann, T. a Shaler, M.E. Sowa, E.J. Bennett, C.M. Richter, R.E. Tyler, E.J. Greenblatt, J.W. Harper, and R.R. Kopito. 2011. Defining human ERAD networks through an integrative mapping strategy. *Nat. Cell Biol.* 14:93–105. doi:10.1038/ncb2383.
- Das, R., J. Mariano, Y.C. Tsai, R.C. Kalathur, Z. Kostova, J. Li, S.G. Tarasov, R.L. McFeeters, A.S. Altieri, X. Ji, R.A. Byrd, and A.M. Weissman. 2009. Allosteric activation of E2-RING finger-mediated ubiquitylation by a structurally defined specific E2-binding region of gp78. *Mol. Cell.* 34:674–85. doi:10.1016/j.molcel.2009.05.010.
- Duncan, L.M., J. a. Nathan, and P.J. Lehner. 2010. Stabilization of an E3 Ligase–E2–Ubiquitin Complex Increases Cell Surface MHC Class I Expression. *J. Immunol.* 184:6978–6985. doi:10.4049/jimmunol.0904154.
- Dunn, W., C. Chou, H. Li, R. Hai, D. Patterson, V. Stolc, H. Zhu, and F. Liu. 2003. Functional profiling of a human cytomegalovirus genome. *Proc. Natl. Acad. Sci. U. S. A.* 100:14223–8. doi:10.1073/pnas.2334032100.
- Flierman, D., C.S. Coleman, C.M. Pickart, T.A. Rapoport, and V. Chau. 2006. E2-25K mediates US11-triggered retro-translocation of MHC class I heavy chains in a permeabilized cell system. *Proc. Natl. Acad. Sci. U. S. A.* 103:11589–94. doi:10.1073/pnas.0605215103.
- Griffiths, P., I. Baraniak, and M. Reeves. 2015. The pathogenesis of human cytomegalovirus. *J. Pathol.* 235:288–97. doi:10.1002/path.4437.
- Hansen, S.G., C.J. Powers, R. Richards, A.B. Ventura, J.C. Ford, D. Siess, M.K. Axthelm, J.A. Nelson, M.A. Jarvis, L.J. Picker, and K. Früh. 2010. Evasion of CD8+ T cells is critical for superinfection by cytomegalovirus. *Science.* 328:102–6. doi:10.1126/science.1185350.
- Hassink, G., M. Kikkert, S. van Voorden, S.-J. Lee, R. Spaapen, T. van Laar, C.S. Coleman, E. Bartee, K. Früh, V. Chau, and E. Wiertz. 2005. TEB4 is a C4HC3 RING finger-containing ubiquitin ligase of the endoplasmic reticulum. *Biochem. J.* 388:647–55. doi:10.1042/BJ20041241.
- Hengel, H., J.O. Koopmann, T. Flohr, W. Muranyi, E. Goulmy, G.J. Hämmerling, U.H. Koszinowski, and F. Momburg. 1997. A viral ER-resident glycoprotein inactivates the MHC-encoded peptide transporter. *Immunity.* 6:623–32.
- Hewitt, E.W., S.S. Gupta, and P.J. Lehner. 2001. The human cytomegalovirus gene product US6 inhibits ATP binding by TAP. *EMBO J.* 20:387–96. doi:10.1093/emboj/20.3.387.
- Hsu, J.-L., D.J.H. van den Boomen, P. Tomasec, M.P. Weekes, R. Antrobus, R.J. Stanton, E. Ruckova, D. Sugrue, G.S. Wilkie, A.J. Davison, G.W.G. Wilkinson, and P.J. Lehner. 2015. Plasma membrane profiling defines an expanded class of cell surface proteins selectively targeted for degradation by HCMV US2 in cooperation with UL141. *PLoS Pathog.* 11:e1004811. doi:10.1371/journal.ppat.1004811.
- Jo, Y., I.Z. Hartman, and R.A. DeBose-Boyd. 2013. Ancient ubiquitous protein-1 mediates sterol-induced ubiquitination of 3-hydroxy-3-methylglutaryl CoA reductase in lipid droplet-associated endoplasmic reticulum membranes. *Mol. Biol. Cell.* 24:169–83. doi:10.1091/mbc.E12-07-0564.
- Jo, Y., P.C.W. Lee, P. V Sguigna, and R.A. DeBose-Boyd. 2011. Sterol-induced degradation of HMG CoA reductase depends on interplay of two Insigs and two ubiquitin ligases, gp78 and Trc8. *Proc. Natl. Acad. Sci. U. S. A.* 108:20503–8. doi:10.1073/pnas.1112831108.
- Jones, T.R., E.J. Wiertz, L. Sun, K.N. Fish, J.A. Nelson, and H.L. Ploegh. 1996. Human cytomegalovirus US3 impairs transport and maturation of major histocompatibility complex class I heavy chains. *Proc. Natl. Acad. Sci. U. S. A.* 93:11327–33.
- Kikkert, M., R. Doolman, M. Dai, R. Avner, G. Hassink, S. van Voorden, S. Thanedar, J. Roitelman, V. Chau, and

- E. Wiertz. 2004. Human HRD1 is an E3 ubiquitin ligase involved in degradation of proteins from the endoplasmic reticulum. *J. Biol. Chem.* 279:3525–34. doi:10.1074/jbc.M307453200.
- Kleiger, G., A. Saha, S. Lewis, B. Kuhlman, and R.J. Deshaies. 2009. Rapid E2-E3 Assembly and Disassembly Enable Processive Ubiquitylation of Cullin-RING Ubiquitin Ligase Substrates. *Cell.* 139:957–968. doi:10.1016/j.cell.2009.10.030.
- Lee, J.P., A. Brauweiler, M. Rudolph, J.E. Hooper, H. a. Drabkin, and R.M. Gemmill. 2010. The TRC8 ubiquitin ligase is sterol regulated and interacts with lipid and protein biosynthetic pathways. *Mol. Cancer Res.* 8:93–106. doi:10.1158/1541-7786.MCR-08-0491.
- Lehner, P.J., J.T. Karttunen, G.W. Wilkinson, and P. Cresswell. 1997. The human cytomegalovirus US6 glycoprotein inhibits transporter associated with antigen processing-dependent peptide translocation. *Proc. Natl. Acad. Sci. U. S. A.* 94:6904–9.
- Leitman, J., M. Shenkman, Y. Gofman, N.O. Shtern, N. Ben-Tal, L.M. Hendershot, and G.Z. Lederkremer. 2014. Herp coordinates compartmentalization and recruitment of HRD1 and misfolded proteins for ERAD. *Mol. Biol. Cell.* 25:1050–60. doi:10.1091/mbc.E13-06-0350.
- Lilley, B.N., and H.L. Ploegh. 2004. A membrane protein required for dislocation of misfolded proteins from the ER. *Nature.* 429:834–40. doi:10.1038/nature02592.
- Liu, W., Y. Shang, Y. Zeng, C. Liu, Y. Li, L. Zhai, P. Wang, J. Lou, P. Xu, Y. Ye, and W. Li. 2014. Dimeric Ube2g2 simultaneously engages donor and acceptor ubiquitins to form Lys48-linked ubiquitin chains. *EMBO J.* 33:46–61. doi:10.1002/embj.201385315.
- McGeoch, D.J., F.J. Rixon, and A.J. Davison. 2006. Topics in herpesvirus genomics and evolution. *Virus Res.* 117:90–104. doi:10.1016/j.virusres.2006.01.002.
- Miao, H., W. Jiang, L. Ge, B. Li, and B. Song. 2010. Tetra-glutamic acid residues adjacent to Lys248 in HMG-CoA reductase are critical for the ubiquitination mediated by gp78 and UBE2G2. *Acta Biochim. Biophys. Sin. (Shanghai).* 42:303–310. doi:10.1093/abbs/gmq022.
- Mocarski, E.S. 2002. Immunomodulation by cytomegaloviruses: manipulative strategies beyond evasion. *Trends Microbiol.* 10:332–9.
- Noriega, V., V. Redmann, T. Gardner, and D. Tortorella. 2012a. Diverse immune evasion strategies by human cytomegalovirus. *Immunol. Res.* 54:140–151. doi:10.1007/s12026-012-8304-8.
- Noriega, V.M., J. Hesse, T.J. Gardner, K. Besold, B. Plachter, and D. Tortorella. 2012b. Human cytomegalovirus US3 modulates destruction of MHC class I molecules. *Mol. Immunol.* 51:245–253. doi:10.1016/j.molimm.2012.03.024.
- Olzmann, J.A., R.R. Kopito, and J.C. Christianson. 2013. The mammalian endoplasmic reticulum-associated degradation system. *Cold Spring Harb. Perspect. Biol.* 5. doi:10.1101/cshperspect.a013185.
- Oresic, K., C.L. Ng, and D. Tortorella. 2009. TRAM1 participates in human cytomegalovirus US2- and US11-mediated dislocation of an endoplasmic reticulum membrane glycoprotein. *J. Biol. Chem.* 284:5905–14. doi:10.1074/jbc.M807568200.
- Park, B., Y. Kim, J. Shin, S. Lee, K. Cho, K. Früh, S. Lee, and K. Ahn. 2004. Human cytomegalovirus inhibits tapasin-dependent peptide loading and optimization of the MHC class I peptide cargo for immune evasion. *Immunity.* 20:71–85.
- Park, B., E. Spooner, B.L. Houser, J.L. Strominger, and H.L. Ploegh. 2010. The HCMV membrane glycoprotein US10 selectively targets HLA-G for degradation. *J. Exp. Med.* 207:2033–41. doi:10.1084/jem.20091793.
- Preston, G.M., and J.L. Brodsky. 2017. The evolving role of ubiquitin modification in endoplasmic reticulum-associated degradation. *Biochem. J.* 474:445–469. doi:10.1042/BCJ20160582.
- Schuren, A.B., A.I. Costa, and E.J. Wiertz. 2016. Recent advances in viral evasion of the MHC Class I processing pathway. *Curr. Opin. Immunol.* 40:43–50. doi:10.1016/j.coi.2016.02.007.
- Soetandyo, N., and Y. Ye. 2010. The p97 ATPase dislocates MHC class I heavy chain in US2-expressing cells via a

- Ufd1-Npl4-independent mechanism. *J. Biol. Chem.* 285:32352–9. doi:10.1074/jbc.M110.131649.
- Stagg, H.R., M. Thomas, D. van den Boomen, E.J.H.J. Wiertz, H. a Drabkin, R.M. Gemmill, and P.J. Lehner. 2009. The TRC8 E3 ligase ubiquitinates MHC class I molecules before dislocation from the ER. *J. Cell Biol.* 186:685–92. doi:10.1083/jcb.200906110.
- Sun, S., G. Shi, H. Sha, Y. Ji, X. Han, X. Shu, H. Ma, T. Inoue, B. Gao, H. Kim, P. Bu, R.D. Guber, X. Shen, A.-H. Lee, T. Iwawaki, A.W. Paton, J.C. Paton, D. Fang, B. Tsai, J.R. Yates Iii, H. Wu, S. Kersten, Q. Long, G.E. Duhamel, K.W. Simpson, and L. Qi. 2015. IRE1 $\alpha$  is an endogenous substrate of endoplasmic-reticulum-associated degradation. *Nat. Cell Biol.* 17:1546–55. doi:10.1038/ncb3266.
- Tiwari, S., and A.M. Weissman. 2001. Endoplasmic reticulum (ER)-associated degradation of T cell receptor subunits. Involvement of ER-associated ubiquitin-conjugating enzymes (E2s). *J. Biol. Chem.* 276:16193–200. doi:10.1074/jbc.M007640200.
- Wang, X., R. a Herr, M. Rabelink, R.C. Hoeben, E.J.H.J. Wiertz, and T.H. Hansen. 2009. Ube2j2 ubiquitinates hydroxylated amino acids on ER-associated degradation substrates. *J. Cell Biol.* 187:655–68. doi:10.1083/jcb.200908036.
- Van De Weijer, M.L.M.L., M.C. Bassik, R.D.R.D. Luteijn, C.M.C.M. Voorburg, M.A.M.A.M. Lohuis, E. Kremmer, R.C.R.C. Hoeben, E.M.E.M. Leproust, S. Chen, H. Hoelen, M.E.M.E. Rensing, W. Patena, J.S.J.S. Weissman, M.T.M.T. McManus, E.J.H.J.E.J.H.J. Wiertz, and R.J.R.J. Lebbink. 2014. A high-coverage shRNA screen identifies TMEM129 as an E3 ligase involved in ER-associated protein degradation. *Nat. Commun.* 5:3832. doi:10.1038/ncomms4832.
- van de Weijer, M.L.M.L., R.D.R.D. Luteijn, and E.J.H.J.E.J.H.J. Wiertz. 2015. Viral immune evasion: Lessons in MHC class I antigen presentation. *Semin. Immunol.* 27:125–37. doi:10.1016/j.smim.2015.03.010.
- Wiertz, E.J., T.R. Jones, L. Sun, M. Bogyo, H.J. Geuze, and H.L. Ploegh. 1996a. The human cytomegalovirus US11 gene product dislocates MHC class I heavy chains from the endoplasmic reticulum to the cytosol. *Cell.* 84:769–79.
- Wiertz, E.J., D. Tortorella, M. Bogyo, J. Yu, W. Mothes, T.R. Jones, T.A. Rapoport, and H.L. Ploegh. 1996b. Sec61-mediated transfer of a membrane protein from the endoplasmic reticulum to the proteasome for destruction. *Nature.* 384:432–8. doi:10.1038/384432a0.
- Yan, L., W. Liu, H. Zhang, C. Liu, Y. Shang, Y. Ye, X. Zhang, and W. Li. 2014. Ube2g2-gp78-mediated HERP polyubiquitylation is involved in ER stress recovery. *J. Cell Sci.* 127:1417–27. doi:10.1242/jcs.135293.
- Ye, Y., H.H. Meyer, and T.A. Rapoport. 2001. The AAA ATPase Cdc48/p97 and its partners transport proteins from the ER into the cytosol. *Nature.* 414:652–6. doi:10.1038/414652a.
- Ye, Y., Y. Shibata, M. Kikkert, S. van Voorden, E. Wiertz, and T.A. Rapoport. 2005. Recruitment of the p97 ATPase and ubiquitin ligases to the site of retrotranslocation at the endoplasmic reticulum membrane. *Proc. Natl. Acad. Sci. U. S. A.* 102:14132–8. doi:10.1073/pnas.0505006102.
- Ye, Y., Y. Shibata, C. Yun, D. Ron, and T. a Rapoport. 2004. A membrane protein complex mediates retrotranslocation from the ER lumen into the cytosol. *Nature.* 429:841–7. doi:10.1038/nature02656.
- Yin, Q., S.-C. Lin, B. Lamothe, M. Lu, Y.-C. Lo, G. Hura, L. Zheng, R.L. Rich, A.D. Campos, D.G. Myszka, M.J. Lenardo, B.G. Darnay, and H. Wu. 2009. E2 interaction and dimerization in the crystal structure of TRAF6. *Nat. Struct. Mol. Biol.* 16:658–666. doi:10.1038/nsmb.1605.

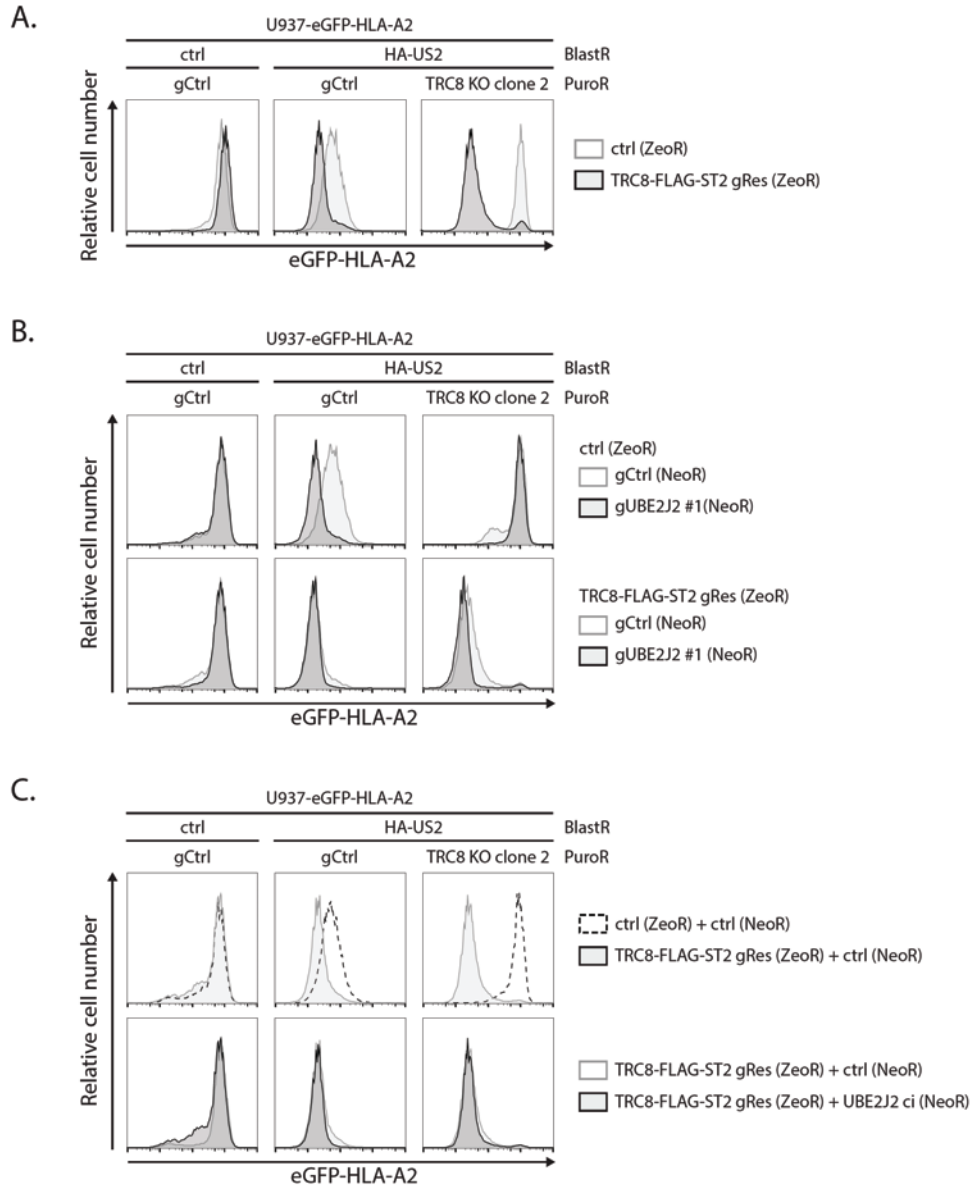


**Supplementary Figure S1. Flow cytometric validation of knockout clones used.** A-B. Independent clones in which the indicated genes were knocked out from U937 cells co-expressing eGFP-HLA-A2, and either HA-US2 (A) or ST2-HA-US2. (B) Cells were assessed for expression levels of the chimeric eGFP-HLA-A2 molecule or cell surface levels of endogenous HLA-A3 by flow cytometry.

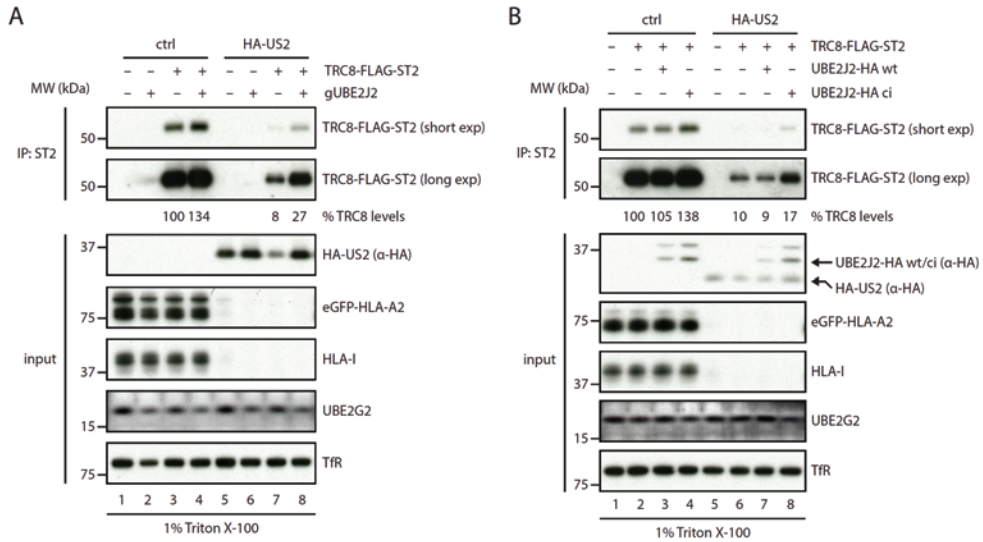
Multiple E2 enzymes regulate HCMV US2-mediated immunoreceptor degradation

<b>HA-US2 + UBE2J2 KO cl.1</b>		<b># reads</b>
<b>wildtype</b>	CTTACCTGGT <u>GTTGCACTTAAACCTCCCGT</u> <u>TGGGAGTGATCATATAGATACTGGG</u>	
<b>Allele 1</b>	CTTACCTGGTGTGCACT-----CGTTGGGAGTGATCATATAGATACTGGG	30
<b>Allele 2</b>	CTTACCTGGTGTGCACTTAAACCTCC-----GGG	58
<b>HA-US2 + UBE2J2 KO cl.2</b>		<b># reads</b>
<b>wildtype</b>	CTTACCTGGT <u>GTTGCACTTAAACCTCC</u> --CGT <u>TGGGAGTGATCATATAGATACTG</u>	
<b>Allele 1</b>	CTTACCTGGTGTGCACTTAAACCTCC <b>TT</b> CGTTGGGAGTGATCATATAGATACTG	320
<b>Allele 2</b>	n/a	-
<b>ST2-HA-US2 + UBE2J2 KO cl.1</b>		<b># reads</b>
<b>wildtype</b>	CTTACCTGGT <u>GTTGCACTTAAACCTCC</u> --CGT <u>TGGGAGTGATCATATAGATACTG</u>	
<b>Allele 1</b>	CTTACCTGGTGTGCACTTAAACC-----TCATATAGATACTG	12
<b>Allele 2</b>	CTTACCTGGTGTGCACTTAAACCTCC <b>TT</b> CGTTGGGAGTGATCATATAGATACTG	63
<b>ST2-HA-US2 + UBE2J2 KO cl.2</b>		<b># reads</b>
<b>wildtype</b>	CTTACCTGGT <u>GTTGCACTTAAACCTCCCGT</u> <u>TGGGAGTGATCATATAGATACTGGG</u>	
<b>Allele 1</b>	CTTACCTGGTGTGCACTTAAA----CCGTTGGGAGTGATCATATAGATACTGGG	107
<b>Allele 2</b>	CTTACCTGGTGTGCACTTAAACC-----TCATATAGATACTGGG	118

**Supplementary Figure S2. Genomic target site sequencing of knockout clones used.** Genomic DNA of the knockout clones established was isolated and PCR amplified. Dual indexing barcodes were added to each sample and genomic target sites were deep sequenced using the Illumina MiSeq platform. Indel formation was assessed using Varscan. PAM motifs are underlined, the gRNA sequences are highlighted in yellow.



**Supplementary Figure S3. gRNA-resistant TRC8-FLAG-ST2 retains function.** (A) A ZeoR-containing vector expressing a gRNA-resistant (gRes) TRC8-FLAG-ST2 was stably introduced in the cell lines indicated, after which total eGFP-HLA-A2 was assessed by flow cytometry. (B) Cells used in (A) were transduced with a NeoR-containing CRISPR/Cas9 control vector (gCtrl), or one targeting UBE2J2 (gUBE2J2 #1). Cells were assessed for eGFP-HLA-A2 expression by measuring eGFP levels using flow cytometry. (C) Cells used in (A) were transduced with a NeoR-containing control vector, or one expressing catalytically UBE2J2 (ci). Cells were assessed for GFP-HLA-A2 expression by measuring eGFP levels using flow cytometry.



**Supplementary Figure S4. Impaired UBE2J2 function leads to TRC8 upregulation (continued from Fig. 4A and 4B).**

(A) TRC8 is upregulated upon UBE2J2 depletion. Control cells (lane 1-4), US2-expressing gRNA-control cells (lane 5-8), or US2-expressing TRC8 KO cells (lane 9-12) were transduced with either a control vector or with a TRC8-FLAG-ST2-expressing vector. After zeocin selection, cells were transduced with a G418-selectable gRNA control vector or anti-gUBE2J2 vector. After G418 selection, cells were lysed in Triton X-100 lysis buffer, and TRC8-FLAG-ST2 was immunoprecipitated by using StrepTactin beads. Immunoprecipitated TRC8-FLAG-ST2 was eluted by using d-Desthiobiotin, after which immunoblot analysis was performed to detect the indicated proteins. Lanes 5-8 from TRC8-Flag-ST2 (long exposure) and Transferrin receptor are shown in figure 4A. (B) TRC8 is upregulated upon expression of catalytically inactive UBE2J2. Control cells (lane 1-4), US2-expressing gRNA-control cells (lane 5-8), or US2-expressing TRC8 KO cells (lane 9-12) were transduced with either a control vector or with a TRC8-FLAG-ST2-expressing vector. After zeocin selection, cells were subjected to a G418-selectable vector expressing either wildtype UBE2J2 (wt) or catalytically inactive UBE2J2 (ci). After G418 selection, cells were lysed in Triton X-100 lysis buffer, and TRC8-FLAG-ST2 was immunoprecipitated by using StrepTactin beads. Immunoprecipitated TRC8-FLAG-ST2 was eluted by using d-Desthiobiotin, after which immunoblot analysis was performed to detect the indicated proteins. Lanes 5-8 from TRC8-Flag-ST2 (long exposure) and Transferrin receptor are shown in figure 4B.

6

## Supplementary Information S01

Number	Name	gRNA sequence*			
1	UBE2A_1	GTGTGGAACGCGGTTCATTTT	47	UBE2J2_3	gTATAGAGACGTCGGACTTCA
2	UBE2A_2	gCAACATAATGGTGTGGAACG	48	UBE2K_1	GATTCGCTGCACC CGCATGT
3	UBE2A_3	gCCGAGAACAACATAATGGTG	49	UBE2K_2	GCAATGACAATAATACCGTG
4	UBE2B_1	gAATCCCGCATGAGCCTCCTC	50	UBE2K_3	GGATGCTGTAGTAGCAAATC
5	UBE2B_2	GGATTTCAAGCGGTTACAAG	51	UBE2L6_1	GTCCGTTCTCGTCCACGTTG
6	UBE2B_3	gTGTTCGACCCCGCCCGGAGG	52	UBE2L6_2	gCACCCCAACGTGGACGAGAA
7	UBE2C_1	GCGTCGCCGCCGCCGTAA	53	UBE2L6_3	gCACGTTGGGGTGGTAGATCT
8	UBE2C_2	gACGGGCGGCGGCAGCCTAG	54	UBE2N_1	GGCGTTGCTCTCATCTGGTT
9	UBE2C_3	GCGGCTGGGTTCGCGGTTTT	55	UBE2N_2	gATAGGAAACCCAGCGTTTGC
10	UBE2D1_1	gCCACCTTGATATGCGCTATC	56	UBE2N_3	gTAACGGGCGTTGCTCTCATC
11	UBE2D1_2	gCCTGATAGCGCATATCAAGG	57	UBE2NL_1	gTAACGGGCGTTGCTTTTCATC
12	UBE2D1_3	GTATTTGTCTCGATATCTCG	58	UBE2NL_2	gATCAAAGGATTCGCCCTTTG
13	UBE2D2_1	gCCATTATTGTAGCTTGCCAA	59	UBE2NL_3	GGTCATTGCTGGGGAATCAA
14	UBE2D2_2	gCCATTGGCAAGCTACAATAA	60	UBE2O_1	gCTGGTTCGGGCGTTACCG
15	UBE2D2_3	GTTTGAAGGGTAATCTGTT	61	UBE2O_2	gCACGGTAACGGCCGACACC
16	UBE2D3_1	GGATTAATAAGGTAACCCGC	62	UBE2O_3	GTGCACGGAGCCACGGTAA
17	UBE2D3_2	GAATACACCGCCTTGATAT	63	UBE2Q1_1	GGCAATGCGGAAGCGCTCG
18	UBE2D3_3	GGTTTGAAGGGTAGTCTGT	64	UBE2Q1_2	GCGGAAGCGCTCGTGGCCG
19	UBE2D4_1	GGAAATTAACCGACTTGCAG	65	UBE2Q1_3	gCTCGAGTCCATCTTCCACCG
20	UBE2D4_2	GGAAATTAACCGACTTGCAGA	66	UBE2Q2_1	gTCTTGTCGAAGATGGACGCC
21	UBE2D4_3	GACAGGTCCTGCAGAACAC	67	UBE2Q2_2	GGAGCATAGTACCGTCGTTG
22	UBE2E1_1	GCCTCCAGGATCCGTGTATG	68	UBE2Q2_3	GCGATTCCGCATCGTCAGT
23	UBE2E1_2	gCCACCCTCATAACCGGATCC	69	UBE2R1_1	GTACGCGGAATCCCTCGAC
24	UBE2E1_3	GAATACACCACCTCATAACA	70	UBE2R1_2	GAGGGATTCCGCGTGACAC
25	UBE2E2_1	gACTAGTGGAGGAAGTTCCGA	71	UBE2R1_3	GAGGGCGATCTATAACACT
26	UBE2E2_2	gCAATTTAGCAGCGGTTTTGC	72	UBE2R2_1	GAAGTAGCCGCTTCGTAGA
27	UBE2E2_3	gCAATTTAGCAGCGGTTTTGC	73	UBE2R2_2	gACGAGTCCGACCTCTACAAC
28	UBE2E3_1	gCCTTCATATAAGAACCCGG	74	UBE2R2_3	GAGGTCGGACTCGTCCACC
29	UBE2E3_2	gTCAACTATACTTGGTCCACC	75	UBE2S_1	GGGGGTAGGTTCTCCACGT
30	UBE2F_1	GCGTCCGACTCGACTCGGA	76	UBE2S_2	GGCGGATGATGTGCGGGGGT
31	UBE2F_2	gCAGCGTCCGACTCGACTCGG	77	UBE2S_3	GGGCATCCGACAGCTACTGC
32	UBE2F_3	GAAACCTCCGAGTTCGAGT	78	UBE2T_1	gCTTGCCAAATGTGATGCCT
33	UBE2G1_1	gACTGTACTGCGAAGACAGC	79	UBE2T_2	gCACCCCGAGGCATCACATGT
34	UBE2G1_2	GACAATGATCTCTACCGAT	80	UBE2T_3	gACCTTTCTCATAAGGTGTGT
35	UBE2G1_3	GATGGGAAGTCCCTATTAT	81	UBE2U_1	gTCTACAGAATTGAGTTTGGC
36	UBE2G2_1	GGAGAAGATCCTGCTGTCGG	82	UBE2U_2	GCCTGTAAGTGAAGATATGA
37	UBE2G2_2	GGACTTAACGGGTAATCAAG	83	UBE2U_3	gTCCATCATATCTTCACTTAC
38	UBE2G2_3	GACTTAACGGGTAATCAAGT	84	UBE2V1_E1_1	gCTAGAAAATTTCACTGCAA
39	UBE2H_1	GCTTGATTTCTTCTGGTCCG	85	UBE2V1_E1_2	gCTTTGCAGTGAATTTTCT
40	UBE2H_2	GCTGCAGCGTCACCATGAG	86	UBE2V1_E4_3	GACACTTACAAGATGGACA
41	UBE2H_3	GAGGCGGATGGACACGGACG	87	UBE2V1_E4_4	GATGGACAGGGATGATAAT
42	UBE2J1_1	GGTCTCCATGGTGGGTCGC	88	UBE2V1_exon_3	gTTACAAAAGGGGGTGCCTTC
43	UBE2J1_2	GTTGTAGCGGTTCTCCATGG	89	UBE2V1_exon_4	gTACAAAAGGGGGTGCCTTCT
44	UBE2J1_3	GAATGGCACTTCACGGTTAG	90	UBE2V2_1	gTCTTCGTAATTTTCGCTTGT
45	UBE2J2_1	GTTGCACTTAAACCTCCCGT	91	UBE2V2_2	gTAGCGCACGGTACAGTTAGC
46	UBE2J2_2	GCTGAATCCCGTTCTGGACG	92	UBE2V2_3	gTCCAACAAGCGAAAATTACG
			93	UBE2W_1	GTGCTCGCGTACGCGCCG



## Multiple E2 enzymes regulate HCMV US2-mediated immunoreceptor degradation

94 UBE2W_2	GTCTCTGGCCTCGCCGGTCT
95 UBE2W_3	gCCATCCCCCAAGACCGGCG
96 UBE2Z_1	GCTGGTGTGTGGCGTTAG
97 UBE2Z_2	GTTGTTGGCGTTAGCGGCAG
98 UBE2Z_3	gCAGCAACGCTGCTCGCCCCG
99 BIRC6_1	GCATGCACTGCGACGCCGAC
100 BIRC6_2	GCATGCACTGCGACGCCGA
101 BIRC6_3	GTGTGATTGTGCTGAGCGC
102 UEVLD_1	GCTGAAATTGCTAATGTGC
103 UEVLD_2	GAAGATTTCAAGGTCCATCG
104 UEVLD_3	gCTGTACAGGGTATTGCAGAC
105 UBE2L3_1	GCCCCTTTTCGTCGATGTT
106 UBE2L3_2	GCCCCTTTTCGTCGATGTT
107 AKTIP_1	gCATCTTGTATAGCGATCTGA
108 AKTIP_2	GGAGTAATATTCATACGGCA
109 gCtrl vector	
110 TRC8_1	GAGGAAGATGACAGGCGTCT
111 UBE2G2_4	CATGGGCTACGAGAGCAGCG
112 UBE2G2_5	GTTGGGATGAAACATCTCAC

\* The crRNA sequence is presented, which is part of the gRNA that directs Cas9 to its target site. A lowercase 'g' residue is not part of the genomic target sequence, but was introduced to allow efficient expression from the U6 promoter



## **CHAPTER 7**

### **Summarizing Discussion**

Michael L. van de Weijer

## Excellent molecular probes

The discovery of herpesvirus immunoevasins in recent years has contributed to the characterization of several cellular pathways. Their specific and potent effect on these cellular processes makes them ideal molecular probes. Especially the HCMV immunoevasions US2 and US11, which specifically target MHC-I for degradation, have been used extensively to study the molecular mechanisms of ERAD. This thesis reports the uncovering of molecular mechanisms of HCMV US2 and US11 by using loss-of-function genetic screens and shows how these findings may shed more light onto ERAD in general.

## Screening for hits

Recent advances in mammalian gene manipulation have created novel ways for extensive, high-throughput studies. In this context, lentivirus-based whole-genome shRNA or CRISPR/Cas9 libraries are instrumental in conducting loss-of-function screens [1]. In **Chapter 2**, we have studied mammalian ERAD by employing the latest RNAi library screening and CRISPR/Cas9 genome-engineering techniques using HCMV US11 as a model.

HCMV US11-mediated degradation of MHC-I molecules serves as a paradigm for ERAD and has facilitated the identification of multiple essential components of this important degradation pathway. In this study, we identified additional essential players of US11-mediated MHC-I downregulation by performing a pooled genome-wide shRNA library screen in human cells expressing the US11 protein. To this end, we constructed a new high-complexity genome-wide shRNA library consisting of around 550,000 different shRNAs. The entire library has been evaluated in a single population of U937 cells. These U937 cells were expressing an HLA-A2 molecule containing an N-terminal eGFP and a Myc-tag (eGFP-Myc-HLA-A2). Both US2 and US11 were able to efficiently degrade eGFP-Myc-HLA-A2 in a proteasome-dependent manner, as exposure to proteasome inhibitors reduced the degradation of eGFP-Myc-HLA-A2. The large difference in HLA-A2 expression between control cells and US11-expressing cells allowed us to greatly increased our chances of obtaining genuine hits in our final hitlist. As such, we have developed a robust and versatile readout system for both US2 and US11 in shRNA- and gRNA-based genetic screens.

This approach proved successful, allowing the identification of several known players, such as p97 and a large compendium of proteasome subunits. Several other proteins known to be involved were absent, such as Derlin-1. This could be due to a number of reasons, including target lethality, timepoint choice, and the effectiveness of shRNAs present in the library. Our hitlist also contained multiple genes of the COPI retrograde transport system. Based on validation experiments, we concluded that the COPI complex is not specifically involved in US11-mediated MHC-I degradation, but that the identification of these subunits in the screen is likely caused by an indirect effect. Lastly, our hit list contained the previously uncharacterized protein TMEM129.

## The ubiquitin ligase exploited by US11

Validation experiments showed that TMEM129 is essentially involved in US11-mediated MHC-I downregulation (**Chapter 3**). Sequence analysis suggested that TMEM129 represents a tri-spanning transmembrane protein containing a long C-terminal tail carrying a non-classical RING domain. A classical RING domain contains three cysteine pairs and one cysteine-histidine pair for the coordination of two zinc-ions. The RING domain of TMEM129 possesses four zinc-coordinating cysteine pairs (C4C4) that are fully conserved among a wide range of TMEM129 orthologs. TMEM129 was proven to be a genuine E3 ubiquitin ligase; the C4C4 RING domain was shown to be essential for its activity. In **Chapter 4**, we confirm the predicted topology of TMEM129 as a tri-spanning transmembrane protein.

The identification of the E3 ubiquitin ligase crucial for US11-mediated MHC-I downregulation has been a subject of intense investigation for over 10 years. The fact that TMEM129 has not been identified earlier is likely due to its low endogenous expression levels, which complicates its identification via standard biochemical approaches. Additionally, bioinformatic approaches to map the complete mammalian E3 landscape failed to classify the proteins containing C4C4 RING domains as E3 ubiquitin ligases, as this configuration is highly unusual. Hence, the identification of a second E3 enzyme containing a C4C4 RING domain next to CNOT4 [2] warrants a revisit of the mammalian E3 landscape, as many more may lay hidden in the mammalian genome.

## Does it take more than one E2 to ubiquitinate?

E3 ubiquitin ligases collaborate with E2 ubiquitin-conjugating enzymes to facilitate polyubiquitination of a target substrate [3]. To investigate the E2 enzymes involved in US11-mediated MHC-I degradation in more detail, focused shRNA- and gRNA-mediated screens were conducted. We found that UBE2J2 and UBE2K/E2-25K were essentially involved in US11-mediated MHC-I degradation. UBE2K has previously been reported to facilitate ubiquitination of MHC-I in permeabilized US11-expressing cells [4]. UBE2J2- and UBE2K-null US11-expressing cells express high levels of MHC-I, which indicates that these two E2 enzymes are not interchangeable and catalyze two different ubiquitination steps essential for the dislocation process.

The idea that the processivity of polyubiquitin formation might be orchestrated by at least two different E2 enzymes, one responsible for ubiquitin chain initiation, while the other E2 promotes ubiquitin chain elongation, is being supported by other studies [5–8]. In the context of US11-mediated MHC-I degradation, mono-ubiquitination of MHC-I is not sufficient to induce dislocation; completion of this reaction requires Lys48-linked polyubiquitination [9,10]. UBE2K is known to catalyze the elongation of Lys48-linked ubiquitin chains, but not ubiquitin-chain initiation [11]. Currently, the type of ubiquitin chain formation catalyzed by

UBE2J2 is not known. However, one might hypothesize that in the context of US11-mediated MHC-I degradation, the membrane-bound UBE2J2 promotes mono-ubiquitination of MHC-I, thereby enabling the cytosolic UBE2K to catalyze Lys48-linked ubiquitin chain elongation. Removal of either UBE2J2 or UBE2K would prevent polyubiquitination of MHC-I and thereby inhibit its dislocation. This hypothesis would be in line with a recent study performed by Weber et al. [5], showing that the ubiquitination of substrates by Doa10, the yeast homolog of TEB4, requires the activity of two E2 enzymes. The non-canonical ubiquitin-conjugating enzyme Ubc6 (yeast homologue of mammalian UBE2J1/UBE2J2) attaches a single ubiquitin moiety not only to lysines, but also to hydroxylated amino acids (cysteines, serines and threonines). These ubiquitin moieties then serve as primers for subsequent poly-ubiquitylation by Ubc7 (yeast homologue of mammalian UBE2G1/UBE2G2).

### Membrane topology of TMEM129

Experimental validation of the membrane topology of ERAD E3 enzymes is key to understanding their function. Prediction of membrane topology of TMEM129 suggested an  $N_{\text{exo}}-C_{\text{cyto}}$  orientation with three transmembrane domains. However, predictions of membrane protein topology are not always accurate. In **Chapter 3**, we experimentally mapped the membrane topology of TMEM129 using *in vitro* translation, truncation scanning, and glycosylation scanning mutagenesis. We demonstrated that TMEM129 is not glycosylated, does not contain disulphide bonds, and contains a non-cleaved signal-anchor sequence. In addition, we showed that TMEM129 contains three transmembrane domains with an overall  $N_{\text{exo}}-C_{\text{cyto}}$  orientation, thereby positioning the C-terminal RING domain in the cytosol. Although we have established that TMEM129 is a tri-spanning ER-resident E3 ubiquitin ligase essentially involved in US11-mediated MHC-I degradation [12,13], its exact role in this process and in ERAD in general remains to be determined.

In the absence of US11, TMEM129 is associated with Derlin-1, p97, and other ERAD factors [12,14]. Hence, it is highly likely that TMEM129 is involved in the turnover of physiological ERAD substrates. A SILAC-based proteomics approach may facilitate the identification of these TMEM129 substrates. Using these substrates as a readout model, a whole-genome CRISPR/Cas9 library screen could be employed to identify the proteins essential for the TMEM129 substrate degradation. A large-scale pulldown of TMEM129 complexes and subsequent identification through mass-spectrometry could shed more light onto associated proteins as well.

## How does the substrate cross the ER membrane?

An important, yet unresolved, question in the field of ERAD is how ER-resident degradation substrates cross the ER membrane. This pertains to membrane proteins such as MHC-I molecules in the presence of US11, but also to soluble ER proteins destined for degradation in the cytosol. Most likely, these proteins are transported back into the cytosol through a channel [15]. Using US2-mediated degradation of MHC-I molecules as a model, a role has been proposed for the Sec61 channel, generally involved in protein import into the ER [16]. This possibility is supported by studies using other proteins as dislocation substrates [17–26]. For US11-mediated degradation of MHC-I molecules, no indications were found for a role of the Sec61 channel in dislocation of the substrate; several other multispinning membrane proteins have been proposed to fulfill this function. These include the Derlins, multispinning membrane proteins widely involved in ERAD [27–32]. Derlin-1 has been shown to contain six transmembrane domains [29] and the protein is involved in the degradation of MHC-I molecules in the context of US11, but not US2 [27,28]. In addition, several E3 ligases that are involved in ERAD are multispinning membrane proteins and may therefore be part of the dislocation channel [33].

The latter hypothesis is supported by experiments involving the *in vitro* reconstitution of dislocation using proteoliposomes and purified *Saccharomyces cerevisiae* proteins. The results indicate that Hrd1p forms a ubiquitin-gated protein-conducting channel [34,35]. Hrd1 forms homo-oligomers consisting of 2 Hrd1p molecules [36–38] and as such could form a protein channel of 12 TM segments. For initiation of dislocation, polyubiquitination of Hrd1p, rather than substrate modification, is necessary. Also, the Cdc48 (yeast homologue of mammalian p97) complex is not essential for dislocation initiation, but is instead required for the subsequent membrane extraction. The role of accessory membrane proteins remained uninvestigated, but they might contribute to the polypeptide conduit within the membrane and may convey certain functions, such as providing substrate specificity.

Mammalian HRD1 likely has an identical topology to yeast Hrd1p with six TMDs [39]. Mammalian TEB4, like its yeast homologue Doa10, has been reported to encompass fourteen TMDs [40]. For mammalian gp78/AMFR, the number of TMDs has been predicted to be between five and seven [41] [40]. TMEM129 contains three TMDs, and may also form (part of) a dislocation channel, especially if TMEM129 is able to form multimers.

## Recruitment of p97

The AAA-ATPase p97 is indispensable for US11-mediated MHC-I degradation. However, the recruitment of p97 to the dislocation complex has remained elusive. It has previously been suggested that VIMP [28] is responsible for p97 recruitment during US11-mediated MHC-I degradation. VIMP was found to link p97 to Derlin-1. Moreover, VIMP was co-precipitated

with US11 and vice-versa. However, no functional experiments were performed to investigate if VIMP would be essential for US11-mediated MHC-I degradation. While we found that VIMP was indeed co-precipitated with US11 (**Chapter 3**), we found that depletion of VIMP did not affect US11-mediated MHC-I degradation, indicating that VIMP is not essential in this context. Another article proposed that UBXD8 is essential for US11-mediated MHC-I degradation [42]. A hypothesized dominant-negative UBXD8 (UBXD8-GFP) negatively affected US11-mediated MHC-I degradation. The UBXD8-GFP also displayed decreased recruitment of p97. These findings suggested that UBXD8 is essential for US11-mediated MHC-I degradation. However, convincing evidence confirming their essential involvement in US11-mediated MHC-I degradation is lacking.

In **Chapter 4**, we set out to identify the p97 cofactors essential for US11-mediated MHC-I degradation using a focused CRISPR/Cas9 library. Our results identified an essential p97 cofactor, namely UBXD8. UBXD8 is localized to the ER [42] and lipid droplets [43,44]. Depletion of UBXD8 stabilizes several ERAD substrates, supporting a role for UBXD8 in general protein degradation [45–48]. It is thought that UBXD8 functions as an ERAD scaffolding coordinator. UBXD8 belongs to a subfamily of hairpin proteins, i.e. it contains a membrane insertion region that dips into the outer leaflet of the ER lipid bilayer. Thus, the N-terminus containing the UBA domain and the C-terminus containing the UBX domain are exposed to the cytosol [49,50].

Our data indicate that the UBA domain of UBXD8 is dispensable for US11-mediated MHC-I degradation. UBA domains in general interact with polyubiquitinated proteins [51]. We found that the UBX domain of UBXD8 is essential for US11-mediated MHC-I degradation. The UBX domain of UBXD8 is required for p97 recruitment [42,45,52] and for the degradation of at least one ERAD substrate [45]. Pulldown experiments on UBXD8 revealed that the UBX-deletion mutant is severely impaired in its ability to recruit p97. Surprisingly, the levels of p97 recruited to the US11-exploited complexes were largely unaffected upon UBXD8 knockout, indicating that UBXD8 is not primarily responsible for the recruitment of p97 to the dislocation complex.

Various domains for binding p97 exist in p97 cofactors within the dislocation complex. UBX, UBX-like, SHP, VBM, and VIM domains interact with the N-terminus of p97, while PUB and PUL domains interact with its C-terminal tail [53]. E3 ubiquitin ligases and the Derlin proteins can also directly recruit p97 [29,53,54]. However, neither a UBXD8 nor a TMEM129 knockout had an effect on the levels of p97 recruited to the US11-exploited complexes. Only Derlin-1 knockout resulted in a relative decrease of p97 recruitment. However, an SHP-deletion mutant of Derlin-1 could still support US11-mediated MHC-I degradation in Derlin-1 knockout cells. Thus, we hypothesize that Derlin-1 indirectly recruits p97 through an unknown factor. In this context, UBXD8 might mediate proper spatial and/or temporal arrangement of p97 complexes. Alternatively, UBXD8 may prevent the binding of cofactors negatively affecting the dislocation process.



## US2-mediated MHC-I degradation

Like US11, US2 hijacks the ERAD pathway to force degradation of MHC-I, but US2 employs a different strategy. As discussed above, US11 exploits Derlin-1 and the E3 ubiquitin ligase TMEM129 in cooperation with the E2 ubiquitin-conjugating enzymes UBE2J2 and UBE2K to dislocate MHC-I [4,12,14,27]. US2 does not depend on any of these proteins but rather appropriates the E3 ubiquitin ligase TRC8 to mediate MHC-I downregulation [55]. On the cytosolic side, both US2 and US11 rely on the ATPase p97 to shuttle MHC-I to the proteasome for degradation [54,56].

In US2-mediated degradation of MHC-I, the function of TRC8 as E3 ligase is relatively well documented [55,57,58]. However, no specific E2 ubiquitin-conjugating enzymes have been implicated in this process. In **Chapter 5**, we constructed a lentiviral CRISPR/Cas9-based library targeting all known human E2 enzymes and used this resource to screen for E2 enzymes that regulate US2-mediated MHC-I downregulation. We identify UBE2G2 as an essential E2 enzyme for this process. Upon UBE2G2 depletion, MHC-I molecules are detected in an ER-resident US2- and TRC8-containing complex, possibly because ubiquitination may be required for extraction of the class I molecules from the ER membrane. In line with our findings for MHC-I, the immunoreceptors integrin- $\alpha$ 2, integrin- $\alpha$ 4, and thrombomodulin are also degraded by US2 in an UBE2G2-dependent manner. Immunoblot analysis of total MHC-I protein levels revealed that a UBE2G2 knockout rescued MHC-I to levels observed in TRC8-knockout conditions.

Interestingly, our screen identified UBE2J2 as a counteracting E2 enzyme, of which depletion further downregulates MHC-I in US2-expressing cells. The immunoreceptors integrin- $\alpha$ 2, integrin- $\alpha$ 4, and thrombomodulin were similarly affected upon UBE2J2 knockout. We hypothesized that either UBE2J2 competes with UBE2G2 for binding to TRC8 or that UBE2J2 regulates the turnover of TRC8. In the first case, depletion of UBE2J2 would provide UBE2G2 with more binding sites. In the second case, depletion of UBE2J2 would cause a decreased turnover of TRC8 and hence an increase in TRC8 protein levels. Both would ultimately lead to enhanced degradation of MHC-I by US2. Because the expression of a catalytically inactive UBE2J2 mutant had a similar effect on US2-mediated MHC-I degradation as the depletion of UBE2J2, this led us to believe that UBE2J2 regulates the turnover of TRC8. Indeed, either expression of catalytically inactive UBE2J2 or depletion of UBE2J2 caused increased protein levels of TRC8. Also, more TRC8 was present in the US2-exploited complexes compared to control conditions. However, whether this is also true for endogenous TRC8 remains to be determined. In conclusion, we show that the E2 ubiquitin-conjugating enzymes UBE2G2 and UBE2J2 are broadly involved in regulating the downregulation of immunoreceptors targeted by HCMV US2.

## Concluding remarks

US2- and US11-mediated degradation of MHC-I serve as a very useful system for studying ERAD. Genome-wide loss-of-function screens and the CRISPR/Cas9 genome-engineering tool have facilitated the identification of multiple essential components of this important degradation pathway, as illustrated in this thesis. A combination of these genetic power tools with SILAC-based proteomic identification of substrates, and large-scale purification of dislocation complexes is anticipated to unveil novel insights into ERAD and will reveal new avenues for research into this intriguing pathway.

## References

- [1] M.C. Bassik, R.J. Lebbink, L.S. Churchman, N.T. Ingolia, W. Patena, E.M. LeProust, M. Schuldiner, J.S. Weissman, M.T. McManus, Rapid creation and quantitative monitoring of high coverage shRNA libraries., *Nat. Methods.* 6 (2009) 443–5. doi:10.1038/nmeth.1330.
- [2] H. Hanzawa, M.J. de Ruwe, T.K. Albert, P.C. van Der Vliet, H.T. Timmers, R. Boelens, The structure of the C4C4 ring finger of human NOT4 reveals features distinct from those of C3HC4 RING fingers., *J. Biol. Chem.* 276 (2001) 10185–90. doi:10.1074/jbc.M009298200.
- [3] R.J. Deshaies, C.A.P. Joazeiro, RING domain E3 ubiquitin ligases., *Annu. Rev. Biochem.* 78 (2009) 399–434. doi:10.1146/annurev.biochem.78.101807.093809.
- [4] D. Flierman, C.S. Coleman, C.M. Pickart, T.A. Rapoport, V. Chau, E2-25K mediates US11-triggered retrotranslocation of MHC class I heavy chains in a permeabilized cell system., *Proc. Natl. Acad. Sci. U. S. A.* 103 (2006) 11589–94. doi:10.1073/pnas.0605215103.
- [5] A. Weber, I. Cohen, O. Popp, G. Dittmar, Y. Reiss, T. Sommer, T. Ravid, E. Jarosch, Sequential Polyubiquitylation by Specialized Conjugating Enzymes Expands the Versatility of a Quality Control Ubiquitin Ligase, *Mol. Cell.* 63 (2016) 827–839. doi:10.1016/j.molcel.2016.07.020.
- [6] A.J. Fletcher, D.L. Mallery, R.E. Watkinson, C.F. Dickson, L.C. James, Sequential ubiquitination and deubiquitination enzymes synchronize the dual sensor and effector functions of TRIM21., *Proc. Natl. Acad. Sci. U. S. A.* 112 (2015) 10014–9. doi:10.1073/pnas.1507534112.
- [7] M.C. Rodrigo-Brenni, D.O. Morgan, Sequential E2s drive polyubiquitin chain assembly on APC targets., *Cell.* 130 (2007) 127–39. doi:10.1016/j.cell.2007.05.027.
- [8] K. Wu, J. Kovacev, Z.-Q. Pan, Priming and extending: a UbcH5/Cdc34 E2 handoff mechanism for polyubiquitination on a SCF substrate., *Mol. Cell.* 37 (2010) 784–96. doi:10.1016/j.molcel.2010.02.025.
- [9] C.E. Shamu, D. Flierman, H.L. Ploegh, T.A. Rapoport, V. Chau, Polyubiquitination is required for US11-dependent movement of MHC class I heavy chain from endoplasmic reticulum into cytosol., *Mol. Biol. Cell.* 12 (2001) 2546–55. <http://www.pubmedcentral.nih.gov/articlerender.fcgi?artid=58612&tool=pmcentrez&rendertype=abstract> (accessed September 7, 2013).
- [10] D. Flierman, Y. Ye, M. Dai, V. Chau, T.A. Rapoport, Polyubiquitin serves as a recognition signal, rather than a ratcheting molecule, during retrotranslocation of proteins across the endoplasmic reticulum membrane., *J. Biol. Chem.* 278 (2003) 34774–82. doi:10.1074/jbc.M303360200.
- [11] D.E. Christensen, P.S. Brzovic, R.E. Klevit, E2-BRCA1 RING interactions dictate synthesis of mono- or specific polyubiquitin chain linkages., *Nat. Struct. Mol. Biol.* 14 (2007) 941–8. doi:10.1038/nsmb1295.
- [12] M.L.M.L. Van De Weijer, M.C. Bassik, R.D.R.D. Luteijn, C.M.C.M. Voorburg, M.A.M.A.M. Lohuis, E. Kremmer, R.C.R.C. Hoeben, E.M.E.M. Leproust, S. Chen, H. Hoelen, M.E.M.E. Ressing, W. Patena, J.S.J.S. Weissman,

- M.T.M.T. McManus, E.J.H.J.E.J.H.J. Wiertz, R.J.R.J. Lebbink, A high-coverage shRNA screen identifies TMEM129 as an E3 ligase involved in ER-associated protein degradation., *Nat. Commun.* 5 (2014) 3832. doi:10.1038/ncomms4832.
- [13] M.L. Van De Weijer, G.H. Van Muijwijk, L.J. Visser, A.I. Costa, E.J.H.J. Wiertz, R.J. Lebbink, The E3 ubiquitin ligase TMEM129 is a tri-spanning transmembrane protein, *Viruses*. 8 (2016). doi:10.3390/v8110309.
- [14] D.J.H. van den Boomen, R.T. Timms, G.L. Grice, H.R. Stagg, K. Skødt, G. Dougan, J.A. Nathan, P.J. Lehner, TMEM129 is a Derlin-1 associated ERAD E3 ligase essential for virus-induced degradation of MHC-I., *Proc. Natl. Acad. Sci. U. S. A.* 111 (2014) 11425–30. doi:10.1073/pnas.1409099111.
- [15] J.C. Christianson, Y. Ye, Cleaning up in the endoplasmic reticulum: ubiquitin in charge., *Nat. Struct. Mol. Biol.* 21 (2014) 325–35. doi:10.1038/nsmb.2793.
- [16] E.J. Wiertz, D. Tortorella, M. Bogyo, J. Yu, W. Mothes, T.R. Jones, T.A. Rapoport, H.L. Ploegh, Sec61-mediated transfer of a membrane protein from the endoplasmic reticulum to the proteasome for destruction., *Nature*. 384 (1996) 432–8. doi:10.1038/384432a0.
- [17] R.K. Plempner, S. Böhmeler, J. Bordallo, T. Sommer, D.H. Wolf, Mutant analysis links the translocon and BiP to retrograde protein transport for ER degradation., *Nature*. 388 (1997) 891–5. doi:10.1038/42276.
- [18] M. Pilon, R. Schekman, K. Römisch, Sec61p mediates export of a misfolded secretory protein from the endoplasmic reticulum to the cytosol for degradation, *EMBO J.* 16 (1997) 4540–4548. doi:10.1093/emboj/16.15.4540.
- [19] R.K. Plempner, J. Bordallo, P.M. Deak, C. Taxis, R. Hitt, D.H. Wolf, Genetic interactions of Hrd3p and Der3p/Hrd1p with Sec61p suggest a retro-translocation complex mediating protein transport for ER degradation., *J. Cell Sci.* (1999) 4123–34. <http://www.ncbi.nlm.nih.gov/pubmed/10547371> (accessed February 22, 2017).
- [20] M. Zhou, R. Schekman, The engagement of Sec61p in the ER dislocation process., *Mol. Cell.* 4 (1999) 925–34. <http://www.ncbi.nlm.nih.gov/pubmed/10635318> (accessed February 22, 2017).
- [21] P. Gillece, M. Pilon, K. Römisch, The protein translocation channel mediates glycopeptide export across the endoplasmic reticulum membrane., *Proc. Natl. Acad. Sci. U. S. A.* 97 (2000) 4609–14. doi:10.1073/pnas.090083497.
- [22] B.M. Wilkinson, J.R. Tyson, P.J. Reid, C.J. Stirling, Distinct domains within yeast Sec61p involved in post-translational translocation and protein dislocation., *J. Biol. Chem.* 275 (2000) 521–9. <http://www.ncbi.nlm.nih.gov/pubmed/10617647> (accessed February 22, 2017).
- [23] A. Schmitz, H. Herrgen, A. Winkeler, V. Herzog, Cholera toxin is exported from microsomes by the Sec61p complex., *J. Cell Biol.* 148 (2000) 1203–12. <http://www.ncbi.nlm.nih.gov/pubmed/10725333> (accessed February 22, 2017).
- [24] D.C. Scott, R. Schekman, Role of Sec61p in the ER-associated degradation of short-lived transmembrane proteins., *J. Cell Biol.* 181 (2008) 1095–105. doi:10.1083/jcb.200804053.
- [25] M. Willer, G.M.A. Forte, C.J. Stirling, Sec61p is required for ERAD-L: genetic dissection of the translocation and ERAD-L functions of Sec61P using novel derivatives of CPY., *J. Biol. Chem.* 283 (2008) 33883–8. doi:10.1074/jbc.M803054200.
- [26] A. Schäfer, D.H. Wolf, Sec61p is part of the endoplasmic reticulum-associated degradation machinery, *EMBO J.* 28 (2009) 2874–2884. doi:10.1038/emboj.2009.231.
- [27] B.N. Lilley, H.L. Ploegh, A membrane protein required for dislocation of misfolded proteins from the ER., *Nature*. 429 (2004) 834–40. doi:10.1038/nature02592.
- [28] Y. Ye, Y. Shibata, C. Yun, D. Ron, T. a Rapoport, A membrane protein complex mediates retro-translocation from the ER lumen into the cytosol., *Nature*. 429 (2004) 841–7. doi:10.1038/nature02656.
- [29] E.J. Greenblatt, J.A. Olzmann, R.R. Kopito, Derlin-1 is a rhomboid pseudoprotease required for the dislocation of mutant  $\alpha$ -1 antitrypsin from the endoplasmic reticulum., *Nat. Struct. Mol. Biol.* 18 (2011) 1147–52. doi:10.1038/nsmb.2111.

- [30] J. Wahlman, G.N. DeMartino, W.R. Skach, N.J. Bulleid, J.L. Brodsky, A.E. Johnson, Real-time fluorescence detection of ERAD substrate retrotranslocation in a mammalian in vitro system., *Cell*. 129 (2007) 943–55. doi:10.1016/j.cell.2007.03.046.
- [31] C.-H. Huang, H.-T. Hsiao, Y.-R. Chu, Y. Ye, X. Chen, Derlin2 protein facilitates HRD1-mediated retrotranslocation of sonic hedgehog at the endoplasmic reticulum., *J. Biol. Chem.* 288 (2013) 25330–9. doi:10.1074/jbc.M113.455212.
- [32] H. Hoelen, A. Zaldumbide, W.F. van Leeuwen, E.C.W. Torfs, M.A. Engelse, C. Hassan, R.J. Lebbink, E.J. de Koning, M.E. Ressing, A.H. de Ru, P.A. van Veelen, R.C. Hoeben, B.O. Roep, E.J.H.J. Wiertz, Proteasomal Degradation of Proinsulin Requires Derlin-2, HRD1 and p97., *PLoS One*. 10 (2015) e0128206. doi:10.1371/journal.pone.0128206.
- [33] J.H.L. Claessen, L. Kundrat, H.L. Ploegh, Protein quality control in the ER: balancing the ubiquitin checkbook., *Trends Cell Biol.* 22 (2012) 22–32. doi:10.1016/j.tcb.2011.09.010.
- [34] A. Stein, A. Ruggiano, P. Carvalho, T.A. Rapoport, Key steps in ERAD of luminal ER proteins reconstituted with purified components., *Cell*. 158 (2014) 1375–88. doi:10.1016/j.cell.2014.07.050.
- [35] R.D. Baldrige, T.A. Rapoport, Autoubiquitination of the Hrd1 Ligase Triggers Protein Retrotranslocation in ERAD., *Cell*. 166 (2016) 394–407. doi:10.1016/j.cell.2016.05.048.
- [36] P. Carvalho, A.M. Stanley, T.A. Rapoport, Retrotranslocation of a misfolded luminal ER protein by the ubiquitin-ligase Hrd1p., *Cell*. 143 (2010) 579–91. doi:10.1016/j.cell.2010.10.028.
- [37] S.C. Horn, J. Hanna, C. Hirsch, C. Volkwein, A. Schütz, U. Heinemann, T. Sommer, E. Jarosch, Usa1 functions as a scaffold of the HRD-ubiquitin ligase., *Mol. Cell*. 36 (2009) 782–93. doi:10.1016/j.molcel.2009.10.015.
- [38] K.M. Bernardi, J.M. Williams, M. Kikkert, S. van Voorden, E.J. Wiertz, Y. Ye, B. Tsai, The E3 ubiquitin ligases Hrd1 and gp78 bind to and promote cholera toxin retro-translocation., *Mol. Biol. Cell*. 21 (2010) 140–51. doi:10.1091/mbc.E09-07-0586.
- [39] E. Nadav, A. Shmueli, H. Barr, H. Gonen, A. Ciechanover, Y. Reiss, A novel mammalian endoplasmic reticulum ubiquitin ligase homologous to the yeast Hrd1., *Biochem. Biophys. Res. Commun.* 303 (2003) 91–7. doi:10.1016/S0006-291X(03)00279-1.
- [40] S.G. Kreft, L. Wang, M. Hochstrasser, Membrane topology of the yeast endoplasmic reticulum-localized ubiquitin ligase Doa10 and comparison with its human ortholog TEB4 (MARCH-VI), *J. Biol. Chem.* 281 (2006) 4646–53. doi:10.1074/jbc.M512215200.
- [41] M. Fairbank, P. St-Pierre, I.R. Nabi, The complex biology of autocrine motility factor/phosphoglucose isomerase (AMF/PGI) and its receptor, the gp78/AMFR E3 ubiquitin ligase., *Mol. Biosyst.* 5 (2009) 793–801. doi:10.1039/b820820b.
- [42] B. Mueller, E.J. Klemm, E. Spooner, J.H. Claessen, H.L. Ploegh, SEL1L nucleates a protein complex required for dislocation of misfolded glycoproteins., *Proc. Natl. Acad. Sci. U. S. A.* 105 (2008) 12325–30. doi:10.1073/pnas.0805371105.
- [43] P. Liu, Y. Ying, Y. Zhao, D.I. Mundy, M. Zhu, R.G.W. Anderson, Chinese hamster ovary K2 cell lipid droplets appear to be metabolic organelles involved in membrane traffic., *J. Biol. Chem.* 279 (2004) 3787–92. doi:10.1074/jbc.M311945200.
- [44] Y. Fujimoto, H. Itabe, J. Sakai, M. Makita, J. Noda, M. Mori, Y. Higashi, S. Kojima, T. Takano, Identification of major proteins in the lipid droplet-enriched fraction isolated from the human hepatocyte cell line HuH7., *Biochim. Biophys. Acta*. 1644 (2004) 47–59. <http://www.ncbi.nlm.nih.gov/pubmed/14741744> (accessed December 20, 2016).
- [45] M. Suzuki, T. Otsuka, Y. Ohsaki, J. Cheng, T. Taniguchi, H. Hashimoto, H. Taniguchi, T. Fujimoto, Derlin-1 and UBXD8 are engaged in dislocation and degradation of lipidated ApoB-100 at lipid droplets., *Mol. Biol. Cell*. 23 (2012) 800–10. doi:10.1091/mbc.E11-11-0950.
- [46] J.C. Christianson, J. a Olzmann, T. a Shaler, M.E. Sowa, E.J. Bennett, C.M. Richter, R.E. Tyler, E.J. Greenblatt,

- J.W. Harper, R.R. Kopito, Defining human ERAD networks through an integrative mapping strategy., *Nat. Cell Biol.* 14 (2011) 93–105. doi:10.1038/ncb2383.
- [47] J.N. Lee, X. Zhang, J.D. Feramisco, Y. Gong, J. Ye, Unsaturated fatty acids inhibit proteasomal degradation of Insig-1 at a postubiquitination step., *J. Biol. Chem.* 283 (2008) 33772–83. doi:10.1074/jbc.M806108200.
- [48] V.T. Phan, V.W. Ding, F. Li, R.J. Chalkley, A. Burlingame, F. McCormick, The RasGAP proteins Ira2 and neurofibromin are negatively regulated by Gpb1 in yeast and ETEA in humans., *Mol. Cell. Biol.* 30 (2010) 2264–79. doi:10.1128/MCB.01450-08.
- [49] J.N. Lee, H. Kim, H. Yao, Y. Chen, K. Weng, J. Ye, Identification of Ubx8 protein as a sensor for unsaturated fatty acids and regulator of triglyceride synthesis., *Proc. Natl. Acad. Sci. U. S. A.* 107 (2010) 21424–9. doi:10.1073/pnas.1011859107.
- [50] B. Schrul, R.R. Kopito, Peroxin-dependent targeting of a lipid-droplet-destined membrane protein to ER subdomains, *Nat. Cell Biol.* 18 (2016) 740–51. doi:10.1038/ncb3373.
- [51] A. Buchberger, From UBA to UBX: new words in the ubiquitin vocabulary., *Trends Cell Biol.* 12 (2002) 216–21. <http://www.ncbi.nlm.nih.gov/pubmed/12062168> (accessed December 7, 2016).
- [52] G. Alexandru, J. Graumann, G.T. Smith, N.J. Kolawa, R. Fang, R.J. Deshaies, UBX7 binds multiple ubiquitin ligases and implicates p97 in HIF1 $\alpha$  turnover., *Cell.* 134 (2008) 804–16. doi:10.1016/j.cell.2008.06.048.
- [53] A. Stolz, W. Hilt, A. Buchberger, D.H. Wolf, Cdc48: a power machine in protein degradation, *Trends Biochem. Sci.* 36 (2011) 515–523. doi:10.1016/j.tibs.2011.06.001.
- [54] Y. Ye, Y. Shibata, M. Kikkert, S. van Voorden, E. Wiertz, T.A. Rapoport, Recruitment of the p97 ATPase and ubiquitin ligases to the site of retrotranslocation at the endoplasmic reticulum membrane., *Proc. Natl. Acad. Sci. U. S. A.* 102 (2005) 14132–8. doi:10.1073/pnas.0505006102.
- [55] H.R. Stagg, M. Thomas, D. van den Boomen, E.J.H.J. Wiertz, H. a Drabkin, R.M. Gemmill, P.J. Lehner, The TRC8 E3 ligase ubiquitinates MHC class I molecules before dislocation from the ER., *J. Cell Biol.* 186 (2009) 685–92. doi:10.1083/jcb.200906110.
- [56] N. Soetandyo, Y. Ye, The p97 ATPase dislocates MHC class I heavy chain in US2-expressing cells via a Ufd1-Npl4-independent mechanism., *J. Biol. Chem.* 285 (2010) 32352–9. doi:10.1074/jbc.M110.131649.
- [57] J.-L. Hsu, D.J.H. van den Boomen, P. Tomasec, M.P. Weekes, R. Antrobus, R.J. Stanton, E. Ruckova, D. Sugrue, G.S. Wilkie, A.J. Davison, G.W.G. Wilkinson, P.J. Lehner, Plasma membrane profiling defines an expanded class of cell surface proteins selectively targeted for degradation by HCMV US2 in cooperation with UL141., *PLoS Pathog.* 11 (2015) e1004811. doi:10.1371/journal.ppat.1004811.
- [58] D.J.H. Van den Boomen, P.J. Lehner, Identifying the ERAD ubiquitin E3 ligases for viral and cellular targeting of MHC class I, *Mol. Immunol.* 68 (2015) 106–111. doi:10.1016/j.molimm.2015.07.005.



## **ADDENDUM**

### **Nederlandse Samenvatting Dankwoord Curriculum Vitae**

**Michael L. van de Weijer**

## NEDERLANDSE SAMENVATTING VOOR NIET-INGEWIJDEN

Gedurende miljoenen jaren hebben virussen en hun gastheren tegenover elkaar gestaan in een strijd om het bestaan. Het virus heeft de gastheer nodig om zich te vermeerderen. De gastheer heeft deze indringers liever niet op bezoek. Deze confrontatie tussen beide partijen heeft ervoor gezorgd dat de gastheer aan de ene kant een immuunsysteem tegen deze virussen heeft ontwikkeld, en dat aan de andere kant virussen op hun buurt weer strategieën hebben ontwikkeld om dit immuunsysteem te tarten, te ontwijken en zelfs in hun eigen voordeel te gebruiken.

### Herpesvirussen

Herpesvirussen zijn DNA virussen, d.w.z. hun genetische informatie ligt opgeslagen op DNA-moleculen in het virus zelf. Herpesvirussen behoren tot de Herpesvirus familie van virussen die weer onderverdeeld kan worden in een  $\alpha$ -,  $\beta$ -, en  $\gamma$ -subfamilie. Er zijn negen herpesvirussen waarvan bekend is dat zij mensen kunnen infecteren: herpes simplex virus type 1 en 2 (HSV-1 en HSV-2); varicella-zoster virus (VZV); Epstein-Barr virus (EBV); human cytomegalovirus (HCMV); human herpesvirus 6A, 6B, en 7 (HHV-6A, HHV-6B, en HHV-7); en Kaposi's sarcoma-associated herpesvirus (KSHV).

Als je eenmaal geïnfecteerd bent door een herpesvirus, draag je dit voor de rest van je leven bij je. Bijna iedereen is op deze manier drager van een of meerdere herpesvirussen. Gelukkig hebben mensen normaliter weinig tot geen last van een herpesvirusinfectie. Echter, onder bepaalde omstandigheden kunnen herpesvirussen ernstige complicaties veroorzaken. Wanneer bijvoorbeeld het immuunsysteem verzwakt is, bijvoorbeeld bij HIV patienten, of wanneer het immuunsysteem onderdrukt wordt, zoals bij transplantatie patiënten, kunnen herpesvirussen weer de kop op steken en levensbedreigende complicaties veroorzaken. Een ander voorbeeld van een ernstige complicatie is het veroorzaken van aangeboren afwijkingen door HCMV. Tenslotte kunnen EBV en KSHV bepaalde type tumoren veroorzaken. Samenvattend zijn herpesvirussen doorgaans onschuldige virussen, maar als ze eenmaal de kans krijgen, kunnen ze veel leed veroorzaken.

### Verstopperkje spelen

Herpesvirussen zijn heer en meester in het om te tuin leiden van het immuunsysteem van de gastheer, doordat zij tijdens een infectie verscheidene eiwitten produceren die aangrijpen op verschillende delen van het immuunsysteem. Bovendien zijn herpesviruses extreem goed in verstoppertje spelen. Herpesvirussen kunnen zich voor langere tijd verschuilen binnenin een gastheercel zonder dat het immuunsysteem dat doorheeft. Het virus houdt zich daar rustig. Dit wordt ook wel *latentie* van het herpesvirus genoemd.



HCMV is een uitstekend voorbeeld van hoe herpesvirussen het immuunsysteem kunnen misleiden. Tijdens een infectie produceert HCMV een vijftal eiwitten die de *MHC klasse I antigeen presentatie route* van het immuunsysteem lamleggen. De MHC klasse I antigeen presentatie route is gedurende de evolutie ontstaan om virale infecties te kunnen signaleren aan het immuunsysteem om vervolgens de geïnfecteerde cellen op te kunnen ruimen. Virussen hebben dit natuurlijk liever niet. Daarom hebben een aantal virussen, waaronder HCMV, methoden ontwikkeld om het MHC klasse I systeem uit te schakelen.

## Hoofdpijnen van dit proefschrift

In dit proefschrift ligt de nadruk op twee HCMV-eiwitten genaamd US2 en US11 die aangrijpen op de MHC klasse I antigeen presentatie route. Deze twee eiwitten zorgen ervoor dat MHC klasse I wordt afgebroken in de cel, waardoor de cel niet meer kan signaleren aan het immuunsysteem dat het geïnfecteerd is door HCMV. Bij deze methode gebruiken deze twee virale eiwitten, US2 en US11, vele andere eiwitten van de gastheercel om de afbraak van MHC klasse I te bewerkstelligen. Deze gebruikte eiwitten spelen normaliter een belangrijke rol bij de centrale afvalverwerking van eiwitten in de cel. Door de werkwijze van US2 en US11 te bestuderen kunnen we dus niet alleen meer te weten komen over hoe dit virus de *MHC klasse I antigeen presentatie route* weet plat te leggen, maar ook hoe de afvalverwerking van eiwitten in de cel werkt. Dit is een fundamenteel biologisch proces essentieel voor het overleven van de cel en het organisme. Dit wordt vooral duidelijk wanneer dit proces verstoord is. Enkele ziektes, met name neurodegeneratieve ziekten, worden veroorzaakt door verstoringen in het afbraakproces.

In **hoofdstuk 1 en 2** wordt een samenvatting gegeven van de methodes die virussen hebben ontwikkeld om de *MHC klasse I antigeen presentatie route* onklaar te maken. Daarin ligt de nadruk op de vele methoden die door herpesvirussen worden gebruikt om het immuunsysteem te slim af te zijn.

In **hoofdstuk 3** hebben wij systematisch gezocht naar eiwitten van de gastheercel die gebruikt worden door het HCMV-eiwit US11. Dit heeft een aantal interessante ontdekkingen opgeleverd, waaronder het gastheereiwit TMEM129. TMEM129 speelt een centrale rol bij de afbraak van MHC klasse I door US11. TMEM129 voorziet MHC klasse I van een label dat dit eiwit naar de afvalverwerking dirigeert. Bovendien hebben wij aanwijzingen gevonden dat TMEM129 ook betrokken is bij de centrale afvalverwerking van eiwitten in de cel. Echter, meer onderzoek zal nodig zijn om dit verder uit te zoeken.

In **hoofdstuk 4** hebben wij de ruimtelijke oriëntatie van het gastheereiwit TMEM129 bestudeerd. De ruimtelijke oriëntatie van eiwitten is doorgaans redelijk te voorspellen met behulp van computeralgoritmen, maar voorspellingen blijven voorspellingen. Door gebruik te maken van een aantal verschillende technieken, hebben wij de voorspelling kunnen bevestigen. Deze bevindingen zullen ons meer inzicht verschaffen in de normale functie van



het TMEM129 eiwit.

In **hoofdstuk 5** hebben wij onderzocht hoe een andere gastheercel-eiwit, genaamd p97, door US11 wordt gebruikt in het proces van MHC klasse I afbraak. P97 wordt gezien als het motortje dat zorgt voor verplaatsing van het af te breken eiwit richting het proteasoom ("de verbrandingsoven"). Normaliter heeft p97 hulp nodig om op de juiste plek en het juiste tijdstip te zijn waar het nodig is. Door systematisch bekende hulpjes van p97 uit te schakelen, en te kijken of de afbraak van MHC klasse I door US11 nog steeds werkt, hebben wij gevonden dat het gastheercel-eiwit UBXD8 hierbij betrokken is.

In **hoofdstuk 6** hebben wij ons geconcentreerd op het HCMV eiwit US2. Dit eiwit zorgt ook voor afbraak van MHC klasse I, maar ten opzichte van US11 doet US2 dit op een andere manier. US2 leent weer andere gastheerceleiwitten. Het TMEM129 equivalent voor US2 is TRC8. TRC8 speelt, zoals TMEM129 bij US11, een centrale rol bij MHC klasse I afbraak door US2. De rol van TRC8 hierbij is het labelen van MHC klasse I voor afbraak. Bij dit markeren voor afbraak heeft TRC8 de hulp nodig van zogenaamde E2 enzymen. In het proces van MHC klasse I afbraak door US2 is de identiteit van deze E2 eiwitten niet bekend. Door systematisch deze E2 eiwitten één voor één weg te halen, en te kijken of de afbraak van MHC klasse I door US2 nog steeds werkt, hebben wij enkele E2 eiwitten kunnen identificeren die hierbij een rol spelen. Uiteindelijk levert dit niet alleen nieuwe inzichten op in dit specifieke proces, maar ook in de algemene afvalverwerking van eiwitten in de cel.

In het laatste hoofdstuk, **hoofdstuk 7**, worden alle bevindingen in dit proefschrift op een rij gezet en bekeken hoe onze bevindingen niet alleen meer inzicht hebben opgeleverd in het proces van virale subversie van het immuunsysteem, maar ook hoe onze bevindingen kunnen bijdragen aan het ophelderen van fundamentele biologische processen. Dit is uiteindelijk van cruciaal belang om aandoeningen met verstoringen van het afbraakproces als oorzaak, beter te kunnen doorgronden en nieuwe therapieën te kunnen ontwikkelen.



## DANKWOORD

### Ouders

*“Wetenschap kan je niet met een schaarstje knippen.”*

Lieve ma en pa. Bedankt voor jullie onvoorwaardelijke zorg en liefde in goede en in slechte tijden. In jullie opvoeding hebben jullie hebben mij de vrijheid en de mogelijkheid gegeven om mijn nieuwsgierigheid voor de wetenschap te ontwikkelen, waardoor ik nu mijn dromen kan najagen. Mijn dank is groot.

### Emmanuel Wiertz

*“Van die dingen.”*

Jouw positieve visie en grenzenloos vertrouwen zal ik gaan missen. Als ik het zo nu en dan niet meer zag zitten, wist je het altijd weer van een positieve kant te benaderen. Dank voor het creëren van de mogelijkheden en steun de afgelopen jaren, waardoor ik mij ten volle heb kunnen ontplooiën.

### Robert Jan Lebbink

Jouw praktische tips over kloneren, het doen van screens, en andere aanverwante labzaken hebben mij meermaals uit de spreekwoordelijke brand geholpen. Jouw passie voor het aanwenden van de nieuwste technieken in de moleculaire biologie is een springplank gebleken voor de vele projecten beschreven in deze thesis. Dank daarvoor!

Niet te vergeten, jouw practical jokes zijn uniek. En daarom het vermelden waard!

*“I am very sorry to inform you that due to a human error we accidently mixed your samples with that of another customer. Could you send us additional material to run the analysis on. We are closed for operation the next two weeks due to a holiday. Could you send us the samples at the earliest at July 1st? We are very sorry for the inconvenience. As a service to you, we will apply an additional 2% discount on your next order from over 50 samples.”*

### Ferdy van Diemen

*“A good plan violently executed now is better than a perfect plan executed next week”*

- George S. Patton

Sinds je komst op de afdeling, ben je een onverwoestbare sparringspartner gebleken op het gebied van wetenschap, geschiedenis, en life in general; en bovenal een goede vriend. De tijden van Deutsche Schlagers die rondschallen in het lab op volumestand 10 mis ik nu al. Het lab in Oxford heeft namelijk geen muziekinstallatie...

**Rutger D. Luteijn**

*“We hebben al zo ver moeten kruipen, het laatste stuk zal ook wel gaan.”*

Jouw gevoel voor humor en muziek zijn een geval apart! Dank voor de protocollen die ik in de jaren van je heb mogen gebruiken. En bovenal, bedankt voor je hulp bij de totstandkoming van deze thesis. Succes en veel plezier in the USA! Ik heb er alle vertrouwen in dat je ook het lab daar op stellen gaat zetten. Doe Sanne de hartelijke groeten!

**Manouk Vrieling**

Jouw humor en wijsheden hebben mij meermaals uit het spreekwoordelijke dal geholpen! Dank ook voor je hulp bij het vervaardigen van deze thesis. Nu ben je trots lid van de MMB UK delegatie, waar ik eveneens sinds kort deel van mag zijn. Ik wens je veel succes en plezier in de UK! Niet te veel smikkelen van die Schotse Haggis, he!

**Anouk Schuren**

Mijn ERAD opvolger! Met een eigenwijs iemand zoals ik was het niet altijd even makkelijk samenwerken. Om hoofdstuk 6 tot een publiceerbaar manuscript te verwerken, was dan ook een hele excersitie, maar het resultaat liegt er niet om! Succes met de laatste loodjes! Die wegen vaak het zwaarst. Laat je vooral niet van de wijs brengen. Zoals Rutger en ik vaak zeggen: *“We hebben al zo ver moeten kruipen, het laatste stuk zal ook wel gaan”*.

**(Ex-)kamerogenoten**

Hartelijk dank voor de gezellige jaren, de tal van roomdiners met al dat overheerlijke eten, en jullie humor!

**Weirdo's! (© R.D. Luteijn)**

Bedankt voor de waardevolle discussies, prettige werksfeer en gezellige tijd!

**Studenten Linda Visser, Guus van Muijlwijk, en Rik Haagmans**

Dank voor jullie tijd en inzet! Jullie werk heeft een mooie bijdrage geleverd aan deze thesis.



## **CURRICULUM VITAE**

Michael (Mike) Laurentius van de Weijer was born on September 29, 1988 in Baarn, The Netherlands. He graduated *cum laude* from his pre-university education (Gymnasium “Physics & Biology” and “Physics & Chemistry” with Ancient Greek and Latin) in 2006 at the Baarnsch Lyceum in Baarn. In the same year, he was admitted to study Biomedical Sciences in Utrecht (Utrecht University). In 2009, he received his Bachelor of Science degree *cum laude*. After his graduation, he was admitted to the Infection & Immunity Master program at the University of Utrecht. During his Master studies in 2009-2010, he worked under supervision of Prof Dr. Linde Meyaard at the Wilhemina Children’s Hospital (University Medical Center Utrecht). From 2010-2011, he worked under supervision of Dr. Berend Jan Bosch at the Faculty of Veterinary Medicine (Utrecht University). His master thesis was written under supervision of Prof. Dr. Emmanuel Wiertz and Dr. Ir. Robert Jan Lebbink at the Department of Medical Microbiology of the University Medical Center Utrecht. Michael obtained his Master of Science degree in 2011, and started as a PhD student in the lab of Prof. Dr. Emmanuel Wiertz and Dr. Ir. Robert Jan Lebbink. Here, he studied the molecular mechanisms of MHC class I degradation by the human cytomegalovirus proteins US2 and US11. The results of his studies are described in this thesis. In early 2017, he continued his scientific career as a postdoctoral researcher in the lab of Prof. Dr. Pedro Carvalho at the Sir William Dunn School of Pathology (University of Oxford) in Oxford, UK, to study the molecular mechanisms of mammalian protein degradation.